IDENTIFICATION OF A HYPOTHALAMIC NEURAL SYSTEM THAT CAN REDUCE BODY WEIGHT AND ADIPOSE MASS IN DIET-INDUCED OBESITY

Rashmita Basu

Submitted to the faculty of the University Graduate School
in partial fulfillment of the requirements
for the degree
Doctor of Philosophy
in the Department of Pharmacology and Toxicology
Indiana University

November 2024

Accepted by the Graduate Faculty of Indiana University, in partial fulfillment of the requirements for the degree of Doctor of Philosophy.

Doctoral Committee

Jonathan N. Flak, Ph.D., Chair

Amelia K. Linnemann, Ph.D.

August 30, 2024

Carol A. Witczak, Ph.D.

Patrick L. Sheets, Ph.D.

Travis J. Jerde, Ph.D.

© 2024

Rashmita Basu

DEDICATION

I dedicate my dissertation to my beloved parents, for their endless love, encouragement, and unwavering support - without which this journey would not have been possible.

And to my mother, who has been my guiding star, teaching me the true meaning of perseverance and grace and that the sky is the limit. Your strength, wisdom, and boundless love have been my guiding light.

You are the roots of my strength and the wings of my aspirations. Thank you for believing in me, even when I doubted myself. This achievement is as much yours as it is mine.

ACKNOWLEDGEMENT

As I reach the culmination of this incredible journey, I am deeply aware that this thesis is not just a reflection of my hard work, but also of the unwavering support, love, and guidance from so many extraordinary people.

First and foremost, I would like to express my deepest gratitude to my PhD advisor, Dr. Jonathan Flak. Your unwavering support, insightful guidance, and passion for science have been a constant source of inspiration. Your belief in my abilities and dedication to my growth as a scientist have been instrumental in my success. I owe much of my growth as a scientist to your invaluable advice. You have supported me immensely in taking multidisciplinary approaches to make scientific discoveries and has cultivated my ability to clearly reason and make convincing arguments based on evidence. I am forever thankful for your extensive support in helping me to realize my professional goals and motivating me to achieve those goals. My journey would not have been the same without the support of my lab members: Andrew J. Elmendorf, Connor A. Mahler, Betty Lorentz, Britany App and the lab interns. Thank you for your friendship, collaboration, and support and who selflessly sharing your knowledge with me. Working alongside you has been a privilege, and I have learned so much from our shared experiences in the lab.

To my incredible dissertation committee members: Dr. Amelia Linnemann, Dr. Carol Witczak, Dr. Patrick Sheets and Dr. Travis Jerde - your thoughtful feedback, challenging questions, invaluable suggestions and unwavering support have enriched my research and pushed me to strive for excellence. Your belief in me, even when I doubted

myself, has been a beacon of hope and encouragement. Thank you for your time, effort, and commitment to my academic journey.

I owe a special thanks to the Dr. Jenelle Richardson, Amy Lawson, Jan Scully, Susan Gunter from the IUSM department of pharmacology; Dr. Thomas Hurley, Brandy Wood, Britney Hieser, Ruth Clark and Tara Hobson from the IBMG; Sylvia Robertson, Olivia Lazaro, Soumya Yennapureddy, Dr. Travis Johnson, Dr. Mike Kalwat, Dr. Andrew Templin, Dr. Robert Considine, Natalie Stull and all other members of the Indiana Biosciences Research Organization. Your support, whether it was advice, helping me troubleshoot and conduct experiments or assisting with administrative tasks was crucial to the success of this work. Your kindness and willingness to help made all the difference during challenging times.

This work would not have been possible without funding support from the American Diabetes Association Pathway to Stop Diabetes Grant 17-INI-15, NIH R01DK136897 grant, Ralph W. and Grace M. Showalter Trust, the IU CDMD Pilot and Feasibility Program, and funds from the Indiana Biosciences Research Institute.

Finally, to my husband and my wonderful family, especially my parents, you have been my pillars of strength. Your unconditional love, patience, and encouragement have been my refuge in the stormy seas of this journey and your steadfast belief in me have been the foundation of everything I have achieved. This journey began with your dreams for me, and I hope I have made you proud.

This thesis is dedicated to all of you, for without your support, none of this would have been possible. Thank you from the bottom of my heart.

Rashmita Basu

IDENTIFICATION OF A HYPOTHALAMIC NEURAL SYSTEM THAT CAN REDUCE BODY WEIGHT AND ADIPOSE MASS IN DIET-INDUCED OBESITY

Dynamic hypothalamic circuits balance energy intake with expenditure to protect individuals from obesity. Lasting negative energy balance, however, triggers a compensatory decrease in energy expenditure, hindering progressive weight loss. While we understand some key players underlying energy balance, the detailed neural underpinnings remain unclear. Here I will delineate the functional efferent circuitry from the ventromedial hypothalamic nucleus (VMN) that facilitates weight loss and prevents rebound weight gain.

VMN neurons have long been linked to a role in energy balance. Both vesicular communication by VMN steroidogenic factor 1 (SF1) neurons and pituitary adenylate cyclase activating peptide (PACAP) release from VMN neurons are essential for maintaining body weight and activating VMN^{Sf1} neurons curbs diet-induced obesity without altering food intake. However, the exact pathway of this VMN signal is unclear because the VMN does not directly communicate with preganglionic sympathetic neurons, indicating signal transmission through an efferent node. Of the few brain sites they communicate with, VMN^{Sf1} neurons sends the densest projections to the caudal preoptic area (POA) and the anterior bed nucleus of stria terminalis (BNST). Stimulating VMN^{PACAP} axonal fibers in the caudal POA, but not anterior BNST, induced thermogenesis in brown and beige adipose tissues in both sexes of mice.

To identify caudal POA populations in body weight regulation, I activated excitatory (glutamatergic) and inhibitory (GABAergic) caudal POA cells in diet-induced obese male mice and found that both glutamatergic and GABAergic caudal POA neurons can reduce diet-induced obesity through separate means. While there is intra-POA communication, my data supports efferent communication with separate downstream circuits by glutamate and GABA caudal POA cells in ameliorating diet-induced obesity.

Because the POA and BNST are extremely complex regions with diverse functions, I then employed deep transfer learning to pinpoint obesity and diabetes risk-associated cell subsets in the POA and BNST. Using single nuclei RNA sequencing on >200,000 nuclei from both sexes of mice, I identified 6 specialized sets of caudal POA and BNST neuronal subtypes that increased in obese and glucose-intolerant mice on a high-fat diet. Targeting these newly identified pathways and neuron subtypes could lead to future obesity and diabetes therapeutics.

Jonathan N. Flak, Ph.D., Chair

Amelia K. Linnemann, Ph.D.

Carol A. Witczak, Ph.D.

Patrick L. Sheets, Ph.D.

Travis J. Jerde, Ph.D.

TABLE OF CONTENTS

List of Tables xiii
List of Figures xiv
List of Abbreviations xvi
Chapter 1: Introduction 1
Obesity epidemic 1
Current anti-obesity treatments: drawbacks 3
Energy balance and its role in obesity 5
CNS control of energy balance 14
Set point theory of body weight regulation 19
Hypothalamic neural circuits regulating energy homeostasis 20
Extra-hypothalamic control of energy homeostasis 45
Key metabolic mechanisms regulating energy homeostasis 48
Gaps in knowledge 58
Goals and hypotheses 59
Chapter 2: Materials and methods 63
Animals 63
Reagents 64
Stereotaxic injections of viral constructs 64
Phenotypic studies 66
Temperature measurement at adipose tissue depots 67
Acute brain slice preparation 68
Electrophysiological recordings 68
Optogenetics studies 69
Terminal tissue collection and perfusion 70
Perfusion and Immunohistochemistry 71
Total RNA sequencing 72
Single nuclei RNA isolation 74
Single nuclei RNA sequencing 75
Quantitative real-time PCR 77
RNAscope in-situ hybridization 78
Cell counts 79
Statistics 79
Chapter 3: Ventromedial hypothalamic nucleus subset stimulates tissue thermogenesis via preoptic area outputs 81
Background and rationale 82
Results 85
Activating VMN^{Sf1} neurons blunts diet induced obesity in male mice 85
VMN^{PACAP} neurons send projections to the POA, thereby activating these neurons via glutamatergic signaling 89
Activating VMN^{PACAP} → caudal POA signaling induces tissue thermogenesis in both sexes of mice 94
After 24 hours fasting, activation of VMN^{PACAP} → caudal POA signaling

restores thermogenic activity in both sexes of mice 97
Acute activation of VMN^{PACAP} → caudal POA neurons induces distinct molecular programs within brown and beige adipose tissue in both sexes of mice 100
Activation of the VMN^{PACAP} neurons leads to highest neuronal activation at caudal POA, among all collaterals, via the VMN^{PACAP} projections 104
Activating VMN^{PACAP} neurons with simultaneous inhibition of the caudal POA neurons blunts adipose tissue thermogenesis in both sexes of mice 107
Overall model 109
Discussion 111
Conclusion 118
Acknowledgement 118
Chapter 4: Distinct populations of neurons in the caudal POA ameliorate diet-induced obesity via distinct pathways 120
Background and rationale 121
Results 125
Activating both glutamatergic and GABAergic neurons in the caudal POA ameliorate diet-induced obesity 126
Activating glutamatergic neurons in the caudal POA increased iBAT and iWAT temperature 130
Activating glutamatergic neurons in the caudal POA induces thermogenic gene expression in iBAT 132
Inhibiting glutamatergic neurons in the caudal POA also curbs diet-induced obesity potentially via distinct mechanism 135
Glutamatergic and GABAergic caudal POA neurons send distinct efferent projections 139
Overall model 141
Discussion 142
Conclusion 149
Chapter 5: Identification of cells in the preoptic area and bed nucleus of the stria terminalis, impacted by obesity and diabetes in both male and female mice 150
Background and rationale 151
Results 155
Dissecting the complexity of the POA and BNST in obesity and diabetes through single nuclei sequencing 155
Validation and identification of glutamatergic and GABAergic cluster in the POA over-expressed in obese and diabetic mice 162
Discussion 166
Conclusion 172
Acknowledgement 173
Chapter 6: Discussions 174
Summary and conclusions 174
Discussion and limitations 180
Future directions 184
Appendices 188
Supplementary figures 188

References.....197
Curriculum Vitae

LIST OF TABLES

Table 1: Hypothalamic nuclei and their role in the control of energy balance.....39

LIST OF FIGURES

Figure 1.1: The role of energy homeostasis in obesity 7
Figure 1.2: Components of total daily energy expenditure (TDEE).....10
Figure 1.3: Brain driving iBAT thermogenesis 19
Figure 1.4: The hypothalamic nuclei 23
Figure 1.5: VMN neural circuits involved in direct and indirect mechanisms governing energy homeostasis 28
Figure 1.6: POA neural circuits involved in direct and indirect mechanisms governing energy homeostasis 33
Figure 1.7: Summary of the major hypothalamic pathways regulating energy balance....40
Figure 1.8: Key metabolic mechanisms regulating body weight.....57
Figure 1.9: Schematic of hypothesized neural circuit by which VMN^{PACAP} acts to regulate body weight.....62
Figure 3.1: Activating VMN^{Sf1} neurons blunts diet induced obesity in male mice.....86
Figure 3.2: Activating VMN^{Sf1} neurons increases energy expenditure and iBAT thermogenic gene expression in diet induced obese male mice 88
Figure 3.3: VMN^{PACAP} neurons send projections to the POA, thereby activating these neurons via glutamatergic signaling 93
Figure 3.4: Activating VMN^{PACAP} → caudal POA signaling induces tissue thermogenesis in both sexes of mice 96
Figure 3.5: After 24 hours fasting, activation of VMN^{PACAP} → caudal POA neurons restores thermogenic activity in both sexes of mice 99
Figure 3.6: Acute activation of VMN^{PACAP} → caudal POA neurons induces distinct molecular programs in brown and beige adipose tissue in both sexes of mice 101
Figure 3.7: Acute activation of VMN^{PACAP} → caudal POA neurons induces distinct molecular programs but with similar peripheral functions in brown and beige adipose tissue in both sexes of mice 103
Figure 3.8: Activation of the of VMN^{PACAP} neurons leads to highest neuronal activation at caudal POA, among all collaterals, via the VMN^{PACAP} projections.....106
Figure 3.9: Activating VMN^{PACAP} neurons with simultaneous inhibition of the caudal POA neurons blunts adipose tissue thermogenesis in both sexes of mice 109
Figure 3.10: Overall model.....111
Figure 4.1: Activating both vGLUT2 and vGAT caudal POA neurons ameliorate diet-induced obesity.....127
Figure 4.2: Activating both vGLUT2 and vGAT caudal POA neurons ameliorate diet-induced obesity without changing activity 129
Figure 4.3: Activating vGLUT2, but not vGAT, caudal POA neurons increases iBAT and iWAT temperature 131
Figure 4.4: Activating vGLUT2 caudal POA neurons induces iBAT and iWAT thermogenesis 134
Figure 4.5: Model for inhibiting vGLUT2 caudal POA neurons to test their potential for ameliorating diet-induced obesity 136
Figure 4.6: Inhibiting vGLUT2 caudal POA neurons ameliorate diet-induced obesity

by inducing hypophagia and increasing iBAT and iWAT temperature.....138
Figure 4.7: Glutamatergic and GABAergic caudal POA neurons send distinct efferent projections 140
Figure 4.8: Overall Model.....142
Figure 5.1: Selection criteria for mice used in snRNASeq.....157
Figure 5.2: Single-nuclei RNA sequencing of POA.....160
Figure 5.3: Single-nuclei RNA sequencing of BNST.....161
Figure 5.4: RNA in situ hybridization of glutamatergic markers in the POA 164
Figure 5.5: RNA in situ hybridization of GABAergic markers in the POA.....165
Figure S1: Schematic of $AAV^{DIO\text{-}hM3dq\text{-}mCherry}$ injection site in $Sf1^{Cre}$ mice, $AAV^{DIO\text{-}ChR2\text{-}eYFP}$ injection site and optrode placements in $Adcyap1^{Cre}$ mice 188
Figure S2: VMN^{PACAP} neurons project to sites outside of the POA and activate neurons in these sites in both sexes of mice 190
Figure S3: Stimulating VMN^{PACAP} → caudal POA neurons with blue light, in absence of ChR2, does not induce tissue thermogenesis in both sexes of mice 192
Figure S4: Validation of the top differentially expressed genes in iBAT and iWAT found in bulk RNA-sequencing 193
Figure S5: Schematic of $AAV^{DIO\text{-}ChR2\text{-}eYFP}$ and $AAV^{hM4Di\text{-}mCherry}$ injection site and optrode placements in $Adcyap1^{ChR2\text{-}eYFP}$ mice 194
Figure S6: Schematic of $AAV^{DIO\text{-}hM3dq\text{-}mCherry}$ injection site in $vGLUT2^{Cre}$ and $vGAT^{Cre}$ mice, $AAV^{DIO\text{-}hM4di\text{-}mCherry}$ injection site in $vGLUT2^{Cre}$ mice 195
Figure S8: Single-nuclei RNA sequencing showing hybrid neuronal populations within POA and BNST 196

LIST OF ABBREVIATIONS

3V - 3rd Ventricle
AAV - Adeno-Associated Virus
ABCs - Arachnoid Barrier Cells
AC - Anterior Commissure
Adcyap1 - Adenylate Cyclase Activating Polypeptide 1
AgRP - Agouti-Related Peptide
Amp 1/2/3 - Amplification steps in RNAscope
AMPK – Adenosine-Mono Phosphate-activated Protein Kinase
ANS – Autonomic nervous System
AP - Anteroposterior
Aq – Aqueduct
ARC - Arcuate Nucleus
ASIC2 - Acid-Sensing Ion Channel 2
ATg - Anterior Tegmental Area
AVP - Arginine Vasopressin
BDNF - Brain-Derived Neurotrophic Factor
BMR - Basal Metabolic Rate
BNST - Bed Nucleus of the Stria Terminalis
BRS3 - Bombesin-like Receptor 3
CCK - Cholecystokinin
ChR2 - Channelrhodopsin-2
cFos - Cellular Immediate Early Gene Fos
CNO - Clozapine-N-Oxide
CNS – Central Nervous System
COL11A1 - Collagen Type XI Alpha 1 Chain
CRH - Corticotropin-Releasing Hormone
D3V - Dorsal 3rd Ventricle
DAPI - 4',6-diamidino-2-phenylindole
DBNST - Dorsal Bed Nucleus of the Stria Terminalis
DG - Dentate Gyrus
DGKG - Diacylglycerol Kinase Gamma
DMN - Dorsomedial Hypothalamic Nucleus
DNP - 2,4-Dinitrophenol
DV – Dorsoventral
EAT - Exercise Activity Thermogenesis
Erα - Estrogen Receptor Alpha
eYFP - Enhanced Yellow Fluorescent Protein
EtOH - Ethanol
FL v2 HRP - Fluorescent v2 Horseradish Peroxidase
FOXP2 - Forkhead Box P2
GABA - Gamma-Aminobutyric Acid
GC - Genome Copies
GLP1 - Glucagon-Like Peptide 1

GPC5 – Glypican 5
Hb - Habenular Commissure
HFD - High-Fat Diet
hM3Dq - Human M3 Muscarinic Dq Receptor
hM4Di - Human M4 Muscarinic Di Receptor
IC - Inferior Colliculus
iBAT - Inter-scapular Brown Adipose Tissue
IRS4 - Insulin Receptor Substrate 4
iWAT - Inguinal White Adipose Tissue
Kcnip1 – Potassium voltage (Kv) Channel-Interacting Protein 1
LepR - Leptin Receptor
LHA - Lateral Hypothalamic Area
LPAG - Lateral Periaqueductal Gray
LV - Lateral Ventricle
MC4R - Melanocortin 4 Receptor
ML - Mediolateral
MnR - Median Raphe Nucleus
NEAT - Non-Exercise Activity Thermogenesis
NOS1 - Nitric Oxide Synthase 1
NPY - Neuropeptide Y
NREE - Non-Resting Energy Expenditure
NTS - Nucleus of the Solitary Tract
OPCs - Oligodendrocyte Precursor Cells
PACAP - Pituitary Adenylate Cyclase-Activating Polypeptide
PAG - Periaqueductal Gray
PBS - Phosphate-Buffered Saline
PCR - Polymerase Chain Reaction
PHA - Posterior Hypothalamic Area
PNS – Peripheral Nervous System
POA - Preoptic Area
POMC – Proopiomelanocortin
PSNS - Parasympathetic Nervous System
PTPRD - Receptor-Type Protein Tyrosine Phosphatase D
PVT - Paraventricular Thalamus
PVN - Paraventricular Hypothalamic Nucleus
PYY - Peptide YY
qRT-PCR - Quantitative Real-Time Polymerase Chain Reaction
RM ANOVA - Repeated Measures Analysis of Variance
RMR – Resting Metabolic Rate
RRID - Research Resource Identifier
RYR3 - Ryanodine Receptor 3
SCN - Suprachiasmatic Nucleus
SEM - Standard Error of the Mean
SF1 - Steroidogenic Factor 1
snRNASeq - Single-Nuclei RNA Sequencing
SNS – Sympathetic Nervous System

SSC - Saline-Sodium Citrate
TDEE - Total Daily Energy Expenditure
TRH - Thyrotropin-Releasing Hormone
TRKB - Tropomyosin Receptor Kinase B
TRPC4 - Transient Receptor Potential Cation Channel Subfamily C Member 4
UCP1 - Uncoupling Protein 1
VLMCs - Vascular and Leptomeningeal Cells
VBNST - Ventral Bed Nucleus of the Stria Terminalis
VLPAG - Ventrolateral Periaqueductal Gray
VMN - Ventromedial Nucleus
VTA - Ventral Tegmental Area
vGAT - Vesicular GABA Transporter
vGLUT2 - Vesicular Glutamate Transporter 2

Chapter 1: Introduction

Obesity epidemic

Global rates of obesity have surged significantly over the past three decades, with more than 42% adults classified as overweight or obese as of 2022 and it is projected to increase >51% by 2035. The obesity crisis is particularly severe in the United States, where nearly 70% of adults have a BMI over 25 kg/m², and minority populations are disproportionately affected. Childhood obesity is also alarmingly high, with 23% of children aged 6-19 qualifying as obese nationwide and rates exceeding over 20% worldwide. Obese children are 80% more likely to be obese adults and face increased risks of early death (Organization 2024). Obesity has surpassed undernutrition as a leading cause of death and disability worldwide and is associated with the risk of developing chronic conditions such as type 2 diabetes, cardiovascular diseases, cancer, fatty liver disease, and kidney disease, all of which are expensive to treat and reduce quality of life (Ogden, Yanovski et al. 2007 6, Organization 2024).

The healthcare systems worldwide are already strained by the high incidence of obesity, and the rising costs of treating obesity and its complications will become unsustainable without intervention. As of 2022, it poses a growing financial burden with $200 billion in the US and over $4 trillion worldwide being spent annually on treating obesity and health conditions that arise from it (Finkelstein, Trogdon et al. 2009, Federation 2023). Curtailing the obesity pandemic is thus a global health concern of paramount importance.

Despite the overwhelming prevalence of obesity and overweight, few medical strategies to date have proven effective in maintaining long-term weight loss. The first-line prescription for weight reduction is diet and exercise. While many individuals initially lose weight through dieting, most do not maintain the weight loss long-term. Adherence to lifestyle modification, combining diet and exercise, is notoriously challenging, leading to a vicious cycle of weight cycling or fad dieting, which increases the risk of heart disease, stroke, and diabetes. Current obesity drugs often have unpleasant side effects like nausea, vomiting, aversion to food intake, loss of lean muscle mass etc. The effectiveness of these medications is, substantial when one is on the drug, but once the patient stops using the drug there can be rebound weight gain (Chakhtoura, Haber et al. 2023, Qi, Cox et al. 2024). Therefore, there is a clear need to develop better strategies to promote weight loss and prevent weight gain to improve health outcomes for overweight and obese individuals.

Understanding why the surge in overweight and obesity has occurred is also vital, as it may inform the design of interventions to manage body weight. Average caloric intake has increased by around 240 kcals/day since 1970, primarily due to higher carbohydrate consumption. Meanwhile, fat intake has decreased over the same period, suggesting that excess caloric intake, rather than high dietary fat, potentiates weight gain. Concurrently, occupational-associated energy expenditure has progressively declined since 1960, and only 1 in 5 adults fulfill the recommended amount of daily physical activity. Thus, the obesity epidemic is likely fueled by excess caloric intake combined with reduced physical activity. While this explains what causes obesity, it does not elucidate why individuals overeat and move less. The increasing availability of palatable,

calorie-rich, and inexpensive food has contributed to rising obesity rates, but what permits caloric intake more than metabolic demands remains unclear. Energy intake is normally coordinated with energy expenditure to defend body weight, but these mechanisms are not completely understood and are influenced by numerous variables such as food palatability, genetics, and a sedentary lifestyle.

Current anti-obesity treatments: drawbacks

The primary recommendation for obesity treatment involves lifestyle changes, including diet and exercise. Popular diets such as Atkins, ketogenic, and intermittent fasting are widely adopted but often come with side effects like ketosis, acidosis, hypoglycemia, gastrointestinal distress, dyslipidemia, lethargy, and unbalanced nutrition. Additionally, adherence to these diets is challenging, leading many individuals to regain weight. Exercise, although beneficial for health, is often insufficient alone for significant weight loss without dietary changes.

Another significant challenge in maintaining weight loss is the adaptation of the resting metabolic rate (RMR), which decreases more than expected based on body composition. The mechanisms underlying RMR control are not well understood. Historical use of 2,4-Dinitrophenol (DNP) illustrates this challenge. DNP was effective for weight loss by stimulating RMR but caused dangerous side effects, including hyperthermia and cardiac arrest, leading to its market withdrawal in 1938. This highlights the need for a better understanding of the biology controlling RMR to develop safer therapeutic targets (Chakhtoura, Haber et al. 2023, Qi, Cox et al. 2024).

A variety of pharmacologic agents have been developed to aid in weight loss, but they generally have limited effectiveness and potential side effects. Sympathomimetic drugs like benzphetamine, phentermine, and phenylephrine promote weight loss by increasing energy expenditure but can cause cardiovascular problems and have a risk of addiction. Phentermine/Topiramate increases energy expenditure and reduces appetite but has numerous side effects, including metabolic acidosis, renal stones, and increased risk of depression and anxiety (Chakhtoura, Haber et al. 2023, Qi, Cox et al. 2024). A variety of GLP-1 agonists drugs such as semaglutide, tirzepatide, liraglutide are approved for type-2 diabetes and weight loss but are expensive and come with side effects such as nausea, vomiting, aversion to food intake and lean mass loss. Liraglutide is a GLP-1 agonist that helps with weight loss and glycemic control but can cause gastrointestinal issues and potentially increase the risk of pancreatitis and thyroid carcinoma (Chakhtoura, Haber et al. 2023, Qi, Cox et al. 2024). Various other drugs are available, but most achieve only modest weight loss (around 5% body weight) and their long-term efficacy is often unproven. Setmelanotide is approved for specific genetic obesity types and increases satiety and energy expenditure, but its mechanism is not fully understood. Orlistat inhibits lipases to prevent fat absorption in the small intestine but commonly causes gastrointestinal issues like fecal incontinence and oily spotting. Naltrexone/Bupropion is a combination drug that suppresses appetite through different mechanisms but can cause severe nausea and insomnia (Chakhtoura, Haber et al. 2023, Qi, Cox et al. 2024).

Bariatric surgery, particularly the Roux-en-Y gastric bypass, another very effective obesity treatment, has a very high cost of surgery and risk of complications,

including hypoglycemia, hernia, perforation of the stomach or intestine, and nutritional deficiencies, limit its use to morbidly obese individuals. This leaves moderately overweight or obese individuals with fewer effective options for weight control and risk non-compliance.

Given the limitations of current treatments, there is a pressing need to develop more effective and safer strategies to promote sustained weight loss and prevent weight gain (Chakhtoura, Haber et al. 2023, Qi, Cox et al. 2024). Research into understanding the underlying causes of obesity, such as increased caloric intake, reduced physical activity, mechanisms of energy balance, the role of neural circuits in feeding behavior, and the influence of genetics and environment on obesity is crucial. Advancements in understanding these areas could lead to the identification of new therapeutic targets and the development of interventions that promote sustained weight loss and improved health outcomes for obese individuals.

Here, I aim to identify the mechanisms to elevate energy expenditure in a long-term manner to facilitate sustained weight loss. By exploring the complex interplay of neural circuits, hormones, and genetic factors, I hope to uncover novel pathways that can be targeted for therapeutic intervention, providing new hope for those struggling with obesity.

Energy balance and its role in obesity

Obesity develops when the balance between the energy intake and energy expenditure is disrupted. This balance between energy intake and energy expenditure, known as energy homeostasis, is crucial for maintaining a healthy weight (Fig. 1.1).

Factors like over-consumption, especially consumption of calorie-dense foods, and decreased energy expenditure contribute to the disruption of energy homeostasis, leading to a positive energy balance and weight gain. Over time, the body responds less effectively to mechanisms that regulate hunger and metabolism, make it harder to metabolize, feel full and maintain a stable weight, further promoting obesity. On the other hand, promoting energy expenditure and decreasing calorie intake leads to weight loss via a negative energy balance.

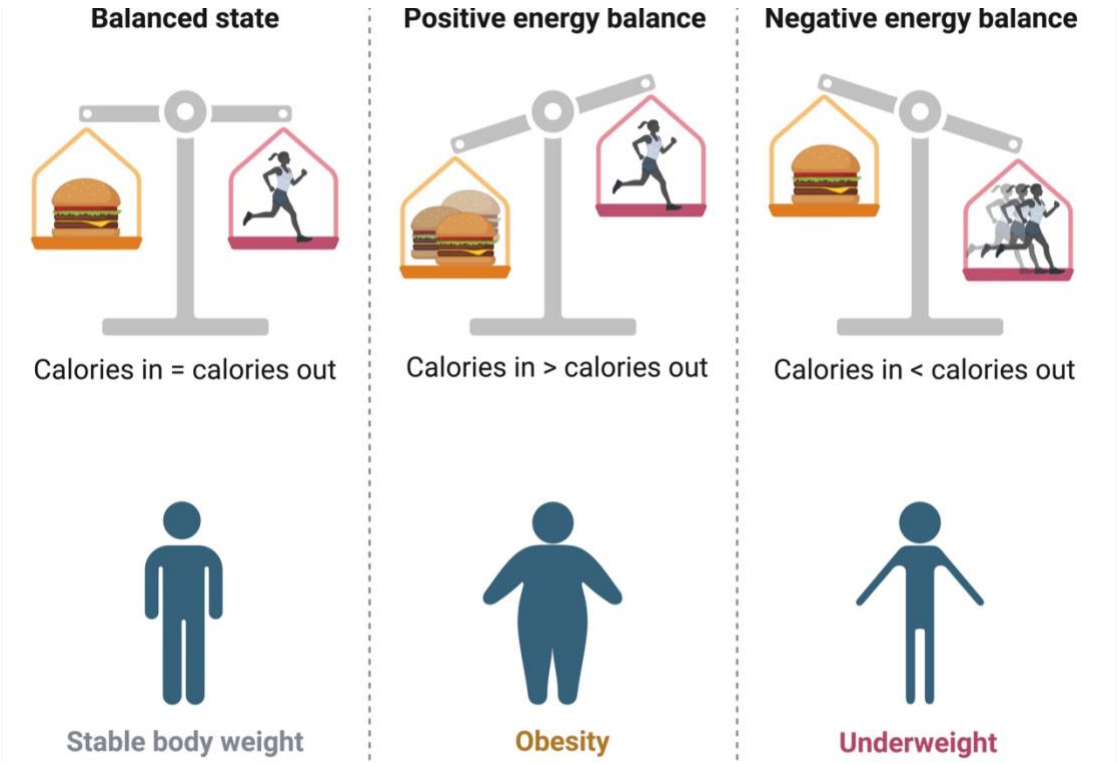

Figure 1.1: The role of energy homeostasis in obesity. The concept of energy balance refers to the relationship between energy intake (from food and beverages) and energy expenditure (through physical activity, metabolic processes, and other bodily functions). When the energy intake and energy expenditure are equal, there is said to be an energy balance. When the energy intake is greater than the energy expenditure, a positive energy balance occurs, resulting in weight gain. Lasting weight gain causes obesity. Conversely, when the energy expenditure is greater than the energy intake, a negative energy balance occurs, resulting in weight loss. Lasting weight loss can cause malnutrition and lead to underweight. Created with Biorender.com.

The control of energy expenditure is a complex physiological process that matches whole body energy utilization to current demands measured in terms of total daily energy expenditure (TDEE), i.e., total calories burnt by a person in a day (Fig. 1.2). It is broadly categorized as resting energy expenditure (REE) and non-resting energy expenditure (NREE), each consisting of distinct components (Novak and Levine 2007,

Tseng, Cypess et al. 2010). REE, comprising of basal metabolic rate (BMR), refers to the amount of energy expended by the body at rest to maintain basic physiological functions such as respiration, circulation, and cellular processes (Fig. 1.2). BMR, also known as the resting metabolic rate (RMR), is the energy expended at rest under standardized conditions (e.g. mild fasting, thermoneutral conditions). Genetic factors, but not environmental factors, influence both REE and RMR, which accounts for most of the individual variability in energy expenditure. Variations in genes related to energy metabolism also influences RMR via thermogenic activity. The other component of TDEE, i.e. NREE, encompasses energy expenditure associated with physical activity, thermic effect of food (TEF), and other non-exercise activities. NREE can be further divided into (1) exercise activity thermogenesis (Patel, Braun et al. 2023), (2) non-exercise activity thermogenesis (NEAT), and (3) thermic effect of food (TEF) and (4) adaptive thermogenesis (Fig. 1.2) (Kassir, Debs et al. 2016). EAT refers to the energy expended during structured physical activities such as exercise, including cardiovascular workouts, strength training, and sports (Fig. 1.2). The intensity, duration, and type of exercise significantly impact EAT, with higher intensity activities generally resulting in greater energy expenditure. NEAT encompasses the energy expended during spontaneous, non-exercise activities such as walking, standing, fidgeting, and maintaining posture (Fig. 1.2). NEAT varies widely among individuals and is influenced by factors such as occupation, lifestyle, and environmental conditions. TEF represents the energy expenditure associated with the digestion, absorption, and metabolism of food (Fig. 1.2). Different macronutrients have varying thermic effects, with protein having the highest thermic effect, followed by carbohydrates and fats (Gao and Horvath 2007).

Adaptive thermogenesis refers to the regulation of energy expenditure in response to changes in environmental conditions, energy intake, and metabolic demands (Fig. 1.2). It includes both shivering thermogenesis and non-shivering thermogenesis. Shivering thermogenesis is a mechanism whereby the body generates heat through involuntary muscle contractions, primarily mediated by the activation of interscapular brown adipose tissue (iBAT). Unlike REE, NREE is primarily shaped by environmental factors like food intake, physical activity, hormones. The brain, via the central nervous system (CNS) and sympathetic nervous system (SNS), detects and integrates these environmental stimuli and shapes body weight, by mediating adaptive changes to energy availability and energy expenditure (Schwartz and Porte 2005, Cannon and Nedergaard 2011).

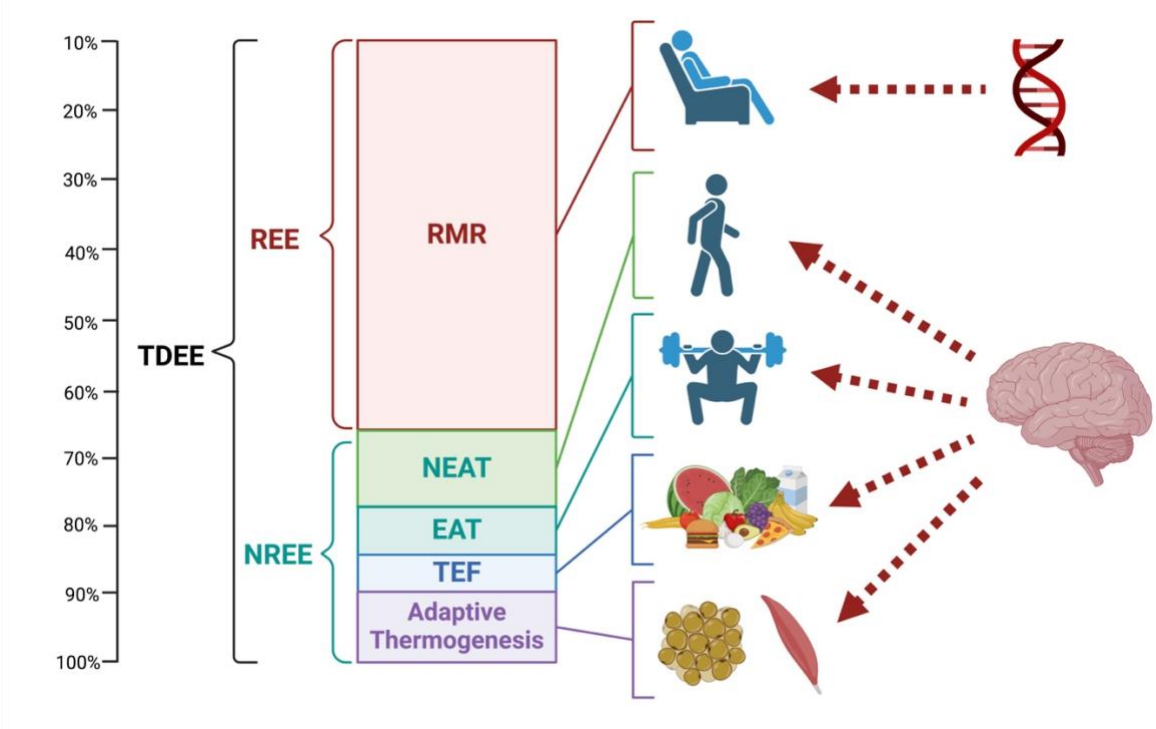

Figure 1.2: Components of total daily energy expenditure (TDEE). TDEE comprises of resting energy expenditure (REE) and non-resting energy expenditure (NREE). REE comprises of resting metabolic rate (RMR) which is primarily governed by genetics. NREE on the other hand, comprises of non-exercise activity thermogenesis (NEAT), exercise activity thermogenesis (Patel, Braun et al.), thermic effect of food (TEF) and adaptive thermogenesis. The components of NREE are modulated by the brain in response to environmental signals. Created with Biorender.com.

Several factors influence energy expenditure, including:

a. Body Composition: Lean mass utilizes and consumes nutrients more than fat mass via maintenance, repair, and protein turnover. Consequently, individuals with higher lean mass have higher RMR and TDEE.

b. Physical Activity: Physical activity stimulates mitochondrial biogenesis and improves insulin sensitivity and thus elevates energy expenditure via energy expended during structured physical activities such as exercise and sports and through

spontaneous activities such as walking, standing, and fidgeting. Physical activity levels increase lean mass composition that is more favorable to energy expenditure. Higher order brain regions that control voluntary movement and locomotion, such as the motor cortex, basal ganglia, and brainstem nuclei, increase energy expenditure and physical activity levels when activated by the individual. Additionally, the motor cortex plans and executes voluntary movements, while the basal ganglia and brainstem nuclei coordinate movement patterns and stimulate muscle tone. Hypothalamic and brainstem systems influence these functions according to environmental stimuli to increase TDEE.

c. Hormone Levels: Hormone levels vary between individuals and mediate differences in TDEE. Thyroid hormones, including triiodothyronine (T3) and thyroxine (T4), stimulate cellular metabolism and thermogenesis, thereby increasing TDEE. Insulin promotes glucose uptake and storage in peripheral tissues, elevating energy utilization and expenditure. Sex hormones, such as estrogen and testosterone, affect body composition, metabolic rate, and energy expenditure, contributing to sex differences in energy metabolism.

d. Diet: TEF represents the energy expended during the digestion, absorption, and metabolism of nutrients consumed in the diet. Consuming larger meals and meals rich in protein elicits a greater thermic response, leading to increased TDEE. Additionally, dietary factors such as meal frequency, nutrient composition, and food processing influences TEF and overall energy balance.

e. Temperature: Brain regions involved in thermoregulation, such as the hypothalamus and brainstem, adjust TDEE and metabolic rate in response to changes in ambient temperature. iBAT contains a high density of mitochondria and is specialized in

dissipating energy as heat through uncoupling protein 1 (UCP1) activation (Fig. 1.3). Non-shivering thermogenesis involves the modulation of metabolic rate without shivering. This occurs through various mechanisms, including sympathetic nervous system activation, thyroid hormone regulation, and the stimulation of iBAT activity. Cold exposure stimulates thermogenesis via non-shivering mechanisms, activating iBAT and increasing SNS activity. iBAT thermogenesis, driven by UCP1, dissipates energy as heat (Morrison, Madden et al. 2014, Labbe, Caron et al. 2015, Sidossis and Kajimura 2015, Contreras, Nogueiras et al. 2016, Betz and Enerback 2018). Conversely, heat exposure triggers mechanisms like sweating and vasodilation for heat dissipation. Changes in ambient temperature indirectly affect metabolic rate by influencing TDEE related to physical activity and RMR. Additionally, deviations from normal body temperature, such as fever or hypothermia, prompt adaptive metabolic responses. Fever elevates metabolic rate to support immune function, while hypothermia slows metabolism to conserve energy.

f. Height: Taller individuals have larger body surface areas, which leads to greater heat loss and increased TDEE for thermoregulation than shorter individuals.

g. Age: As individuals age, decreased lean body mass, mitochondrial function and metabolic rate reduce RMR. Additionally, age-related declines in hormone levels, such as growth hormone and testosterone further reduce TDEE.

h. Sex: Males typically have more lean and less adipose mass compared to females, resulting in higher RMR and overall TDEE. Additionally, hormonal differences, such as higher levels of testosterone in males and estrogen in females, modulate metabolic function and TDEE through their effects on hypothalamic nuclei and

peripheral tissues, such as, estrogen action on insulin sensitivity and fat oxidation, while testosterone increases muscle mass and metabolic rate.

i. Emotion & Stress Level: Acute stress triggers the release of stress hormones like cortisol and adrenaline, which mobilize energy stores and enhance metabolic activity to cope with perceived threats. Chronic stress, however, disconnects these pathways, disrupting appetite, food intake patterns, and metabolic balance. Stress-induced cortisol release increases adipose mass, favors visceral fat, and exacerbates metabolic imbalance. Moreover, emotional states such as anxiety and depression impact appetite, food choices, and energy balance, contributing to weight fluctuation and metabolic disturbance.

Disruption of energy homeostasis is a key factor in the development of obesity. Normally, energy homeostasis is regulated by complex neuroendocrine signals involving the brain, gut, and adipose tissues. In obesity, this delicate balance is disrupted, often due to factors such as overnutrition, sedentary lifestyle, and genetic predispositions that alter metabolic processes. Overnutrition, particularly from calorie-dense diets, coupled with reduced physical activity, leads to an energy surplus, which the body stores as fat. Hormonal signals crucial for signaling satiety and regulating glucose metabolism, may become less effective due to the development of resistance in these pathways. This hormonal dysregulation skews the body's natural feedback mechanisms that regulate hunger and metabolic rate, making it difficult to maintain a healthy weight. Moreover, chronic low-grade inflammation, commonly observed in obesity, can interfere with hypothalamic function—the brain's key area for appetite regulation and energy expenditure—further exacerbating metabolic dysregulation and energy imbalance. As the

body stores more fat, the adipose tissue itself becomes not just a storage site but an active endocrine organ, secreting hormones and inflammatory markers that perpetuate metabolic dysfunction and complicate the return to a balanced state of energy homeostasis. Thus, the breakdown in the mechanisms that maintain energy balance is central to the pathophysiology of obesity. Addressing these disruptions through lifestyle changes, medical interventions, and potentially targeting specific molecular pathways offers avenues for restoring energy balance and managing and potentially reversing obesity.

CNS control of energy balance

The nervous system integrates all the factors mentioned above to maintain energy homeostasis within the body by balancing energy expenditure with energy intake(Gao and Horvath 2007). Since the nervous system acts as a master regulator to maintain energy homeostasis, understanding the neural factors that controls energy metabolism is crucial. This intricate system comprises several components, including the CNS, SNS, parasympathetic nervous system (PSNS), and peripheral nervous system (PNS). Each component exerts unique effects on energy expenditure, contributing to the overall balance of energy within the body. The CNS, particularly the hypothalamus of the brain, integrates sensory and hormonal inputs to govern energy intake, expenditure, and storage. The SNS and PSNS convey neural signals from the CNS to peripheral organs, with SNS activity promoting energy expenditure and PSNS activity favoring conservation. Meanwhile, the PNS relays information from peripheral organs back to the CNS, facilitating bidirectional communication crucial for maintaining energy homeostasis. This integrated framework underscores the interconnectedness of central, autonomic, and peripheral pathways in regulating metabolic responses to internal and external cues

(Hyun and Sohn 2022). Understanding the interplay between these systems is crucial for comprehending the complex regulation of metabolic processes.

The CNS, consisting of the brain and spinal cord, serves as the central control center for coordinating various physiological functions, including energy metabolism. Specific regions within the brain, particularly the hypothalamus, plays pivotal roles in appetite, energy intake, and expenditure. The hypothalamus integrates signals from peripheral organs, and neuronal circuits activate suitable responses in the form of appetite and metabolism. For instance, genetically similar neuronal populations within the hypothalamus, such as those expressing proopiomelanocortin (POMC) and Agouti-related peptide (AgRP), respond to peripheral signals such as hormones like leptin, an adipose-derived hormone, and insulin to suppress appetite and increase energy expenditure or to ghrelin to stimulate feeding and increase energy intake (Huo, Gamber et al. 2009, Yang and Ruan 2015, Yang and Xu 2020). Moreover, the cerebral cortex, involved in higher cognitive functions, controls behaviors such as physical activity and dietary choices through the integration of sensory inputs and cognitive processes that impacts energy expenditure (Clapham 2012).

The autonomic nervous system (ANS) governs involuntary bodily functions, including heart rate, digestion, metabolism and respiration. It comprises two main divisions: the SNS and the PSNS, both of which work synergistically to maintain physiological equilibrium, including energy balance. The SNS, involved in the "fight or flight" system, is activated during stressful situations or periods of heightened activity, characterized by increased heart rate, blood pressure, and energy mobilization. SNS activation releases catecholamines such as epinephrine and norepinephrine, which

stimulate glycogenolysis and lipolysis. Lipolysis in adipose tissue liberates free fatty acids (FFAs) into circulation, which serve as substrates for energy production during times of increased metabolic demand. Specifically, SNS activation enhances thermogenesis by promoting iBAT activity and inducing the expression of thermogenic genes such as UCP1. iBAT-mediated thermogenesis dissipates energy as heat, contributing to the regulation of body temperature and energy balance (Cannon and Nedergaard 2011, Wu, Jun et al. 2015, Patel, Braun et al. 2023). Moreover, the SNS stimulates substrate utilization and glucose metabolism in both muscle and liver according to energy balance state. Additionally, SNS activation increases heart rate and cardiac output, thereby elevating metabolic rate and energy expenditure to meet the demands of physical activity or stress.

In contrast to the SNS, the PSNS is often associated with the "rest and digest" response that favors energy conservation and storage. PSNS activity decreases heart rate, vasodilation, and enhanced gastrointestinal motility, facilitating nutrient absorption and storage. While traditionally considered less involved in energy expenditure regulation compared to the SNS, emerging evidence suggests that the PSNS also plays a role in metabolic homeostasis (Buhmann, le Roux et al. 2014, Asadi, Shadab Mehr et al. 2022, Imai and Katagiri 2022). The vagal system, a key component of the PSNS, serves as a major pathway for bidirectional communication between the gut and the brain. Through its efferent fibers, the vagus nerve innervates various organs involved in metabolic processes, including the gastrointestinal tract, liver, and adipose tissue. Stimulation of the vagus nerve promotes nutrient absorption, insulin secretion, and glycogen synthesis, thereby influencing energy utilization and storage in peripheral tissues and organs.

Sensory fibers of the vagus nerve innervating the gastrointestinal tract also detect changes in gut microbiota composition, microbial metabolites, and gut wall integrity . These signals are then relayed to the brainstem nuclei, including the nucleus tractus solitarius (NTS), which integrate visceral sensory information and modulate autonomic and neuroendocrine responses. Additionally, the vagus nerve modulates gut hormone secretion and secretion of neurotransmitters such as serotonin, gamma-aminobutyric acid (GABA), and dopamine by the gut microbiome and transmitting information about gastric distension, appetite regulation, energy metabolism to the brain (Buhmann, le Roux et al. 2014, Asadi, Shadab Mehr et al. 2022, Imai and Katagiri 2022). Furthermore, the PSNS stimulates gut microbiota, which contribute to harvest energy and metabolism through fermentation of dietary substrates.

The PNS consists of nerves and ganglia that extend beyond the CNS including sensory neurons, motor neurons, and autonomic neurons and these nerves innervate various organs and tissues throughout the body. Peripheral nerves innervate metabolic tissues such as adipose tissue, skeletal muscle, and the liver, enabling bidirectional communication between the CNS and peripheral organs. For instance, sensory neurons within adipose tissue detect changes in adiposity and nutrient availability, relaying this information to the CNS to modulate appetite, thermogenesis, and energy balance. Similarly, motor neurons innervating skeletal muscle regulate physical activity levels and energy expenditure in response to CNS signals and environmental stimuli (Lenard and Berthoud 2008, Yoo, Yu et al. 2021).

Thus, the CNS, ANS, and PNS work in concert to maintain energy homeostasis by integrating signals from internal and external environments and orchestrating appropriate physiological responses. For instance:

a. Integration of Metabolic Signals: The hypothalamus receives input from peripheral signals, such as hormones (e.g., leptin, insulin, ghrelin) and nutrient levels, to regulate appetite, energy expenditure, and metabolic rate accordingly.

b. Balance between SNS and PSNS: The balance between sympathetic and parasympathetic tone determines the overall level of energy expenditure. During periods of increased energy demand, the SNS predominates, promoting lipolysis, thermogenesis, and cardiovascular function to meet metabolic needs.

c. Adaptation to Environmental Challenges: The nervous system enables adaptive responses to environmental challenges, such as cold exposure or dietary fluctuations, through adjustments in energy expenditure and thermoregulation mediated by sympathetic outflow and peripheral nervous signaling.

Thus, the nervous system exerts profound effects on energy expenditure and homeostasis through intricate neuroendocrine pathways and autonomic regulation. The interplay between the CNS, ANS, and PNS ensures dynamic adjustments in metabolic rate and energy balance to meet the demands of changing physiological conditions and environmental challenges. Dysfunction in these neural circuits leads to metabolic disorders such as obesity or metabolic syndrome, highlighting the critical relationship between the brain, nervous system, and energy expenditure. A comprehensive understanding of these regulatory mechanisms is essential for developing interventions to combat metabolic disorders and promote overall health and well-being.

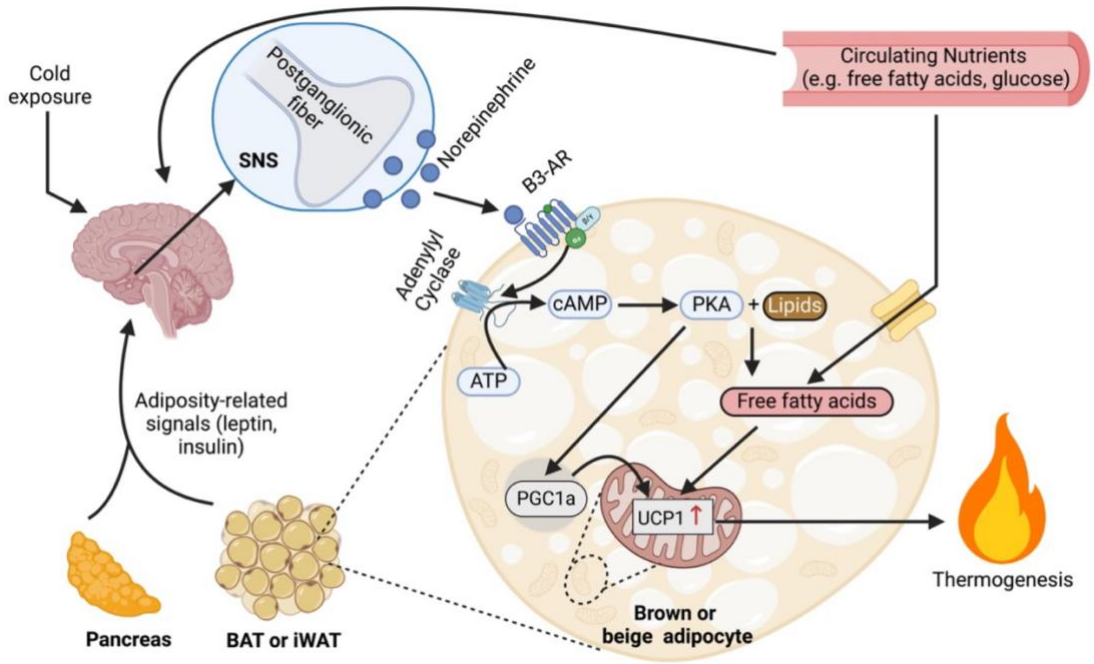

Figure 1.3: Brain driving iBAT thermogenesis. The hypothalamus of the brain, integrates hormonal, nutritional and environmental signals and engages the different components of the CNS ANS and PNS to influence the whole-body physiology as well as key mechanisms, such as iBAT thermogenesis, to influence energy homeostasis and body weight. Created with Biorender.com.

Set point theory of body weight regulation

The set point theory posits that the body naturally regulates its weight around an internally set point, much like it regulates temperature or blood pressure, primarily controlled by genetic and biological factors. Central to this regulation is the hypothalamus, which responds to hormonal signals from leptin—produced by fat cells—to manage food intake and energy expenditure based on fat stores (Schwartz, Woods et al. 2000). If weight decreases below this set point, leptin levels drop, stimulating appetite

and reducing energy expenditure to regain weight. Adaptive thermogenesis also plays a role, where the body adjusts its energy expenditure in response to calorie intake changes, complicating long-term weight loss and promoting weight regain when normal eating resumes (Rosenbaum and Leibel, 2010). This theory is bolstered by genetic studies showing a high heritability of body weight, indicating a pre-set range of weight that individuals tend to maintain (Gagnon, Mauriege et al. 1996).

However, the set point theory does not fully account for the modern increase in obesity, often criticized for overlooking significant environmental and lifestyle factors. Moreover, insulin and ghrelin, along with leptin, contribute to weight regulation, influencing appetite and energy balance (Faber, Matsen et al. 2018). For obesity treatment, this suggests the necessity of approaches that can adjust the biological set point beyond mere diet and exercise, potentially involving pharmacological treatments or lifestyle changes that significantly impact the body's weight-regulating mechanisms. This understanding encourages a multifaceted, personalized approach to effective long-term weight management, recognizing the complex interplay of genetic, hormonal, and metabolic factors in weight regulation.

Hypothalamic neural circuits regulating energy homeostasis

The hypothalamus, located within the ventral diencephalon, consists of several smaller regions, called nuclei, with each of these hypothalamic nuclei contain specialized neurons that play key roles in maintaining other physiological functions. The hypothalamic nuclei that are key regulators of energy homeostasis are the anterior hypothalamic area (AHA), preoptic area (POA), bed nucleus of the stria terminalis

(BNST), suprachiasmatic nucleus (SCN), paraventricular hypothalamic nucleus (PVN), ventromedial hypothalamic nucleus (VMN), dorsomedial hypothalamic nucleus (DMN), arcuate nucleus (ARC), lateral hypothalamic area (LHA) and supraoptic nucleus (SON) (Fig. 1.4) (Jenkins 1972).

The hypothalamus stands out as a dynamic and adaptable region capable of rapid responses to changes in the environment that exhibits high degrees of anatomical and cellular plasticity, enabling it to adapt quickly to alterations in firing patterns and connectivity within neuronal networks (Coll and Yeo 2013). The precision with which the brain responds to nutritional signals, emphasizes the hypothalamus's capacity to compensate for disturbances induced by feeding, exercise, or changes in ambient temperature. As the central hub for processing these signals, the hypothalamus integrates inputs from various sources, including sensory information, internal physiological cues and humoral factors. This integration allows the brain to accurately interpret the nutritional state and make appropriate adjustments in food intake and energy expenditure. Sensory inputs, central integrative circuits, and motor outputs, exemplify the extensive communication between the nervous system and peripheral organs such as the gastrointestinal tract, liver, pancreas, and adipose tissues, and integrating this information to regulate energy production, storage, mobilization, and utilization (Coll and Yeo 2013, Timper and Bruning 2017).

Research in both human and mice have shown that the hypothalamus acts as a superordinate master regulator of whole-body energy homeostasis by regulating the intricate web of mechanisms governing energy homeostasis and expenditure. From evolutionary adaptations to precise neural control, the hypothalamus integrates genetic,

environmental, and physiological factors to maintain energy balance by regulating food intake and energy expenditure. This area, containing cell populations critical for homeostatic functions, rapidly adapts to changes in the environment to ensure energy supplies for cellular functions and protection against energy scarcity. Recognizing the multifaceted nature and the intricacy of hypothalamic function is paramount for developing targeted interventions to address the escalating challenges of metabolic disorders in modern societies. Current research in this field holds the promise of unraveling new insights into the neural control of metabolic states, offering avenues for targeted therapeutic interventions and preventative strategies that leverage the sophisticated regulatory capabilities of the hypothalamus in maintaining energy balance at both the molecular and systems levels. Here, I summarize the hypothalamic regulation of energy expenditure at the organism level, its components and how they are controlled by the hypothalamic neural circuits.

In the following sections I will delve deeper into each of the hypothalamic nuclei that play a key role in the regulation of energy balance by modulating all the different factors mentioned earlier, such as body composition, physical activity, hormonal and dietary cues, ambient temperature, sexual dimorphism, emotion and stress levels.

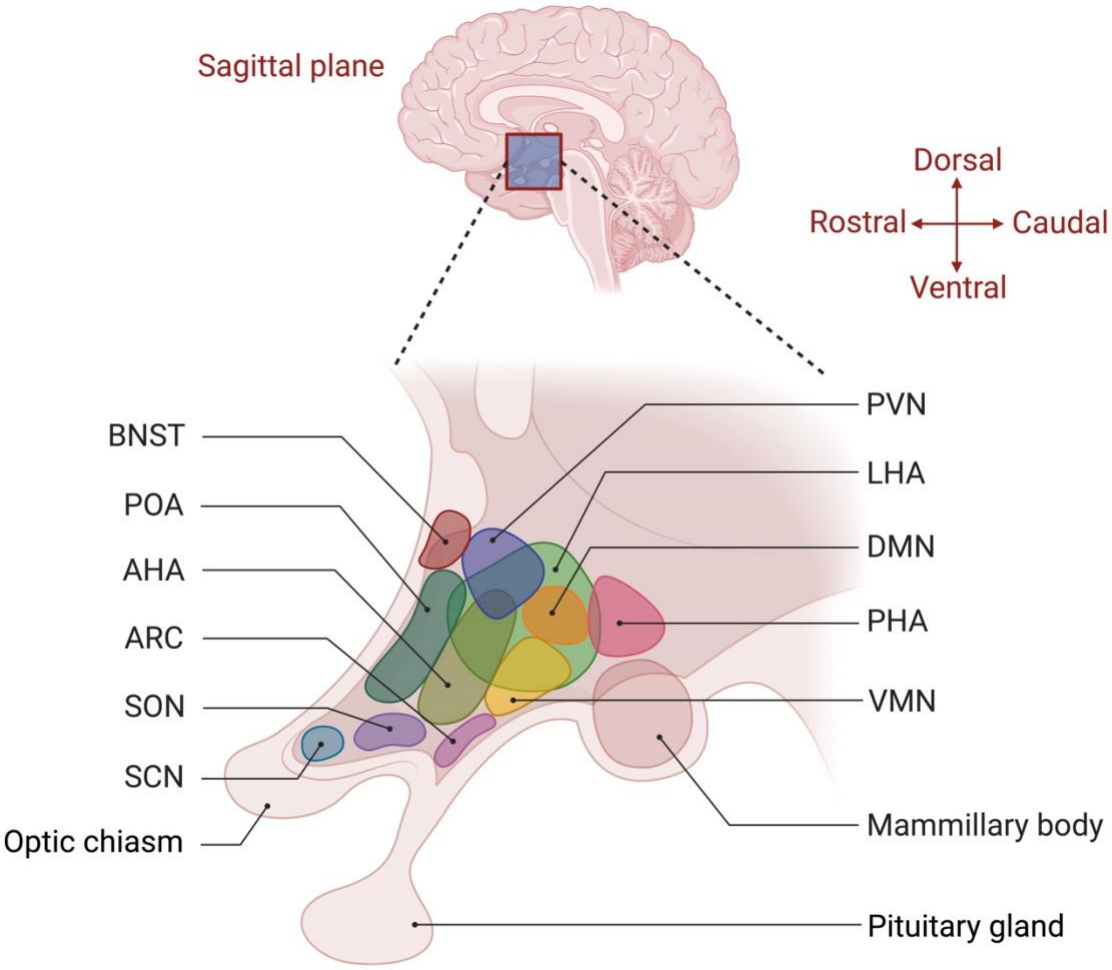

Figure 1.4: The hypothalamic nuclei. Sagittal section of the brain showing the hypothalamic nuclei and their location within the diencephalon. The nuclei are located dorsal to the pituitary gland and optic chiasm and rostral to the mammillary body. AHA = anterior hypothalamic area, POA = preoptic area, BNST = bed nucleus of the stria terminalis, SCN = suprachiasmatic nucleus, PVN = paraventricular hypothalamic nucleus, VMN = ventromedial hypothalamic nucleus, DMN = dorsomedial hypothalamic nucleus, ARC = arcuate nucleus, LHA = lateral hypothalamic area, SON = supraoptic nucleus, PHA = posterior hypothalamic area. Created with Biorender.com.

Ventromedial hypothalamic nucleus

The VMN integrates peripheral signals related to nutrient availability and energy status, thereby controlling feeding behavior, energy expenditure, thermogenesis, and glucose levels. Within the VMN, diverse populations of neurons, including glutamatergic, steroidogenic factor 1 (SF1), pituitary adenylate cyclase activating peptide (PACAP), estrogen receptor alpha (ERα), LepR, work in concert to orchestrate metabolic responses to maintain energy homeostasis. The vast majority of VMN neurons are glutamatergic neurons that relay peripheral signals related to nutrient availability to downstream brain regions involved in energy regulation, including direct hormonal signals such as leptin and insulin, where leptin suppress appetite and increase energy expenditure and insulin impacts glucose metabolism and satiety There is evidence of an extremely modest population of GABAergic neurons that presumably exert inhibitory control over neuronal circuits, sense circulating glucose levels, and contribute to the regulation of feeding behavior and energy balance. The VMN modulates sympathetic outflow to metabolic tissues, including iBAT and skeletal muscle, thereby influencing thermogenesis and fat utilization. These mechanisms driven by the VMN can have implications on nutrient partitioning, particularly via melanocortin action on VMN melanocortin receptor 3 (Nogueiras, Wiedmer et al. 2007). Through partitioning of energy substrates, energy expenditure, and heat dissipation, VMN neurons help to regulate energy homeostasis and metabolism (Fujikawa, Castorena et al. 2017). Furthermore, SF1 expressing cells within the VMN play a crucial role in coordinating metabolic responses to changes in energy status. SF1 is a transcription factor involved in the development and function of hypothalamic neurons and is essential for the regulation

of energy metabolism. SF1 expressing neurons in the VMN integrate hormonal and nutrient signals to modulate sympathetic outflow and metabolic rate, thereby influencing thermogenesis, energy expenditure, and glycemic control (Labbe, Caron et al. 2015, Caron and Richard 2017, Flak, Goforth et al. 2020, Khodai and Luckman 2021, Basu, Elmendorf et al. 2024). Additionally, a subset of SF1 neurons expressing PACAP projects to the POA where it acts on the PAC1R neurons through efferent communication to control body weight and iBAT thermogenesis (Liao, de Molliens et al. 2019, Bozadjieva-Kramer, Ross et al. 2021, Khodai and Luckman 2021).

Collectively, these functions driven by the VMN have the potential for wide - ranging effects on peripheral tissue function independently from food intake. This is particularly underscored through the connection with the VMN and exercise responses. SF-1 is required for the metabolic benefits from exercise. These benefits are driven through the induction of PGC1a in skeletal muscle and triggered by a combination of muscarinic and noradrenergic activation on the VMN. Evidence points to the role of sympathetic activation mediating these beneficial effects of exercise and the potential of harnessing the VMN for obesity treatments (Fujikawa, Castorena et al. 2016, Fujikawa, Castorena et al. 2017).

Activation of SF1 neurons, co-expressing ERα, in the VMN leads to the upregulation of key metabolic genes involved in fatty acid oxidation and thermogenesis, such as UCP1 and peroxisome proliferator-activated receptor-gamma coactivator 1α (PGC-1α). Estrogen-ERα signaling enhances sympathetic tone, promoting the release of norepinephrine, which stimulates iBAT thermogenesis and inhibits lipid storage in gonadal white adipose tissue (WAT) (Caron and Richard 2017, Contreras, Nogueiras et

al. 2017, van Veen, Kammel et al. 2020, Khodai and Luckman 2021, Torres Irizarry, Jiang et al. 2022). Furthermore, estrogen signaling in the VMN increases the expression of POMC neurons, which produce anorexigenic neuropeptides like α-melanocyte-stimulating hormone (α-MSH), leading to reduced food intake and increased energy expenditure. BDNF neurons in the VMN contribute to energy metabolism regulation through BDNF released by these neurons, which activates its receptor, TRKB, initiating signaling cascades that enhance neuronal survival and synaptic plasticity. TRKB activation leads to the phosphorylation of downstream targets such as phospholipase C-gamma (PLC-γ) and ERK, which modulate neuronal excitability and synaptic transmission. BDNF-TRKB signaling in the VMN enhances the activity of POMC neurons while inhibiting AgRP neurons, thereby promoting satiety and increasing energy expenditure (Contreras, Gonzalez et al. 2015, Contreras, Nogueiras et al. 2017).

LepR neurons in the VMN suppress appetite and increase energy expenditure via the action of leptin on SF1 neurons (Flak and Myers 2016, Contreras, Nogueiras et al. 2017, Hirschberg, Sarkar et al. 2020). Leptin, secreted by adipocytes in proportion to fat stores, acts on LepR expressed by neurons in the AHA to inhibit food intake and increase energy expenditure, promoting weight loss. Leptin binding to LepR activates signaling pathways such as Janus kinase 2 (JAK2)-signal transducer and activator of transcription 3 (STAT3) and AMP-activated protein kinase (AMPK), leading to changes in neuronal excitability and gene expression. Activation of LepR-positive neurons in the AHA increases sympathetic outflow to iBAT and skeletal muscle, promoting thermogenesis and fat oxidation (Contreras, Gonzalez et al. 2015, Contreras, Nogueiras et al. 2016, Torres Irizarry, Jiang et al. 2022).

In summary, the VMN plays a crucial role in integrating peripheral signals related to nutrient availability and energy status to regulate feeding behavior, energy expenditure, thermogenesis, and glycemic control. Through the concerted actions of all the above-mentioned neurons, the VMN fine-tunes metabolic responses to maintain energy homeostasis in the face of changing nutritional and metabolic demands (Fig. 1.5).

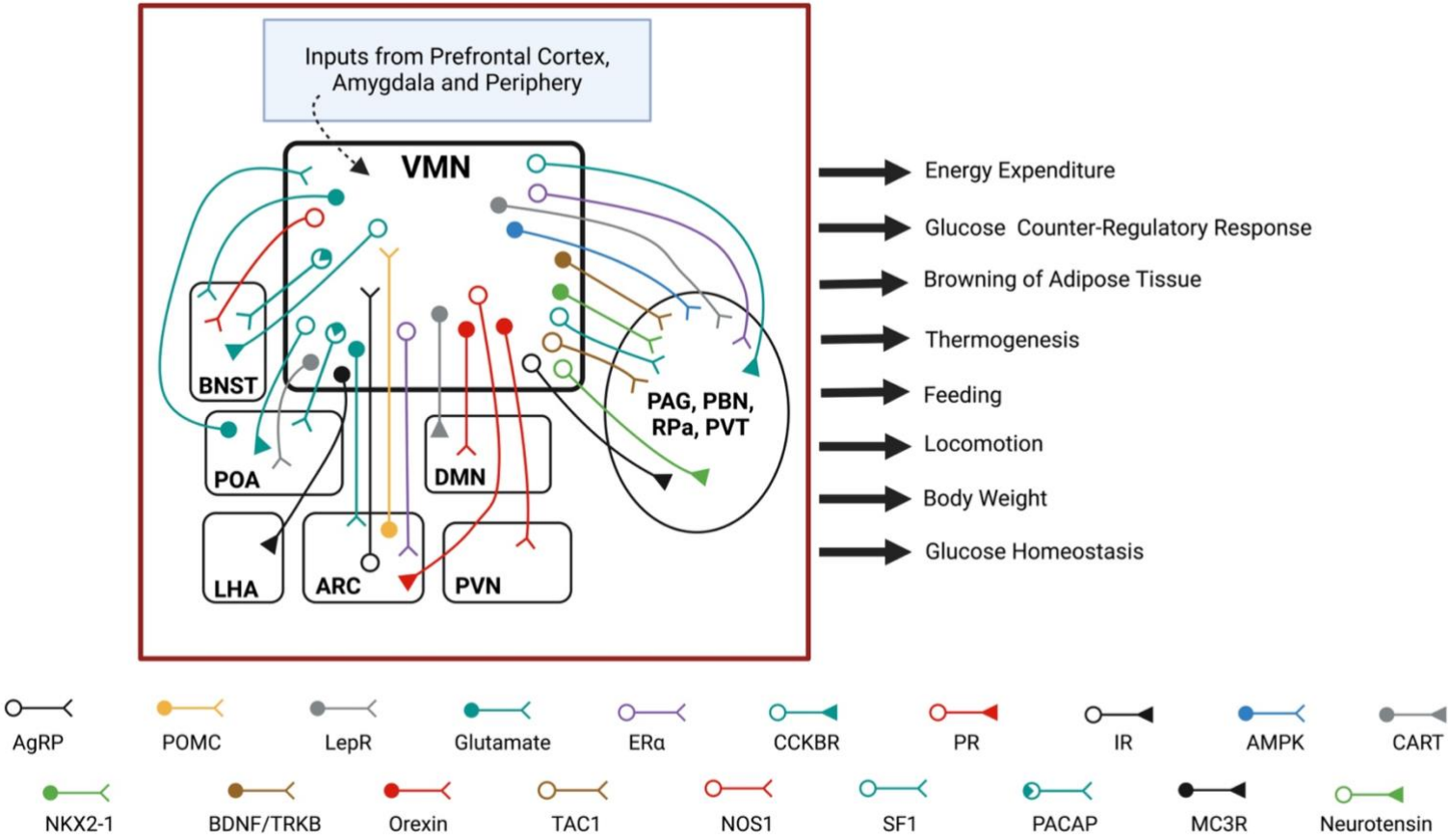
Inputs from Prefrontal Cortex, Amygdala and Periphery
VMN
BNST
POA
LHA
ARC
DMN
PVN
PAG, PBN, RPa, PVT
Energy Expenditure
Glucose Counter-Regulatory Response
Browning of Adipose Tissue
Thermogenesis
Feeding
Locomotion
Body Weight
Glucose Homeostasis
AgRP
POMC
LepR
Glutamate
ERα
CCKBR
PR
IR
AMPK
CART
NKX2-1
BDNF/TRKB
Orexin
TAC1
NOS1
SF1
PACAP
MC3R
Neurotensin

Figure 1.5: VMN neural circuits involved in direct and indirect mechanisms governing energy homeostasis. The VMN is known to be responsible for mediating a multitude of physiological functions the periphery. The VMN receives inputs from prefrontal cortex and amygdala of the brain as well as hormonal and nutritional cues from the periphery (denoted by black dotted arrow). The VMN contains neurons, primarily glutamatergic in nature, that project across the different parts of the VMN, interconnecting each region with the others. The VMN also contains several different types of neurons (indicated by combinations of different color and shapes of neurons, in the figure legend), which project to various outputs within the hypothalamus as well as different regions of the thalamus and hindbrain. VMN = Ventromedial hypothalamic nucleus. POA = Preoptic area. BNST = Bed nucleus of stria terminalis. LHA = Lateral hypothalamic area. ARC = Arcuate nucleus. DMN = Dorsomedial hypothalamic nucleus. PVN = Paraventricular hypothalamus. PAG = Periaqueductal gray. PBN = Parabrachial nucleus. RPa = Raphe pallidus. PVT = Paraventricular thalamus. AgRP = Agouti-related peptide. POMC = Proopiomelanocortin. LepR = Leptin receptor. ERa = Estrogen receptor type a. CCKBR = Cholecystokinin B receptor. PR = Progesterone receptor. IR = Insulin receptor. AMPK = 5' adenosine monophosphate-activated protein kinase. CART = Cocaine and amphetamine regulated transcript. NKX2-1 = Thyroid transcription factor 1 (TIF1). BDNF = Brain-derived neurotrophic factor. TRKB = Tropomyosin receptor kinase B. TAC1 = Tachykinin precursor 1. NOS1 = Nitric oxide synthase 1. SF1 = Steroidogenic factor 1. PACAP = Pituitary adenylate cyclase-activating polypeptide. MC3R = Melanocortin 3 receptor. The schematics were created using The Mouse Brain in Stereotaxic Coordinates Fourth Edition (Paxinos and Franklin) and Biorender.com.

Preoptic area

The preoptic area (POA) of the hypothalamus controls thermoregulation and energy expenditure, with distinct neuronal populations distributed across its subregions—such as the median preoptic nucleus (MnPO), ventromedial preoptic area (VMPO) and medial preoptic area (MPO) - each playing specialized roles. Across the POA, the leptin receptor (LepR) expressing neurons, which are sensitive to the adipose-derived hormone leptin are key regulators of energy balance, influencing metabolic processes. Activation of LepR neurons within the POA by leptin signals, which influences energy expenditure (Zhang, Kerman et al. 2011, Contreras, Gonzalez et al. 2015, Yang and Ruan 2015,

Torres Irizarry, Jiang et al. 2022). Furthermore, neurons expressing GABA (i.e. GABAergic neurons) and those that express glutamate (i.e. glutamatergic neurons) within the POA sense temperature changes and activate the ANS to coordinate thermoregulatory responses. GABAergic neurons inhibit local neuronal circuits to activate sympathetic outflow to peripheral tissues such as iBAT and skeletal muscle. Conversely, glutamatergic neurons facilitate excitatory neurotransmission and relay temperature signals to respond to environmental temperature changes. Moreover, these diverse neuronal populations form intricate neural networks that connect both temperature and energy expenditure to environmental cues and internal metabolic states.

Cold-sensing subsets of GABAergic and glutamatergic neurons in the MnPO/MPO detect decreases in temperature and initiate thermogenic responses to maintain body temperature, such as increasing sympathetic outflow to iBAT and skeletal muscle to generate heat. Conversely, warm-sensing subsets of GABAergic and glutamatergic neurons in the MnPO/MPO respond to increases in temperature by promoting heat dissipation mechanisms (Labbe, Caron et al. 2015, Yang, Xie et al. 2023). Neurons expressing bombesin-like receptor 3 (BRS3) in the MnPO/VMPO, act as cold sensors, triggering thermogenic responses and playing a part in fever and torpor induction by modulating sympathetic outflow to iBAT and skeletal muscle. Conversely, warm-sensitive neurons in the VMPO, expressing brain-derived neurotrophic factor (BDNF) and PACAP, respond to heat by activating cooling mechanisms such as vasodilation and sweating (Tan, Cooke et al. 2016, Tan and Knight 2018). During febrile responses, the cold-sensing neurons in VMPO/MnPO may contribute to the initiation of fever by signaling to higher brain centers, such as the hypothalamus, to raise the body's set point

temperature. This process involves the release of prostaglandins and other inflammatory mediators, which act on subsets of cold-sensing and warm-sensing POA neurons to elevate body temperature through mechanisms such as increased metabolic rate and shivering. In conditions of torpor, where animals enter a state of reduced metabolic activity and decreased body temperature to conserve energy, these neurons likely play a role in coordinating the transition to and from torpor states (Cerri 2017, Machado, Bandaru et al. 2020, Zhang, Reis et al. 2020, Nakamura, Yahiro et al. 2022, Saper and Machado 2022, Machado, Raffin et al. 2023). Cold-sensing neurons may help initiate torpor by reducing sympathetic outflow and metabolic rate, while warm-sensing neurons may facilitate arousal from torpor by promoting thermogenesis and increasing metabolic activity. Moreover, in response to ambient temperature change, BRS3 neurons in the POA act via their projection to PVN, DMN and brainstem to induce febrile response or torpor and regulate heart rate and locomotor activity (Pinol, Mogul et al. 2021, Pinol and Reitman 2022).

Also, the POA receives projections from the VMN^{PACAP} neurons, where the neuropeptide PACAP exerts pleiotropic functions, including roles in neurotransmission, neuroprotection, and endocrine regulation. PACAP acts via their primary receptor, PACAP receptor 1 (PAC1R), expressed within the POA neurons, to regulate glucose metabolism and adipose tissue thermogenesis. As a signal within the VMN, PACAP signaling can activate feeding behavior, energy expenditure, and thermogenesis. In addition to receiving PACAP signals, PACAP-containing POA cells sense warm temperature and engage systems to lower core body temperature in mice. This highlights the complexity of the function of neuropeptides within specialized circuits. In addition to

temperature signals, this area also senses other types of signals that directly impact TDEE (Liao, de Molliens et al. 2019, Basu, Elmendorf et al. 2024).

Additionally, other subtypes of neurons within the POA, such as those expressing neuropeptides like thyrotropin-releasing hormone (TRH) and neuropeptide Y (NPY), further activate energy expenditure and temperature responses. TRH neurons within the POA release thyroid-stimulating hormone (TSH) from the anterior pituitary, increasing thyroid hormone secretion and subsequent activation of metabolic rate and energy expenditure (Munzberg, Qualls-Creekmore et al. 2016 Morrison, & Yu, 2016 49). NPY-expressing neurons stimulate sympathetic outflow and iBAT activity, promoting heat generation and energy expenditure during cold exposure. Thus, the POA serves as a crucial hub for both thermoregulation and energy expenditure, with distinct subsets of neurons playing specialized roles in these processes. The integration of signals from leptin, GABAergic, glutamatergic, TRH, NPY, and other neuronal populations within the POA enables precise adjustment of body temperature and metabolic rate in response to environmental challenges, ensuring the maintenance of thermal and energy homeostasis. Dysfunction of these neuronal circuits in the POA disrupts energy expenditure and thermoregulation, contributing to metabolic disorders such as obesity and metabolic syndrome.

Overall, the diverse populations of GABAergic and glutamatergic neurons within the POA contribute to the finely tuned regulation of thermoregulation and energy metabolism, allowing organisms to adapt to changing environmental conditions while maintaining physiological homeostasis (Fig. 1.6).

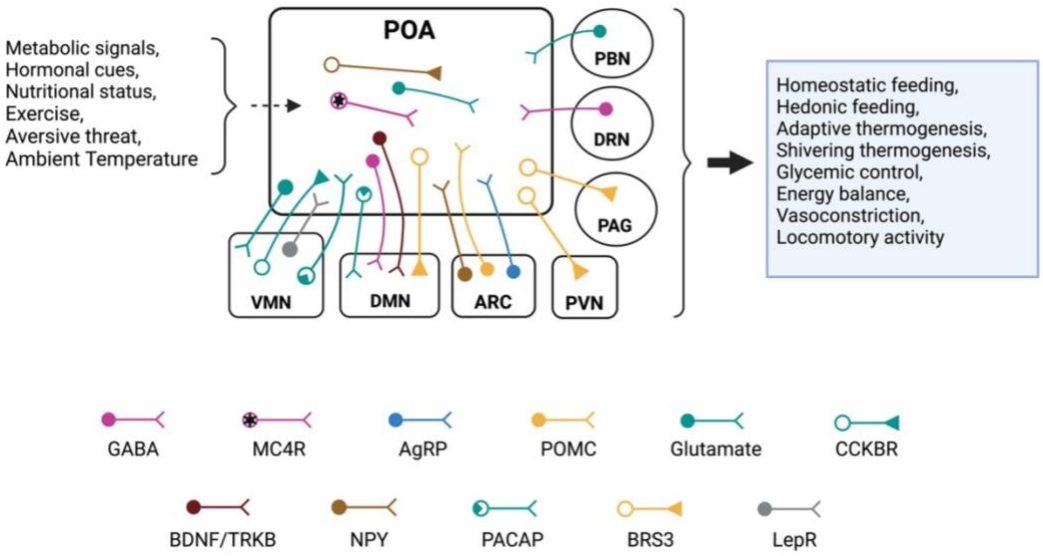

Figure 1.6: POA neural circuits involved in direct and indirect mechanisms governing energy homeostasis. The POA is known to be responsible for mediating a multitude of physiological functions the periphery. The POA receives inputs from the other hypothalamic nuclei of the brain as well as other regions of the midbrain and hindbrain, and it intergrates environmental, hormonal and nutritional cues from the periphery (denoted by black dotted arrow). The POA contains neurons that project across the different parts of the VMN, interconnecting each region with the others. The VMN also contains several different types of neurons (indicated by combinations of different color and shapes of neurons, in the figure legend), which project to various outputs within the hypothalamus as well as different regions of the midbrain and hindbrain. VMN = Ventromedial hypothalamic nucleus. POA = Preoptic area. ARC = Arcuate nucleus. DMN = Dorsomedial hypothalamic nucleus. PVN = Paraventricular hypothalamus. PAG = Periaqueductal gray. PBN = Parabrachial nucleus. PAG = Periaqueductal gray. DRN = Dorsal Raphe Nucleus. AgRP = Agouti-related peptide. POMC = Proopiomelanocortin. LepR = Leptin receptor. CCKBR = Cholecystokinin B receptor. BDNF = Brain-derived neurotrophic factor. TRKB = Tropomyosin receptor kinase B. MC4R = Melanocortin 4 receptor. GABA = Gamma amino butyric acid. BRS3 = Bombesin receptor subtype 3. The schematics were created using The Mouse Brain in Stereotaxic Coordinates Fourth Edition (Paxinos and Franklin) and Biorender.com.

Bed nucleus of the stria terminalis

The BNST integrates signals from higher order brain areas, such as the amygdala and prefrontal cortex. As such, the BNST is not only implicated in stress responses but also other emotional states and metabolic signals as well. Neurons within the BNST exert profound effects on thermogenesis, energy expenditure, and metabolic regulation in concert with other hypothalamic nuclei. Within the BNST, diverse populations of neurons, including glutamatergic, GABAergic, and peptidergic neurons, activate sympathetic outflow and hormonal stress responses.

Glutamatergic neurons within the BNST transmit stress signals to hypothalamic and brainstem systems that maintain energy balance and thermogenesis. GABAergic neurons, on the other hand, primarily act locally for similar overall functions (Crestani, Alves et al. 2013). Additionally, neuropeptides such as corticotropin-releasing hormone (CRH), expressed by neurons within the BNST, share the same functions but play roles in both local as well as distal neural circuit control. CRH signaling within the BNST stimulates the hypothalamic-pituitary-adrenal (HPA) axis, leading to the release of glucocorticoids that activate energy metabolism, gluconeogenesis, and glycemic control. Furthermore, CRH neurons in the BNST project to hypothalamic nuclei, including the PVN and the DMN, to induces sympathetic and hormonal responses to stress (Schneeberger, Parolari et al. 2019, Maita, Bazer et al. 2021, Young and Tong 2021). The BNST has additional functions, not necessarily directly due to emotional responses that are instead maintain energy balance and metabolic homeostasis, which include efferent connections with the hypothalamus and amygdala. To underscore this function, decreased BNST function is associated with obesity, insulin resistance, and dysglycemia.

In summary, the BNST serves as a crucial nexus for the integration of stress, emotional, and metabolic signals, exerting profound effects on thermogenesis, energy expenditure, and metabolic regulation. Through its modulation of sympathetic outflow and interactions with other hypothalamic nuclei, the BNST plays a central role in coordinating adaptive responses to stressors and maintaining metabolic homeostasis.

Other hypothalamic nuclei involved in energy homeostasis

In addition to the above hypothalamic nuclei, many other hypothalamic regions contribute to mediate energy expenditure either via independent mechanisms or via interaction between the different nuclei across the hypothalamus. Each of these hypothalamic regions utilizes distinct neuronal populations and signaling mechanisms to orchestrate a comprehensive response to internal and external cues, ensuring optimal energy utilization and metabolic equilibrium.

DMN (Dorsomedial Hypothalamic Nucleus): The DMN is integral to coordinating physiological processes that control energy homeostasis, thermoregulation, and behavioral responses to stress and arousal. Neurons in the DMN, including those expressing glutamatergic, GABAergic, and dopaminergic neurotransmitters, interact complexly to influence sympathetic outflow to iBAT, thereby regulating thermogenesis and body temperature. DMN neurons also integrate hormonal signals from leptin and insulin to modulate energy expenditure and food intake, responding adaptively during states of energy deficit or surplus. Recent studies highlight the DMN's role in synchronizing circadian rhythms of feeding and activity, emphasizing its connection to

the light cycle and sleep patterns, which in turn affects metabolic rate and overall energy balance (Morrison et al., 2014; Nakamura & Morrison, 2022).

ARC (Arcuate Nucleus): The ARC serves as a critical neural hub for the regulation of appetite and body weight. It houses two important populations of neurons: anorexigenic pro-opiomelanocortin (POMC) neurons and orexigenic agouti-related peptide (AgRP) neurons. These neurons are highly responsive to peripheral metabolic cues such as hormones leptin and ghrelin, which inform the brain about the body's energy status. POMC neurons stimulate the release of alpha-melanocyte-stimulating hormone (α-MSH), which promotes satiety, while AgRP neurons release neurotransmitters that encourage food intake and reduce metabolic rate. The ARC also communicates with other hypothalamic and brainstem regions to coordinate complex behaviors related to hunger, satiety, and reward (Li et al., 2019; Contreras et al., 2017).

LHA (Lateral Hypothalamic Area): The LHA is known as the feeding center, playing a pivotal role in regulating hunger and satiety. It contains diverse neuron types, including those producing orexin/hypocretin and melanin-concentrating hormone (MCH), both of which significantly influence energy balance, wakefulness, and reward systems. Orexin neurons are particularly important for initiating feeding and increasing arousal, while MCH neurons tend to promote feeding and reduce metabolic rate. The LHA interacts with various other brain regions to modulate not only metabolic processes but also emotional and cognitive aspects of eating, such as food reward and pleasure (Rossi, 2023; Berthoud & Munzberg, 2011).

PVN (Paraventricular Nucleus): The PVN orchestrates a variety of neuroendocrine, autonomic, and behavioral responses critical for energy balance and

stress adaptation. It releases neuropeptides such as corticotropin-releasing hormone (CRH), oxytocin, and vasopressin, which regulate stress responses, blood pressure, and renal function, in addition to energy homeostasis. The PVN regulates the autonomic nervous system, controlling the release of thyroid hormones and adrenal corticoids through interactions with the pituitary gland. Neurons in the PVN also receive significant input from the ARC and other hypothalamic nuclei to ensure appropriate responses to changes in energy availability, influencing processes like appetite, thermogenesis, and glucose metabolism. These connections make the PVN a crucial mediator in the interactions between energy homeostasis and stress responses (Sutton et al., 2016; Labbe et al., 2015).

SCN (Suprachiasmatic Nucleus): The SCN acts as the master circadian regulator, aligning physiological processes including metabolism with environmental light cycles. It influences energy metabolism and thermogenesis through neural pathways controlling sympathetic activity, and its regulation of hormonal rhythms like leptin and ghrelin orchestrates feeding behaviors in sync with circadian cycles (Faber et al., 2021).

AHA (Anterior Hypothalamic Area): The AHA maintains thermal homeostasis by responding to temperature changes through transient receptor potential (TRP) channel-expressing neurons. These neurons activate thermogenic processes in iBAT during cold exposure and coordinate heat dissipation responses during warmth, playing a key role in energy expenditure and temperature regulation (Kozyreva et al., 2019; Schneeberger et al., 2022).

The regulation of energy homeostasis, essential for survival, relies on complex neural circuits responsive to nutrient and hormonal signals, with the hypothalamus at its

core (Fig. 1.7). All the above-mentioned hypothalamic nuclei are highly plastic, adapting rapidly to changes in the environment to maintain energy balance and play specialized roles in energy regulation, as summarized below in Table. 1, by integrating sensory information, physiological cues, and humoral factors, coordinating food intake and energy expenditure through extensive communication with peripheral organs such as the gastrointestinal tract, liver, pancreas, and adipose tissues (Fig. 1.7).

Table 1: Hypothalamic nuclei and their role in the control of energy balance

Function		AH	POA	BNST	SCN	PVN	VMN	DMN	ARC	LHA
Thermogenesis	Sympathetic nerve activity mediated	√	√	√		√	√	√	√	√
	iBAT differentiation						√			
	Tissue thermogenesis	√	√			√	√	√	√	√
	TRH mediated		√							
	Cold exposure mediated	√	√							
	Torpor		√					√		
	Febrile responses		√					√		
Locomotory Activity			√				√			√
Regulation of feeding	Orexigenic control						√	√	√	√
	Anorexigenic control	√				√	√	√	√	√
	Leptin sensitivity	√	√			√	√	√	√	
	Hedonic feeding									√
Regulation of drinking						√				√
Glucose Homeostasis	Glucose sensing			√		√	√	√	√	√
	Insulin sensitivity			√		√	√	√		
Lipid Metabolism	Lipolysis and β-oxidation					√	√		√	
	ER stress mediated lipotoxicity						√			
Stress response	HPA axis regulation			√		√				
ERα mediated sexual dimorphism							√			
Circadian rhythm					√			√		√
AVP mediated fluid balance	Osmoregulation				√	√				
	Dehydration induced anorexia	√								√
Cardiovascular regulation	Blood pressure control			√				√		
	Heart rate control			√				√		
Sleep-Wakefulness cycle							√			√

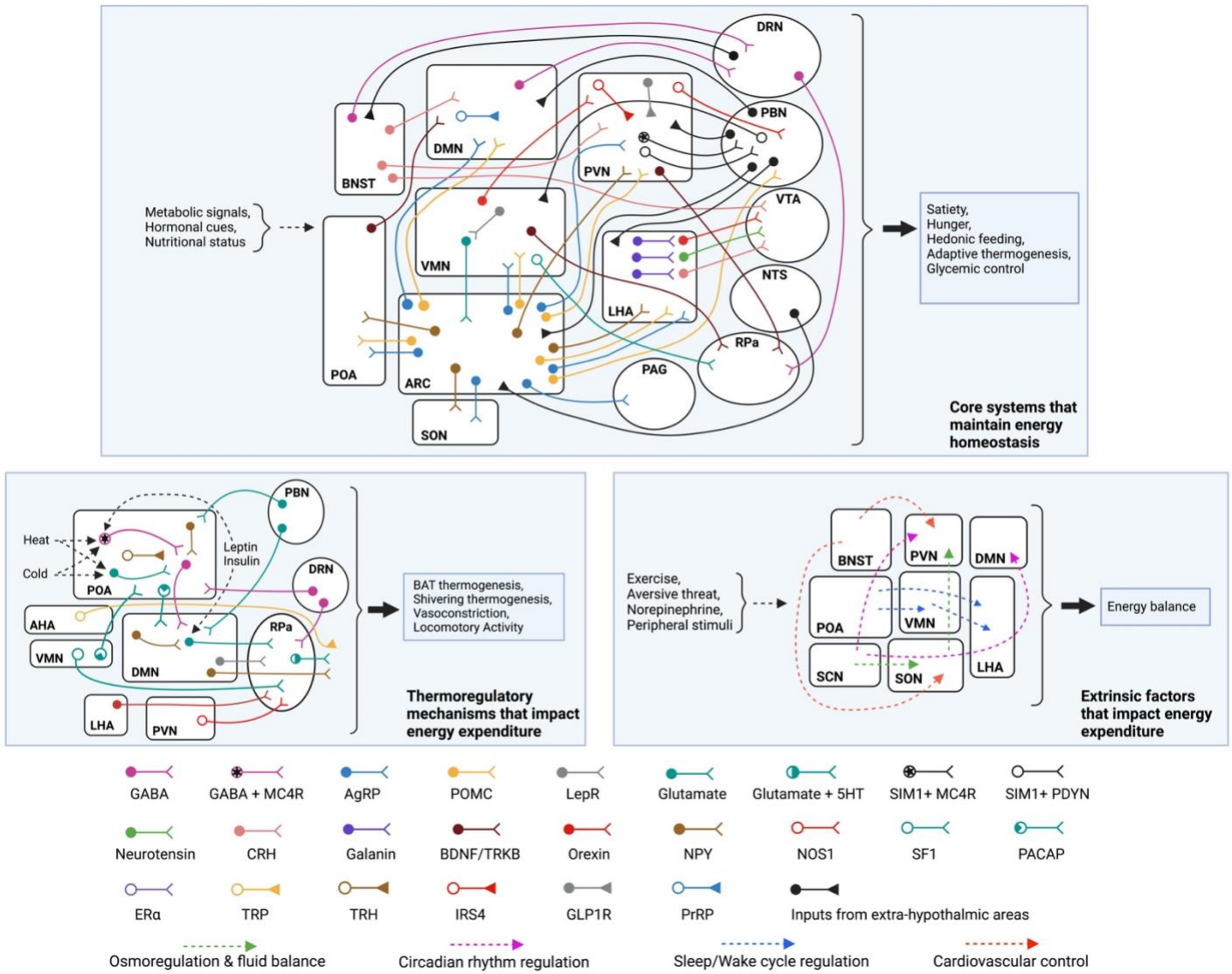
Metabolic signals,
Hormonal cues,
Nutritional status
BNST
DMN
PVN
DRN
PBN
VTA
NTS
VMN
LHA
RPa
PAG
POA
ARC
SON
Satiety,
Hunger,
Hedonic feeding,
Adaptive thermogenesis,
Glycemic control
Core systems that maintain energy homeostasis
Heat
Cold
POA
Leptin
Insulin
PBN
DRN
AHA
VMN
DMN
RPa
LHA
PVN
BAT thermogenesis,
Shivering thermogenesis,
Vasoconstriction,
Locomotory Activity
Thermoregulatory mechanisms that impact energy expenditure
Exercise,
Aversive threat,
Norepinephrine,
Peripheral stimuli
BNST
PVN
DMN
POA
VMN
SCN
SON
LHA
Energy balance
Extrinsic factors that impact energy expenditure
GABA
GABA + MC4R
AgRP
POMC
LepR
Glutamate
Glutamate + 5HT
SIM1+ MC4R
SIM1+ PDYN
Neurotensin
CRH
Galanin
BDNF/TRKB
Orexin
NPY
NOS1
SF1
PACAP
ERα
TRP
TRH
IRS4
GLP1R
PrRP
Inputs from extra-hypothalmic areas
Osmoregulation & fluid balance
Circadian rhythm regulation
Sleep/Wake cycle regulation
Cardiovascular control

Figure 1.7: Summary of the major hypothalamic pathways regulating energy balance. The different hypothalamic nuclei receive a multitude of environmental and metabolic signals from the periphery and each hypothalamic nucleus interact with the other hypothalamic nuclei and with the extra-hypothalamic areas (brain nuclei outside the hypothalamus like regions in the prefrontal cortex, amygdala, thalamus, hindbrain etc.) via several different types of neurons (indicated by combinations of different color and shapes of neurons, in the figure legend). Together these areas integrate all the peripheral signals and in turn modulate the metabolic and energy status of the body. VMN = Ventromedial hypothalamic nucleus. POA = Preoptic area. BNST = Bed nucleus of stria terminalis. LHA = Lateral hypothalamic area. ARC = Arcuate nucleus. DMN = Dorsomedial hypothalamic nucleus. PVN = Paraventricular hypothalamus. SCN = Suprachiasmatic nucleus. AHA = Anterior hypothalamic area. SON = Supraoptic nucleus. PAG = Periaqueductal gray. PBN = Parabrachial nucleus. RPa = Raphe pallidus. PVT = Paraventricular thalamus. GABA = Gamma aminobutyric acid. MC4R = Melanocortin 4 receptor. AgRP = Agouti-related peptide. POMC = Proopiomelanocortin. LepR = Leptin receptor. 5HT = 5-hydroxytryptamine (serotonin). SIM1 = Single minded 1. PDYN = Prodynorphin. CRH = Corticotropin releasing hormone. NPY = Neuropeptide Y. TRP = Transient receptor potential. TRH = Thyrotropin-releasing hormone. IRS4 = Insulin receptor substrate 4. GLP1R = Glucagon-like peptide-1 receptor. PrRp = Prolactin-releasing peptide. ERa = Estrogen receptor type a. BDNF = Brain-derived neurotrophic factor. TRKB = Tropomyosin receptor kinase B. NOS1 = Nitric oxide synthase 1. SF1 = Steroidogenic factor 1. PACAP = Pituitary adenylate cyclase-activating polypeptide. The schematics were created using The Mouse Brain in Stereotaxic Coordinates Fourth Edition (Paxinos and Franklin) and Biorender.com.

Hypothalamic dysfunction in energy imbalance and obesity

The hypothalamus is the master regulator of energy balance and thermoregulation. It functions as the central integrator of sensory inputs and motor outputs, thus enabling feedback regulation of specific metabolic functions. The hypothalamus has evolved to navigate periods of scarcity and abundance, with genetic factors influencing an organism's ability to efficiently store and utilize energy resources. The 'thrifty genotype' hypothesis suggests that alleles conducive to energy storage were selected for during human evolution, providing a survival advantage in energy-scarce environments (Neel 1962). However, in the context of modern environments with excess caloric availability, these genetic predispositions contribute to the rising challenges of

obesity and metabolic diseases. Dysfunction in the mechanisms governed by the hypothalamus, results in impaired energy metabolism that leads to obesity (Labbe, Caron et al. 2015). For instance, while impaired leptin signaling in the ARC, due to genetic mutations or leptin resistance, has been thought to result in uncontrolled appetite and weight gain (Myers, Leibel et al. 2010), recent research suggests that obesity might be more closely linked to dysfunction in the neural circuits rather than reduced leptin signaling per se. This is evidenced by studies showing that despite high leptin levels, the signaling pathways remain unresponsive, indicating a circuit-level dysfunction (Ottaway, Mahbod et al. 2015, Friedman 2016). Leptin, a hormone produced by adipocytes, normally acts on the hypothalamus to inhibit food intake and increase energy expenditure. In leptin resistance, despite elevated leptin levels, the hypothalamic neurons fail to respond adequately, leading to continued hunger and reduced energy expenditure. When leptin receptors in the hypothalamic neurons become insensitive to leptin, it disrupts the normal regulatory mechanisms, leading to hyperphagia and decreased thermogenesis. This dysfunction is often associated with the inflammation of hypothalamic tissues, particularly in obesity induced by high-fat diets, which exacerbates leptin resistance. Leptin resistance is also marked by impaired intracellular signaling pathways, such as the JAK2-STAT3 pathway, critical for leptin's regulatory effects on food intake and energy balance.

Disruptions in melanocortin signaling within the PVN also contributes to obesity (Krude, Biebermann et al. 1998). Imbalances in AgRP and POMC signaling in the ARC contribute to hyperphagia and metabolic dysfunction (Andermann and Lowell 2017). AgRP neurons, which are normally inhibited by leptin, become overactive in leptin-

resistant states, leading to increased appetite and reduced energy expenditure. Similarly, POMC neurons, which are stimulated by leptin to release anorexigenic peptides, fail to respond adequately, resulting in impaired satiety signals (Schwartz, Woods et al. 2000). Studies have shown that mice with targeted deletions of the LepR gene in hypothalamic neurons exhibit obesity due to increased food intake and decreased energy expenditure (Munzberg, Flier et al. 2004). This genetic model highlights the critical role of leptin signaling in the ARC in maintaining energy balance. Additionally, the VMN is crucial for sensing and responding to glucose levels, and its dysfunction is associated with metabolic disturbances and obesity (King 1991). Leptin resistance in the VMN disrupts glucose homeostasis and impairs energy regulation, further contributing to the obesity phenotype.

Additionally, inflammation in both the hypothalamus and peripheral tissues contributes to obesity, but hypothalamic inflammation is a primary driver. Chronic inflammation in the hypothalamus impairs neuronal function and disrupts regulatory pathways of energy balance (Thaler, Yi et al. 2012). Research indicates that hypothalamic inflammation is associated with damage and maladaptive responses, contributing to the pathogenesis of obesity (De Souza, Araujo et al. 2005, Wisse and Schwartz 2009). Factors such as high-fat diets can induce hypothalamic inflammation, leading to obesity (Cai and Liu 2011). Inflammatory signals in the hypothalamus disrupt the normal regulation of appetite and energy expenditure, exacerbating weight gain and metabolic dysfunction. Understanding these mechanisms is crucial for developing targeted interventions to address obesity and its related metabolic disorders.

Moreover, as mentioned before, variations in genes related to energy metabolism also influences metabolic rate by modulating thermoregulation and contributes to obesity.

Enhanced UCP1 function, at iBAT, due to certain genetic variants increase energy dissipation as heat, elevating RMR and protecting against weight gain through a combination of thyroid hormone signaling, thermogenesis, and sympathetic nervous system activity. For example, variants in the promoter region of the UCP1 gene, such as the -3826A/G polymorphism, have been associated with increased basal expression of UCP1. Individuals with the -3826G allele exhibit higher UCP1 mRNA levels, which enhances thermogenic capacity and energy expenditure (Esterbauer, Oberkofler et al. 1998, Dinas, Nintou et al. 2022).

Also, the Trp64Arg polymorphism in the beta-adrenergic receptors (e.g., ADRB3) gene is associated with reduced receptor function, leading to decreased iBAT activation and lower thermogenesis (Widen, Lehto et al. 1995, Gagnon, Mauriege et al. 1996). Conversely, other variants may enhance receptor sensitivity, promoting UCP1-mediated thermogenesis. Genetic variations in thyroid hormone receptors (e.g., TRH and TRβ) can affect how these hormones influence UCP1 activity. Enhanced thyroid hormone signaling due to specific receptor polymorphisms upregulate UCP1 expression and increase thermogenesis (Iglesias and Diez 2007, Boelen, Wiersinga et al. 2008). Also, PGC-1α is a transcriptional coactivator that regulates genes involved in energy metabolism, including UCP1.

Variants in the PGC-1α gene increases UCP1 expression and iBAT activity, enhancing thermogenesis (Puigserver and Spiegelman 2003, Handschin and Spiegelman 2006). Moreover, the PRDM16 (*PR domain containing 16)* and CIDEA (cell death-inducing DNA fragmentation factor alpha-like effector A) genes are involved in the differentiation and function of brown adipocytes. Certain genetic variants promote the

browning of white adipose tissue, increasing the number of mitochondria and UCP1 in the cells and thus enhancing thermogenic capacity (Seale, Bjork et al. 2008, Wu, Zhou et al. 2014). The combined effect of these genetic variants impacts an individual's ability to dissipate energy as heat through UCP1 function. Thermogenic efficiency directly impacts RMR to protect against weight gain and obesity, even in the presence of high caloric intake. Moreover, individual genetic and environmental diversity underlies differences in energy metabolism and body composition that contributes to the susceptibility to metabolic disorders.

In conclusion, the hypothalamic regulation of energy balance is intricate and essential for maintaining metabolic homeostasis. Genetic variations that enhance iBAT thermogenesis and the thrifty genotype hypothesis illustrate how evolutionary adaptations now contribute to obesity in calorie-rich environments. Thus, addressing hypothalamic dysfunction and understanding mechanisms within the hypothalamus to enhance energy expenditure are crucial for developing targeted therapies to combat obesity and related metabolic disorders.

Extra-hypothalamic areas interacting with the hypothalamic nuclei to control energy homeostasis

Extra-hypothalamic areas such as the raphe pallidus (RPa), parabrachial nucleus (PBN), periaqueductal gray (PAG), dorsal raphe nucleus (DRN), nucleus tractus solitarius (NTS), and paraventricular thalamus (PVT) that receive inputs from the hypothalamic nuclei such as the VMH, the ARC, the LH, the DMH and the PVH, are integral components of the neural circuitry regulating energy balance. These regions

serve as relay stations and modulators, receiving inputs from hypothalamic nuclei involved in energy homeostasis and transmitting hypothalamic signals to the periphery via various sensory and hormonal signals related to energy status.

For instance, the RPa, for example, orchestrates thermoregulation and energy metabolism by integrating hypothalamic signals with serotonergic modulation. The PBN receives projections from hypothalamic areas and transmits various gustatory and visceral signals to the periphery, thus, contributing to the regulation of feeding behavior and energy expenditure (Dodd, Worth et al., 2014). The PAG, known for its role in pain modulation and stress responses, also interacts with hypothalamic nuclei to influence energy balance in response to acute stressors (Schneeberger, Brice et al., 2019). The DRN, a serotonergic nucleus, receives projections from the hypothalamus and in response relays inputs related to mood and emotional states, and contributes to the integration of emotional cues into energy regulation. The NTS serves as a primary site for visceral sensory integration and communicates with hypothalamic nuclei to regulate energy intake and expenditure in response to changes in nutrient availability. Lastly, the PVT, an important relay between the limbic system and hypothalamus, integrates motivational and reward-related signals with metabolic cues to modulate feeding behavior and energy expenditure. Collectively, these extra-hypothalamic areas form a complex network that integrates diverse inputs from the hypothalamic nuclei and transmits signals that modulate the physiology at the periphery to maintain energy balance in response to internal and external cues (Adjeitey, Mailloux et al. 2013, Munzberg, Qualls-Creekmore et al. 2016, Basu and Flak 2024).

RPa (Raphe Pallidus): The RPa integrates signals from various hypothalamic nuclei like the POA, VMN, DMN, PVN, and LHA, coordinating thermoregulation and energy metabolism. It modulates sympathetic outflow to iBAT and skeletal muscle, affecting thermogenesis and energy expenditure. Serotonergic neurons in the RPa influence body temperature and metabolic rate by regulating iBAT thermogenesis during cold exposure. These neurons also play a key role in glycemic control by influencing hepatic glucose production and insulin secretion.

PBN (Parabrachial Nucleus): Situated in the rostral hindbrain, the PBN acts as a critical relay center, integrating signals from hypothalamic areas like the ARC, VMN, LHA, and PVN with sensory inputs from the gastrointestinal tract. This integration allows the PBN to modulate feeding behavior and metabolic responses effectively. The PBN also plays a role in coordinating thermoregulatory responses through inputs from thermosensitive hypothalamic neurons, adapting energy expenditure and food intake based on energy status and hormonal cues.

PAG (Periaqueductal Gray): The PAG, central to pain modulation and stress responses, also interacts with hypothalamic nuclei to influence energy balance under stress. It receives inputs concerning energy status, nutrient availability, and thermoregulatory cues from the hypothalamus, which enable the PAG to coordinate adaptive autonomic and behavioral responses. Activation of PAG neurons can induce thermogenic responses and modulate behavioral responses to environmental stressors that affect energy expenditure.

DRN (Dorsal Raphe Nucleus): The DRN integrates hormonal and neural signals from hypothalamic regions to modulate mood, satiety, and thermogenesis. It regulates

serotonin release, which affects mood and energy balance, influencing feeding behavior and metabolic rate. The DRN also interacts with the hypothalamus to modulate responses to stress, which can impact energy metabolism and behavioral responses related to feeding and energy expenditure.

NTS (Nucleus Tractus Solitarius): The NTS, a primary visceral sensory integration site, receives inputs from the gastrointestinal tract and hypothalamic nuclei, allowing it to adjust feeding behavior and energy expenditure in response to nutrient signals and energy status. It modulates sympathetic nervous system activity, influencing thermogenesis and metabolic rate. The NTS also integrates cardiovascular and respiratory signals, playing a broader role in physiological homeostasis.

PVT (Paraventricular Thalamus): The PVT integrates motivational and reward-related signals with metabolic cues from the hypothalamus to modulate feeding behavior and energy expenditure. It acts as a relay between limbic structures and hypothalamic nuclei, influencing responses to environmental cues that affect energy balance. The PVT's role in regulating stress responses and emotional behavior also impacts metabolic processes, linking emotional states with feeding behavior and energy expenditure.

These extra-hypothalamic areas, through their extensive interactions with the hypothalamus, form a complex network that regulates energy homeostasis by integrating diverse physiological signals and coordinating adaptive responses to internal and external changes.

Key metabolic mechanisms regulating energy homeostasis

The hypothalamus serves as a critical hub for integrating signals that regulate energy balance, interfacing extensively with peripheral and central inputs. This central mechanism involves the key nuclei which process signals from hormones like leptin, ghrelin, and insulin and from sensory inputs related to temperature, stress, and emotions. These nuclei orchestrate responses that regulate feeding, energy expenditure, thermogenesis, and glycemic control. The comprehensive network formed by the interactions between the hypothalamic and extra-hypothalamic nuclei ensures nuanced regulation of metabolism, responding adaptively to a variety of physiological and environmental changes. This system's complexity is further enriched by the integration of signals related to peripheral inflammation, the gut microbiome, and immune system interactions, which influence hypothalamic function and overall metabolic regulation (Fig. 1.8). Disruptions in these pathways, such as from chronic inflammation or stress, can lead to metabolic dysfunctions, emphasizing the critical role of the hypothalamus and its associated networks in maintaining energy homeostasis and metabolic health.

Adipose tissue negative feedback

More than 60 years ago, Kennedy proposed that energy homeostasis is maintained through signals proportional to body fat mass that inform the brain of current energy stores via a negative feedback loop (Kennedy, 1953). Insulin and leptin are key hormones in this feedback loop, circulating in proportion to body fat. During negative energy balance, such as fasting or weight loss, their levels decrease (Bagdade, Bierman, and Porte, 1967; Considine et al., 1996). These hormones enter the CNS in proportion to their

plasma levels and act on receptors in the hypothalamus, a critical area for energy regulation (Baura et al., 1993; Schwartz et al., 1996; Baskin, Breininger, and Schwartz, 1999).

Leptin and insulin reduce food intake and increase energy expenditure, including thermogenesis, by activating the sympathetic nervous system (SNS) to iBAT (Campfield et al., 1995; Zhang Y et al., 1994). iBAT generates heat through uncoupling protein 1 (UCP1), contributing to overall energy expenditure. In leptin deficiency, as seen in ob/ob mice and certain humans, hyperphagia and reduced energy expenditure lead to obesity, which can be reversed by leptin administration (Montague et al., 1997; Farooqi et al., 2007).

However, most obesity cases involve leptin resistance, where high leptin levels fail to suppress appetite or increase thermogenesis due to impaired leptin transport across the blood-brain barrier (BBB) or hypothalamic inflammation (Myers et al., 2010; Thaler and Schwartz, 2010; Thaler et al., 2012). Insulin also influences energy balance and thermogenesis via its central actions, enhancing SNS outflow to iBAT (Woods et al., 1979).

Hunger and satiety perception

The hypothalamus processes peripheral signals of hunger and satiety, including ghrelin, which stimulates appetite, and satiety peptides like peptide YY (PYY), glucagon-like peptide 1 (GLP1), and cholecystokinin (CCK). These peptides are secreted by gastrointestinal cells in response to ingested nutrients: CCK from the proximal gut and GLP1 and PYY from the distal intestine. These satiety peptides reduce food intake by

promoting meal termination. In contrast, ghrelin, secreted from stomach cells, increases food intake and fat mass, particularly before meals when levels rise sharply. Both types of signals activate the vagus nerve, which transmits information about ingested nutrients to the brain's nucleus of the solitary tract (NTS). However, the effects of satiety peptides are short-lived, often leading to increased meal frequency despite reduced meal size, limiting their therapeutic potential for weight loss.

Adiposity signals like leptin and insulin further modulate these satiety signals. Leptin enhances the satiety response to peptides like CCK, reducing meal size. During conditions of low leptin, such as prolonged fasting or weight loss, sensitivity to satiety signals decreases, leading to larger meals and increased energy intake. Elevated ghrelin levels during weight loss, coupled with reduced leptin and insulin, drive weight regain.

Reward driven mechanisms

Energy homeostasis is also influenced by hedonic and reward mechanisms involving the hypothalamus and its connections with the limbic system, particularly the nucleus accumbens and the ventral tegmental area. These areas regulate the rewarding aspects of food intake, driven by dopamine signaling. Obesity treatments targeting these pathways aim to modulate the reward system to reduce overeating and food addiction, addressing the emotional and pleasure-driven components of eating behavior.

Allostasis

Allostasis refers to the process by which the body achieves stability through change, adapting to stressors and maintaining homeostasis. The hypothalamus plays a

central role in allostatic regulation by coordinating responses to various stressors, including changes in energy availability, environmental conditions, and psychological stress. By modulating hormonal, neural, and behavioral responses, the hypothalamus ensures that energy balance is maintained under varying conditions. Chronic stress and allostatic overload can disrupt hypothalamic function, leading to metabolic imbalances and obesity. Understanding and targeting allostatic mechanisms in the hypothalamus can help develop strategies to improve resilience and maintain energy homeostasis in the face of chronic stress and other challenges.

Thermoregulation and Brown Adipose Tissue Activation

The hypothalamus regulates thermogenesis through the sympathetic nervous system, particularly by stimulating iBAT to produce heat via UCP1. This process increases energy expenditure, making thermoregulation a vital aspect of energy balance. Targeting hypothalamic circuits that control iBAT activation can enhance thermogenesis and promote weight loss, providing a novel approach for obesity treatment.

Glucose Metabolism and Insulin Sensitivity

Hypothalamic regulation of glucose metabolism and insulin sensitivity is critical for energy homeostasis. The hypothalamus senses blood glucose levels and modulates peripheral glucose production and utilization through hormonal and neural signals. Dysregulation in these pathways can lead to insulin resistance and type 2 diabetes, commonly associated with obesity. Therapies targeting hypothalamic control of glucose

metabolism aim to improve insulin sensitivity and glucose homeostasis, contributing to weight management and metabolic health.

Circadian Rhythms and Sleep-Wake Cycle

The hypothalamus orchestrates circadian rhythms and the sleep-wake cycle, which are closely linked to energy balance. Disruptions in these rhythms, such as those caused by irregular sleep patterns, can lead to metabolic dysregulation and obesity. The suprachiasmatic nucleus (SCN) of the hypothalamus synchronizes peripheral clocks, coordinating feeding behavior, hormone release, and energy expenditure with the light-dark cycle. Targeting hypothalamic regulation of circadian rhythms and improving sleep quality can enhance metabolic health and aid in obesity prevention and treatment.

HPA Axis and Stress Response

The HPA axis, regulated by the hypothalamus, plays a role in energy balance through its influence on stress responses and cortisol secretion. Chronic stress and elevated cortisol levels can promote fat accumulation, particularly visceral fat, and disrupt appetite regulation. Interventions that modulate the HPA axis and reduce stress can positively impact energy homeostasis and support weight management efforts.

Reproduction

Reproductive function, governed by the hypothalamus, is linked to energy status. Energy deficiency can suppress reproductive hormones to conserve energy, while adequate energy availability supports reproductive health. Leptin plays a pivotal role in

signaling energy sufficiency to the reproductive axis. Understanding these connections can aid in developing treatments that address reproductive health in the context of obesity and metabolic disorders.

Thermoregulatory and Energy Expenditure Pathways

The hypothalamus plays a key role in regulating body temperature and energy expenditure through pathways that influence iBAT activity and shivering thermogenesis. These mechanisms help maintain energy balance by adjusting metabolic rate in response to environmental and internal cues. Enhancing these pathways can increase energy expenditure and aid in weight management.

Neuroinflammation

Chronic inflammation in the hypothalamus, often seen in obesity, impairs its ability to regulate energy balance. This neuroinflammation disrupts signaling pathways involved in appetite control and energy expenditure. Targeting inflammatory processes within the hypothalamus offers a potential strategy for treating obesity and restoring normal energy homeostasis.

Gut-Brain Axis and Microbiome Interactions

The hypothalamus is influenced by signals from the gut microbiome through the gut-brain axis. Gut-derived metabolites and microbial composition can affect hypothalamic function and energy regulation. Modulating the gut microbiome through

diet, probiotics, or other interventions can impact hypothalamic control of metabolism and offer new avenues for obesity treatment.

Ventromedial hypothalamic pituitary adenylate cyclase activating peptide in curbing obesity

Pituitary adenylate cyclase-activating polypeptide (PACAP) is a crucial neuropeptide involved in the regulation of energy homeostasis and the prevention of obesity. Belonging to the secretin-glucagon superfamily of peptide hormones, PACAP interacts with class B1 G protein-coupled receptors, exerting its effects through both central and peripheral mechanisms (Basu et al., 2024; Bozadjieva-Kramer et al., 2021). In the hypothalamus, particularly the ventromedial hypothalamic nucleus (VMN), PACAP plays a pivotal role in regulating feeding behavior, energy expenditure, and thermogenesis.

The VMN, which contains the densest population of PACAP-expressing neurons in the medial hypothalamus, is integral to PACAP's effects on energy balance (Basu et al., 2024). Central injections of PACAP into the VMN reduce food intake and increase metabolic rate, emphasizing its anorectic and thermogenic properties (Basu et al., 2024; Bozadjieva-Kramer et al., 2021). PACAP achieves these effects through interactions with the PAC1 receptor (PAC1R) and modulation of glutamate neurotransmission, specifically through NMDA receptor activity (Marquette University, 2014). This signaling pathway enhances satiety by inhibiting ghrelin and increasing levels of satiety-promoting hormones like GLP-1 and leptin.

PACAP's role extends to the modulation of energy expenditure. It stimulates iBAT thermogenesis, a critical process for maintaining energy balance and combating obesity. PACAP-expressing neurons in the VMN project to the caudal POA, which in turn activates thermogenesis in iBAT and beige adipose tissues, even during fasting (Basu et al., 2024). The importance of PACAP in this neurocircuit is highlighted by the fact that its inhibition can abolish the thermogenic response.

Furthermore, PACAP in the mediobasal hypothalamus (MBH) modulates sympathetic nervous system activation, influencing blood glucose levels, thermogenesis, energy expenditure, and food intake (Bozadjieva-Kramer et al., 2021). Conditional ablation of the Adcyap1 gene encoding PACAP in the VMN leads to rapid weight gain, increased adiposity, hyperinsulinemia, and severe obesity, underscoring PACAP's critical role in metabolic homeostasis (Bozadjieva-Kramer et al., 2021).

In summary, PACAP in the VMN is a key regulator of energy homeostasis and a promising target for obesity treatment. Its multifaceted actions in reducing food intake, enhancing metabolic rate, and stimulating thermogenesis through central and peripheral mechanisms highlight its potential for therapeutic interventions aimed at managing obesity (Basu et al., 2024; Bozadjieva-Kramer et al., 2021).

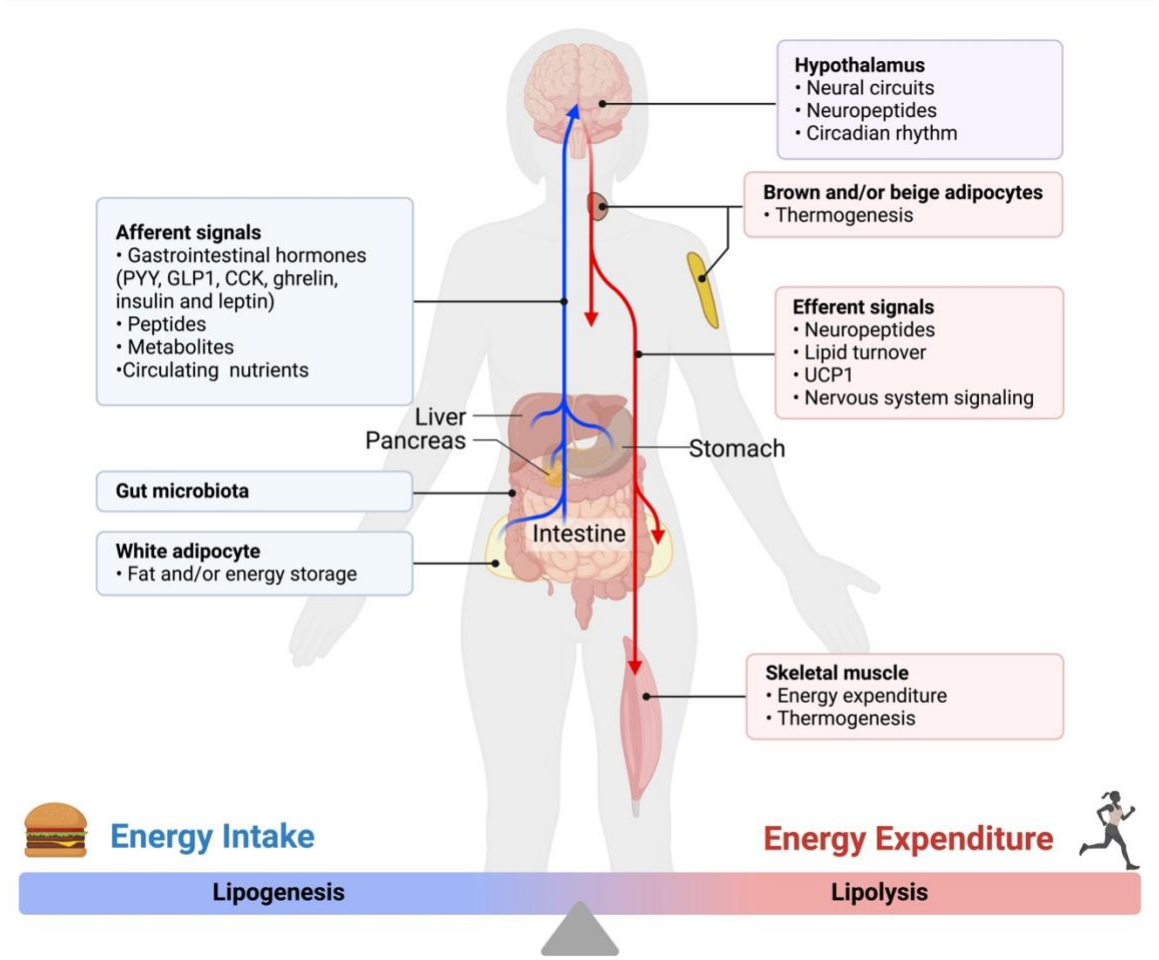

Figure 1.8: Key metabolic mechanisms regulating body weight. Food intake induces production of a range of signals, including gut hormones, peptides, metabolites and the nutrients contained in food, which affect different mechanisms in the brain for activating processes in the body, such as appetite control, or thermogenesis and vital functions, which are as simple as breathing, or maintaining the metabolic functions will use the nutrients and food ingested to induce fermentative processes and synthesize metabolites, such as short-chain fatty acids. All these processes correspond to the blue lines, which lead to energy intake. Also, in the brain, efferent signals are produced and sent to different tissues for promoting thermogenesis and/or energy storage, which correspond to the red lines, and contribute to energy expenditure. UCP1 = Uncoupling protein 1. PYY = Peptide YY (Peptide tyrosine tyrosine). GLP1 = Glucagon-like peptide 1. CCK = Cholecystokinin. Created with Biorender.com.

Gaps in knowledge

In mammals, improper energy balance leads to the development of obesity and energy expenditure acts as a major player in body weight control. Long-term negative energy balance caused by fasting and dieting triggers a compensatory mechanism and lowers energy expenditure which hinders weight loss. Current anti-obesity therapies often yield only modest, short-term effects and can be costly or come with severe side effects due to a fundamental gap in my understanding of obesity mechanisms. This project aims to deepen my understanding of the neural circuits that regulate energy expenditure, focusing on the neural circuit originating from VMN, which can be manipulated to promote weight loss. The VMN is recognized as a key player in energy regulation, but its downstream pathways, particularly those projecting to pre-ganglionic sympathetic neurons, remain poorly defined. Notably, the VMN stimulates thermogenesis in iBAT, and is involved in body weight regulation. Identifying which specific subsets of neurons are involved is critical for mapping the neural circuits that control body weight and energy expenditure.

This study introduces novel approaches to understanding how hypothalamic neurons control energy expenditure, setting the groundwork for innovative obesity treatments. By leveraging genetically engineered mouse models, this research will illuminate unknown hypothalamic mechanisms crucial for energy homeostasis. Such insights are pivotal for developing new strategies that enhance energy expenditure and promote sustainable weight loss. Through this research, I also aim to uncover the downstream neural circuitry extending from the VMN that governs energy balance and

weight management, providing a foundation for potential therapeutic interventions in obesity.

Goals and hypotheses

The purpose of my dissertation is thus to provide an overview of energy balance physiology and describe how hypothalamic dysfunction and disruption of the neural circuit originating in the VMN, contributes to the development of obesity and how manipulating the components of this neural circuit induces thermogenesis and curbs diet-induced obesity, thus making the as a novel target for weight control.

As such, the major goals of this dissertation are (Fig. 1.9):

Aim 1: Defining the downstream output from VMN that induces tissue thermogenesis and body weight loss (Chapter 3)

Here, I investigated the downstream mechanisms by which VMN neurons stimulate adipose tissue thermogenesis. I manipulated subsets of VMN neurons and studied its effect on tissue thermogenesis and body weight control, using $Sf1^{Cre}$ and $Adcyap1^{Cre}$ mice and measured physiological parameters under both high-fat diet and standard chow diet conditions. To determine the node efferent to these VMN neurons, that is involved in modulating energy expenditure, I employed electrophysiology and optogenetics experiments combined with measurements using tissue-implantable temperature microchips.

Aim 2: Examining the role of glutamatergic and GABAergic neurons in the caudal POA, downstream to the VMN neurons, in tissue thermogenesis and body weight regulation

The POA is a complex structure containing intermingled clusters of both excitatory (i.e. Glutamatergic) and inhibitory (i.e. GABAergic) neuronal subpopulations along with other cells. Without clear targets within these intermingled clusters, I explored both the glutamatergic and GABAergic signaling in the caudal POA by either activating or inhibiting the vGLUT2 (Glutamatergic; containing vesicular glutamatergic transporter 2) or vGAT (GABAergic; containing vesicular GABAergic transporter) neurons in the caudal POA of knock-in *vGLUT2*^{Cre} or *vGAT*^{Cre} diet-induced obese male mice. To pinpoint the cellular population involved, I targeted the vGLUT2 and vGAT neurons in the anterior portion of the caudal POA (+0.3mm to -0.1mm bregma) and called it the rostral POA and as well as the posterior portion of the caudal POA (-0.1mm to -.34mm bregma) and called it the caudal POA.

Aim 3: Dissecting the neuronal subpopulation in the POA relevant to obesity and type-2 diabetes (Chapter 5)

I employed single-nuclei RNA sequencing (snRNASeq) to characterize the cellular diversity within this region by analyzing over 200,000 nuclei, the largest dataset of this brain region to date, from a cohort of mixed-sex mice, including obese and glucose-intolerant individuals on a high-fat diet. This comprehensive analysis identified six high-resolution cellular subtypes that were significantly enriched in obese and glucose-intolerant mice. To refine my understanding of these subtypes, I utilized

advanced deep-transfer learning techniques, which enabled us to identify cellular subsets associated with increased obesity and type-2 diabetes risk.

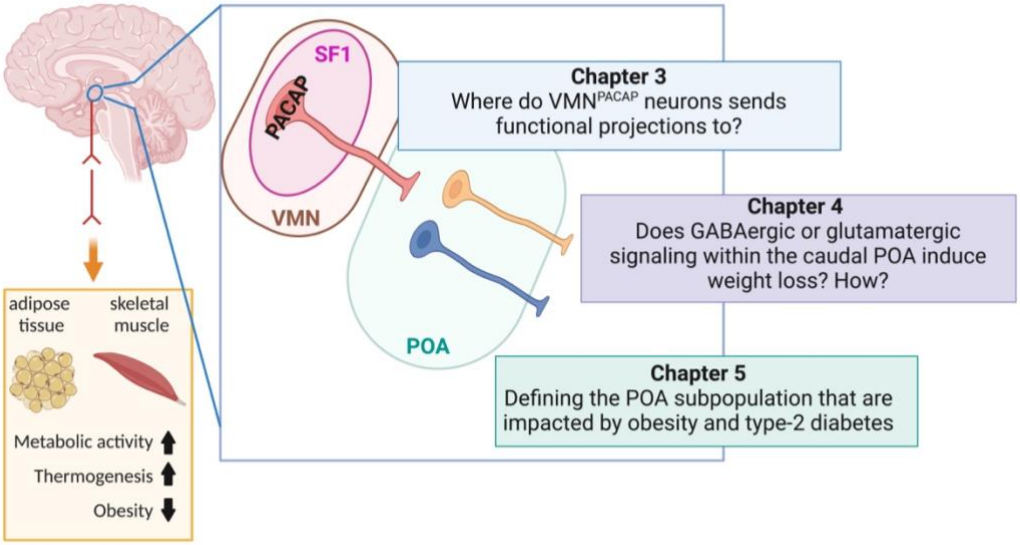

Figure 1.9: Schematic of hypothesized neural circuit by which VMN^{PACAP} acts to regulate body weight. Key questions addressed in each chapter of the dissertation to investigate how VMN^{PACAP} acts to regulate body weight. Created with Biorender.com.

Chapter 2: Materials and methods

Animals

The procedures included in this manuscript were approved by the Committee on the Use and Care of Animals at Indiana University (Indianapolis, IN). All mice were provided with standard chow diet and water *ad libitum*, unless noted otherwise, and kept in a temperature-controlled (23°C) room on a 12-hour light-dark cycle. *C57BL/6J* mice (RRID:IMSR_JAX:000664) were purchased from The Jackson Laboratory. *Sf1*^{Cre} mice (RRID:IMSR_JAX:037533) (Dhillon, Zigman et al. 2006), *Vglut2-ires-cre* (*vGLUT2*^{Cre}) mice (RRID:IMSR_JAX:016963) and *Vgat-ires-cre* (*vGAT*^{Cre}) (RRID:IMSR_JAX:01696) (Vong, Ye et al. 2011) were generated by Bradford Lowell (Beth Israel deaconess Med Centre (Harvard)), *Adcyap1-2A-Cre* (*Adcyap1*^{Cre}) mice were generated by Zachary Knight (University of California, San Francisco (UCSF)) (RRID:IMSR_JAX:030155) (Tan, Cooke et al. 2016). All experiments were carried out using approximately equal numbers of male and female mice, unless noted otherwise. For HFD studies only male mice were used, since prevalent data shows female mice are resistant to diet-induced obesity. These mice were provided with high fat diet regimen (HFD; 45% kcal from fat, high sugar, D12451, Research Diets), starting from 8-10 weeks of age, till 40-44 weeks of age until they were at least 35g body weight. Mice that weighed less than 35g after 44 weeks age were removed from the study. Mice were group-housed prior to stereotaxic surgery in all cohorts, but single-housed post-operatively for body weight and food intake studies, indirect calorimetry, optogenetics and temperature measurements at adipose tissue depots. Otherwise, animals continued to

be housed with their littermates. Unless stated, male and female mice were included for the analysis. All cre-driver mice were used in the homozygous state. All transgenic mice were maintained on a mixed background and have been described previously (Flak, Patterson et al. 2014, Flak, Arble et al. 2017, Flak, Goforth et al. 2020, Bozadjieva-Kramer, Ross et al. 2021). All mice were genotyped via polymerase chain reaction (PCR) across the genomic region of interest prior to study and only mice heterozygous for *Sf1*^{Cre} or homozygous for *Adcyap1*^{Cre}, *vGLUT2*^{Cre} and *vGAT*^{Cre} were included in the study. All mice were bred via in-house colonies. For studies, animals were processed in the order of their ear tag number, which was randomly assigned at the time of tailing (prior to genotyping). Investigators were blinded to genotype/treatment for all studies except knock-out experiments.

Reagents

All the AAVs were acquired from Addgene (Addgene HQ Addgene, Watertown, Massachusetts). All AAVs were aliquoted into 3ul stocks upon arrival and stored at -80C. *AAV-hSyn-DIO-hM3Dq-mCherry* (2.1x10^13 GC/ml), Addgene plasmid 44361, serotype 8; *AAV-hSyn-DIO-mCherry* (2.2x10^13 GC/ml), Addgene plasmid 50459, serotype 8; *AAV-Ef1a-DIO-hChR2-eYFP* (2.2x10^13 GC/ml), Addgene plasmid 35507, serotype 9; *AAV-Ef1a-DIO -eYFP* (2.2x10^13 GC/ml), Addgene plasmid 35507, serotype 9; *AAV-hSyn-hM4Di-mCherry* (2x10^13 GC/ml), Addgene plasmid 50475, serotype 8, [gifted by Bryan Roth, UNC to Addgene].

Stereotaxic injections of viral constructs

Craniotomy was performed on *Sf1*^{Cre}, *vGLUT2*^{Cre} and *vGAT*^{Cre} mice aged 18-20 week-old mice that weighed at least 35 grams. *Adcyap1*^{Cre} mice received a craniotomy at ages 8-14 weeks old. All mice were anesthetized with 1.5-2% isoflurane, in preparation for craniotomy. Successful anesthesia of the mice was tested by hind-leg pinch. The animal was placed on a warm water heating pad, kept at 37°C, on the stereotaxic platform (Kopf) and its head was fixed using the ear-bars and nose piece. The eyes were covered with Artificial Tears ointment (Pivetal) to avoid drying of the eyes. The scalp was shaved, and the shaved area was disinfected with 10% iodine solution (PVP) (Medline) followed by sterile PBS. After exposing the skull with an incision, bregma and lambda were leveled, a hole was drilled, and the contents of a pulled pipette at the coordinates of my target were released at ~10nl/min. For the VMN-directed injections in *Sf1*^{Cre} mice, 150nl of virus were injected at anteroposterior (AP) -1.05, mediolateral (ML) +/- 0.35, dorsoventral (DV) -5.55. For the tracer studies 75nl of virus was injected at the VMN of *Adcyap1*^{Cre} mice at AP -1.05, ML +/- 0.35, DV -5.55. For optogenetic studies using *Adcyap1*^{Cre} mice, 75nl of virus was injected unilaterally at the VMN, at AP -1.05, ML - 0.35, DV -5.55, followed by mono fiber-optic cannula (Doric lenses, size 5.8mm) implantation at a 45° angle at the VMN unilaterally at AP -1.05, ML - 2.05, DV -5.4. Additionally, another mono fiber-optic cannula (Doric lenses, size 5.8mm for caudal POA or 4.5mm for the bed nucleus of stria terminalis (BNST) was implanted unilaterally at either of the two VMN outputs: (1) for caudal POA at AP +0.1, ML - 0.56, DV -5.3; (2) BNST at AP +0.6, ML - 0.65, DV -4.3. The mono fiber-optic cannulas were fixed with 2 mixtures: (i) and (ii). Mixture (i) contained C&B METABOND and

AMALGAMBOND: 5mg AMALGAMBOND, 4 drops of B METABOND and 1 drop of C Universal catalyst. This was allowed to solidify for 3 minutes and was followed by mixture (ii), a dental cement (mixture of Contemporary Ortho-Jet Powder and Contemporary Ortho-Jet liquid, Lang Dental Manufacturing Co., Inc.) on top of the skull. For optogenetic activation at VMN combined with inhibition at caudal POA studies using *Adcyap1*^{Cre} mice, 75nl of AAV-Ef1a-DIO-hChR2-eYFP virus (for cre-dependent expression) was injected at the VMN, at AP -1.05, ML - 0.35, DV -5.55, and AAV-hSyn-hM4Di-mCherry virus (for cre-independent local neuronal expression) was injected at the caudal POA, at AP +0.1, ML - 0.56, DV -5.54 followed by a mono fiber-optic cannula (Doric lenses, size 5.8mm) implantation unilaterally at caudal POA at AP +0.1, ML -0.56, DV -5.3. For the rostral POA directed injections in *vGLUT2*^{Cre} and *vGAT*^{Cre} mice, 75nl of virus were injected at AP +0.01, ML +/-0.509, DV -5.54 and for the more caudal POA directed injections in *vGLUT2*^{Cre} and *vGAT*^{Cre} mice, 75nl of virus were injected at AP +0.22, ML +/-0.519, DV -5.54. For all surgeries, I allowed at least 5 minutes for the virus to diffuse into the brain and the pipette was raised slowly out of the hole in the skull. The hole in the skull where the virus was injected was filled with bone wax. The skin incision was closed with surgical glue (VetBond, 3M). Analgesics (Carprofen, 5mg/kg) were administered prophylactically to all mice to prevent post-surgical pain. The mice were allowed four weeks to recover from surgery before any experimental manipulation. Either mCherry or YFP fluorescent reporters were used to confirm proper targeting of the brain region in all studies. If fluorescence was not observed within the targeted injection site, these cases were omitted from analyses.

Phenotypic studies

Body weight and food intake were monitored weekly in all mice post-surgery. Body weight and food were weighed weekly on a precision balance (OHAUS Corporation, model # SPX421). For all glycemic measures, mice were fasted for 5 hours prior to testing and blood glucose was measured with a One Touch Ultra 2 glucometer (Johnson and Johnson) by tail vein draw. Additionally for the glycemic measures in fasted state, mice were fasted for 24 hours before measuring blood glucose. Body composition data was collected with assistance from Indiana University School of Medicine Mouse Metabolic Phenotyping Center from the EchoMRI™-100H Body Composition Analyzer. TSE Phenomaster cages were used for indirect calorimetry measurement, with assistance from the Indiana University School of Medicine Mouse Metabolic Phenotyping Center. Indirect calorimetry data was used to calculate fat oxidation and glucose oxidation via the Weir equation (Weir, et.al. 1949).

Temperature measurement at adipose tissue depots

During stereotaxic surgeries, temperature programmable microchips (UCT-2112 Temperature Microchip), from UID (Lake Villa, Illinois), were implanted using UPGI-Q Pistol Grip Injector from UID, directly underneath the skin, above the iBAT and inguinal white adipose tissue (iWAT; also known as beige or brite adipose tissue; metabolically active with some thermogenic capacity) in mice. Animals were allowed 4-week recovery and acclimation was performed by handling them and using the handheld reader system (UID, model URH-1HP) or the automated system (UID, home cage monitoring system) for 5 consecutive days before taking the final measurements. Data were collected using

the handheld reader system at the time points indicated or continuously using the automated system.

Acute brain slice preparation

After the recovery from intracranial injections, acute brain slices were prepared as described previously. Mice were briefly (~15 seconds) anesthetized with 99.9% isoflurane (Patterson Veterinary) and quickly decapitated. Brains were rapidly dissected and submerged in an ice-cold choline solution containing the following (in mM): 110 choline chloride, 25 $NaHCO_3$, 25 D-glucose, 11.6 sodium ascorbate, 7 $MgSO_4$, 3.1 sodium pyruvate, 2.5 KCL, 1.25 NaH_2PO_4, and 0.5 $CaCl_2$). Coronal brain slices containing the pre-optic region (spine of the blade tilted rostrally 15° off vertical plane, 300-µm thick) were prepared with a vibratome (VT1200S; Leica). Slices were transferred to a 37°C artificial CSF (ACSF) bath containing the following (in mM): 127 NaCl, 25 $NaHCO_3$, 25 D-glucose, 2.5 KCl, 1$MgCl_2$, 2 $CaCl_2$, and NaH_2PO_4 for 30 min. Slices were subsequently incubated for at least 45 minutes in ACSF at room temperature before being transferred to the recording chamber.

Electrophysiological recordings

Slices were placed in the recording chamber of a SliceScope Pro 6000 (Scientifica) and continuously perfused with the ACSF (30-32°C) at the rate of ~1 mL per minute. Slices were held in place with a slice anchor (Warner Instruments). Recording pipettes were made from borosilicate capillaries with filaments (G150-F; Warner Instruments) using a horizontal pipet puller (P-97; Sutter Instruments). Preoptic

neurons approximately 40 µm or deeper from the surface of the slice were targeted for recording. After establishing a Gigaohm (GΩ) seal between the pipette tip and the cell membrane gentle negative pressure was applied from inside the pipette to open the cell membrane. After the opening of the cell membrane, neurons were allowed to stabilize for 5 minutes before recording. The patch electrode (2.5-3.5 MΩ resistance) was filled with a cesium-based internal was used: 60 mM CsMeSO3, 60 mM CsCl2, 10 mM HEPES, 0.2 mM EGTA, 8 mM NaCl, 2 mM MgCl2, 3 mM MgATP, 0.3 mM NaGTP, 5 mM lidocaine, 10 mM phosphocreatine. Whole-cell patch-clamp recordings were performed at 30-32°C, amplified and filtered at 4 kHz, and digitized at 10 kHz using a Multiclamp 700B amplifier (Molecular Devices). Evoked excitatory postsynaptic currents and evoked inhibitory postsynaptic currents (eEPSCs/eIPSCs) were generated by initiating blue lights using a LED illumination system (CoolLED pE-4000) using a 490 nm wavelength LED with a GFP filter (ET FITC/GFP, Olympus). Membrane potential was held at -60 mV in a voltage-clamp mode for eEPSCs and at +10 mV for eIPSCs. No synaptic blockers were added during evoked electrophysiological recordings. After the recording, CPP and NBQX (Tocris, Bristol, UK; 5 µM) were added to the ACSF to block glutamatergic (excitatory) inputs; SR 95531 hydrobromide (GABAzine, Tocris, Bristol, UK; 10 µM) was added to the ACSF to block GABAergic (inhibitory) inputs. Pipette capacitance was compensated, and the inclusion of data required a series resistance < 35 MΩ.

Optogenetics studies

For the optogenetic measurements, the optical fibers in the head of the singly housed *Adcyap1*^{Cre} mice were connected to a blue light (450nm) emitting optical system

(Doric Lenses, LED Illumination system), using fiber optic patch cords, that were attached to fiber optic cannulas on the skull, and stimulated at VMN along with either of the two VMN efferents (either caudal POA or BNST). Blue light stimulation was done using 120mA current at 40Hz frequency for 5.0ms. Glycemic measures and measurements for temperature at the different adipose tissue depots were done- first without blue light stimulation for 90 minutes and then with lights on for 120 minutes. For the studies with optogenetic activation at VMN combined with hM4Di mediated inhibition at caudal POA, the *Adcyap1*^{Cre} mice were injected with clozapine-N-oxide (CNO) (.3 mg/kg, IP) 30 minutes prior to blue light stimulation. For these mice the optogenetic stimulation was done following CNO injection, as mentioned above. All mice in the optogenetics studies were acclimated for at least a week to the laser equipment and procedure room prior to testing to ensure a low stress environment. Mice were tested within their home-cages and were allowed to freely move around their home-cage.

Terminal tissue collection and perfusion

After completion of phenotypic and/or physiological studies, the mice were terminally sacrificed for tissue harvesting. For studies with hM3dq or hM4di, the mice were injected with CNO (.3 mg/kg, IP) 2 hours prior to tissue collection. For optogenetic studies, mice were either stimulated with blue light or no blue light for the respective control group for 2 hours prior to tissue collection. At the end of the 2 hours of treatment, mice were anesthetized with isoflurane for harvesting. All mice were anesthetized with isoflurane. When deeply anesthetized, adipose tissues: iBAT, iWAT and perigonadal

white adipose tissue (pgWAT) were collected immediately prior to transcardial perfusion and immediately placed on dry ice.

Perfusion and Immunohistochemistry

Brains from mice were collected and processed as previously described (Flak, Patterson et al. 2014, Flak, Arble et al. 2017, Flak, Goforth et al. 2020, Bozadjieva-Kramer, Ross et al. 2021). Following terminal tissue harvest, transcardial perfusion was performed on the mice with phosphate buffered saline (PBS) followed by 10% neutral buffered formalin (NBF) (Fisher brand, catalog #245685). Brains were removed and placed into 10% NBF overnight, followed by 30% sucrose for at least 36 hours. Brains were cut into 30μm sections on a freezing microtome in four series and stored in antifreeze solution (25% ethylene glycol, 25% glycerol). For immunohistochemistry staining sections were washed with PBS and then treated sequentially with 1% hydrogen peroxide/ 0.3% sodium hydroxide, 0.3% glycine, and 0.03% sodium dodecyl sulfate. Pretreatment was followed by an hour in blocking solution (PBS containing 2.5% triton, 3% Normal Donkey Serum (Lampire Biological Laboratories, catalog # 7332100)), followed by overnight incubation in blocking solution containing either chicken anti-GFP (GFP-1020, RRID: AB_1000240, Aves, 1:1000) or rabbit Living Colors DsRed Polyclonal Antibody (632496, RRID: AB_10013483, Takara Bio 1:1000). The next day, the sections were incubated with fluorescent secondary antibodies: either Cy™3 AffiniPure Donkey Anti-Rabbit IgG (H+L) (711165152, RRID: AB_2307443, Jackson) with DsRed or Alexa Fluor® 488 AffiniPure Donkey Anti-Chicken IgY (IgG) (H+L) (703-545-155, RRID: AB_2340375, Jackson) with anti-GFP. cFos staining was done

additionally to the slices to quantify neuronal activation. For this cFos staining was done in day 1 of staining using Rabbit anti-c-Fos antibody (2250S c-Fos 9F6, Cell Signaling) followed by Peroxidase AffiniPure Donkey Anti-Rabbit IgG (H+L) (711-035-152, RRID: AB_10015282, Jackson). This was followed by the DsRed or GFP staining as described above. The stained sections were mounted onto slides and cover slipped with Fluoromount-G (Southern Biotech).

Total RNA sequencing

100mg of iBAT and iWAT were each homogenized using Bullet Blender. Steel beads were used to homogenize iBAT and zirconium oxide beads were used to homogenize iWAT. RNA was extracted from the homogenized tissue using the TRIzol® Reagent (15596018, Ambion) and PureLink™ RNA Mini Kit with on-column DNase I (Zymo Research DNase I; catalog # E1010). The RNA quality and concentration was checked by Nanodrop 2000 (Thermo Scientific). Total RNA sequencing was done by the Centre for Medical Genomics Core at Indiana University School of Medicine. The RNA sequencing data was then analyzed by Olivia Lazaro under the supervision of Dr. Travis Johnson. Analysis was performed separately for each type of adipose tissue parallely using RStudio (version 4.1.1). The reads were aligned using the package Rsubread (version 1.22.2) and annotated using the GRCm38 primary assembly through the index building function in Rsubread (Smyth 2005, Law, Chen et al. 2014, Ritchie, Phipson et al. 2015, Law, Alhamdoosh et al. 2016, Wickham 2016, Pagès, Carlson et al. 2021, Yu 2022). The BAM files generated through paired end alignment were then mapped to obtain read counts. These counts were annotated based on experimental group and sex,

then filtered for expression to remove genes with an average expression of less than 1 CPM across all samples. The filtered data was then used to create a design matrix using model.matrix () from the limma package (version 3.50.1) with explanatory variables based on sample sex and treatment group for both sexes combined, but adjacently the same pipeline was run for each individual sex for comparative analysis using only the explanatory variable of treatment group. This design matrix is used for the standard limma RNAseq pipeline (Law, Chen et al. 2014, Ritchie, Phipson et al. 2015, Law, Alhamdoosh et al. 2016) consisting firstly of the voom function, which estimates the mean-variance of the log-counts, then generates precision weights for each observation, which are used for linear model fitting for each gene. The generated linear model is then used to compute an array containing the logFC (log fold change) value, p value, adjusted p value (by Benjamini-Hochberg procedure), average expression, and log-odds of differential expression for each gene using the empirical Bayes method (Smyth 2005). This array was filtered for all genes meeting the criteria of having an adjusted p value less than .05 and a logFC value greater than 0.58 or less than -0.58, which were considered to be differentially expressed. Volcano plots were generated using the ggplot2 package (version 3.3.6) to visualize the genes based on scaled (from -1.0 to 1.0) logFC values and scaled (from 0 to 1) adjusted p values, and heatmaps using the heatmap3 package (version 1.1.9) based on gene expression for each of the top 20 DEGs for each group. Finally, the expression values for all upregulated and downregulated DEGs are subset and used for functional enrichment using clusterProfiler (version 4.2.2) with annotation sourced from AnnotationDbi (version 1.56.2) (Wickham 2016, Pagès, Carlson et al. 2021, Yu 2022) and visualization of results using enrichplot (version 1.14.2).

Single nuclei RNA isolation

Single nuclei isolation was performed following a modified protocol, which is described in detail below. At first the brains of anesthetized mice were collected and placed on ice. Then very quickly the POA and BNST were dissected from brains using a stainless-steel brain matrix (Kent Scientific Corporation). Once dissected the brain sections were put in 1.5ml sterile Eppendorf tubes and flash frozen in liquid nitrogen and stored at -80ºC. Then the frozen brain tissue samples were transferred to a pre-chilled glass Dounce homogenizer (2ml grinder A and B; Sigma-Aldrich) with ice-cold lysis buffer, containing EZ Prep Lysis Buffer (Sigma-Aldrich, NUC101-1KT), 1M DTT (Thermo-Fisher) and Protector RNase inhibitor (Sigma-Aldrich, 3335399001). The initial homogenization was performed with grinder A, followed by grinder B. The homogenized sample was then filtered through a 30 µm MACS strainer (Myltenyi, 130-098-458) and the nuclei were pelleted by centrifugation at 500 rcf for 5 minutes at 4 °C. The supernatant was carefully discarded to avoid disturbing the loose pellet, and the nuclei were resuspended in wash buffer 1, containing 1M $MgCl_2$, 1M Tris Buffer (pH 8.0), 2M KCl, BSA, 1mM DTT and Protector RNase inhibitor. The nuclei suspension was again filtered through a 30 µm MACS strainer and the nuclei were pelleted by centrifugation at 500 rcf for 5 minutes at 4 °C, the supernatant was carefully removed, and the pellet was resuspended in wash buffer 1. For nuclei staining, propidium iodide (ThermoFisher P3566) solution was added to the nuclei suspension. An optional step was performed to count the nuclei by placing 1µL of the sample on a slide, covering it with a coverslip, and visualizing it under a TRITC channel using a fluorescence microscope. Nuclei were counted using ImageJ software with the cell counter plugin. The stained nuclei were then

transferred to tubes pre-coated with wash buffer 1 and were sorted by FACS sorting. The sorted nuclei were then subjected to single nuclei RNA sequencing. For genomics and sequencing, propidium iodide -negative samples were isolated in parallel with the experimental samples.

Single nuclei RNA sequencing

The isolated nuclei were processed by the Centre for Genomics Core at Indiana University School of Medicine, according to the 10× Chromium workflow as outlined by the manufacturer. The Chromium Next GEM Single Cell 5′ Kit v2 (10X Genomics PN-1000263) was used, followed by the corresponding library construction kit (10× Genomics PN-1000190). The resulting libraries were evaluated with the Bioanalyzer 2100 instrument (Agilent), and cDNA quantity was measured using a Qubit fluorometer (Thermo Fisher Scientific). The libraries were then sequenced on a NovaSeq 6000 S4 flow cell (Illumina), aiming for 10,000 reads per cell with 100-bp paired-end sequencing. The FastQ files were generated by the 10X Genomics standard sequencing protocol and sent to me for analysis. Cell Ranger 7.1.0 was used to align the raw fastq files to the mm10 mouse reference genome (version 2020-A) and generate UMI counts. The filtered gene-barcode matrices were used as input in R to create Seurat objects including only the cells with at least 100 observable features. All objects were split into male and female samples before proceeding with quality control of each object at a time. Cells expressing an outlying number of features and/or an abnormally large mitochondrial DNA percentage were considered poor quality. Each object was normalized using the sctransform package, variable features were identified, all Seurat objects were merged,

and PCA was ran on the merged data. Afterwards, the harmony package was used to integrate the data. Sample sex was included as a covariate to account for batch effects. To cluster cells, UMAP was ran on the first 10 harmony embeddings and a Shared Nearest Neighbor (SNN) graph was computed using the same harmony embeddings. Twenty-nine clusters were identified at a resolution of 0.5 and labeled based on their canonical marker expression. To identify subclusters, different cell types were subset based on the following variables: brain region (BST or POA), sex, and sex-specific cells within a brain region (male BST cells, female BST cells, male POA cells, or female POA cells). All subsets were clustered the same way as the larger object, except only the first 7 harmony embeddings were used and a value of k = 10 (instead of the default value of 20) was used to build the SNN graph. The number of clusters identified varies for each subcluster.

The Seurat format datasets for comprehensive brain regions and gender datasets of all cell types were analyzed using PCA for dimensionality reduction. Based on PCs and elbow plot, dimensions were reduced to 1:15, and the top 15 PCs were used for further UMAP analysis using Seurat (v.5.1.0). A KNN graph based on Euclidean distance was constructed using the FindNeighbors function, and clustering was performed with FindClusters using a resolution of 0.5, increasing the number of clusters. UMAP visualization showed clustering of cells. Differentially expressed markers were identified using the Wilcoxon rank-sum test with FindAllMarkers (logfc.threshold 0.25, min.pct 0.1), and the top 5 markers of each cluster were extracted using dplyr, generating a heatmap for markers with average log fold change > 1. Logistic regression was performed for comprehensive datasets, considering diet, sex, and brain region information, fitting generalized linear models for each cluster. Significant clusters were

identified with p-values < 0.05 for diet, brain region, and their interactions, but > 0.05 for sex and its interactions. Similar logistic regression was done for brain region datasets (bst and poa) and gender datasets (male and female). Functional enrichment analysis was conducted for biological processes, cellular components, and molecular functions using enrichGO (p-value and q-value cut-off 0.05). Top 20 KEGG pathways were identified using enrichKEGG. Significant clusters and genes were subset and visualized using featureplot from Seurat.

Quantitative real-time PCR

RNA was isolated in a similar fashion as described previously. cDNA was synthesized by reverse transcription from mRNA (extracted using the method described above) using the SuperScript VILO cDNA Synthesis Kit (Invitrogen). Gene expression was performed by quantitative real time PCR (qRT-PCR) using Taqman gene expression assays using TaqMan Fast Advanced Master Mix (Thermo Fisher) with a standard protocol using the applied biosystems' setup and Quantstudio 5 and Quantstudio 3 (Thermo Fisher Scientific). Gene expression was measured for *Ucp1* (Mm01244861_m1), *Dio2* (Mm00515664_m1), *Ppargc1a* (Mm01208835_m1), *Prdm16* (Mm00712556_m1), *Cidea* (Mm00432554_m1), *Elovl3* (Mm00468164_m1), *Zbtb16* (Mm01176868_m1), *MaeA* (Mm00491367_m1), *Slc26a8* (Mm00524836_m1), *Ppt1* (Mm00477078_m1), *Kdm6b* (Mm01332680_m1), *Adrb1* (Mm00431701_s1), *Adrb3* (Mm02601819_g1). Relative abundance for each transcript was calculated by a standard curve of cycle thresholds and normalized to TBP (Mm01277042_m1).

RNAscope *in-situ* hybridization

Multiplex *in-situ* hybridization was performed using the RNAscope MultiPlex v2 assay (Advanced Cell Diagnostics, Inc.) with 4 probes: *Asic2*, *Ptprd*, *Kcnip1* and *Gpc5*. Three coronal sections of POA were sampled at bregma 0.26mm, 0.02mm, -0.34mm and -0.70mm for each mouse (total n = 4) and an area of 1.8mm (height) X 2.1mm (width) was scanned for each brain section. DAPI was used as a signal as a reference. First, on the day before the experiment, one or two brains were sectioned at 14 microns and placed in an 8-section series across six slides, with sections stored in antifreeze. Slides were air-dried at -20°C for 2 hours, then transferred to -80°C for at least 16 hours before further processing. Then on day 1, the oven was preheated to 60°C and then the slides were washed with 1X PBS for 5 minutes. The slides were baked at 60°C for 30 minutes, then immersed in pre-chilled formalin for 15 minutes at 4°C. During this time, the oven was set to 40°C, and a humidity tray was prepared with distilled water. The target retrieval solution was heated to approximately 99°C on a hot plate, which was maintained at 300°C. Post-formalin treatment, slides were immersed in a series of ethanol washes: 50% EtOH for 5 minutes, 70% EtOH for 5 minutes, and two rounds of 100% EtOH for 5 minutes each. 5-8 drops of hydrogen peroxide were applied to cover the sections completely for 10 minutes at room temperature, followed by rinsing with distilled water. Slides were then transferred to a metal slide tray and placed in boiling target retrieval solution on a hot plate for 5 minutes. Afterward, slides were rinsed with distilled water and immersed in 100% EtOH for 3 minutes before drying at room temperature for 5 minutes. A hydrophobic barrier was drawn around the sections, and RNA Scope Protease III was applied for 30 minutes at 40°C. During this incubation, I prepared the RNAscope

Multiplex Fluorescent Detection Reagents v2, 1X wash buffer, and 5X SSC. Hybridization probes were mixed and applied to the sections for 2 hours at 40°C. After washing with 1X wash buffer, slides were processed using FL v2 Amp 1, Amp 2, and Amp 3, each incubated for 30 minutes at 40°C, with intermediate washes. TSA fluorophores were prepared, and FL v2 HRP channels were developed sequentially with respective incubations and washes for C1, C2, and C3 probes. Finally, slides were counterstained with DAPI, mounted with a coverslip, and dried overnight in the dark. Slides were stored at 2-8°C and imaged within two weeks.

Cell counts

Images from 30μm thick sections containing DsRed or GFP alone or with cFos antibody staining were collected in the VMN, POA, BNST, PVT, MnR, VTA and PAG using an Echo Fluorescent microscope with a 4X or 10X objective. The target regions were identified by overlaying the corresponding bregma level from an anatomical reference using The Mouse Brain in Stereotaxic Coordinates Fourth Edition (Paxinos and Franklin) on microscope images. Images were collected with the same exposure settings on the microscope. They were counted by eye using the counting feature in ImageJ by someone blind to treatment. Total number of cFos-IR nuclei were counted for each brain area.

Statistics

Time-course data for the following studies: body weight, blood glucose and temperature at adipose depots, were analyzed by two-way repeated measures ANOVA

with Fisher's LSD post hoc test. Data in Figures 3.1C, 3.3C-3.3K, 3.4B-3.4J, 3.7B, 3.7E, 4.1D, 4.1H, 4.1L, 4.1P, 4.2A-4.2H, 4.5A, 4.5E, 4.5F, 4.5G, 4.5K, 4.5L, 5.1B, S3A-S3F, S7A-S7D were analyzed by two-way repeated measures ANOVA with Fisher's LSD post hoc test. Data in Figures 3.1D-3.1F, 3.2H, 3.6C, 3.6F, 3.6I, 3.6J, 3.6M, 3.6P, 3.6Q, 3.7D, 3.7G, 4.1E-4.1G, 4.1I-4.1K, 4.1M-4.1O, 4.1Q-4.1S, 4.3A-4.3D, S2D, S2G, S2K, S20, S2R, S4A-S4B, S5C, S5F, S5I, S5J, S5M, S5P, S5Q were analyzed by student's t-test. Data in Figures 3.1M, 4.5B-4.5D, 4.5H-4.5J, 5.1A, 5.1C analyzed by multiple student's t-test. Data in Figures 3.1G-3.1L, 3.7C, 3.7F, 4.5M-4.5N were analyzed by one-way ANOVA. Data was expressed as mean +/- SEM. No data were removed unless the injection missed the targeted location, or the animal was sick or injured at the time of the experiment (loss of > 10% body weight). Significance was determined at $p \leq 0.05$. All data were analyzed using Prism (GraphPad, La Jolla, California).

Chapter 3: Ventromedial hypothalamic nucleus subset stimulates tissue thermogenesis via preoptic area outputs

Abstract

Hypothalamic signals potently stimulate energy expenditure by engaging peripheral mechanisms to restore energy homeostasis. Previous studies have identified several critical hypothalamic sites (e.g. POA and VMN) that could be part of an interconnected neurocircuit that controls tissue thermogenesis, essential for body weight control, but the key neurocircuit that can stimulate energy expenditure has not yet been established.

Here, I investigated the downstream mechanisms by which VMN neurons stimulate adipose tissue thermogenesis. I manipulated subsets of VMN neurons and studied its effect on tissue thermogenesis and body weight control, using *Sf1*^{Cre} and *Adcyap1*^{Cre} mice and measured physiological parameters under both high-fat diet and standard chow diet conditions. To determine the node efferent to these VMN neurons, that is involved in modulating energy expenditure, I employed electrophysiology and optogenetics experiments combined with measurements using tissue-implantable temperature microchips.

Activation of the VMN neurons that express the Sf1 (VMN^{Sf1} neurons) reduced body weight, adiposity and increased energy expenditure in diet-induced obese mice. This function is likely mediated, at least in part, by the release of the PACAP neuropeptide (encoded by the *Adcyap1* gene) by the VMN neurons, since I previously demonstrated that PACAP, at the VMN, plays a key role in energy expenditure control.

Thus, I then shifted focus to the subpopulation of VMN^{Sf1} neurons that contain the neuropeptide PACAP (VMN^{PACAP} neurons). Since the VMN neurons do not directly project to the peripheral tissues, I traced the location of the VMN^{PACAP} neurons' efferents. I identified that VMN^{PACAP} neurons project to and activate neurons in the caudal regions of the POA whereby these projections stimulate tissue thermogenesis in brown and beige adipose tissue. I demonstrated that selective activation of caudal POA projections from VMN^{PACAP} neurons induces tissue thermogenesis, most potently in negative energy balance and activating these projections lead to some similar, but mostly unique, patterns of gene expression in brown and beige tissue. Finally, I demonstrated that the activation of the VMN^{PACAP} neurons' efferents that lie at the caudal POA are necessary for inducing tissue thermogenesis in brown and beige adipose tissue.

These data indicate that VMN^{PACAP} connections with the caudal POA neurons impact adipose tissue function and are important for induction of tissue thermogenesis. My data suggests that the VMN^{PACAP} → caudal POA neurocircuit and its components are critical for controlling energy balance by activating energy expenditure and body weight control.

Background and rationale

Upon a change in energy status, neural circuits dynamically balance caloric intake with energy expenditure to maintain body weight; obesity arises when these responses are no longer adequate. My lack of understanding of the components and mechanisms that promote energy expenditure, are a barrier for obesity-treatment.

BMR accounts for about 70% of total energy expenditure, followed by activity-induced thermogenesis from exercise and non-exercise activities (10–15% of total energy expenditure) and adaptive thermogenesis from ingesting food or being exposed to cold temperatures (10–15% of total energy expenditure) (Ogden, Yanovski et al. 2007). Unlike BMR, which is largely shaped by genetics, the other two are regulated by environmental stimuli such as temperature, hormone levels, and nutritional status. The brain integrates these environmental cues via bi-directional communication between the CNS and the PNS that together regulate energy expenditure (Schwartz and Porte 2005, Cannon and Nedergaard 2011, Wu, Jun et al. 2015, Tran, Park et al. 2022). The sympathetic nervous system, stimulated by the CNS, induces adaptive thermogenesis in iBAT and iWAT (Tseng, Cypess et al. 2010, Berg and Jensen 2013) to stimulate metabolic rate and promote weight loss via the action of norepinephrine (Leblanc, Dussault et al. 1982, Berg and Jensen 2013, Wu, Jun et al. 2015, Yu, Qualls-Creekmore et al. 2016). CNS signals stimulate norepinephrine release from neurons in the sympathetic chain in response to exercise, cold temperature, and diet related signals, which then induces mitochondrial UCP1 expression and lipolysis in brown and beige adipocytes. This triggers fatty acid oxidation and mitochondrial uncoupling, accompanied by heat production or thermogenesis as a by-product (Adjeitey, Mailloux et al. 2013, Yu, Qualls-Creekmore et al. 2016) which is an adaptive and plastic way to metabolize and remove excess nutrients from the system.

The VMN, a region within the medio-basal hypothalamus of brain, traditionally known for mediating glucose homeostasis, induces iBAT thermogenesis, and downstream communication initiated by VMN neurons is crucial for energy expenditure

control (Seoane-Collazo, Ferno et al. 2015, Roh, Song et al. 2016). lab has shown that lesioning of the VMN leads to increased body weight and adipose mass along with a decrease in lean mass in mice compared to their littermate controls (Flak, Goforth et al. 2020). A subpopulation of VMN neurons densely expresses a neuropeptide called PACAP, encoded by *Adcyap1*. PACAP administration induces sympathetic nervous system activity, panic behavior, anorexia, and thermogenesis (Tanida, Shintani et al. 2010, Tanida, Hayata et al. 2013). In addition, I previously demonstrated that loss of PACAP at the VMN, induces obesity without inducing hyperphagia and that VMN^{PACAP} neurons control energy balance by promoting energy expenditure (Bozadjieva-Kramer, Ross et al. 2021). Suppression of this neuropeptide within only the VMN occurs naturally in response to both fasting and decrease in leptin levels (Hawke, Ivanov et al. 2009), which could be a critical signal to match energy expenditure with food intake.

Recent evidence indicates that distinct VMN neuron subsets project to different areas of the brain and mediate separate physiological effects via distinct neural circuits (Meek, Nelson et al. 2016, Faber, Matsen et al. 2018, Zhang, Chen et al. 2020). However, the neural circuit and the node downstream of VMN, that is involved in energy expenditure and body weight control remains undefined. Here, I aim to dissect the components and nodes of this neural circuit. Even though the VMN^{PACAP} neurons are a major regulator of energy expenditure and body weight, the mechanistic details are still unclear. Dissecting the physiological, cellular, and molecular bases of this neural circuit is key to understanding the central control of energy balance and its dysfunction during obesity. By doing this, I will expand our knowledge of the key neural systems that govern body weight independent from food intake.

Results

Activating VMN^{Sf1} neurons blunts diet induced obesity in male mice

Previous studies from our lab showed that silencing the Sf1 neurons in the VMN (VMN^{Sf1}) led to obesity with a decrease in energy expenditure (Flak, Goforth et al. 2020). But their role in ameliorating diet induced obesity has not been identified. To test the potential for VMN^{Sf1} neurons to reduce body weight and adiposity in diet induced obesity, I put male *Sf1^{Cre}* mice on HFD. I first looked at pertinent phenotypic alterations. *Sf1^{Cre}* male mice and their littermate (WT) male controls were given HFD, beginning at 8-10 weeks of age, for 40-44 weeks of age until they weighed at least 35 grams. I then performed craniotomy to administer *AAV$^{DIO\text{-}hM3dq\text{-}mCherry}$* (Fig. 3.1A; Supplementary Fig. S1A) into the VMN of these mice (Supplementary Fig. S1B-S1C) and monitored their body weight, body composition, food intake and energy expenditure (Fig. 3.1B). For the phenotypic measurements, *Sf1^{hM3dq}* mice and their WT littermate controls were acclimated for 7 days with once daily intraperitoneal (IP) saline injection. For the next 3 days they were injected with IP CNO, twice daily (every 12 hours). Both groups of mice weighed the same before and 4-weeks post-surgery. After activating the *Sf1^{hM3dq}* neurons with IP CNO injection, *Sf1^{hM3dq}* mice lost 1g body weight in just 3 days, in contrast to the WT controls (Fig. 3.1C), without altering food intake (Fig. 3.1D). I then calculated the percentage of adipose and lean mass change in these mice and compared between the groups. I calculated change in the percentage of adipose or lean mass normalized to pre-CNO body weight for each mouse and found that these mice had 15% reduced adiposity (Fig. 3.1E), and 5% increased lean mass (Fig. 3.1F).

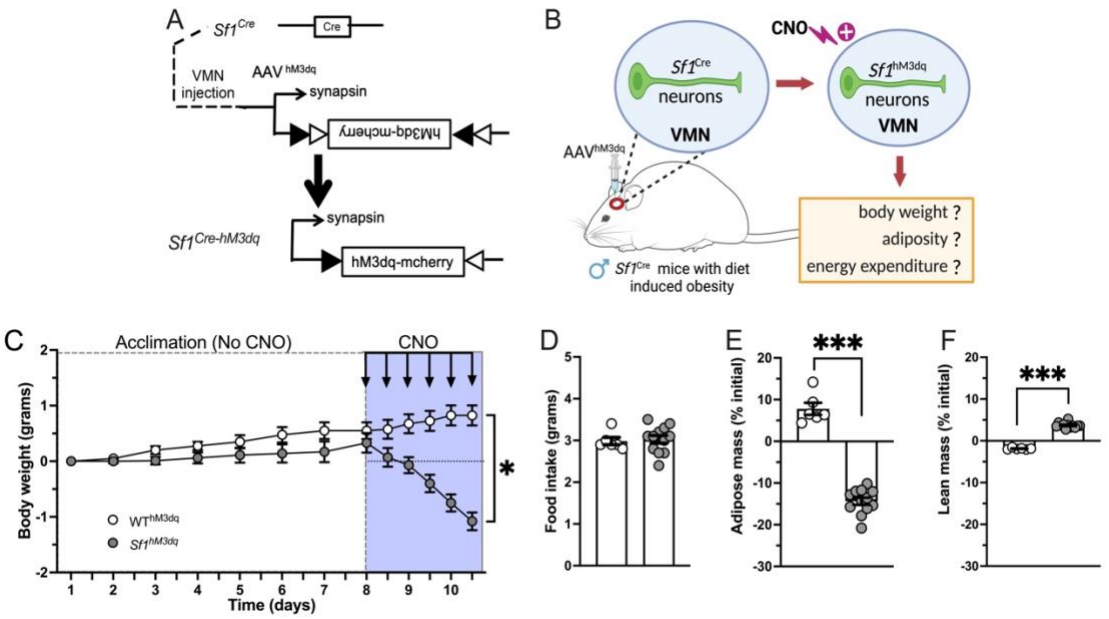

Figure 3.1: Activating VMN^{Sf1} neurons blunts diet induced obesity in male mice. I introduced *AAV$^{DIO\text{-}hM3dq\text{-}mCherry}$* into the VMN of either *Sf1^{Cre}* mice or their wild-type littermate controls (A). Then I tested the potential for activating VMN neurons in diet-induced following Clozapine-N-oxide (CNO) IP injection (B) and measured body weight (C) food intake (D), adiposity (E) and lean mass (F). n=5-12 male mice. Data expressed as mean ± SEM and analyzed by either two-way RM ANOVA (C), by student's t-test (D-F). *p<0.05, **p<0.01, ***p<0.0001.

To perform indirect calorimetry measurements, I included a separate cohort of these mice groups that were placed into the TSE metabolic chambers. Then mice were acclimated for 4 days with once daily IP saline injection. The next 3 days they were injected with IP CNO, once daily. I compared the oxygen consumption (vO2), respiratory exchange rate (RER), energy expenditure, locomotor activity, fat oxidation and glucose oxidation between *Sf1^{hM3dq}* mice and the WT control groups, as well as the levels of those parameters at 3 hours before IP CNO injection (pre-CNO) and 3 hours after IP CNO

injection (post-CNO). vO2 (Fig. 3.2A) and energy expenditure (Fig. 3.2C) were elevated, with no change in RER (Fig. 3.2B), post-CNO injection in the *Sf1*^{hM3dq} mice. These mice also exhibited higher locomotory activity (Fig. 3.2D). After calculating the fat and glucose oxidation rates in these mice using Weir equation, I found elevated fat oxidation rate when normalized to their lean body mass (Fig. 3.2E), with no change in the rate of glucose oxidation when normalized to their lean body mass (Fig. 3.2F). I next measured expression of targets associated with thermogenesis (Fig. 3.2G) in iBAT, using qRT-PCR, from iBAT harvested after 2-hour stimulation with IP CNO injection. Mitochondrial uncoupling protein 1 (*Ucp1*) (Fig. 3.2G), iodothyronine deiodinase 2 (*Dio2*) (Fig. 3.2G), cell death-inducing DNA fragmentation factor-like effector A (*Cidea*) (Fig. 3.2G) and peroxisome proliferator-activated receptor gamma coactivator 1-alpha (*Ppargc1a*) (Fig. 3.2G) were all upregulated in the *Sf1*^{hM3dq} mice compared to the controls. However, I did not observe any differences in the PR domain containing 16 (*Prdm16*) (Fig. 3.2G) and elongation of very long chain fatty acids-3 (*Elovl3*) (Fig. 3.2G). These data, taken together with the indirect calorimetry and phenotypic measurements, indicate that the mice with activated VMN^{Sf1} neurons have an elevated capacity for thermogenesis, which could contribute to their loss of body weight and adipose mass.

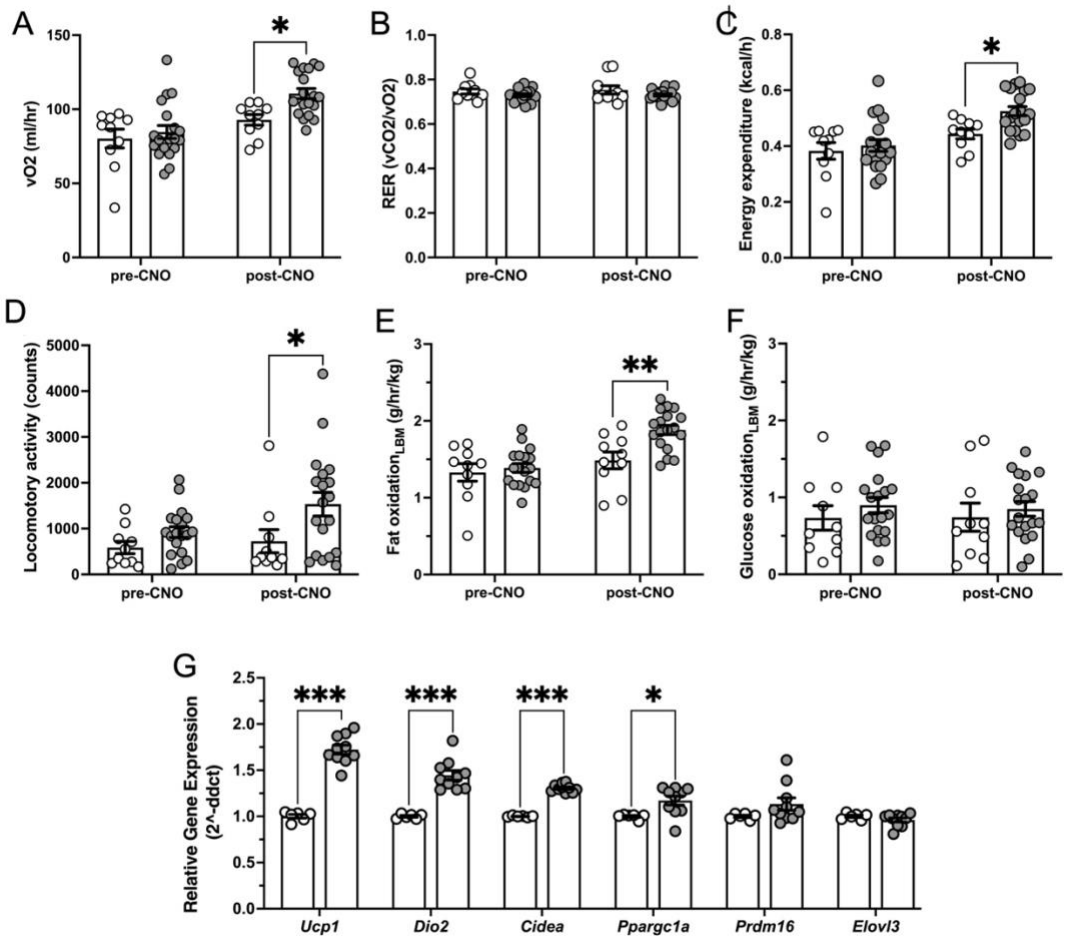

Figure 3.2: Activating VMN^{Sf1} neurons increases energy expenditure and iBAT thermogenic gene expression in diet induced obese male mice. I introduced *AAV$^{DIO\text{-}hM3dq\text{-}mCherry}$* into the VMN of either *Sf1^{Cre}* mice or their wild-type littermate controls (A). Then I tested the potential for activating VMN neurons in diet-induced following Clozapine-N-oxide (CNO) IP injection and measured vO2 (A), RER (B), energy expenditure (C), locomotory activity (D) using TSE chambers, and compared the parameters between the *Sf1^{Cre}* mice and their wild-type littermate controls as well as between 3 hours pre-CNO and 3 hours post-CNO. I also measured fat oxidation (E) and glucose oxidation (F) using the Weir equation and compared the parameters between the *Sf1^{Cre}* mice and their wild-type littermate controls as well as between 3 hours pre-CNO and 3 hours post-CNO. qRT-PCR was done for thermogenic markers in iBAT (G), which was harvested post- 2 hours IP CNO injection and before perfusion. n=5-12 male mice. Data expressed as mean ± SEM and analyzed by either one-way ANOVA (A-F) or multiple student's t-test (G). *p<0.05, **p<0.01, ***p<0.0001.

VMN^{PACAP} neurons send projections to the POA, thereby activating these neurons via glutamatergic signaling

I next investigated the efferent nodes of the VMN^{PACAP} neurons through which they transmit the signal downstream to the periphery (Fig. 3.3A). To test where these neurons project to, I administered *AAV$^{DIO\text{-}syn\text{-}mRuby}$* at the VMN of 8-12 weeks-old *Adcyap1^{Cre}* mice to identify where the terminals are most concentrated in the brain (Fig 3.3B, 3.3E, S2A, S2H, S2L). In a separate cohort of mice, I administered *AAV$^{DIO\text{-}hM3dq\text{-}mCherry}$* or *AAV$^{DIO\text{-}mCherry}$* at the VMN of 8-12 weeks-old *Adcyap1^{Cre}* mice to identify which of the projection sites exhibit cFos after activating VMN^{PACAP} neurons. I activated the VMN^{PACAP} neurons using IP CNO injections and observed projections (Fig. 3.3B, 3.3E) from the VMN^{PACAP} neurons and cFos following IP CNO (Fig. 3.3C-3.3D, 3.3F-3.3G) in the POA using fluorescence and counted the cFos induction (Fig. 3.3H). I observed that the VMN^{PACAP} neurons efferently project to relatively few places in the brain, but the most prominent projections are in the POA. These projections particularly overlay in the caudal POA (Fig. 3.3B, 3.3E), defined from +0.3 to -0.34mm bregma, that are just lateral to the suprachiasmatic nucleus (SCN), above optic tract (OPT), but not in the traditional more rostral (+0.6 to +0.3mm bregma) regions required for stable body temperature. Besides the caudal POA, I also found VMN^{PACAP} projections in the BNST (Supplementary Fig. S2A-S2G), followed by lesser dense projections in the PVT (Supplementary Fig. S2H-S2K) and PAG (Supplementary Fig. S2L-S2R). I measured cFos induction at all the projection sites following IP CNO injection and compared them between PACAP^{hM3dq} mice (Fig. 3.3D, 3.3G; Supplementary Fig. S2C, S2F, S2J, S2N, S2Q) and PACAP^{mCherry} control mice (Fig. 3.3C, 3.3F; Supplementary Fig. S2B, S2E,

S2I, S2M, S2P) and counted the cFos at each of these projection sites (Fig. 3.3H; Supplementary Fig. S2D, S2G, S2K, S2O, S2R). I found that cFos in the $PACAP^{hM3dq}$ mice were increased compared to the control mice in both sexes and at all projection sites.

Because the POA has been known to be critical for energy expenditure and tissue thermogenesis (Clapham 2012, Morrison, Madden et al. 2014, Yu, Francois et al. 2018) and this was the site where I observed the densest collection of synaptic terminals, I investigated whether the functional output of the VMN^{PACAP} neurons is at the caudal POA. I tested whether VMN^{PACAP} neurons directly activate cells in the caudal POA by measuring mini excitatory postsynaptic potential within neurons in the caudal POA following local stimulation of ChR2 in axonal terminals. For this, I unilaterally administered channelrhodopsin (ChR2) via $AAV^{DIO\text{-}ChR2\text{-}eYFP}$ at the VMN of 8-12 weeks-old $Adcyap1^{Cre}$ mice. ChR2 is expressed throughout the axon; thus, fiber optic light stimulation at the projection site will release vesicle pools from neurons that project to that site, but not from neurons that project elsewhere. Following sufficient time to induce expression of ChR2 throughout the neurons (4 weeks post-surgery), we performed electrophysiologic recording from neurons in apposition to ChR2-positive fibers using optogenetics, commonly referred to ChR2-assisted circuit mapping (CRACM) (Cheriyan, Kaushik et al. 2016, Cheriyan and Sheets 2020, Li and Sheets 2020) (Fig. 3.3I-3.3J). In a CRACM experiment, excitatory signal transmission between neurons is studied using optogenetics and electrophysiology. Presynaptic neurons expressing light-sensitive ChR2 are activated by photo-stimulation, leading to glutamate release. This glutamate binds to postsynaptic AMPARs (α-amino-3-hydroxy-5-methyl-4-isoxazolepropionic acid

receptor), generating an excitatory postsynaptic current via sodium influx. If the depolarization is sufficient, NMDARs (N-methyl-D-aspartate receptor) also open, allowing calcium influx, which contributes to synaptic plasticity. Patch-clamp recordings capture these responses, revealing functional synaptic connections and excitatory circuit dynamics. We stimulated the VMN axonal inputs of these mice with blue light (490nm) and recorded from the caudal POA (Fig. 3.3I). Electrophysiological responses recorded in artificial cerebrospinal fluid (aCSF) alone revealed an excitatory current followed by an inhibitory current after stimulation of VMN inputs (Fig. 3.3J). Addition of glutamatergic blockers (CPP and NMQX 5μM) eliminated both the excitatory and inhibitory responses, which inhibits that VMN inputs are excitatory and drive feed-forward inhibition of caudal POA neurons via activation of local inhibitory neurons (Fig. 3.3J). The percentage of cells activated and/or inhibited at either caudal POA or SCN (control region) were calculated in both sexes of mice (Fig. 3.3K). I found that in both sexes of mice, VMN stimulation evoked both excitatory and inhibitory responses at caudal POA (11 of 14 neurons in males; 4 of 6 neurons in females). In males, 3 out 14 recorded caudal POA neurons did not respond to optogenetic stimulation of VMN inputs in slices where responses in other neurons were detected (Fig. 3.3K). In females, one caudal POA neuron displayed only an inhibitory response to VMN stimulation with one other neuron showing no response (Fig. 3.3K). Minimal responses were measured in SCN neurons following VMN input stimulation. Only 1 in 5 SCN neurons in male mice displayed both excitatory and inhibitory responses with the remaining 4 neurons showing no response (Fig. 3.3K). In females, 2 out of 4 SCN neurons responded to VMN stimulation; one

producing only an excitatory response with the other producing only an inhibitory response (Fig. 3.3K).

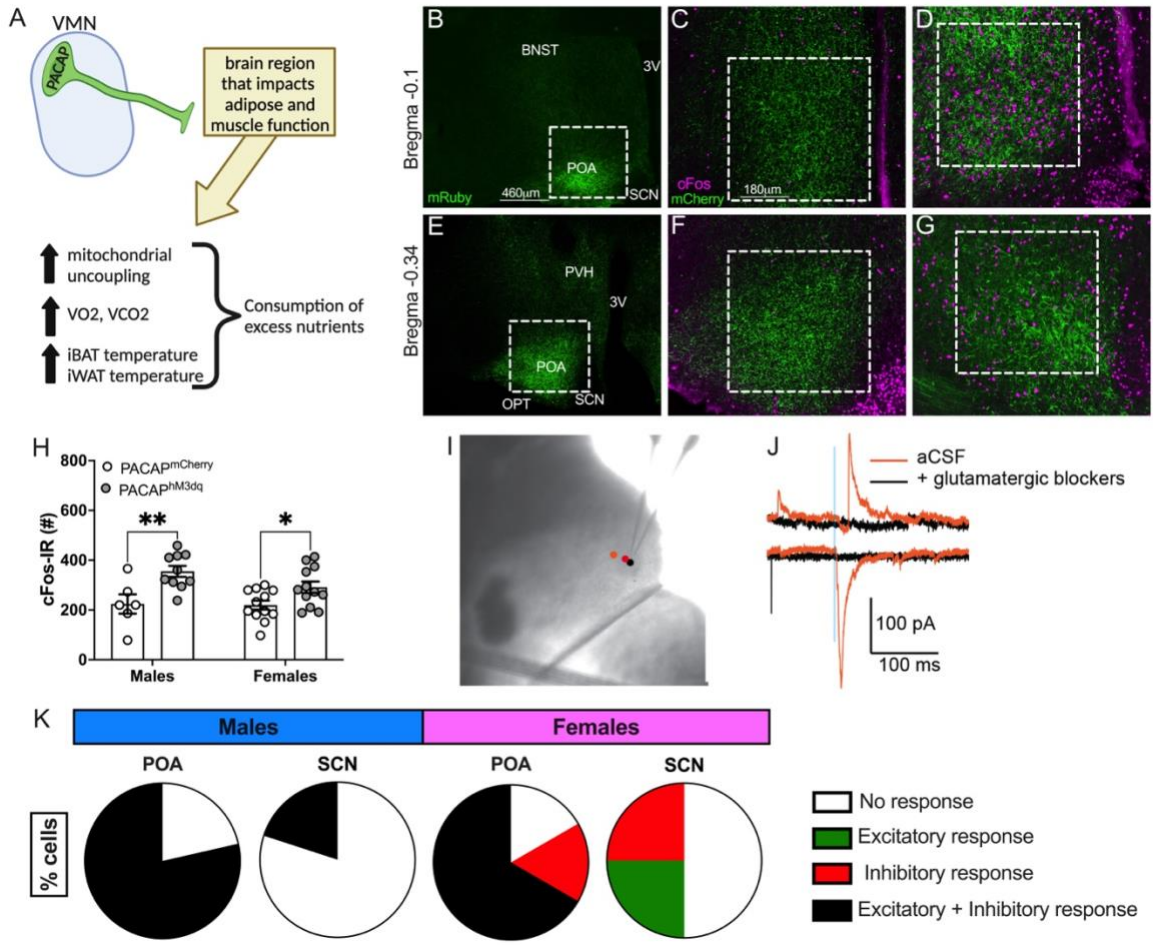

Figure 3.3: VMN^{PACAP} neurons send projections to the POA, thereby activating these neurons via glutamatergic signaling. I identified a new site that VMN^{PACAP} neurons project to, using *AAV$^{DIO\text{-}syn\text{-}mRuby}$* to see the projections from VMN and AAV$^{DIO\text{-}hM3dq}$ to measure neuronal activation via cFos induction. I observed projections (B,E) from VMN *Adcyap1^{Cre}* neurons and cFos following IP CNO (C-D, F-G) in the POA and counted (H). Scalebar = 180µm. In addition, I recorded from 12 caudal POA neurons while activating ChR2-positive fibers from VMN *Adcyap1^{ChR2}* neurons in both normal CSF and in the presence of either glutamate (CPP and NMQX, 5µM) blockers and the percentage of caudal POA neurons activated or inhibited are counted (I-K). Representative traces are included (I). (H) N=6-10 mice. (J-K) N=19 cells (14 POA, 5 SCN) from 3 male mice and N=10 cells (6 POA, 4 SCN) from 3 female mice. 3V = 3rd ventricle. PVN = Paraventricular hypothalamic nucleus. SCN = Suprachiasmatic nucleus. OPT = Optic tract. Data expressed as mean ± SEM and analyzed by student's t-test (H), *p<0.05, **p<0.01.

Activating VMN^{PACAP} → caudal POA signaling induces tissue thermogenesis in both sexes of mice

I next tested the functional role for VMN^{PACAP} projections to the caudal POA and used the BNST as a control, given that projections from the VMN potently stimulate hyperglycemia which could be the mechanistic explanation for increasing energy expenditure and thermogenesis. For this I unilaterally administered *AAV$^{DIO\text{-}ChR2\text{-}eYFP}$* at the VMN of 8-12 weeks-old *Adcyap1^{Cre}* mice, combined sexes, as previously described (Flak, Patterson et al. 2014, Flak, Arble et al. 2017, Flak, Goforth et al. 2020) and implanted optical fiber (optrode) at either the caudal POA efferents or the BNST efferents as well as at the VMN somas (Fig. 3.4A-3.4B), to stimulate the optrodes using blue light to activate the ChR2 that was expressed along the axon and terminals of the VMN neurons. Additionally, I implanted temperature-sensing microchips at iBAT and iWAT. Following sufficient time to induce expression of ChR2 throughout the neurons (4 weeks post-surgery), I began the experiments. I measured temperature at iBAT (Fig. 3.4C, 3.4F, 3.4I) and iWAT (Fig. 3.4D, 3.4G, 3.4J) and blood glucose (Fig. 3.4E, 3.4H, 3.4K) over the course of 2 hours following the onset of blue light flash into the optrodes. I ran each experiment two times: once with blue light on and once with no blue light and the treatments were flipped for the experiments. Activating VMN^{PACAP} somas containing ChR2, via blue light, increased iBAT (Fig. 3.4C) and iWAT (Fig. 3.4D) temperature by 1°C and .5°C respectively and blood glucose by ~10mg/dL compared to the no blue light stimulation control. Blue light stimulation of the efferents containing ChR2 at the caudal POA, showed a similar increase in iBAT (Fig. 3.4F) and iWAT (Fig. 3.4G) temperature as well as blood glucose (Fig. 3.4H) compared to the no light stimulation control.

However, blue light stimulation of the efferents containing ChR2 at the BNST did not show a change in temperature at iBAT (Fig. 3.4I) or iWAT (Fig. 3.4J) but elevated blood glucose (Fig. 3.4K) compared to the control.

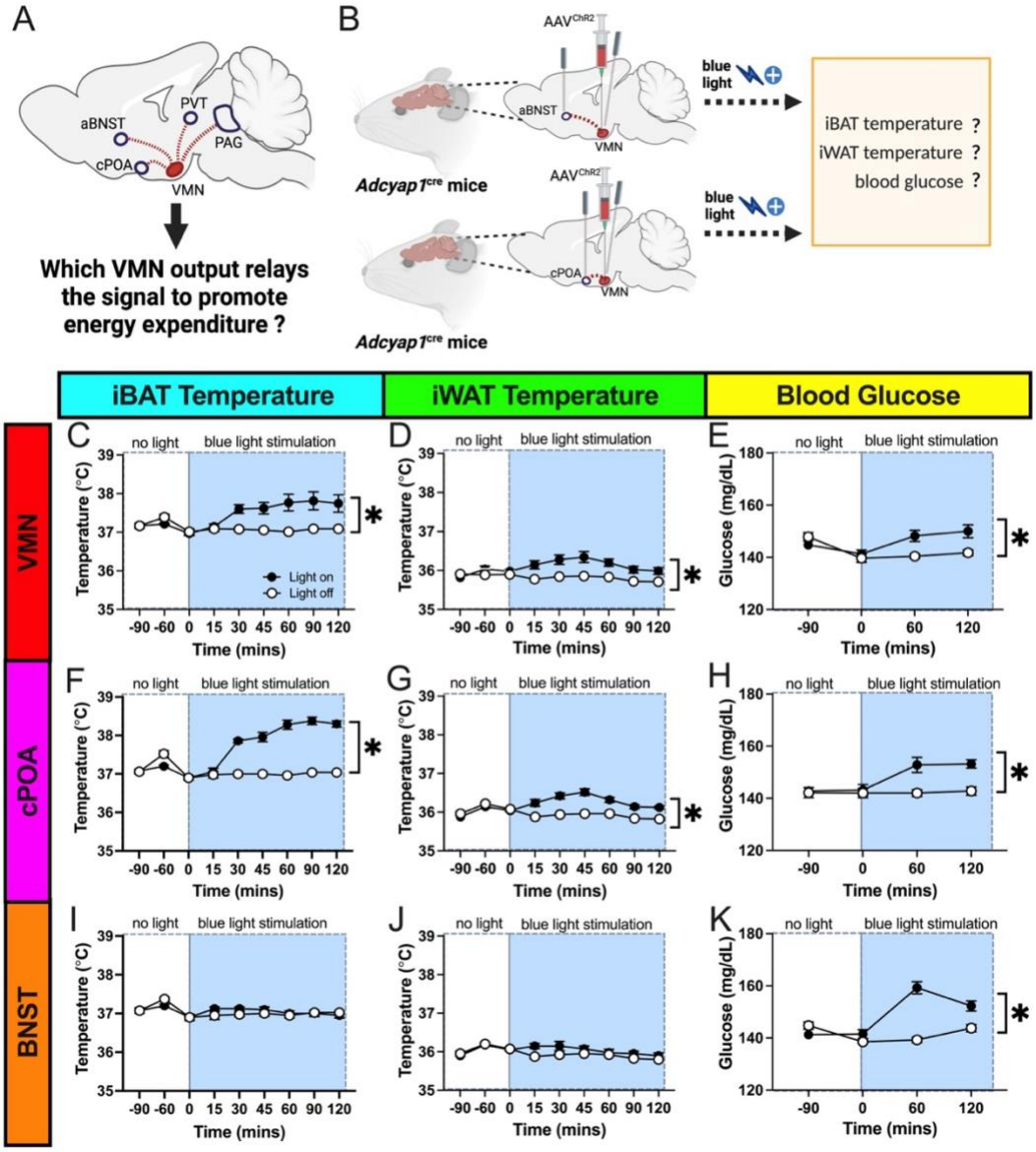

Figure 3.4: Activating VMN^{PACAP} → caudal POA signaling induces tissue thermogenesis in both sexes of mice. To test functional output of VMN^{PACAP} neurons (A), I introduced *AAV$^{DIO\text{-}ChR2\text{-}eYFP}$* in *Adcyap1^{Cre}* mice and implanted optrodes at VMN somas as well as at either caudal POA efferents or BNST efferents (B) and temperature microchips at iBAT and iWAT. To activate VMN^{PACAP} neurons at either cell body (C-E), caudal POA efferents (F-H), or BNST efferents (I-K), I stimulated either of the optrodes with blue light for 2 hours and measured temperature above iBAT (C-I) and iWAT (D-J) and blood glucose (E-K). Data expressed as mean ± SEM and analyzed by two-way RM ANOVA, N=7-14, *p<0.05. (A-B) Created with Biorender.com.

After 24 hours fasting, activation of VMN^{PACAP} → caudal POA signaling restores thermogenic activity in both sexes of mice

I then tested the effect of dietary signals and changes to feeding conditions on VMN^{PACAP} → caudal POA signaling and its thermogenic control. Importantly fasting reduces thermogenesis in adipose tissue depots, which could also suppress the ability for VMN^{PACAP} neurons to induce thermogenesis, but VMN^{PACAP} could also be effective at inducing thermogenesis when suppressed during negative energy balance. *Adcyap1^{ChR2}* mice from the previous set of optogenetics experiment in chapter 2, were fasted for 24 hours and then tested to determine if suppression of thermogenesis due to fasting can be overridden by activating these projections (Fig. 3.5A). I measured temperature at iBAT (Fig. 3.5B, 3.5E, 3.5H) and iWAT (Fig. 3.5C, 3.5F, 3.5I) and blood glucose (Fig. 3.5D, 3.5G, 3.5J) over the course of 2 hours following the onset of blue light flash into the optrodes. I ran each experiment 3 times: (1) before fasting began with blue light off, (2) after 24-hour fasting with blue light on and (3) after 24-hour fasting with blue light off, and the treatments were flipped for the experiments. 24-hour fasting led to a drop in iBAT temperature (Fig. 3.5B, 3.5E, 3.5H), iWAT temperature (Fig. 3.5C, 3.5F, 3.5I) and blood glucose levels (Fig. 3.5D, 3.5G, 3.5J) in the mice compared to the pre-fasting levels (control). Activating VMN^{PACAP} somas containing ChR2, via blue light, restored iBAT temperature (Fig. 3.5B) and blood glucose (Fig. 3.5D) to pre-fasting levels, however iWAT temperature (Fig. 3.5C) was not restored. Blue light stimulation of the efferents containing ChR2 at the caudal POA, showed a restoration of both iBAT (Fig. 3.5E) and iWAT (Fig. 3.5F) temperatures but not blood glucose (Fig. 3.5G) compared pre-fasting levels. In contrast, blue light stimulation of the efferents containing ChR2 at

the BNST did not restore iBAT (Fig. 3.5H) or iWAT (Fig. 3.5I) temperatures but restored blood glucose level (Fig. 3.5J) to pre-fasting levels.

To eliminate the possibility that ChR2 expression or the blue light itself is leading to any unwanted physiological effects, I administered $AAV^{DIO\text{-}\,eGFP}$ at the VMN of a separate cohort of 8-12 weeks-old $Adcyap1^{Cre}$ mice, combined sexes and performed identical optogenetics experiment as discussed above. I ran each experiment 4 times: (1) before fasting began with blue light on, (2) before fasting began with no blue light, (3) after 24-hour fasting with blue light on and (4) after 24-hour fasting with no blue light, and the treatments were flipped for the experiments. Blue light stimulation of the efferents at the caudal POA after 24-hour fasting, showed no change in iBAT (Supplementary Fig. S3A) or iWAT (Supplementary Fig. S3B) temperatures or blood glucose levels (Supplementary Fig. S3C) compared pre-fasting levels. Similarly, blue light stimulation of the efferents at the BNST showed no difference in iBAT (Supplementary Fig. S3D) or iWAT (Supplementary Fig. S3E) temperatures or blood glucose level (Supplementary Fig. S3F) compared to pre-fasting levels. Also, when temperatures at iBAT or iWAT and blood glucose levels were compared between similar groups with blue light on versus groups with blue light off, no difference was found.

In summary, these data indicate that VMN^{PACAP} → caudal POA connection is necessary for tight thermogenic control when feeding conditions change. All these together indicate, VMN^{PACAP}, as well as associated signaling targets, are critical components to the control of energy balance by activating energy expenditure that impact adipose tissue function.

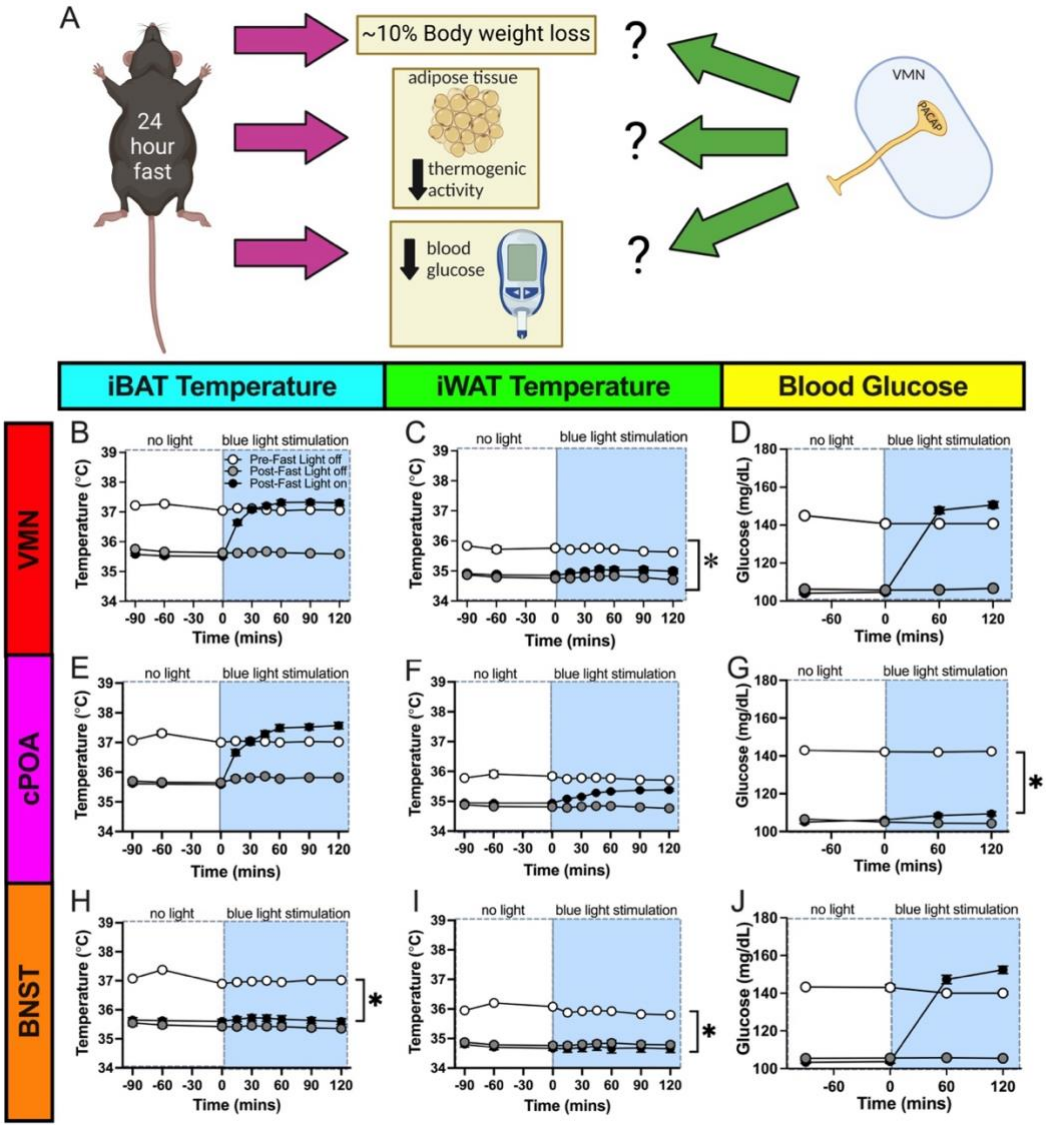

Figure 3.5: After 24 hours fasting, activation of VMN^{PACAP} → caudal POA neurons restores thermogenic activity in both sexes of mice. In *Adcyap1*^{Cre} mice, I introduced *AAV*$^{DIO\text{-}ChR2\text{-}eYFP}$ and implanted optrodes at VMN somas as well as at either caudal POA efferents or BNST efferents and temperature microchips at iBAT and iWAT. Then, I subjected the mice to blue light stimulation or without blue light stimulation for 2 hours to test the potential for *Adcyap1* neurons to impact brown and beige fat thermogenesis during fasting to restore normal levels of thermogenesis (A). I fasted the mice from figure 4 for 24 hours and then stimulated either at VMN somas (B-D), caudal POA efferents (E-G), or BNST efferents (H-J) with blue light for 2 hours and measured temperature above iBAT (B,E,H) and iWAT (C, F, I) temperature and blood glucose (D-J). All data expressed as mean ± SEM and analyzed by two-way RM ANOVA. N=7-14 mixed male and female mice. *p<0.05. (A) Created with Biorender.com.

Acute activation of VMN^{PACAP} → caudal POA neurons induces distinct molecular programs within brown and beige adipose tissue in both sexes of mice

I next investigated how the VMN^{PACAP} → caudal POA signaling affects the molecular programs within the iBAT and iWAT. I administered *AAV$^{DIO\text{-}ChR2\text{-}eGFP}$* at the VMN of 8-12 weeks-old *Adcyap1^{Cre}* mice, combined sexes, in a separate cohort of mice, as described previously, and implanted optrodes at the caudal POA efferents. Then, I subjected them to blue light stimulation or without blue light stimulation for 2-hours and tested them for temperatures at iBAT and iWAT, as described previously, and then the iBAT and iWAT harvested from the mice after anesthesia, prior to transcardial perfusion. Total RNA from the iBAT and iWAT was isolated and sequenced. Total RNA-sequencing (RNA-seq) analysis (Fig. 3.5A) was performed in the iBAT (Fig. 3.6B-3.6E) and iWAT (Fig. 3.6F-3.6I) of these mice 6 weeks after viral injection. Functional enrichment analysis, also called gene set analysis (GSA), was performed in iBAT (Fig. 3.6D-3.6E) and iWAT (Fig. 3.6H-3.6I) to discover biological annotations that are upregulated (Fig. 3.6D, 3.6H) or downregulated (Fig. 3.6E, 3.6I), within the list of top 20 differentially expressed genes (Fig. 3.6B-3.6C, 3.6F-3.6G).

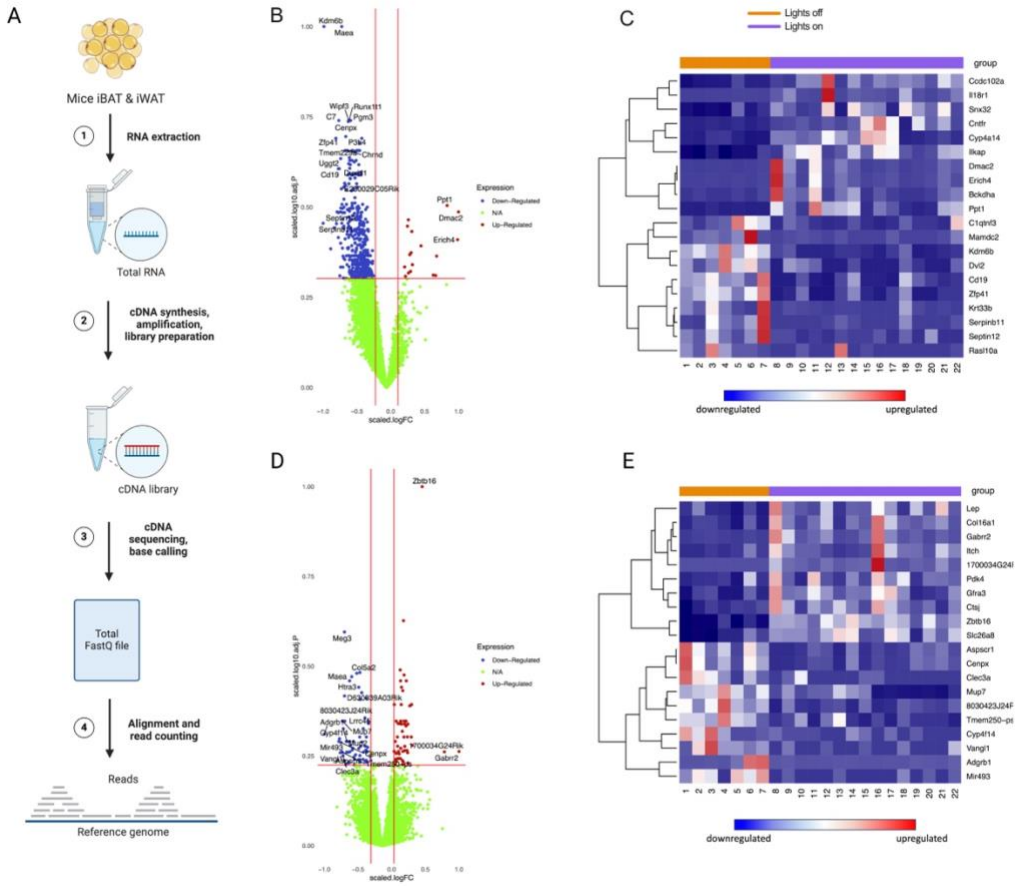

Figure 3.6: Acute activation of VMN^{PACAP} → caudal POA neurons induces distinct molecular programs in brown and beige adipose tissue in both sexes of mice. In *Adcyap1^{Cre}* mice, I introduced *AAV$^{DIO\text{-}ChR2\text{-}eYFP}$* and implanted optrodes at VMN somas and at either caudal POA efferents or BNST efferents and temperature microchips at iBAT and iWAT. Then, I subjected the mice to blue light stimulation or without blue light stimulation for 2 hours and then the iBAT and iWAT were harvested from the mice after anesthesia, prior to transcardial perfusion. I then isolated total RNA from the iBAT and iWAT and performed total RNA-sequencing (A) of iBAT and iWAT isolated from mice after acute activation of VMN^{PACAP} → caudal POA neurons using optogenetics. Volcano plots (B,D), heatmaps (C,E) from iBAT (B,C) and iWAT (D,E) were generated. N=12-14 mixed male and female mice. (A) Created with Biorender.com.

Comparison between molecular mechanisms and biological processes that are associated with mice with blue light stimulation versus control mice without blue light stimulation. In iBAT, I found molecular mechanisms contributing to the mitochondrial electron transport chain and cellular proliferation to be upregulated (Fig. 3.7A) whereas molecular mechanisms aiding in lipid metabolism and cellular structural organization and protein post-translational modification/degradation pathways were downregulated (Fig. 3.7B). However, in iWAT, I found the pathways facilitating nuclear and cellular restructure and remodeling to be upregulated (Fig. 3.7C), while some downregulation in molecular pathways contributes to cell differentiation (Fig. 3.7D)

I also validated the top 3 hits from the RNA-sequencing analysis, using qRT-PCR of iBAT (Supplementary Fig. S4A) or iWAT (Supplementary Fig. S4B). I found *Ppt1*, *Kdm6b* to be upregulated in iBAT and *Zbtb16* and *Slc26a8* to be upregulated in iWAT, whereas the gene *MaeA* was downregulated in both iBAT and iWAT, confirming what I found in the RNA-sequencing results. In iBAT, *Ppt1* encodes an enzyme involved in lysosomal hydrolysis of fatty acids, potentially regulating energy metabolism, and *Kdm6b* promotes browning of iWAT. In iWAT, *Zbtb16* induces mitochondrial fatty acid oxidation and uncoupling, while *Slc26a8* enhances anion transport, impacting ATP synthesis and energy expenditure. *MaeA*, downregulated in both iBAT and iWAT, may influence nutrient sensing and energy metabolism through its role in autophagy and maintenance of hematopoietic stem cells. These findings highlight distinct genetic programs in brown and beige adipose depots, key for energy balance and thermogenic adaptation.

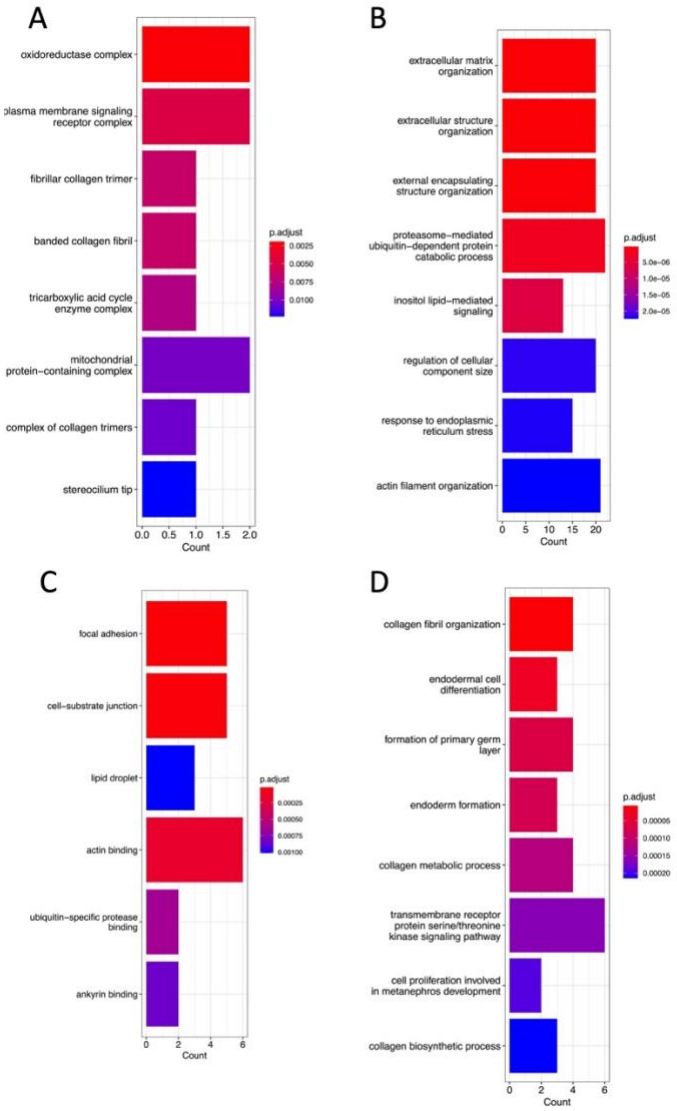

Figure 3.7: Acute activation of VMN^{PACAP} → caudal POA neurons induces distinct molecular programs but with similar peripheral functions in brown and beige adipose tissue in both sexes of mice. In *Adcyap1^{Cre}* mice, I introduced *AAV$^{DIO\text{-}ChR2\text{-}eYFP}$* and implanted optrodes at VMN somas and at either caudal POA efferents or BNST efferents and temperature microchips at iBAT and iWAT. Then, I subjected the mice to blue light stimulation or without blue light stimulation for 2 hours and then the iBAT and iWAT were harvested from the mice after anesthesia, prior to transcardial perfusion. I then isolated total RNA from the iBAT and iWAT and performed total RNA-sequencing of iBAT and iWAT isolated from mice after acute activation of VMN^{PACAP} → caudal POA neurons using optogenetics. Functional enrichment plots with upregulated genes

(A,C) and downregulated genes (B,D) from iBAT (A,B) and iWAT (C,D) were generated. N=12-14 mixed male and female mice. (A) Created with Biorender.com.

Activation of the of VMN^{PACAP} neurons leads to highest neuronal activation at caudal POA, among all collaterals, via the VMN^{PACAP} projections

I then tested whether activation of VMN^{PACAP} neurons' efferents at caudal POA, and not any other collateral nuclei like BNST, PVT or PAG, are responsible for tissue thermogenesis at iBAT and iWAT in mice. Since, cFos induction is a marker of neuronal activation, I first observed projections (Fig. 3.8A, 3.8D, 3.8G, 3.8K, 3.8N) from the VMN^{PACAP} neurons *AAV$^{DIO\text{-}syn\text{-}mRuby}$* at the VMN of 8-12 weeks-old *Adcyap1^{Cre}* mice to identify where the terminals are most concentrated in the brain. Then using brain sections from *Adcyap1^{Cre}* mice included in aforementioned experiments and counted cFos (Fig. 3.8B, 3.8E, 3.8L, 3.8O) in all those nuclei where the VMN^{PACAP} neurons projected to, i.e., caudal POA, BNST, PVT and PAG and compared them. I counted cFos induction in the mice with blue light stimulation (light on) and compared them with the group with no blue light stimulation (light off) (Fig. 3.8C, 3.8F, 3.8I, 3.8J, 3.8M, 3.8P, 3.8Q). I also compared cFos induction between the contralateral (in relation to side with unilateral AAV injection and optrode placement) and ipsilateral sides of the mice with blue light stimulation (light on) (Fig. 3.8C, 3.8F, 3.8I, 3.8J, 3.8M, 3.8P, 3.8Q). I found that blue light stimulation (light on) at VMN lead to increased cFos induction when compared to the light off group (Fig. 3.8C, left) as well as the ipsilateral sides when compared to the contralateral sides (Fig. 3.8C, right) of the mice that received blue light stimulation (light on). Blue light stimulation (light on) at the caudal POA lead to a similar increase in cFos induction when compared to the light off group (Fig. 3.8F, left) and a similar increase on

the ipsilateral sides when compared to the contralateral sides (Fig. 3.8F, right) of the mice that received blue light stimulation (light on). On the contrary when I counted cFos induction at BNST (Fig. 3.8H) and measured cFos at both the dorsal BNST (Fig. 3.8I) and ventral BNST (Fig. 3.8J) after blue light stimulation (light on) of that node, I did not see a significant change in the cFos induction when compared to the light off group (Fig. 3.8I, left) and neither did I find any significant change in the cFos induction when the ipsilateral sides were compared to the contralateral sides (Fig. 3.8I, right) of the mice that received blue light stimulation (light on). I also did not find any significant change in the cFos induction at PVT (Fig. 3.8L) when comparing light on and light off groups (Fig. 3.8M, left) or the contralateral versus ipsilateral sides (Fig. 3.8M, right) of the mice that received blue light stimulation (light on). When measuring activity at PAG (Fig. 3.8O), I found that blue light stimulation (light on) at VMN lead to increased cFos induction at dorsal PAG when compared to the light off group (Fig. 3.8P, left) as well as the ipsilateral sides when compared to the contralateral sides (Fig. 3.8P, right) of the mice that received blue light stimulation (light on). But the at the ventral PAG there was no significant change in cFos induction when comparing light on and light off groups (Fig. 3.8Q, left) or the contralateral versus ipsilateral sides (Fig. 3.8Q, right) of the mice that received blue light stimulation (light on). These results validated that, activation of VMN^{PACAP} neurons' efferents at caudal POA, and not any other collateral nuclei, are responsible for tissue thermogenesis at iBAT and iWAT in mice.

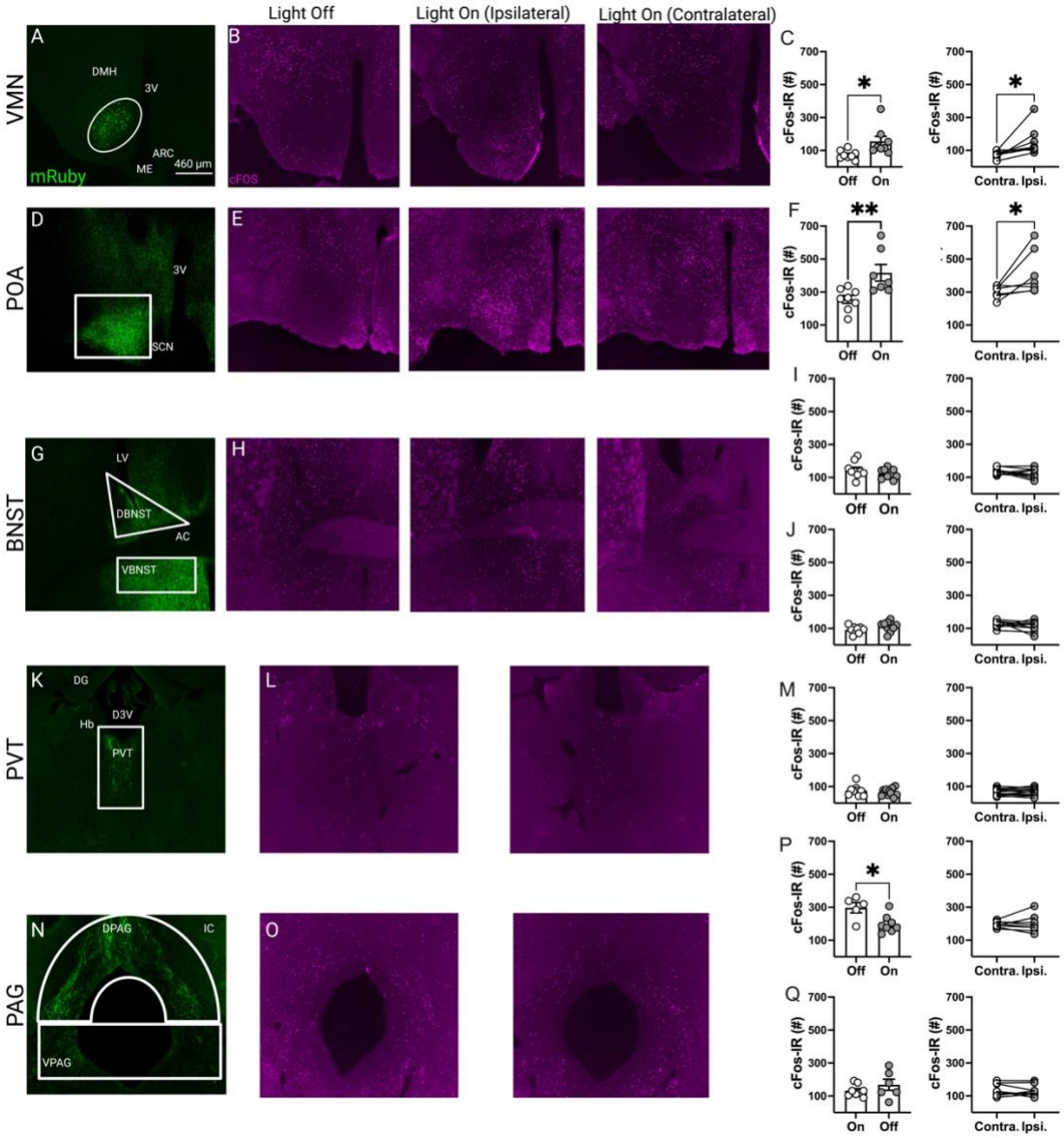

Figure 3.8: Activation of the VMN^{PACAP} neurons leads to highest neuronal activation at caudal POA, among all collaterals, via the VMN^{PACAP} projections. I took brain sections from *Adcyap1^{Cre}* mice included in the previous experiments (Figures 3.3, 3.4, 3.5) and stained for mRuby and for cFos separately. Representative traces showing mRuby at VMN (A), POA (D), BNST(G), PVT (K), PAG (N). Representative traces showing cFos induction during 3 different conditions: (1) light off (left panels of B, E, H, L, O), (2) light on and ipsilateral side (middle panels of B, E, H, L, O) and (3) light on and contralateral side (right panels of B, E, H, L, O). The cFos was observed at VMN (B) and all the projection sites after blue light stimulation: at POA (E), BNST (H), PVT (L), PAG (O) and counted. The cFos induction at each region was counted and compared:

VMN (C), POA (F), dorsal BNST (I), ventral BNST (J), PVT (M), dorsal PAG (P), ventral PAG (Q) and compared between the light off versus light on groups (left panels of C, F, I, J, M, P, Q) and between the contralateral (light on) versus ipsilateral (light on) groups (right panels of C, F, I, J, M, P, Q). In the representative images of cFos counts for PVT (L) and PAG (O), the contralateral and ipsilateral sides are represented together in one image, with the left side of the images showing the ipsilateral side and the right side showing the contralateral side. N=6-10 mice. Scalebar = 460μm (A, D, G, K, N) and 180μm (B, E, H, L, O). LV = Lateral ventricle. 3V = 3rd ventricle. AC = Anterior commissure. DBNST = Dorsal bed nucleus of stria terminalis. VBNST = Ventral bed nucleus of stria terminalis. DG = Dentate gyrus. D3V = Dorsal 3rd ventricle. Hb = Habenular commissure. PVT = Paraventricular thalamus. DPAG = Dorsal periaqueductal gray. VPAG = Ventral periaqueductal gray. IC = Inferior colliculus. Aq = Aqueduct. Data expressed as mean ± SEM and analyzed by student's t-test (left and right panels of C, F, I, J, M, P, Q), *$p<0.05$, **$p<0.01$.

Activating VMN^{PACAP} neurons with simultaneous inhibition of the caudal POA neurons blunts adipose tissue thermogenesis in both sexes of mice

I then tested whether activation of VMN^{PACAP} → caudal POA neurons, indeed, is necessary for tissue thermogenesis at iBAT and iWAT in mice, I activated the VMN^{PACAP} neurons while inhibiting the caudal POA neurons and studied the effect on iBAT and iWAT temperatures in both sexes of mice. For this, I unilaterally administered *AAV$^{DIO\text{-}ChR2\text{-}eYFP}$* at the VMN and *AAV$^{hM4Di\text{-}mCherry}$* at the caudal POA of 8-12 weeks-old *Adcyap1^{Cre}* mice, combined sexes, as previously described (Flak, Patterson et al. 2014, Flak, Arble et al. 2017, Flak, Goforth et al. 2020) to induce cre-dependent expression of ChR2 at the VMN and cre-independent expression of hM4Di at the caudal POA (Fig. 3.9A). I also, implanted an optical fiber (optrode) at the caudal POA efferents (Fig. 3.9A). This was done to stimulate the optrode using blue light to activate the ChR2 that was expressed along the axon and terminals of the VMN neurons and concurrently the inhibit the neurons at the caudal POA via CNO IP injection, where the CNO will work on

the hM4Di receptors expressed in the caudal POA neurons. Additionally, I implanted temperature-sensing microchips at iBAT and iWAT. Following sufficient time to induce expression of cre-dependent ChR2 and cre-independent hM4Di throughout the VMN and caudal POA neurons respectively (4 weeks post-surgery), I began the experiments. I measured temperature at iBAT (Fig. 3.9B, 3.9C, 3.9D) and iWAT (Fig. 3.9E, 3.9F, 3.9G) over the course of 2 hours following the onset of blue light flash into the optrodes. I ran each experiment four times: with blue light on or with no blue light as well as with IP CNO or saline administration and the treatments were flipped for the experiments. Blue light stimulation of the VMN^{PACAP} efferents containing ChR2 at the caudal POA along with IP saline administration, increased iBAT (Fig. 3.9B, 3.9C) by 1°C and with no change in iWAT (Fig. 3.9D, 3.9E) temperature, compared to the no blue light stimulation control. Whereas when the blue light stimulation, to activate VMN^{PACAP} efferents containing ChR2 at the caudal POA, was combined with the IP CNO administration, to inhibit the hM4Di expressing caudal POA neurons, there was no increase in iBAT (Fig. 3.9B, 3.9C) or iWAT (Fig. 3.9D, 3.9E) temperature compared to the no blue light stimulation control.

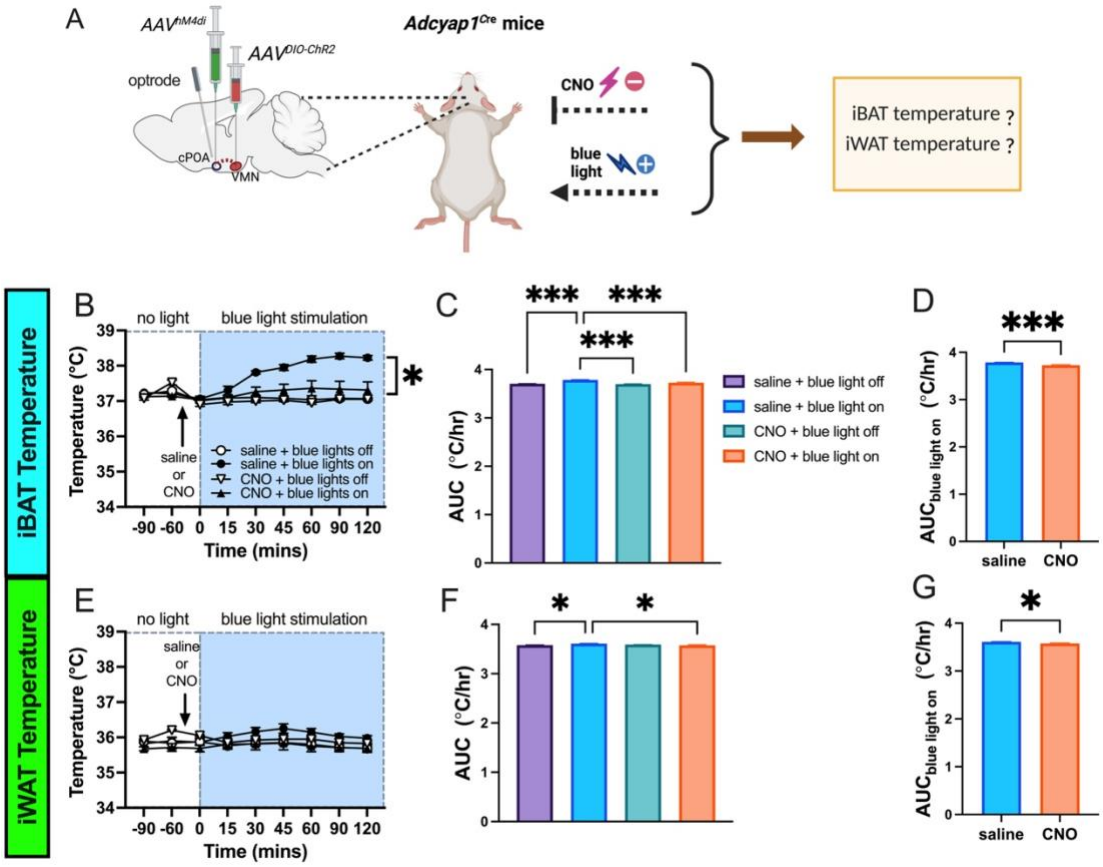

Figure 3.9: Activating VMN^{PACAP} neurons with simultaneous inhibition of the caudal POA neurons blunts adipose tissue thermogenesis in both sexes of mice. I unilaterally administered *AAV$^{DIO\text{-}ChR2\text{-}eYFP}$* at the VMN and *AAV$^{hM4Di\text{-}mCherry}$* at the caudal POA of *Adcyap1^{Cre}* mice and implanted an optrode at the caudal POA efferents (A). I then measured iBAT (B) and iWAT (E) temperatures after activating the VMN^{PACAP} neurons while inhibiting the caudal POA neurons and compared the results between the groups. I also measured the area under the curve at iBAT (C) and iWAT (F) temperatures and compared between the different groups. I then separately compared area under the curve at iBAT (D) and iWAT (G) temperatures in the groups with blue light on and compared between IP saline with Ip CNO injection. N=9 mixed male and female mice. Data expressed as mean ± SEM and analyzed by either two-way RM ANOVA (B, E), one-way ANOVA (C, F) or by student's t-test (D, G). *p<0.05, **p<0.01, ***p<0.0001. (A) Created with Biorender.com.

Overall model

Together data demonstrates that the subpopulation of VMN^{Sf1} neurons expressing the PACAP neuropeptide, projects to caudal POA and transmits the signal downstream to the periphery (Fig. 3.10). These VMN neurons transmit the signal to the periphery to iBAT and iWAT via the preoptic outputs to increase thermogenesis and energy expenditure by means of mitochondrial uncoupling. While acute activation of this neurocircuit promotes thermogenesis at iBAT and induces mechanisms involved in browning, at iWAT; chronic activation of this circuit leads to elevated thermogenic programming in iBAT and iWAT which ultimately improves metabolization of excess energy resulting in weight loss.

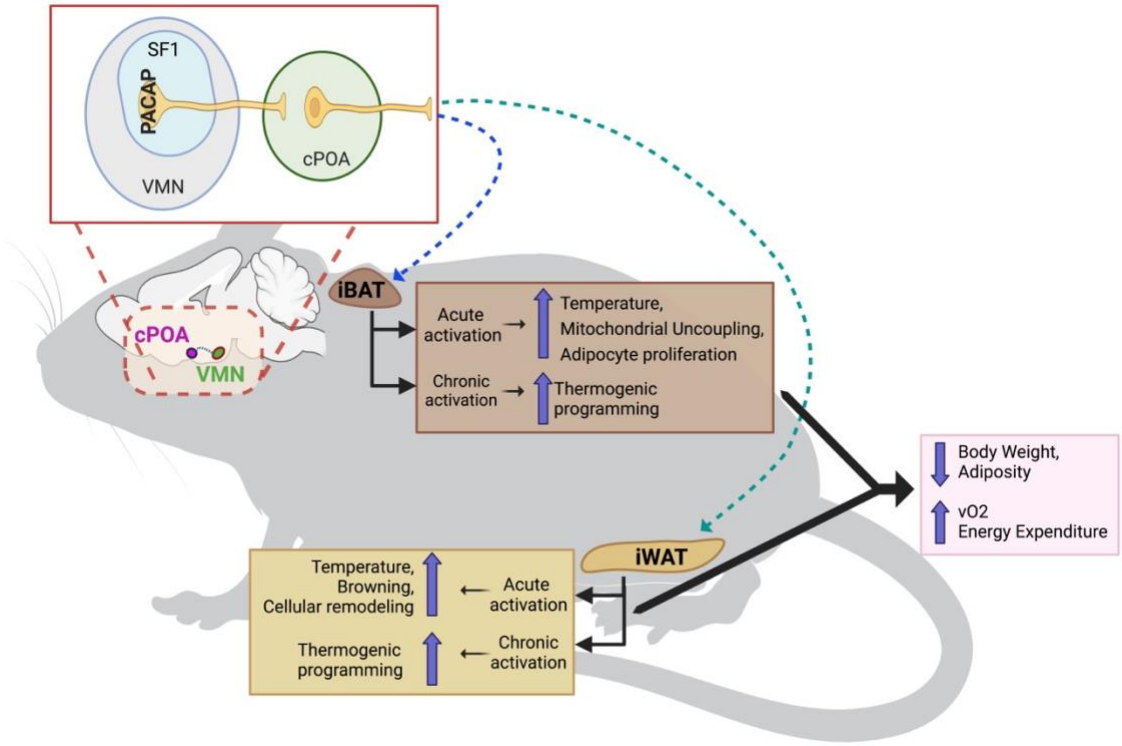

Figure 3.10: Overall model. data indicates that the subpopulation of VMN^{Sf1} neurons expressing the PACAP neuropeptide, projects to caudal POA. These VMN^{PACAP} neurons transmit distinct signals to the periphery to iBAT and iWAT via the caudal POA. Acute activation of this neurocircuit promotes distinct physiological mechanisms at iBAT and iWAT than what chronic activation of this circuit leads to. Together these mechanisms reduce body weight and adiposity and increase vO2 and energy expenditure. Created with Biorender.com.

Discussion

These data demonstrate that a subset of VMN neurons induce tissue thermogenesis via the POA, which can be activated to reduce obesity and increase energy expenditure in diet-induced obese male mice. Proper function and fine tuning of this neurocircuit is essential for the maintenance of energy balance via energy expenditure. Activation of this circuit increases temperature above both the brown and beige adipose

depots and reduces adipose mass in diet-induced obese male mice. Together with historical data linking nutrient sensing with the VMN, data support a model for this circuit is to elevate the metabolization of excess energy, when necessary, but not necessarily for the purpose of temperature control. In support of this notion, *Adcyap1* expression is reduced after both fasting and in *ob/ob* mice, which can each be restored by leptin administration (Zhang, Chen et al. 2020). Taken together with my data, PACAP regulation according to energy status signals is a key regulator of energy expenditure and for whole body energy balance. It remains to be seen if this circuit can be targeted for either body weight loss or normalizing energy expenditure in negative energy balance conditions.

These findings are consistent with the view that there is a subset of VMN cells that are essential in controlling tissue thermogenesis and energy expenditure. These data provide further support that the key subset contains the neuropeptide PACAP. Indeed, I extended upon data included in a previously published manuscript (Bozadjieva-Kramer, Ross et al. 2021) from the lab. In the previous paper, we demonstrated that a VMN-centered PACAP knockout leads to obesity in both male and female mice, that only leads to a modest increase in food intake once the animals are obese (Bozadjieva-Kramer, Ross et al.). Surprisingly, I only observed changes in glycemic responses after the mice had been obese for months, but not three weeks as they were developing the obesity phenotype. However, I observed suppressed energy expenditure during the early development of obesity. Also in this paper, I demonstrated that activating VMN^{PACAP} cells by DREADD-hM3dq induction induced iBAT thermogenesis. I reproduced that finding using ChR2-mediated activation and demonstrated that these cells have the

potential to also stimulate iWAT thermogenesis. These thermogenic functions are most effective during negative energy balance. Taken together with previous evidence that fasting and loss of leptin signaling reduces *Adcyap1* expression, these data demonstrate the potential for this circuit to override suppressed energy expenditure during periods of negative energy balance to metabolize excess nutrients, when necessary, via thermogenic signaling pathways. More investigation is needed to examine the contexts in which this circuit is recruited. While gene expression data suggests that this circuit is activated in energy balance excess and suppressed in negative energy balance, more data is needed. Additionally, there may be other signals that could impact the function of this circuit, including cold temperature.

Originally, it was assumed that energy expenditure stimulating VMN cells act via caudally projecting brainstem mechanisms (Swanson and Kuypers 1980), but the recent evidence using viral tracers has been lacking (Meek, Nelson et al. 2016, Faber, Matsen et al. 2018). Thus, VMN cells are more likely to be present further upstream in energy expenditure-controlling circuits than previously assumed. I and others have demonstrated that there are no projections into the key brain areas that control adipose tissue and muscle function (Meek, Nelson et al. 2016, Faber, Matsen et al. 2018, Sabatini, Wang et al. 2021). Furthermore, projections into the periaqueductal gray potently induce defensive behaviors, which is a shared function of the VMN and the periaqueductal gray (Wang, Chen et al. 2015). Thus, there must be an alternative output that the VMN activates as part of the essential circuit for energy expenditure stimulation by the VMN. Indeed, the VMN sends robust projections to the caudal POA, as I describe, which is a region in temperature control and locomotor activity. Induction of thermogenesis through the POA

likely involves activation of the sympathetic nervous activity. Denervation of the iBAT depletes UCP1 from adipocytes, reduces thermogenesis, leads to cold intolerance, and increases susceptibility to obesity (Morrison, Madden et al. 2014, Lee, Petkova et al. 2015, Rondini, Mladenovic-Lucas et al. 2017, Fischer, Schlein et al. 2019). Furthermore, optogenetic activation of tyrosine-hydroxylase nerves in iBAT induces a very similar rise in iBAT temperature from what I observed in study and involves temperature-responsive pathways through the POA (Morrison, Madden et al. 2014, Lyons, Razzoli et al. 2020). VMN^{PACAP} cells could engage these mechanisms that activate responses to cold and warm temperature or potentially a separate set of cells that don't directly control temperature but instead elevate metabolism in peripheral tissues via thermogenic pathways. Future studies will tease out the mechanisms by which the POA controls this function.

However, VMN^{PACAP} neurons are not a segregated population of VMN neurons and are expressed throughout the nucleus, but particularly in the dorsomedial division of the VMN. Other studies have demonstrated that many VMN neurons are glucose-responsive, but data would support VMN^{PACAP} neurons do not primarily control blood glucose because the induction of hyperglycemia by activating VMN^{PACAP} neurons is not as robust VMN^{Sf1} neurons, or the subset of VMN neurons that contain the cholecystokinin-b receptor (Meek, Nelson et al. 2016, Flak, Goforth et al. 2020). Indeed, I observe that the primary output from VMN^{PACAP} neurons is not the BNST, which is the output that VMN^{Sf1} neurons and VMN^{NOS1} neurons (expressing nitric oxide synthase 1) act via to mobilize blood glucose. While VMN^{PACAP} neurons may be glucose-responsive, the responsiveness to blood glucose may instead tune tissue thermogenesis in adipose tissue. Although, there may just be a small subset of VMN^{PACAP} neurons that participate

in the counterregulatory response to hypoglycemia intermingled with those that control energy expenditure.

There could be other functions for VMN^{PACAP} → caudal POA signaling. For instance, chronic activation may reveal effects outside of thermogenesis. Indeed, a recent study demonstrated that chronic activation of VMN^{Sf1} neurons reduced inflammatory markers within adipose tissue in diet-induced obese mice (Rashid, Kondoh et al. 2023). While this study focused on more acute signaling for thermogenesis, I could be missing long term effects for this circuit that could benefit the individual. In addition to other functions for this circuit, other important VMN functions are likely primarily driven by separate VMN cells. While I did observe an increase in blood glucose after activating projections to the BNST, this is much more modest than what has been observed with other VMN subpopulations (Meek, Nelson et al. 2016, Faber, Matsen et al. 2018, Flak, Goforth et al. 2020). However, continuous induction of thermogenic pathways in the adipose tissue could also impact lipid trafficking and glucose transport, which could have beneficial effects in diabetes and obesity. In addition, separate VMN cells induce stress and anxiety behaviors, which I did observe in the *Sf1*^{Cre} mice, but not in the *Adcyap1*^{Cre} mice. This likely is through a separate output, which is most likely the periaqueductal gray. However, the PVT has also been implicated in these functions and may serve another role, which could lead to anorexia upon activation (Zhang, Chen et al. 2020). More investigation is needed to define the output circuits from the VMN in all the functions related to the nucleus.

RNA-sequencing analysis of the iBAT and iWAT showed that acute activation (2 hours of stimulation) of VMN^{PACAP} → caudal POA signaling engages molecular

mechanisms that ultimately contribute, at least in part, to thermogenesis and improved energy metabolism. Importantly, canonical thermogenic genes are not among most differentially expressed genes in either iBAT or iWAT, likely due to the acute nature of the study only at 2 hours, mainly because thermogenic programming in adipose tissue typically occurs with stimulation over the course of days, (as I saw in study of *Adcyap1*^{VMN}*KO*). The most differentially upregulated genes in iBAT (Supplementary Fig. S6A): *Ppt1*, *Kdm6b* are involved in facilitating energy metabolism. *Ppt1* is known to be encoding an enzyme responsible for hydrolyzing long chain fatty acids from lysosomal cargo and interacts with the mitochondrial F_1 ATP-synthase (Lyly, Marjavaara et al. 2008) but its role in energy metabolism has not been explored. Since lysosomes can sense nutrient availability depending on their cargo storage and regulate energy metabolism (Settembre, Fraldi et al. 2013), I speculate that *Ppt1* contributes to regulation of energy metabolism as well. The gene *Kdm6b* encodes the protein KDM6B which facilitates browning of iWAT (Pan, Huang et al. 2015, Gao, Liu et al. 2021). In iWAT, the most differentially upregulated genes (Supplementary Fig. S6B): *Zbtb16* and *Slc26a8* are also found to be involved in induction of mitochondrial metabolism and uncoupling capacity. *Zbtb16* is a significant energy metabolism modulator and overexpression of the gene has been found to induce thermogenic programming including induction of mitochondrial fatty acid oxidation and uncoupling/electron transport chain (Plaisier, Bennett et al. 2012, Skolnikova, Sedova et al. 2020). The *Slc26a8* gene is known to stimulate anion transport activity of the cystic fibrosis transmembrane conductance regulator (CFTR) which in turn facilitates ATP synthesis, ATP transport, and influences energy expenditure by regulating nutrient absorption and digestion (Wetmore, Joseloff et al. 2010, Bass, Brownell et al.

2021). The gene *MaeA* was found to be most differentially downregulated in both iBAT and iWAT. The protein MaeA is an E3 ubiquitin ligase subunit and is essential for maintenance of hematopoietic stem cells (HSCs) and autophagy (Wei, Pinho et al. 2021). Its role in energy expenditure or metabolism has not been explored much, but since studies show that loss of E3 ubiquitin ligase leads to impaired nutrient sensing and metabolism in peripheral tissues (Lee, Han et al. 2018), MaeA may have an important role to play in control of energy expenditure, especially in presence to dietary signals. These findings together with the GSA result indicate that acute activation of the VMN^{PACAP} → caudal POA circuit leads to a distinct genetic program within each the brown and the beige adipose depots, that together are critical for the maintenance of energy balance. Adipose tissue is highly plastic with a high capacity for remodeling between iBAT to iWAT to pgWAT and vice-versa, in terms of metabolic and thermogenic activity, depending on the hormonal or environmental stimuli (Loncar 1991, Cousin, Cinti et al. 1992, Fisher, Kleiner et al. 2012, Wu, Bostrom et al. 2012, De Fano, Bartolini et al. 2022). Future studies will determine the role of increased proliferation and mitochondrial uncoupling in the brown adipocytes in iBAT and cellular remodeling in iWAT on metabolic health.

I also validated that the projections from VMN^{PACAP} neurons that lie at the caudal POA are indeed necessary for inducing adipose tissue thermogenesis. Acute neuronal activation at the different VMN^{PACAP} neurons' efferents indicated the importance of the VMN^{PACAP} → caudal POA signaling in eliciting thermogenesis. This combined with the fact that inhibition of the caudal POA neurons even after activating the VMN^{PACAP} neurons' efferents at the caudal POA blunted the signaling mechanism that triggered

adipose tissue thermogenesis response. However, in absence of the inhibition of caudal POA neurons, the thermogenic response was restored alone by the activation of the VMN^{PACAP} neurons' efferents at the caudal POA. Currently, I am unable to confirm that this is a direct connection between the VMN^{PACAP} and the caudal POA. Even though this is the most likely explanation, I cannot rule out that there is another neuron between the VMN and the caudal POA that is integral to the function of this circuit. But it is clear from findings that the caudal POA signaling is necessary for VMN^{PACAP} cells to induce adipose tissue thermogenesis.

Conclusion

In all, I define the anatomical output that the VMN uses to stimulate energy expenditure, which is even more effective in negative energy balance to stimulate tissue thermogenesis. I demonstrate that the VMN can activate energy expenditure in diet-induced obese male mice to reduce adipose mass and increase energy expenditure. This effect is associated with an upregulation in the expression of key thermogenic markers in the iBAT. Lastly, I identify the differentially expressed genes in both brown and beige adipose tissue immediately following acute activation of VMN^{PACAP} neurons that project to the caudal POA and demonstrate that there are very different pathways activated that likely lead to the overall goal of stimulating energy expenditure. These findings will provide new avenues to target for future treatment of obesity.

Acknowledgement

I thank Andrew J. Elmendorf, Betty Lorentz, Britany App, Connor A. Mahler, Dr. Patrick Sheets, Olivia Lazzaro, Dr. Shudi Zhou and Dr. Travis Johnson for completing parts of the experiments in this chapter. The data in this chapter has been published (Basu et. al., 2024).

Chapter 4: Distinct populations of neurons in the caudal POA ameliorate diet-induced obesity via distinct pathways

Abstract

VMN cells project to relatively few sites in the brain but the most prominent efferents lie in the caudal POA, defined from +0.3mm to -0.34mm bregma, that are just lateral to the suprachiasmatic nucleus (SCN), above optic tract (OPT), but not in the traditional more rostral (+0.6mm to +0.3mm bregma) regions that have been implicated in body temperature control. Indeed, as shown in chapter 3, I found that stimulating VMN^{PACAP} axonal fibers in the caudal POA induces brown and beige tissue thermogenesis in both sexes of mice, indicating that caudal POA neurons are engaged by VMN^{PACAP} cells for body weight control.

The POA is a complex structure containing intermingled clusters of both excitatory (i.e. Glutamatergic) and inhibitory (i.e. GABAergic) subpopulations along with glia and immune cells. To determine the potential for POA cells to ameliorate obesity, I tested both glutamatergic and GABAergic caudal POA cells by activating the vGLUT2 (Glutamatergic; containing vesicular glutamatergic transporter 2) or vGAT (GABAergic; containing vesicular GABAergic transporter) expressing neurons in diet-induced obese male mice. To determine potential anatomical differences, I targeted the vGLUT2 and vGAT neurons in the anterior portion of the caudal POA (+0.3mm to -0.1mm bregma) and called it the rostral POA and as well as the posterior portion of the caudal POA (-0.1mm to -.5mm bregma) and called it the caudal POA.

I demonstrated that both glutamatergic and GABAergic neurons in the caudal POA can ameliorate diet-induced obesity, with glutamatergic signaling being involved in inducing thermogenesis at iBAT and iWAT. Activation of glutamatergic neurons reduced food intake, adiposity, and increased lean mass, while also enhancing thermogenic gene expression in iBAT. In contrast, GABAergic signaling primarily reduced adiposity without significant effects on food intake or thermogenesis. This does not appear to be due to a local circuit because inhibiting glutamatergic signaling in the caudal POA also led to weight loss and thermogenic responses, indicating the complexity of the underlying neural circuits.

This indicated that there are subtypes of $vGLUT2^{cPOA}$ and $vGAT^{cPOA}$ neurons that act distinctly via separate pathways to influence body weight, adiposity and thermogenesis at iBAT and iWAT in diet-induced obese male mice.

Background and rationale

Energy balance is governed by intricate neural circuits in the brain, with the hypothalamus playing a central role. Within the hypothalamus, the POA is another significant region, traditionally known for its involvement in a multitude of social behaviors such as parenting, mating, and aggression, as well as homeostatic functions, including thermoregulation, sleep, reproduction and thirst, circadian rhythm and hedonic behavior ((Adjeitey, Mailloux et al. 2013)). The POA integrates a wide array of physiological signals to properly calibrate autonomic and endocrine responses. Historically, the POA has been associated with body temperature stability, with early research identifying it as a key site for thermoregulatory control with distinct neuronal

populations, intermingled together, across its subregions playing specialized roles (Swanson 2000, Sternson 2013). Despite its well-established role in thermoregulation and evidence in metabolic processing (Labbe et al., 2015; Yang et al., 2023; Tan et al., 2016; Tan & Knight, 2018; Cerri, 2017; Machado et al., 2020; Machado et al., 2023; Nakamura et al., 2022; Saper & Machado, 2022; Zhang et al., 2020; Pinol et al., 2021; Pinol & Reitman, 2022; Basu et al., 2024; Liao et al., 2019; Munzberg et al., 2016; Morrison, & Yu, 2016), the involvement of the POA in these functions has not been as extensively studied. This leaves a gap in understanding of the POA's contributions to energy balance and metabolic homeostasis.

The POA's thermoregulatory functions have been extensively characterized, with early research demonstrating its critical role in maintaining body temperature. The POA integrates sensory inputs related to ambient temperature and orchestrating appropriate physiological responses, such as shivering or vasodilation, to regulate heat production and dissipation. It also plays a key role in reproductive behaviors, coordinating sexual arousal and mating through its connections with other hypothalamic and limbic structures. Additionally, the POA is involved in circadian rhythm regulation, interacting with the SCN to modulate sleep-wake cycles and other daily physiological rhythms.

As mentioned previously in chapter 1, LepR expressing neurons within the POA are one of the key regulators of energy balance, influencing metabolic processes (Adjeitey, Mailloux et al. 2013). Both cold and warm-sensing neurons within the POA sense temperature changes in the periphery and activate the autonomic nervous system to coordinate thermoregulatory responses, such as increasing heat production in iBAT and skeletal muscle or promoting heat dissipation via vasodilation and sweating (Labbe,

Caron et al. 2015, Yang, Xie et al. 2023) which are crucial for non-shivering thermogenesis and overall energy balance (Morrison, Madden et al. 2014). Additionally, neurons expressing neuropeptides like TRH and NPY further activate energy expenditure and temperature responses, integrating signals to maintain thermal and energy homeostasis (Munzberg, Qualls-Creekmore et al. 2016).

Furthermore, glutamatergic (excitatory) and GABAergic (inhibitory) neurons play pivotal roles in controlling energy expenditure. Glutamatergic neurons in the POA facilitate excitatory neurotransmission and promote energy expenditure through thermogenic responses. Activation of these neurons increases sympathetic outflow to iBAT and skeletal muscle, thereby enhancing heat production and overall metabolic rate (Yang and Ruan 2015). This process is critical for maintaining body temperature and energy balance, especially in response to cold exposure.

Conversely, GABAergic neurons in the POA inhibit local neuronal circuits and play a contrasting role in energy expenditure control. Activation of GABAergic neurons can reduce metabolic rates by inhibiting sympathetic outflow to peripheral tissues such as iBAT, thus decreasing thermogenesis and conserving energy (Sternson 2013). These neurons are crucial for fine-tuning the balance between energy expenditure and conservation, ensuring appropriate physiological responses to varying environmental and metabolic conditions.

The neurotransmitters, GABA, and glutamate are packaged into vesicles inside the neurons, by unique transporters. Inhibitory GABAergic neurons have a single vesicular GABAergic transporter (vGAT), there are three separate vesicular Glutamate transporters (vGLUT; type 1 is vGLUT1, type 2 is vGLUT2 and type 3 is vGLUT3). In

both humans and rodents, vGLUT1 is primarily expressed in the cortex and vGLUT3 in the midbrain. However, thalamic, and hypothalamic regions contain vGLUT2 (Meek, Nelson et al. 2016, Faber, Matsen et al. 2018). So, I used inbred *vGLUT2*^{Cre} mice to target glutamatergic neurons and *vGAT*^{Cre} mice to target GABAergic neurons in region of interest. Using *vGAT*^{Cre} mice helped test if the effects are mediated by the inhibitory signaling, versus using *vGLUT2*^{Cre} tested the effects are mediated via excitatory neurons. The interplay between these excitatory and inhibitory neuronal populations within the POA forms a sophisticated regulatory network that integrates various signals, including hormonal cues like leptin, which influences the activity of both glutamatergic and GABAergic neurons, thereby modulating energy expenditure and maintaining homeostasis.

Given the sheer breadth of functions and properties of cells within the POA, anatomical differences likely play an important role in differentiating separate functional subpopulations in the POA. For instance, the caudal POA has emerged as a significant subregion influencing thermogenesis and energy expenditure. My previous findings have shown that the caudal POA, located laterally to the SCN and above the OPT from +0.3mm to -0.34mm relative to bregma, regulates the function of thermogenic sites such as brown and beige adipose tissues in the periphery (Basu and Flak 2024). This is distinct from the more rostral regions of the POA, traditionally associated with thermoregulation and spanning from +0.6mm to +0.3mm bregma (Satinoff 1978, Zhang, Kerman et al. 2011).

Despite these insights, the specific roles of distinct neuronal subpopulations within the caudal POA remain inadequately understood. The POA itself is a highly

intricate structure, comprising intermingled clusters of both excitatory and inhibitory neuronal subpopulations, along with several other cell types. This complexity is further underscored by the work of Moffit et al. (Moffitt, Bambah-Mukku et al. 2018), which elaborates on the diverse and interwoven nature of these neuronal clusters, that contribute to its multifaceted roles, making it challenging to pinpoint specific targets within the POA for therapeutic interventions. Given the anatomical complexity and functional heterogeneity of the POA, it is crucial to dissect the individual contributions of glutamatergic and GABAergic neurons to thermoregulation and metabolic control.

In this study, I aimed to elucidate the functional roles of vGLUT2 (i.e., glutamatergic) and vGAT (i.e., GABAergic) neurons within the caudal POA of diet-induced obese male mice. Utilizing Cre-loxP recombination, I specifically targeted these neuronal populations to investigate the effects of their activation and inhibition on body weight, adiposity, lean body mass, food intake, and thermogenesis. Since, the caudal POA is still a very broad region, I targeted the vGLUT2 and vGAT neurons in the anterior portion of the caudal POA (+0.3mm to -0.1mm bregma) and called it the rostral POA as well as the posterior portion of the caudal POA (-0.1mm to -.34mm bregma) and called it the caudal POA, to pinpoint the cellular population even better.

By elucidating the specific contributions of these neuronal subpopulations, study advances the understanding of the neurobiological mechanisms governing energy homeostasis and metabolic regulation, providing potential targets for therapeutic interventions in obesity and related metabolic disorders.

Results

Activating both glutamatergic and GABAergic neurons in the caudal POA ameliorate diet-induced obesity

In the previous chapter I showed that VMN^{PACAP} neurons project to the caudal POA and stimulating the axonal fibers of those neurons generate excitatory glutamatergic signaling. But it is not known whether this signal activates glutamatergic or GABAergic neurons in the caudal POA and whether this signal mediates weight loss effect in the periphery. To test this, I used $vGLUT2^{Cre}$ or $vGAT^{Cre}$ male mice and put them on HFD tested the potential for those neurons to reduce body weight and adiposity in diet induced obesity. I first looked at pertinent phenotypic alterations. $vGLUT2^{Cre}$ or $vGAT^{Cre}$ male mice were given HFD, beginning at 8-10 weeks of age, for 40-44 weeks of age until they weighed at least 35 grams. I then performed craniotomy to administer $AAV^{DIO\text{-}hM3dq\text{-}mCherry}$ or $AAV^{DIO\text{-}mCherry}$ (Fig. 4.1A) into either rostral (0.02mm bregma) or caudal (-0.22mm bregma) POA of these mice (Fig. 4.1B; Supplementary Fig. S6A-S6D) and monitored their body weight, body composition and food intake (Fig. 4.1C). For the phenotypic measurements, $vGLUT2^{hM3dq}$ or $vGAT^{hM3dq}$ mice and their respective controls were acclimated for 7 days with once daily intraperitoneal (IP) saline injection. For the next 3 days they were injected with IP CNO, twice daily (every 12 hours). All groups of mice weighed the same before and 4-weeks post-surgery. Activating both the $vGLUT2^{hM3dq}$ and $vGAT^{hM3dq}$ neurons in the rostral and caudal POA with IP CNO injection, led to a loss of body weight by >1g in just 3 days, in contrast to the $vGLUT2^{mCherry}$ and $vGAT^{mCherry}$ controls (Fig. 4.1D, 4.1E, 4.1F, 4.1G).

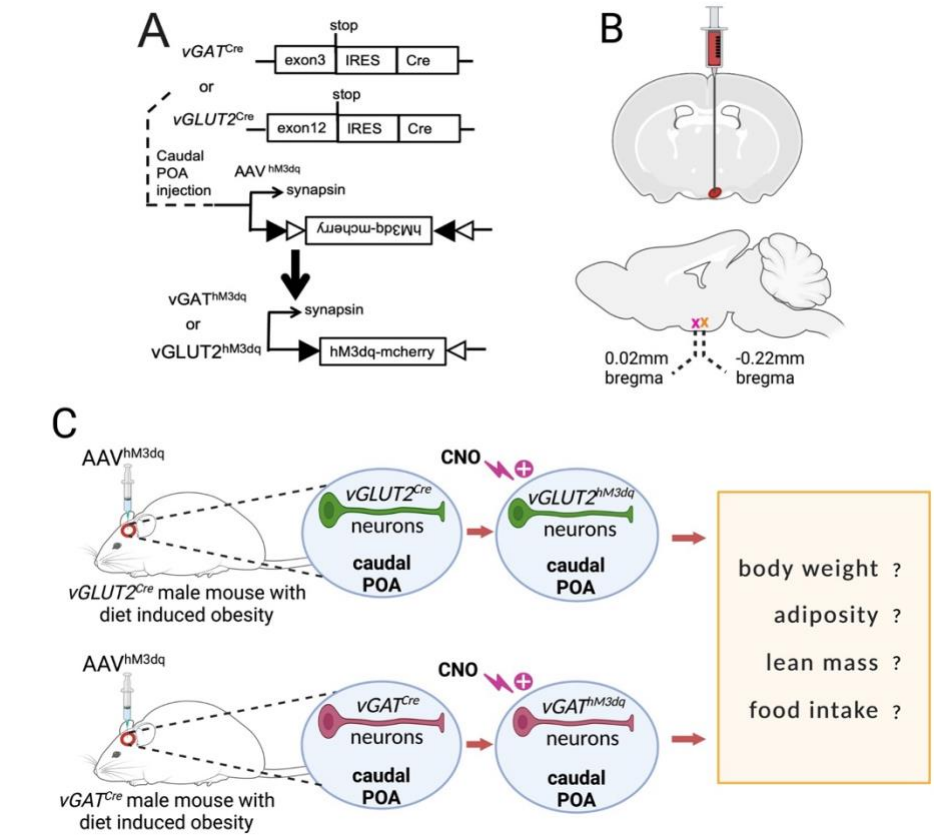
A
vGAT^Cre
stop
exon3
IRES
Cre
or
vGLUT2^Cre
stop
exon12
IRES
Cre
Caudal POA injection
AAV hM3dq
synapsin
hM3dq-mcherry
vGAT^hM3dq
or
vGLUT2^hM3dq
synapsin
hM3dq-mcherry
B
0.02mm bregma
-0.22mm bregma
C
AAV^hM3dq
vGLUT2^Cre male mouse with diet induced obesity
CNO
vGLUT2^Cre neurons
caudal POA
vGLUT2^hM3dq neurons
caudal POA
AAV^hM3dq
vGAT^Cre male mouse with diet induced obesity
CNO
vGAT^Cre neurons
caudal POA
vGAT^hM3dq neurons
caudal POA
body weight ?
adiposity ?
lean mass ?
food intake ?

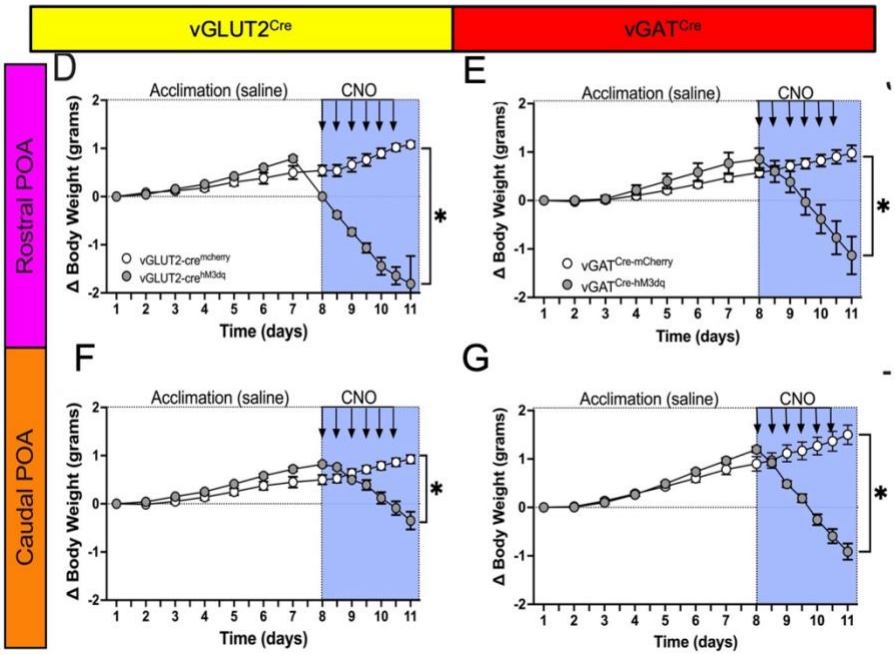
vGLUT2^Cre
vGAT^Cre
Rostral POA
Caudal POA
D
E
F
G
Acclimation (saline)
CNO
Δ Body Weight (grams)
Time (days)
vGLUT2-cre^mcherry
vGLUT2-cre^hM3dq
vGAT^Cre-mCherry
vGAT^Cre-hM3dq
*

Figure 4.1: Activating both vGLUT2 and vGAT caudal POA neurons ameliorate diet-induced obesity. In diet-induced obese and diabetic male mice, I introduced cre-inducible hM3dq via AAV (A) into either glutamatergic (i.e. vGLUT2) or GABAergic (i.e. vGAT) neurons of *vGLUT2*^{Cre} and *vGAT*^{Cre} mice respectively (C) in either rostral POA or caudal POA (B), to test their potential to reduce body weight in diet-induced obesity and I measured body weight (D, E, F, G). n=5-17 male mice. (D, H, L, P) analyzed by two-way RM ANOVA. Data expressed as mean ± SEM. *p<0.05. (B-C) Created with Biorender.com.

Activating the *vGLUT2*^{hM3dq} neurons in the rostral and caudal POA, however, reduced food intake (Fig. 4.2A, 4.2I), while *vGAT*^{hM3dq} neurons did not (Fig. 4.2E, 4.2M), compared to the *vGLUT2*^{mCherry} and *vGAT* ^{mCherry} controls. Additionally, activating the *vGLUT2*^{hM3dq} neurons in both the rostral and caudal POA, reduced both adipose mass (Fig. 4.2B, 4.2J) and lean mass (Fig. 4.2C, 4.2K), however, activation of *vGAT*^{hM3dq} neurons reduced only adipose mass (Fig. 4.2F, 4.2N) and increased lean mass (Fig. 4.2G, 4.2O), when compared to the *vGLUT2*^{mCherry} and *vGAT* ^{mCherry} controls respectively. However, activating the *vGLUT2*^{hM3dq} or *vGAT*^{hM3dq} neurons in the rostral or caudal POA, did not change locomotory activity (Fig. 4.2E, 4.2H, 4.2L, 4.2P).These data indicate that both vGLUT2 and vGAT neurons in both the rostral and caudal POA have therapeutic potential in diet-induced obesity.

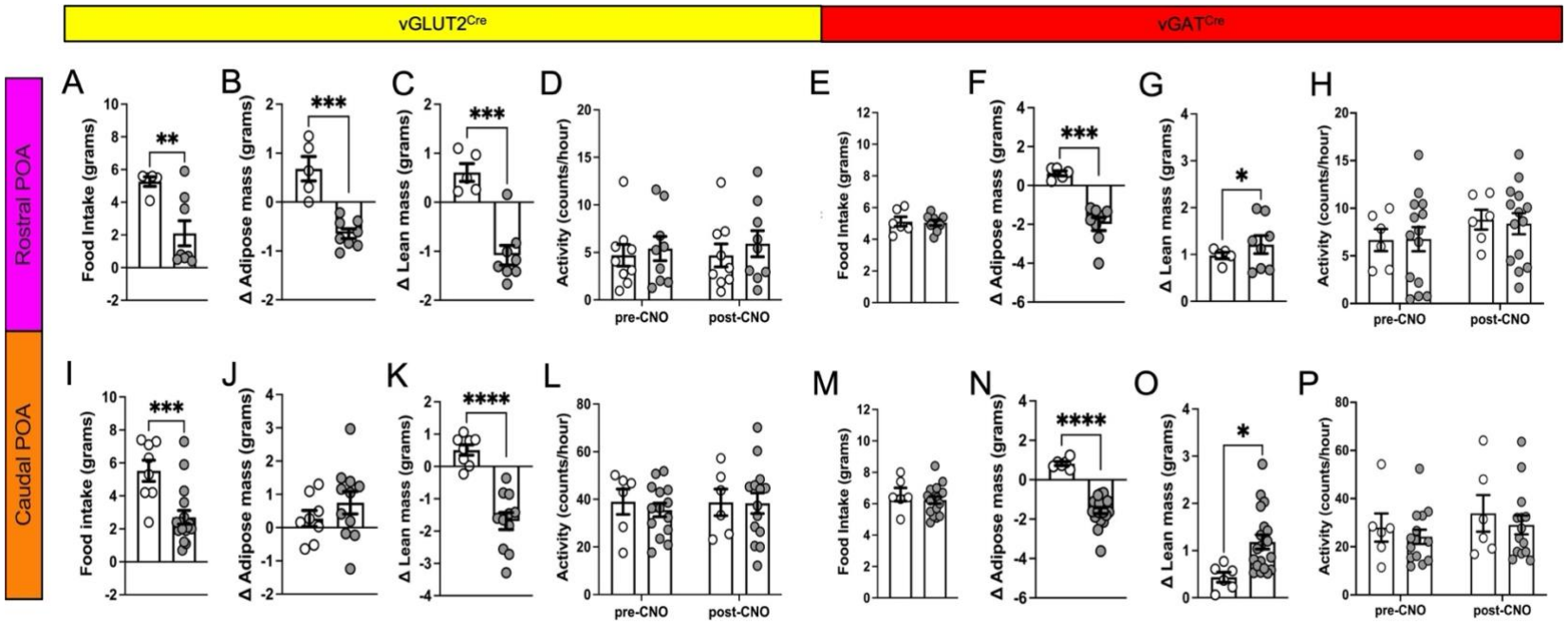

Figure 4.2: Activating both vGLUT2 and vGAT caudal POA neurons ameliorate diet-induced obesity without changing activity. In diet-induced obese and diabetic male mice, I introduced cre-inducible hM3dq via AAV into either glutamatergic (i.e. vGLUT2) or GABAergic (i.e. vGAT) neurons of *vGLUT2^{Cre}* and *vGAT^{Cre}* mice respectively in either rostral POA or caudal POA, to test their potential to reduce body weight in diet-induced obesity. I measured food intake (A, E, I, M), adiposity (B, F, J, N), lean mass (C, G, K, O) and locomotory activity (D, H, L, P) after activating either vGAT or vGLUT2 neurons via CNO administration for 72 hours. n=5-17 male mice. (A-C, E-G, I-K, M-O) analyzed by student's t-test. (D, H, L, P) analyzed by one-way ANOVA. Data expressed as mean ± SEM. *p<0.05, **p<0.01, ***p<0.001, ****p<0.0001.

Activating glutamatergic neurons in the caudal POA increased iBAT and iWAT temperature

I then investigated whether the glutamatergic or GABAergic neurons in rostral versus caudal POA, can induce iBAT and iWAT thermogenesis. For this I used the previous set of diet induced obese *vGLUT2*^{Cre} or *vGAT*^{Cre} male mice with *AAV*$^{DIO\text{-}hM3dq\text{-}mCherry}$ or *AAV*$^{DIO\text{-}mCherry}$ injected in either their rostral or caudal POA. I then tested the potential for the *vGLUT2*^{hM3dq} and *vGAT*^{hM3dq} neurons to induce iBAT (Fig. 4.3A, 4.3 B, 4.3C, 4.3D) and iWAT (Fig. 4.3E, 4.3F, 4.3G, 4.3H) thermogenesis by increasing the temperatures at those depots. Activating the *vGLUT2*^{hM3dq} neurons in the rostral POA with IP CNO injection reduced temperatures at iBAT (Fig. 4.3A) and iWAT (Fig. 4.3E), compared to their *vGLUT2*^{mCherry} controls. Interestingly, activating the *vGLUT2*^{hM3dq} neurons in the caudal POA increased temperatures at iBAT (Fig. 4.3B) and iWAT (Fig. 4.3F), compared to their *vGLUT2*^{mCherry} controls. On the other hand, activating the *vGAT*^{hM3dq} neurons in either the rostral or caudal POA did not alter the temperatures at either iBAT (Fig. 4.3C, 4.3D) or iWAT (Fig. 4.3G, 4.3H) when compared to their *vGAT*^{mCherry} controls. This indicates glutamatergic, but not GABAergic, neurons in the caudal POA are involved in iBAT and iWAT thermogenesis.

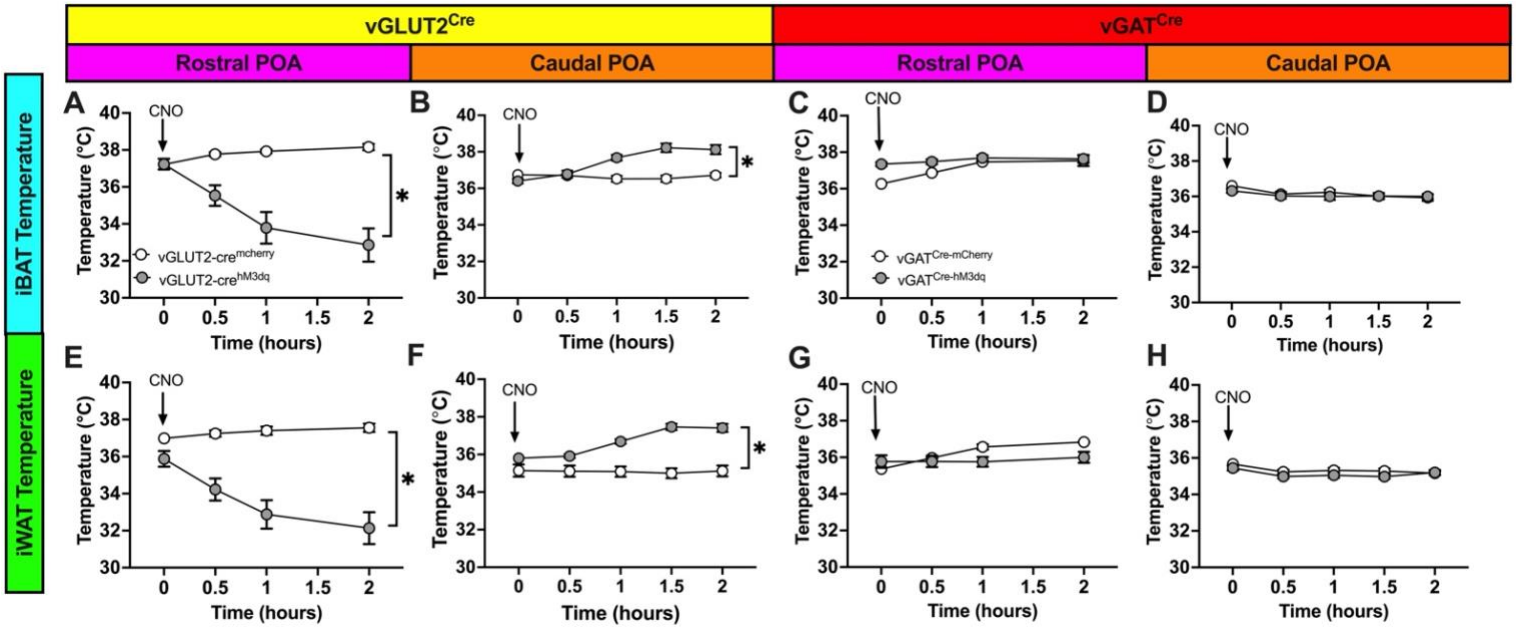

Figure 4.3: Activating vGLUT2, but not vGAT, caudal POA neurons increases iBAT and iWAT temperature. In diet-induced obese and diabetic male mice, I introduced cre-inducible hM3dq via AAV into either vGLUT2 or vGAT neurons of *vGLUT2^{Cre}* and *vGAT^{Cre}* mice respectively in either rostral POA or caudal POA and measured temperature above the iBAT (A-D) and iWAT (E-H). n=5-9 male mice. (A-H) analyzed by two-way RM ANOVA. Data expressed as mean ± SEM. *p<0.05.

Activating glutamatergic neurons in the caudal POA induces thermogenic gene expression in iBAT

Since I found that both glutamatergic and GABAergic neurons in both the rostral and caudal POA are involved in ameliorating diet-induced obesity but only glutamatergic neurons in the caudal POA can impact iBAT and iWAT thermogenesis, I wanted to investigate what happens to the thermogenic gene expression at the iBAT and iWAT after activating glutamatergic and GABAergic signaling. I used the previous set of diet induced obese *vGLUT2*^{Cre} or *vGAT*^{Cre} male mice with *AAV*$^{DIO\text{-}hM3dq\text{-}mCherry}$ or *AAV*$^{DIO\text{-}mCherry}$ injected in either their rostral or caudal POA and tested the potential for the *vGLUT2*^{hM3dq} and *vGAT*^{hM3dq} neurons to induce iBAT and iWAT thermogenic gene expression by using qRT-PCR and calculating fold change (2^-ddct) of iBAT (Fig. 4.4A, 4.4B) or iWAT (Fig. 4.4C, 4.4D) thermogenic genes. I found that activating *vGLUT2*^{hM3dq} neurons in the rostral POA decreased *Ucp1* and *Adrb3* gene expression in iBAT (Fig. 4.4A) and *Adrb1* gene expression in iWAT (Fig. 4.4C), compared to the *vGLUT2*^{mcherry} control neurons. Activating *vGLUT2*^{hM3dq} neurons in the caudal POA, however, induced *Ucp1*, *Ppargc1a*, *Prdm16*, *Adrb1* gene expression in iBAT (Fig. 4.4A), compared to the *vGLUT2*^{mcherry} control neurons; whereas none of the thermogenic genes in the iWAT (Fig. 4.4C) were not altered. On the other hand, activating *vGAT*^{hM3dq} neurons in the rostral POA decreased *Dio2* gene expression and increased *Prdm16* gene expression in iBAT (Fig. 4.4B) whereas none of the thermogenic genes in the iWAT (Fig. 4.4D) were not altered, compared to the *vGLUT2*^{mcherry} control neurons. Additionally, activating *vGAT*^{hM3dq} neurons in the caudal POA increased *Prdm16* and *Adrb1* gene expression in iBAT (Fig. 4.4B) and increased *Prdm16* gene expression in

iWAT (Fig. 4.4D). These data together suggest that glutamatergic neurons in the caudal POA induces thermogenic gene expression in iBAT.

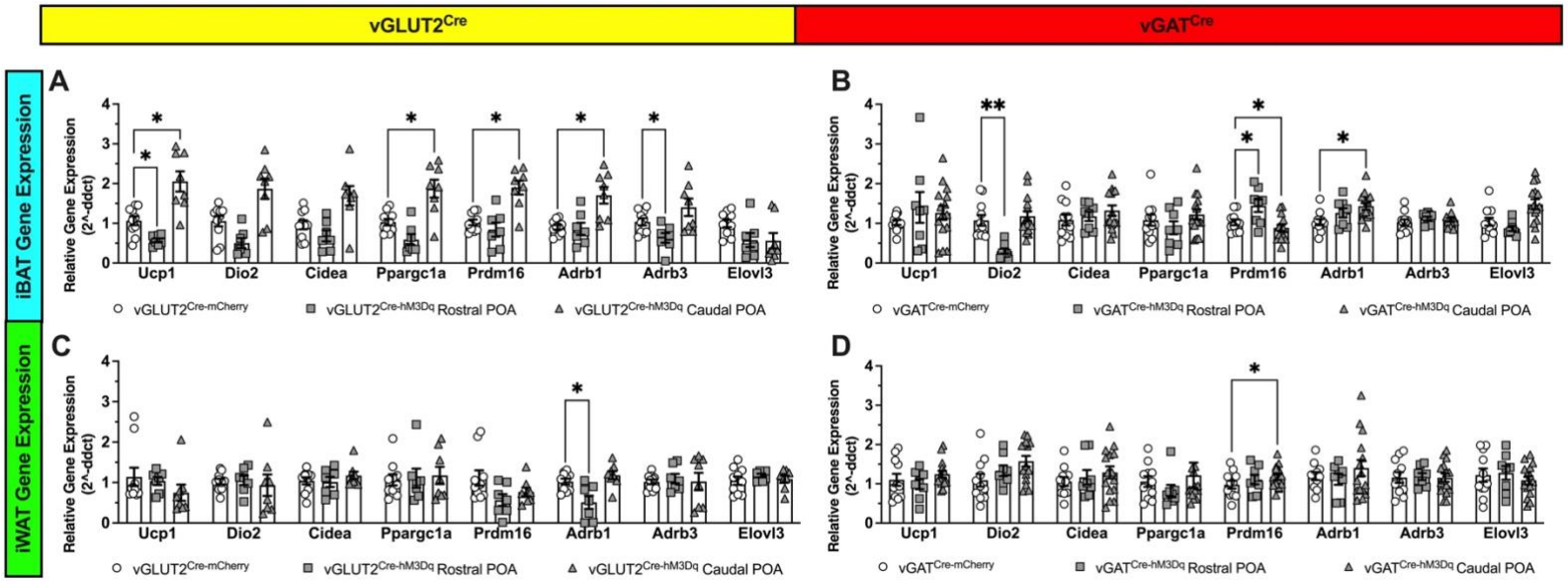

Figure 4.4: Activating vGLUT2 caudal POA neurons induces iBAT and iWAT thermogenesis. In diet-induced obese and diabetic male mice, I introduced cre-inducible hM3dq via AAV into either vGLUT2 or vGAT neurons of *vGLUT2^{Cre}* and *vGAT^{Cre}* mice respectively in either rostral POA or caudal POA and measured thermogenic gene expression using qRT-PCR. I calculated fold change (2^-ddct) of iBAT (A, B) or iWAT (C, D) thermogenic genes. n=5-9 male mice. (A-D) analyzed by multiple student's t-test. Data expressed as mean ± SEM. *p<0.05, **p<0.01.

Inhibiting glutamatergic neurons in the caudal POA also curbs diet-induced obesity potentially via distinct mechanism

I then investigated the effect of inhibiting the glutamatergic neurons in both rostral and caudal POA to test the necessity of glutamatergic signaling within the rostral and caudal POA in ameliorating diet-induced obesity. To test this, I used *vGLUT2*^{Cre} male mice and put them on HFD tested the potential for those neurons to reduce body weight and adiposity in diet induced obesity. *vGLUT2*^{Cre} male mice were given HFD, beginning at 8-10 weeks of age, for 40-44 weeks of age until they weighed at least 35 grams. I then performed craniotomy to administer *AAV*$^{DIO\text{-}hM4di\text{-}mCherry}$ or *AAV*$^{DIO\text{ -}mCherry}$ (Fig. 4.5A) into either rostral or caudal POA of these mice (Fig. 4.5B; Supplementary Fig. S6E-S6F) and monitored their body weight, body composition and food intake (Fig. 4.5C). For the phenotypic measurements, *vGLUT2*^{hM4di} mice and the *vGLUT2*^{mCherry} controls were acclimated for 7 days with once daily IP saline injection. For the next 3 days they were injected with IP CNO, twice daily (every 12 hours). Both groups of mice weighed the same before and 4-weeks post-surgery. Inhibiting the *vGLUT2*^{hM4di} neurons in both the rostral and caudal POA with IP CNO injection, led to a loss of body weight by ~1g in just 3 days (Fig. 4.6A, 4.6H), along with a reduction in food intake (Fig. 4.6B, 4.6I) and adipose mass (Fig. 4.6C, 4.6J), compared to the *vGLUT2*^{mCherry} controls. Inhibiting the *vGLUT2*^{hM4di} neurons in the rostral POA also led to reduction in lean mass (Fig. 4.6D) but inhibiting the *vGLUT2*^{hM4di} neurons in the caudal POA did not alter lean mass (Fig. 4.6K). These data indicate that not a local inhibitory circuit is at play here, which is inhibiting the glutamatergic neurons in the caudal POA.

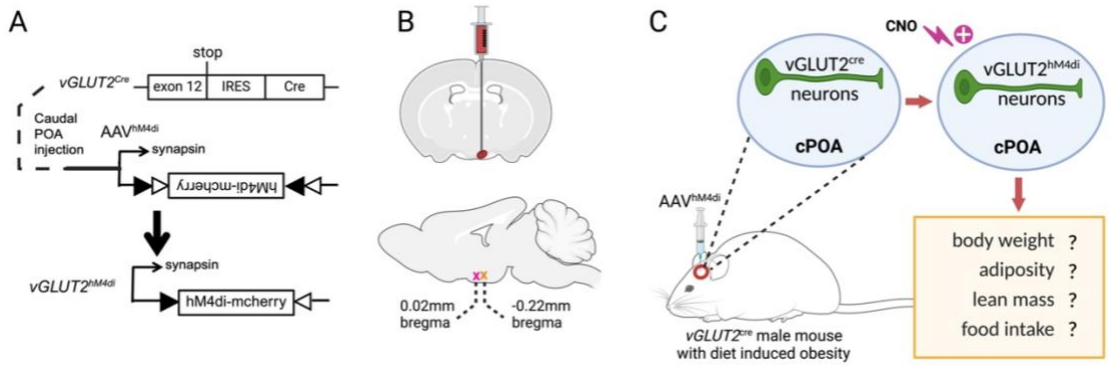

Figure 4.5: Model for inhibiting vGLUT2 caudal POA neurons to test their potential for ameliorating diet-induced obesity. In diet-induced obese and diabetic male mice, I introduced cre-inducible hM4di via AAV (A) into vGLUT2 neurons of *vGLUT2^{Cre}* mice in either rostral POA or caudal POA (B) and measured body weight, food intake, adiposity and lean mass (C) after inhibiting vGLUT2 neurons via CNO administration for 72 hours. (B-C) Created with Biorender.com.

Additionally, inhibiting *vGLUT2^{hM4di}* neurons at the rostral POA did not change locomotory activity (Fig. 4.6E) but when the same was done to the neurons at caudal POA, there was an increase in the locomotory activity (Fig. 4.6L), compared to the *vGLUT2^{mCherry}* controls. Then, I tested the effect of inhibiting the glutamatergic neurons in the caudal POA on iBAT and iWAT thermogenesis. Inhibiting the *vGLUT2^{hM4di}* neurons in the rostral POA did not alter the temperatures at iBAT (Fig. 4.6F) or iWAT (Fig. 4.6G) but doing so in caudal POA, increased the temperatures at iBAT (Fig. 4.6M) and iWAT (Fig. 4.6N) when compared to the *vGLUT2^{mCherry}* controls. Then I calculated the thermogenic gene expression at iBAT (Fig. 4.6O) and iWAT (Fig. 4.6P), using qRT-PCR and calculating fold change (2^-ddct) of the genes. I found that inhibiting the *vGLUT2^{hM4di}* neurons in the rostral POA reduces *Adrb3* gene expression in iBAT (Fig. 4.6O), when compared to the *vGLUT2^{mCherry}* controls. Whereas, inhibiting the

vGLUT2^{hM4di} neurons in the caudal POA reduces *Adrb3* and *Elovl3* gene expression in iBAT (Fig. 4.6O) and *Dio2* gene expression in the iWAT (Fig. 4.6P), when compared to the *vGLUT2*^{mCherry} controls; again, indicating that not a local inhibitory circuit at play that is inhibiting the glutamatergic neurons in the caudal POA. Thus, a local inhibitory neuronal subset may not be involved alone that is responsible for iBAT and iWAT thermogenesis which is being engaged in the weight-lowering effects by activating POA neurons and a more complex circuitry is at play here.

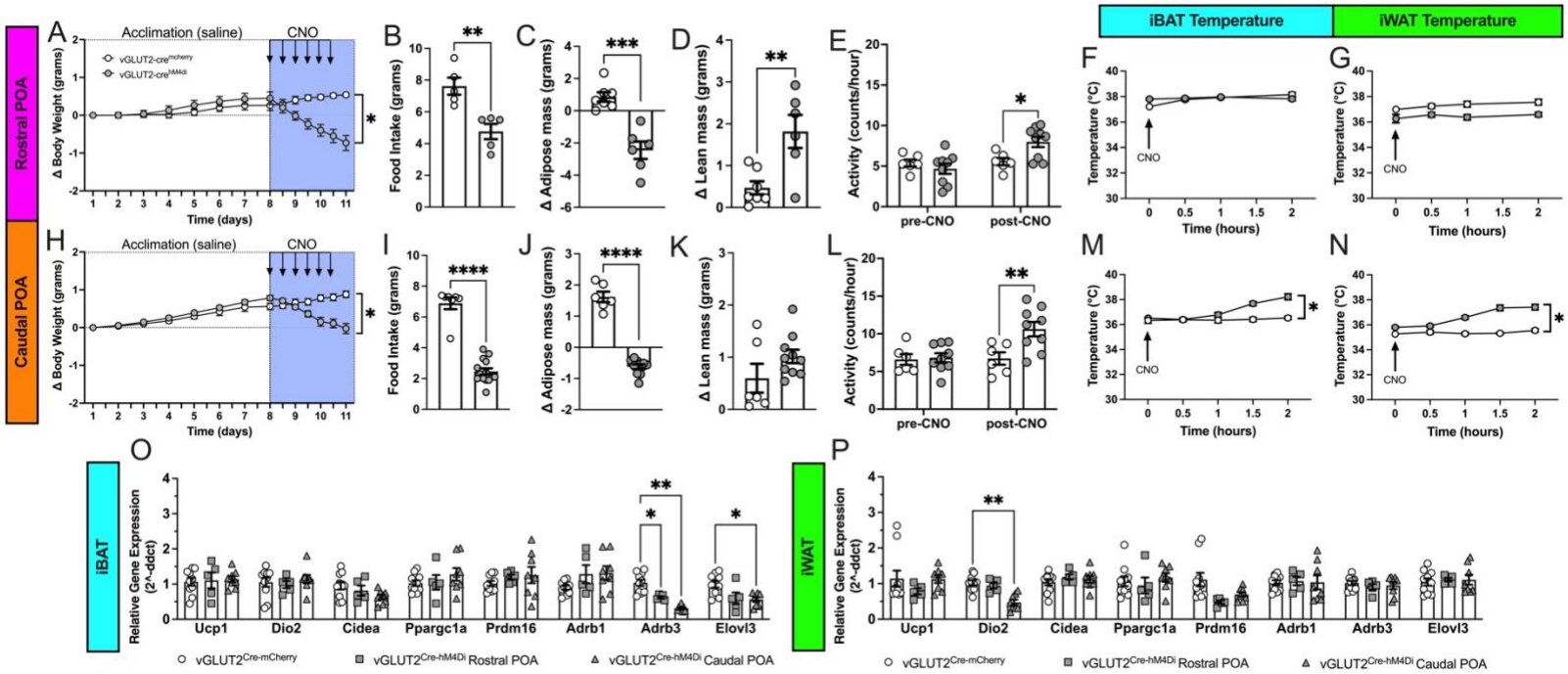

Figure 4.6: Inhibiting vGLUT2 caudal POA neurons ameliorate diet-induced obesity by inducing hypophagia and increasing iBAT and iWAT temperature. I measured body weight (A, G), food intake (B, H), adiposity (C, I) and lean mass (D, J) after inhibiting vGLUT2 neurons via CNO administration for 72 hours in *vGLUT2^{Cre}* diet-induced obese male mice. I also measured temperature above the iBAT (E, K) and iWAT (F, L) and thermogenic gene expression at iBAT (M) and iWAT (N), using qRT-PCR and calculating fold change (2^-ddct) of the genes. n=5-9 male mice. (A, E, F, G, K, L) analyzed by two-way RM ANOVA. (B-D, H-J) analyzed by multiple student's t-test. (M-N) analyzed by one way RM ANOVA. Data expressed as mean ± SEM. *p<0.05, **p<0.01, ***p<0.001, ****p<0.0001.

Glutamatergic and GABAergic caudal POA neurons send distinct efferent projections

The POA does not contain any spinal projecting neurons and must be connected to interneurons or neurons that project to the hindbrain. Thus, to find the next efferent node within this circuit, I next investigated the efferent nodes of the *vGLUT2* and *vGAT* rostral and caudal POA neurons through which they transmit the signal downstream to the periphery (Fig. 4.7). To test where these neurons project to, I administered $AAV^{DIO\text{-}hM3dq\text{-}mCherry}$ at the rostral (0.02mm bregma) and caudal (-0.34mm bregma) POA of 8-12 weeks-old $vGLUT2^{Cre}$ or $vGAT^{Cre}$ mice to identify where the terminals are most concentrated in the brain. I activated the vGLUT2 and vGAT rostral and caudal POA neurons using IP CNO injections and observed projections using fluorescence.

I observed that the $vGLUT2^{\text{rostral POA}}$ neurons (Fig 4.6A) send dense efferent projections to the LHA (Fig 4.7B), LPAG (lateral periaqueductal gray; Fig 4.7C) and VLPAG (ventrolateral periaqueductal gray; Fig.4.7C); whereas, $vGLUT2^{\text{caudal POA}}$ neurons (Fig 4.7E) send dense efferent projections to the VMN (Fig 4.7F), LHA (Fig 4.7F), LPAG (Fig 4.7G) and VLPAG (Fig.4.7G). On the other hand, $vGAT^{\text{rostral POA}}$ neurons (Fig 4.7I) send dense efferent projections to the PMnR (paramedian raphe nucleus; Fig.4.7L), ATg (anterior tegmental nucleus; Fig 4.7L) and MnR (median raphe nucleus, Fig.4.7L); while, $vGAT^{\text{caudal POA}}$ neurons (Fig 4.7M) projects densely to the VMN (Fig 4.7N), LHA (Fig 4.7N) and MnR (Fig.4.7P).

Clearly, these 4 subsets of neurons send distinct projections of the nuclei of the hypothalamus and the hindbrain.

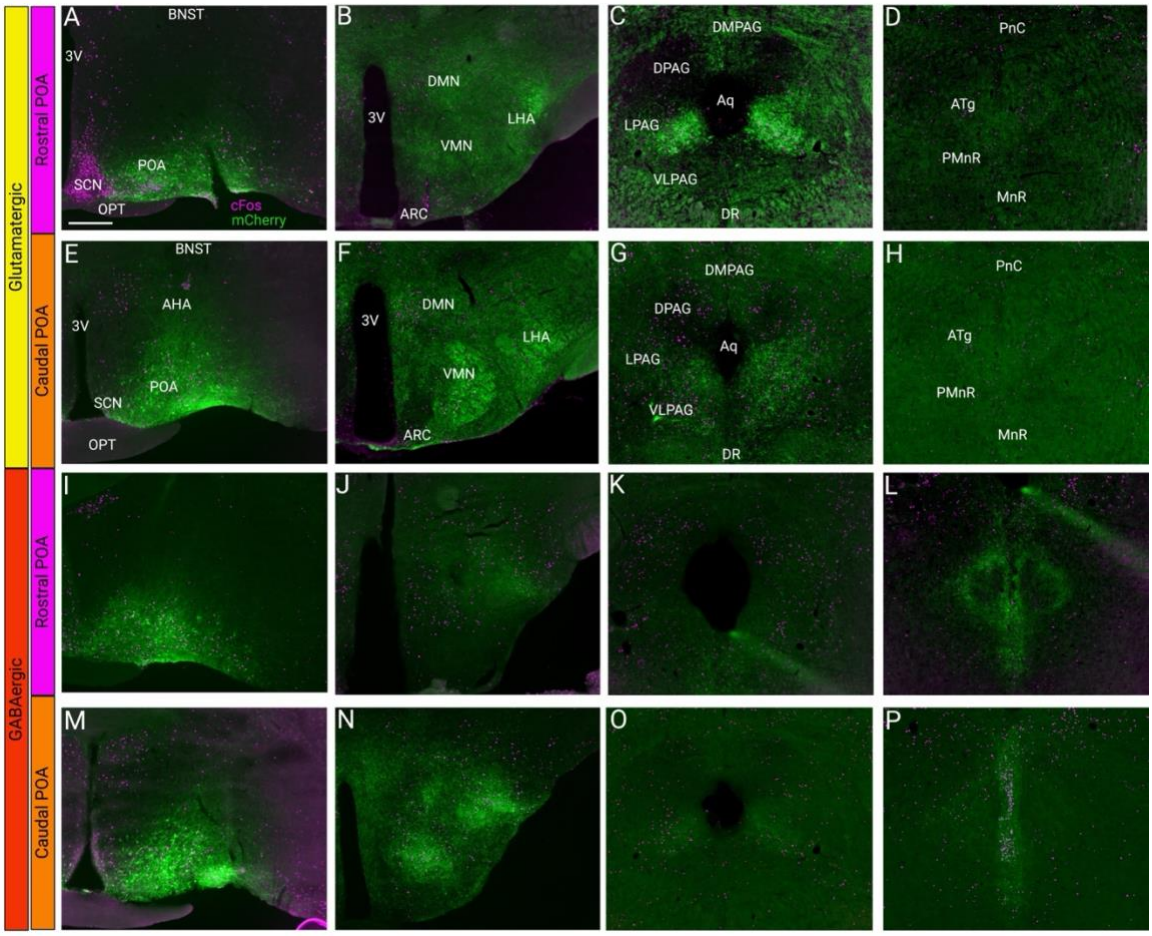

Figure 4.7: Glutamatergic and GABAergic caudal POA neurons send distinct efferent projections. Representative images showing efferent projections from vGLUT2 (A-H) and vGAT (I-P) POA neurons to the other hypothalamic and hindbrain nuclei, with injection of $AAV^{DIO\text{-}hM3dq\text{-}mCherry}$ at either rostral (0.02mm bregma; A-D, I-L) or caudal (-0.34mm bregma; E-H, M-P) POA. We compared anterograde projections of these neurons after activating them with CNO IP injection. mCherry in green and cFos in magenta. Scalebar = 460µm. 3V = 3rd ventricle. AHA = Anterior hypothalamic area. DMH = Dorsomedial hypothalamic nucleus. VMN = Ventromedial hypothalamic nucleus. ARC = Arcuate nucleus. ME = Median eminence. D3V = Dorsal 3rd ventricle. AC = Anterior commissure. cPOA = caudal preoptic area. SCN = Suprachiasmatic nucleus. LV = Lateral ventricle. BNST = Bed nucleus of stria terminalis. Opt = Optic tract. LHA = Lateral hypothalamic area. DMPAG = Dorsomedial periaqueductal gray. DLPAG = Dorsolateral periaqueductal gray. DPAG = Dorsal periaqueductal gray. VPAG = Ventral periaqueductal gray. DR = Dorsal raphe nucleus. Aq = Aqueduct. PnC = Pontine reticular nucleus, caudal part. MnR = Median raphe nucleus. PMnR = Paramedian raphe nucleus. ATg = Anterior tegmental nucleus. The schematics were

created using The Mouse Brain in Stereotaxic Coordinates Fourth Edition (Paxinos and Franklin). Created using Biorender.com.

Overall summary

This study uncovers the intricate roles of glutamatergic and GABAergic neurons in the caudal POA in regulating energy expenditure and body weight. Both glutamatergic and GABAergic neurons in the caudal POA, receive input from the VMN^{PACAP} neurons and contribute to ameliorating diet-induced obesity (Fig 4.8). Using $vGLUT2^{Cre}$ and $vGAT^{Cre}$ mouse models, I found that glutamatergic neurons were particularly effective in promoting thermogenesis at both iBAT and iWAT, leading to reduced food intake, decreased adiposity, and increased lean mass. Additionally, activation of these neurons upregulated thermogenic gene expression in iBAT. Conversely, activation of GABAergic neurons primarily diminished adiposity and body weight , with no impact on food intake or adipose tissue thermogenesis. Moreover, inhibiting glutamatergic signaling in the caudal POA also resulted in weight loss and induced thermogenic responses, highlighting the complexity of the neural mechanisms involved.

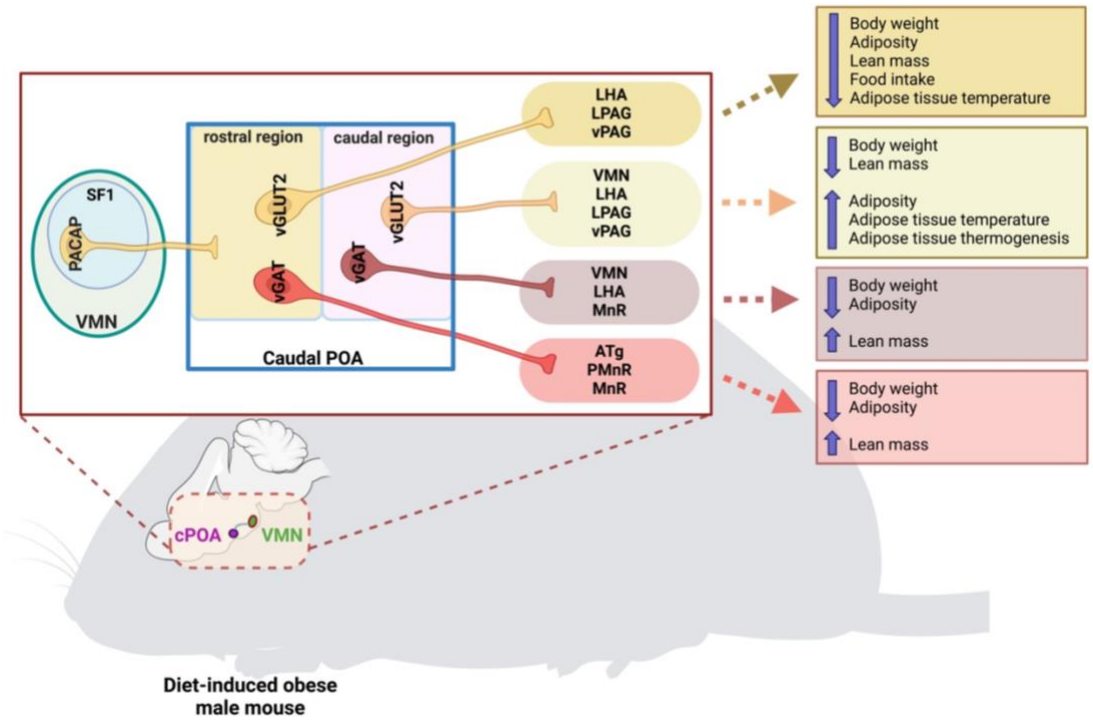

Figure 4.8: Overall Model. Both glutamatergic and GABAergic neurons in the caudal POA (cPOA), receive input from the VMN^{PACAP} neurons, contribute to ameliorating diet-induced obesity. Activation of glutamatergic neurons reduced food intake, adiposity, and increased lean mass, while also enhancing thermogenesis at adipose tissue. In contrast, GABAergic neurons reduced body weight and adiposity and increased lean mass, without significant effects on food intake or thermogenesis. Created with Biorender.com.

Discussion

The activation of both glutamatergic and GABAergic neurons in the rostral POA as well as GABAergic neurons in the caudal POA led to a significant reduction in body weight and adiposity in diet-induced obese male mice, suggesting that these neuronal populations can be engaged to reduce body weight and fat mass. However, data does not support a common mechanism between these populations, but separate mechanisms to

commonly reduce body weight. In addition to adipose tissue loss across all cell types, glutamatergic neurons also reduced food intake and lean mass while GABAergic activation did not, indicates that these neurons might influence energy intake instead of energy expenditure. Glutamatergic neurons likely modulate both food intake and energy storage, whereas GABAergic neurons may primarily influence energy expenditure, adiposity and lean muscle development. Additionally, the fact that activating glutamatergic neurons in the caudal POA, but not the rostral POA, induced thermogenesis in iBAT and iWAT indicates a functional specialization within the caudal POA. This region-specific effect suggests that the caudal POA has distinct neuronal circuits that are more involved in the regulation of peripheral thermogenesis and energy expenditure.

The lack of thermogenic response following the activation of GABAergic neurons suggests that glutamatergic neurons in the caudal POA may be specifically linked to thermogenic processes in peripheral tissues. The upregulation of thermogenic genes in iBAT following the activation of glutamatergic neurons in the caudal POA reinforces the idea that these neurons are pivotal in enhancing thermogenesis and energy expenditure. This gene expression profile aligns with the observed increase in depot temperatures, providing a molecular basis for the thermogenic effects. The increase in Prdm16 gene expression upon GABAergic activation suggests that while these neurons may not directly induce thermogenesis, they could still play a role in modulating iBAT function or differentiation. On the other hand, inhibiting glutamatergic signaling in the caudal POA still resulted in reduced body weight and adiposity, alongside increased thermogenesis in iBAT and iWAT. This indicates that glutamatergic signaling might not be necessary for

these effects and suggests the involvement of a more complex neural circuitry, possibly involving compensatory mechanisms or other unidentified pathways.

Together my data underscores the distinct and complementary roles of glutamatergic and GABAergic neurons in the caudal POA in energy balance regulation. The activation of glutamatergic neurons appears to enhance energy expenditure not only through increased thermogenesis in adipose tissues but also by suppressing appetite, highlighting the excitatory nature of these neurons in promoting metabolic processes. On the other hand, the role of GABAergic neurons seems more limited to adiposity control, suggesting an inhibitory influence on energy conservation mechanisms. The differential effects observed in rostral versus caudal POA regions further suggest a spatially distinct functionality within the POA, with the caudal POA being more influential in thermogenesis. The discrepancy between temperature regulation and body weight effects observed in these studies highlights the complex and distinct roles of glutamatergic and GABAergic signaling within the rostral and caudal POA. The activation of glutamatergic neurons in the caudal POA induced adipose tissue thermogenesis, leading to a reduction in food intake and body weight. This suggests that glutamatergic signaling in the caudal POA directly promotes energy expenditure through thermogenesis. In contrast, activating GABAergic neurons in the same region resulted in reduced adiposity without affecting thermogenesis, indicating that the weight loss mediated by these neurons might involve non-thermogenic mechanisms, such as alterations in metabolic programming or changes in peripheral energy storage. Interestingly, while both neuron types contributed to weight loss, the mechanisms appear distinct, with glutamatergic signaling linked to thermogenesis and GABAergic signaling possibly influencing adipose tissue metabolism

or storage directly. The absence of increased thermogenesis in some cases, despite reduced adiposity, suggests that long-term changes in metabolic programming, possibly through hormonal or autonomic pathways, might underlie the sustained reduction in adipose mass. This distinction between immediate thermogenic responses and long-term metabolic adaptations emphasizes the need to consider both direct and indirect pathways in the regulation of energy balance and the treatment of obesity.

The identification of specific neuronal populations within the caudal POA that regulate body weight and thermogenesis highlights potential targets for therapeutic interventions in obesity and metabolic disorders. Modulating glutamatergic and GABAergic signaling in these regions could offer new strategies for weight loss and metabolic health improvement. Specifically, the ability of glutamatergic neurons to simultaneously reduce food intake and promote thermogenesis makes them a particularly attractive target for anti-obesity strategies. Moreover, the specific activation of these neurons could potentially be used to modulate metabolic rates and energy expenditure without affecting other physiological processes controlled by the POA. The distinct roles of the rostral and caudal POA in thermogenesis and energy expenditure provide insights into the central regulation of these processes. This knowledge could contribute to the development of more precise treatments targeting specific brain regions to enhance metabolic outcomes. The involvement of complex neural circuits in regulating energy balance underscores the need for a comprehensive understanding of the brain's role in metabolic regulation. This complexity also suggests that multiple pathways and neurotransmitter systems may need to be targeted simultaneously for effective obesity treatment.

The different efferent projections from the rostral and caudal POA neurons also may also play an important role in the producing the peripheral effects these circuits produced, as the projection sites are known to play crucial roles in various aspects of human physiology, particularly in regulating energy homeostasis and stress responses. As mentioned in chapter 1, the VMN is pivotal in controlling energy balance, particularly in terminating feeding behavior and is also involved in the counterregulatory response to hypoglycemia, where it stimulates glucagon secretion to restore blood glucose levels. Dysfunction in this region has been linked to obesity, as the VMN is integral to the body's ability to sense and respond to energy surplus and deficits. Targeting VMN pathways could help develop therapies aimed at enhancing satiety or improving glucose regulation in obesity. The LHA regulates feeding behavior and energy homeostasis. It integrates signals related to hunger and energy needs and is considered a critical player in both initiating feeding and in reward-driven eating. Dysregulation in the LHA can lead to overeating and obesity, making it a significant target for anti-obesity drugs aimed at modulating these pathways to reduce excessive food intake. Both the LPAG and VLPAG of the PAG are involved in the modulation of pain and stress responses. While they are not directly involved in feeding, their role in stress-induced eating behavior is crucial. Stress can trigger overeating or binge eating in susceptible individuals, and targeting the PAG could be a novel approach to managing stress-related obesity. Additionally, the MnR is implicated in mood regulation and have connections to pathways that modulate food intake. Given the strong link between mood disorders and obesity, targeting the serotonergic pathways in these nuclei could provide therapeutic benefits for patients who struggle with obesity due to emotional or stress-related eating. The ATg, a part of the

VTA, is involved in motor control and reward systems, which can influence physical activity levels and motivation to engage in behaviors like eating. Modulating this area could help in designing therapies that encourage physical activity or reduce reward-driven eating in obesity. Moreover, the VTA is well known for regulating reward consumption and addiction behaviors and is connected to various other hypothalamic nuclei as well as the spinal neurons. Understanding and dissecting each of these connections and neural circuits could lead to identification of new mechanisms and neural components underlying obesity development.

Prevalent studies utilizing the diet-induced obesity model show that while 70-80% of male mice become diet-induced obese in a short amount of time, only 30-40% of female mice become obese from HFD. Thus, I used male obese mice for these studies as female mice are more resistant to weight gain and including female diet-induced obese mice would have extended the timeline of these studies much further. But future studies should include female mice to explore potential sex differences and the generalizability of these findings. This would help in understanding whether similar mechanisms are at play in different contexts and populations and to provide a more comprehensive understanding. Moreover, females exhibit distinct patterns of body weight control, influenced by estrogen and other hormones, which modulate adiposity, energy expenditure, and thermogenic capacity differently than in males. Incorporating females into future studies is essential for a comprehensive understanding of these mechanisms. This would not only reveal potential sex-specific therapeutic targets but also provide insights into the long-term differences in body weight control between sexes. For instance, females might respond differently to interventions aimed at enhancing

thermogenesis or reducing adiposity, given their unique hormonal milieu and its impact on energy balance and fat distribution over the lifespan. Addressing these differences could lead to more effective, gender-tailored strategies for managing obesity and metabolic disorders. Additionally, while my use of Cre-loxP technology enabled targeted neuronal manipulation, it does not allow for the precise mapping of downstream pathways and circuits involved in the observed phenotypic changes. To gain a more comprehensive understanding of the role of rostral and caudal POA neuronal populations in regulating energy balance, future research should investigate the glutamatergic and GABAergic neuronal sub-populations, including those expressing different neurotransmitters, neuropeptides, or receptors. This could help identify additional targets for therapeutic intervention.

Further mechanistic studies should aim to delineate long-term effects of chronic modulation of glutamatergic and GABAergic signaling in the caudal POA, including potential compensatory changes in other neural circuits or metabolic processes. Additionally, a deeper exploration of the downstream pathways and inter-neuronal communications as well as identifying the downstream targets of the activated or inhibited neurons, provided a more comprehensive understanding of the neural circuitry involved in energy homeostasis. Investigating the roles of other neurotransmitter and neuropeptide systems within the caudal POA, that might interact with glutamatergic and GABAergic signaling in the caudal POA, could also yield further insights into the complex regulation of energy balance. Moreover, translational studies are needed to explore the potential therapeutic applications of these findings in humans, with a focus on the safety and efficacy of targeting specific neuronal populations for obesity treatment.

Conclusion

My study provides novel insights into the role of the caudal POA in regulating energy expenditure and body weight, particularly through the differential involvement of glutamatergic and GABAergic neurons. By utilizing vGLUT2^{Cre} and vGAT^{Cre} mice models, I demonstrated that both glutamatergic and GABAergic neurons in the caudal POA significantly contribute to ameliorating diet-induced obesity, with glutamatergic signaling being particularly pivotal in inducing thermogenesis in iBAT and iWAT. Activation of glutamatergic neurons reduced food intake, adiposity, and increased lean mass, while also enhancing thermogenic gene expression in iBAT. In contrast, GABAergic neuron activation primarily reduced adiposity without significant effects on food intake or thermogenesis. Inhibiting glutamatergic neurons in the caudal POA also led to weight loss and thermogenic responses, indicating the complexity of the underlying neural circuits.

Chapter 5: Identification of cells in the preoptic area and bed nucleus of the stria terminalis, impacted by obesity and diabetes in both male and female mice

Abstract

In the previous study, I found distinct roles of glutamatergic and GABAergic neuronal populations in body weight regulation, adiposity reduction, and thermogenesis induction. However, the cellular makeup of the POA is heterogeneous, and the molecular identities of the body weight regulating cells remain elusive. To gain a more comprehensive understanding of the role of rostral and caudal POA neuronal populations in regulating energy balance, I wanted to investigate the glutamatergic and GABAergic neuronal sub-populations, including those expressing different neurotransmitters, neuropeptides, or receptors. Additionally, as mentioned in chapter 3, the VMN^{PACAP} neurons projected to BNST, besides caudal POA, and activating those projections led to higher blood glucose levels in mice, indicating the VMN^{PACAP} → BNST was responsible for glucoregulatory response. To dissect the cellular and molecular heterogeneity of the POA and BNST, I employed single-nuclei RNA sequencing (snRNASeq), focusing on neuronal subpopulations overexpressed in obese and glucose-intolerant mice, to further elucidate the cellular architecture of these regions and identify potential therapeutic targets for obesity and type-2 diabetes.

I employed snRNASeq to characterize the cellular diversity within this region by analyzing >200,000 nuclei, the largest dataset of this brain region to date, from a cohort of mixed-sex mice, including obese and glucose-intolerant individuals on a high-fat diet. This comprehensive analysis identified six high-resolution cellular subtypes that were

significantly enriched in obese and glucose-intolerant mice. To refine my understanding of these subtypes, I utilized advanced deep-transfer learning techniques, which enabled us to identify cellular subsets associated with increased obesity and type-2 diabetes risk.

These studies provide a detailed cellular and molecular map of the caudal POA, revealing new high-resolution subtypes of neurons and other non-neuronal cell types that may play critical roles in energy balance and metabolic regulation. My findings highlight targetable genes and pathways within these newly identified cell populations, offering novel therapeutic avenues for the treatment of obesity and metabolic disorders. This research represents a significant step forward in understanding the complex neural circuits governing energy homeostasis and offers potential for developing targeted interventions to combat metabolic diseases.

Background and rationale

The POA's thermoregulatory functions have been extensively characterized, with early research demonstrating its critical role in maintaining body temperature. The POA integrates temperature-related sensory to orchestrate appropriate physiological responses, such as shivering or vasodilation, that activate heat production and dissipation. It also plays a key role in reproductive behaviors, coordinating sexual arousal and mating through its connections with other hypothalamic and limbic structures. Additionally, the POA regulates circadian rhythmicity, interacting with the SCN to modulate sleep-wake cycles and other daily physiological rhythms. Despite these well-established roles, the POA's contribution to body weight regulation and metabolic homeostasis remains relatively underexplored. Recent studies have begun to uncover the involvement of the

POA in energy balance, particularly its role in regulating feeding behavior and energy expenditure. However, the specific neuronal subpopulations within the caudal POA that mediate these effects and their potential role in obesity and type-2 diabetes are not fully understood.

The complexity of the POA is underscored by recent findings from Moffitt et al. (Moffitt, Bambah-Mukku et al. 2018), who utilized molecular, spatial, and functional single-cell profiling to uncover a diverse array of cellular subtypes within this region. However, they defined the POA region extremely broadly, including parts of the striatum, lateral septum, and all of the BNST. Despite this issue, their study revealed a rich tapestry of neurons and other cell types, each potentially contributing uniquely to the POA's multifaceted roles. This cellular heterogeneity suggests that the POA may integrate various physiological signals to coordinate responses related not only to traditional functions such as thermoregulation and reproduction but also to energy balance and metabolic regulation. Understanding and dissecting this complexity is crucial, as it could reveal novel cellular targets and pathways for therapeutic intervention in obesity and metabolic disorders. The identification of specific neuronal subtypes and their associated molecular markers provides a foundational map for future studies aiming to elucidate the mechanisms by which the POA influences body weight and energy homeostasis.

In my previous study, I employed chemogenetic approaches to selectively activate or inhibit glutamatergic and GABAergic neurons in the caudal POA of diet-induced obese male mice. This work revealed distinct roles for these neuronal populations in regulating body weight, adiposity, and thermogenesis. Specifically, activation of

glutamatergic signaling in the caudal POA induced thermogenesis in interscapular iBAT and iWAT, leading to significant reductions in body weight and fat mass. In contrast, activation of GABAergic signaling did not elicit similar thermogenic effects. Furthermore, inhibition of glutamatergic signaling, while effective in reducing obesity, failed to induce thermogenesis, indicating a complex and potentially context-dependent interplay of these neuronal pathways.

Previous investigations to study the transcriptomic profile of the POA has mostly focused on the markers within medial POA that are involved social behavior regulation (Eck, Palmer et al. 2022, Guo, Keenan et al. 2024, Polzin, Zhao et al. 2024), but markers overexpressed in metabolic disorders has not been studied. Here, I employed advanced deep transfer learning techniques to identify specific cellular subsets associated with increased risk of obesity and type-2 diabetes. This approach allowed us to refine my understanding of the high-resolution subtypes and to highlight targetable genes and pathways within these populations. My findings offer novel therapeutic avenues for the treatment of obesity and metabolic disorders by potentially modulating these newly identified cell populations to restore energy balance.

The cellular complexity and heterogeneity of the POA pose significant challenges to understanding its precise role in energy balance and metabolic regulation. Traditional techniques have been limited in their ability to resolve the diverse cellular subtypes and their specific contributions to physiological processes (Kim, Kang et al. 2023). To address these limitations, I employed snRNASeq to provide a comprehensive analysis of the caudal POA's cellular landscape. By analyzing over 200,000 nuclei from a cohort of mixed-sex mice, including obese and glucose-intolerant individuals on a high-fat diet, I

generated the largest dataset of this brain region to date. This analysis revealed six high-resolution cellular subtypes significantly enriched in obese and glucose-intolerant mice, underscoring the region's cellular diversity and its potential role in metabolic dysregulation.

To validate the presence and spatial distribution of these cellular subtypes, I utilized RNAscope *in situ* hybridization, a powerful technique for detecting and visualizing specific RNA molecules within tissue sections. RNAscope enabled us to confirm the expression patterns of key markers in identified glutamatergic and GABAergic neuronal clusters, providing a spatially resolved map of these populations within the caudal POA. The advantages of RNAscope include its high sensitivity and specificity, allowing for the detection of low-abundance transcripts and providing precise localization of gene expression within the tissue context. This validation step is critical for ensuring the accuracy of my snRNASeq data and for linking molecular signatures to functional anatomical structures.

This study advances my understanding of the cellular complexity and heterogeneity within the POA and its implications for energy homeostasis. By elucidating the distinct roles of glutamatergic and GABAergic neuronal populations in thermogenesis and metabolic regulation, I provide a foundation for developing targeted interventions to combat obesity and related metabolic diseases. The integration of cutting-edge single-cell technologies, RNAscope validation, and computational approaches in this research underscores the potential for high-resolution cellular mapping to inform therapeutic strategies for complex metabolic disorders.

Results

Dissecting the complexity of the POA and BNST in obesity and diabetes through single nuclei sequencing

A diagram describing the experimental setup and a flow chart explaining the process of selecting mice for the snRNASeq study are shown (Fig. 5.1). I put the C57BL/6J male and female mice were put on HFD or control diet for 12-14 weeks, until they weighed at least 35gm and they were glucose intolerant (Fig. 5.1). Once every week the mice were weighed, and glucose tolerance test (GTT) was performed on them. In the obese and glucose-intolerant group, only mice that were maintained on HFD, weighed at least 35 grams, had >10 grams of adipose mass (Fig. 5.1A) and had a blood glucose level of at least 200mg/dL or >500mg-hr/dL (Fig. 5.1B), n = 10 female and 11 male, were chosen for the snRNASeq. The control group, that were maintained on control diet, contained n = 9 female and 9 male lean and glucose-tolerant mice, with at least 35 grams body weight, <5 grams of adipose mass (Fig. 5.1A) and <200mg/dL or >400mg-hr/dL blood glucose level (Fig. 5.1B).

I dissected the rostral part of the mouse hypothalamus containing the POA region (~1.5mm x 2.3mm x 1.2mm, bregma +0.6mm to −0.6mm) and BNST region (~1.2mm x 2.5mm x 1.2mm, bregma +0.6mm to −0.6mm) from brains of adult female and male mice from the HFD or control groups (Fig. 5.1D). From each of brain areas, i.e., POA and BNST, I dissociated the tissue to get single nuclei using a custom protocol that improved cell survival and FACS capture (as described in the Chapter 2). Following pre-processing steps to remove low-quality nuclei and any outlier samples, the final single-nucleus RNA-seq dataset contained a total of 185,716 nuclei with a mean nuclei number of 9,774

± 1,370 (mean ± SD) per animal for POA, and 218,550 nuclei with a mean nuclei number of 11,302 ± 1,424 (mean ± SD) per animal for BNST. Two rounds of clustering were used to first, separate the major neuronal (inhibitory and excitatory neurons) and non-neuronal cell types and second, to further identify the cellular subgroups among each of these cell types. This led to the delineation of major cell classes including excitatory and inhibitory neurons, microglia, astrocytes, immature oligodendrocytes (newly formed oligodendrocytes and oligodendrocyte progenitor cells), mature oligodendrocytes, ependymal cells, endothelial cells, fibroblasts, macrophages, and mural cells, as well as subdivisions within these cell classes (Fig. 5.2, 5.3).

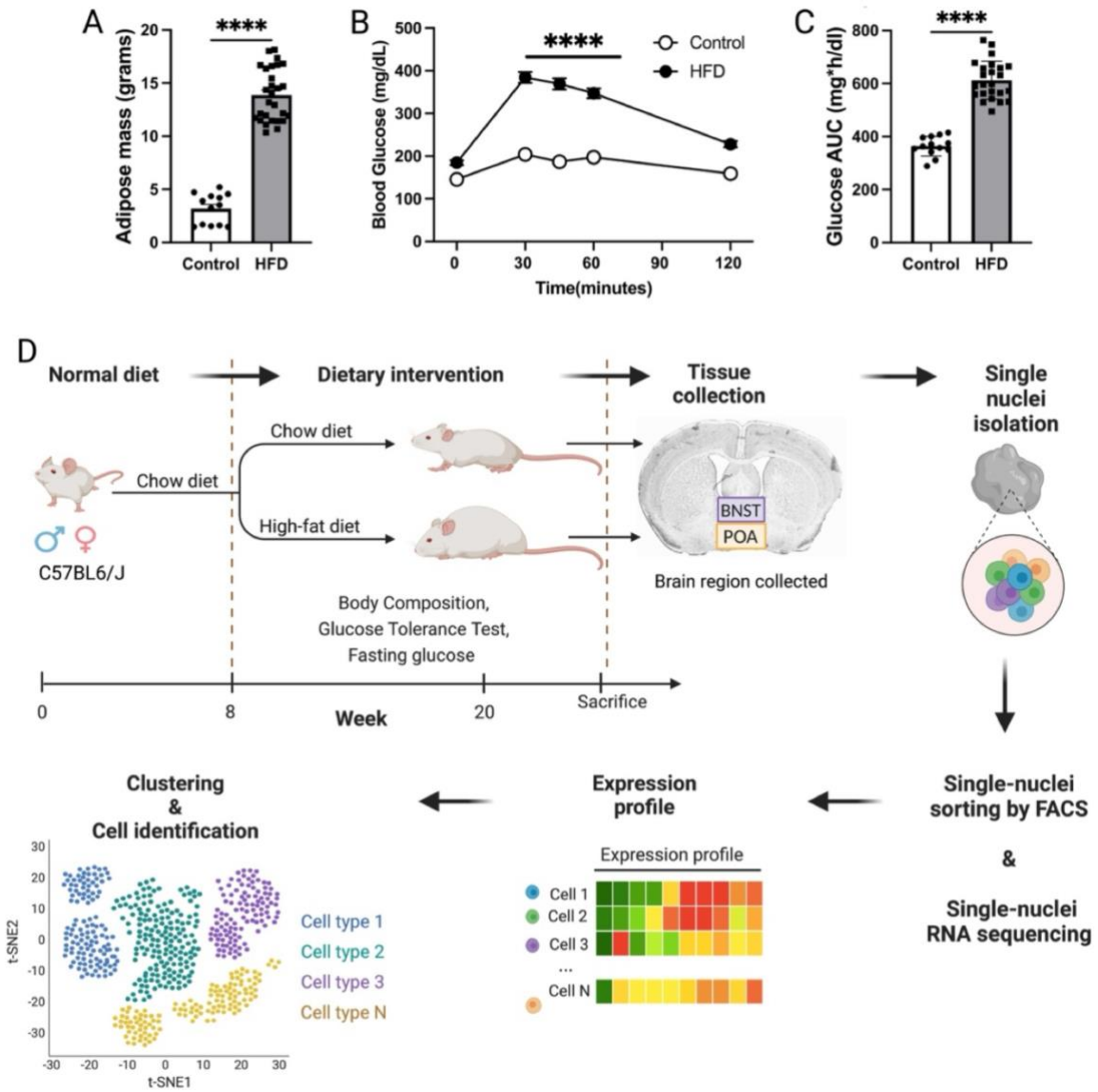

Figure 5.1: Selection criteria for mice used in snRNASeq. C57BL/6J male and female mice were put on HFD or control diet for 12-14 weeks, until they weighed at least 35gm and they were glucose intolerant. In the obese and glucose-intolerant group, only mice that were maintained on HFD, weighed at least 35 grams, had a high adiposity and had a high blood glucose level were chosen for the snRNASeq. The control group, that were maintained on control diet, contained lean and glucose-tolerant mice, with at least 35 grams body weight, normal adiposity and blood glucose level. Design and workflow of snRNA sequencing of POA and BNST (D) in diet induced obese mice or control mice on chow diet, to identify the population of POA and BNST cells responsive to diabetes and obesity. >200,000 single nuclei were analyzed. n = 10 females, 11 males (obese and glucose intolerant) and 9 females, 9 males (control) for both POA and BNST. (A, C)

analyzed by multiple student's t-test. (B) analyzed by two-way RM ANOVA. Data expressed as mean ± SEM. ****p<0.0001.

The first round of clustering in the POA and BNST identified several cell clusters, which are annotated into ten major cell types (Fig. S8, S9) based on the expression of known marker genes, including inhibitory neurons (based on *Gad1*/*Gad2* and *Slc32a1*, encoding vGAT), excitatory neurons (*Slc17a6*, encoding vGLUT2, and *Slc17a8*, encoding vGLUT3), astrocytes (*Slc1a2* and *Slc39a12*), oligodendrocytes (*Mbp* and *St18*), oligodendrocyte precursor cells (OPCs; based on *Vcan* and *Pdgfra*), microglia (*Selplg* and *C1qa*), endothelial cells (*Flt1*), ependymal cells (*Ccdc170* and *DnAHA12*), vascular and leptomeningeal cells (VLMCs; based on *Slc6a13*), and arachnoid barrier cells (ABCs; based on *Slc47a1*). In the POA, second round of clustering of excitatory neurons (1,012 cells) and inhibitory neurons (12,0167 cells) separately revealed 7 and 19 neuronal subpopulations, respectively (Figs. 5.2). In the BNST, further clustering of excitatory neurons (9,459 cells) and inhibitory neurons (11,8250 cells) separately revealed 11 and 23 subpopulations, respectively (Figs. 5.3). I denoted the excitatory and inhibitory neuronal clusters as e1, e2, … and so on; and i1, i2, … and so on, respectively, with the initial letter "e" or "i" for excitatory or inhibitory neurons, respectively, followed by a number indicating the size of the clusters (with 0 indicating the largest cluster).

While most of the identified clusters expressed either excitatory or inhibitory neuronal markers, I observed expression of the GABA synthetic genes *Gad1* and *Gad2* in many excitatory neuronal clusters classified on the basis of expression of the gene for vGLUT2 (*Slc17a6*), with *Gad2* expression being particularly widespread. By contrast,

very few *Slc17a6*-positive clusters expressed the gene for vGAT (*Slc32a1*). These data suggest that *Slc17a6* and *Slc32a1* are better discriminators for excitatory versus inhibitory neurons, corroborating evidence from other brain areas. Interestingly, cells in two neuronal clusters originally designated as inhibitory and one originally designated as excitatory co-expressed *Slc17a6* (or *Slc17a8* for vGLUT3) and *Slc32a1*. These cells were unlikely to be a clustering artifact because individual cells co-expressed both markers, nor did they correspond to doublets, hence they potentially represent hybrid neurons capable of GABA/Glutamate co-release, as characterized in the hypothalamus and a few other brain regions. I denoted these clusters as h1, h2 and h3 (Fig. S8).

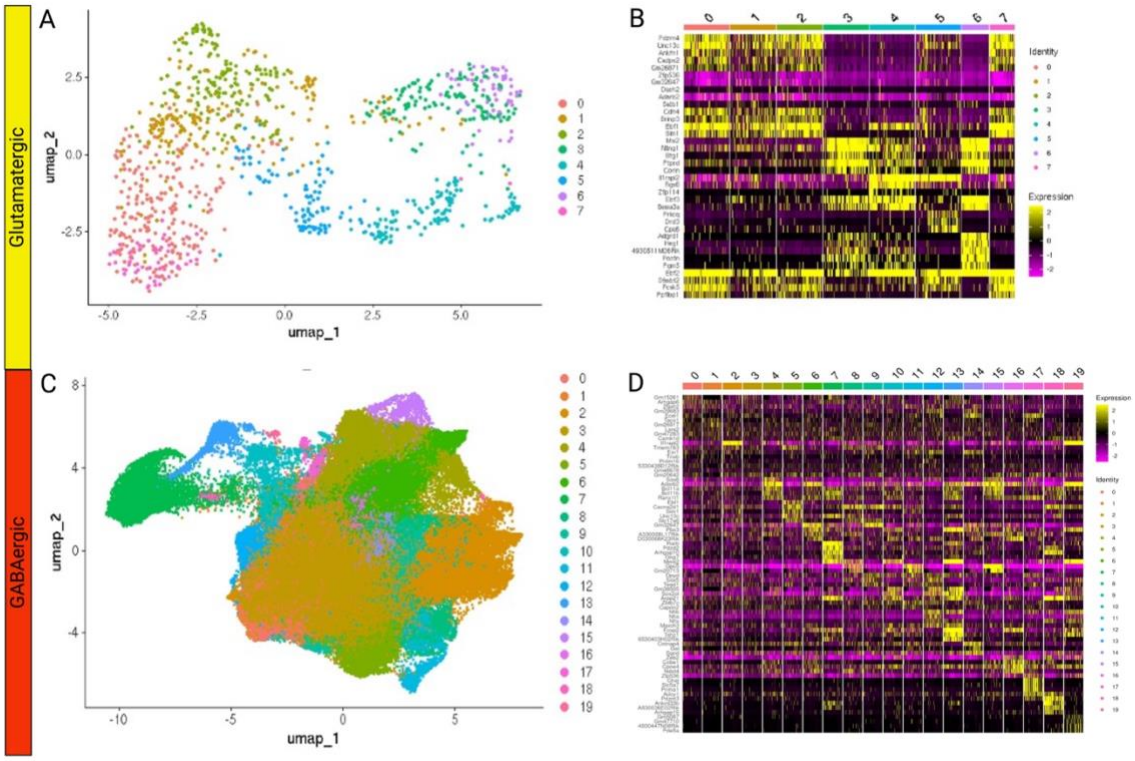

Figure 5.2: Single-nuclei RNA sequencing of POA. Over 200,000 single nuclei were analyzed from the POA of diet induced obese mice or control mice on chow diet, to identify the population of POA cells responsive to diabetes and obesity. Uniform Manifold Approximation and Projection (UMAP) for glutamatergic (a) and GABAergic (C) populations with cells colored by cluster. Numbers on the UMAP indicate the cluster ID. Each color-coded cluster on the UMAP plot represents populations of cells that have the same gene expression profile. Total nuclei numbers for each UMAP plot are 200,000. Heatmap of differentially expressed genes per cluster within the glutamatergic (B) or GABAergic (D) neuron population. n = 10 females, 11 males (obese and glucose intolerant) and 9 females, 9 males (control).

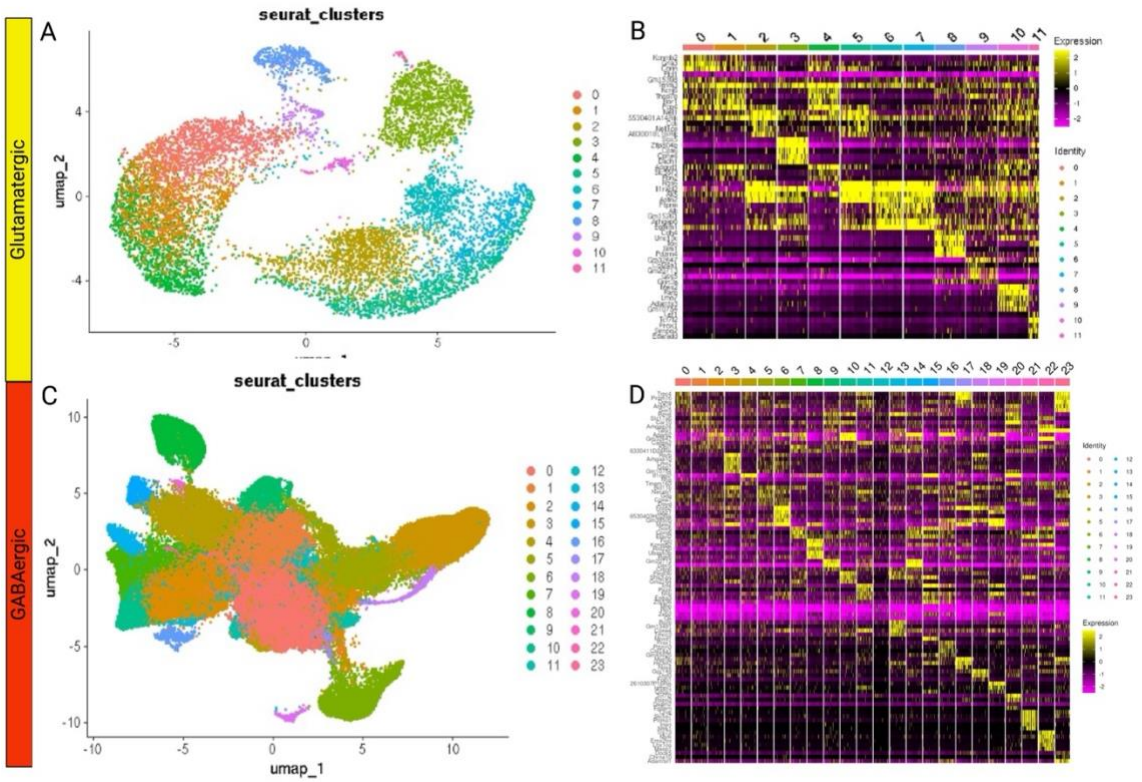

Figure 5.3: Single-nuclei RNA sequencing of BNST. Over 200,000 single nuclei were analyzed from the BNST of diet induced obese mice or control mice on chow diet, to identify the population of BNST cells responsive to diabetes and obesity. Uniform Manifold Approximation and Projection (UMAP) for glutamatergic (a) and GABAergic (C) populations with cells colored by cluster. Numbers on the UMAP indicate the cluster ID. Each color-coded cluster on the UMAP plot represents populations of cells that have the same gene expression profile. Total nuclei numbers for each UMAP plot are 200,000. Heatmap of differentially expressed genes per cluster within the glutamatergic (B) or GABAergic (D) neuron population. n = 10 females, 11 males (obese and glucose intolerant) and 9 females, 9 males (control).

Validation and identification of glutamatergic and GABAergic cluster in the POA over-represented in obese and diabetic mice

To validate and spatially characterize the glutamatergic (e0) and GABAergic clusters (i5) in the caudal portions of the POA, that are over-expressed in obese and diabetic mice, I performed *in situ* hybridization using the RNAscope Multiplex Fluorescent V2 assay to study gene expression in brain tissue sections (Advanced Cell Diagnostics). Coronal sections of the caudal portions of the POA (defined from +0.3mm to -0.7mm bregma, that are just lateral to the SCN, above OPT, but not in the traditional more rostral (+0.6mm to +0.3mm bregma) regions required for stable body temperature) from C57BL/6J mice, were sampled at bregma 0.26mm (Fig. 5.4A, 5.5A), 0.02mm (Fig. 5.4B, 5.5B), -0.34mm (Fig. 5.4C, 5.5C) and -0.70mm (Fig. 5.4D, 5.5D) (n = *4* for each region), and an area of 1.8 mm (height) × 2.1 mm (width) was scanned for each brain section. I studied the localization of the excitatory markers *Asic2* (Acid-sensing ion channel 2) and *Ptprd* (Protein tyrosine phosphatase receptor type D) mRNA expression, co-expressed in the vGLUT2 neurons to characterize the glutamatergic neuronal clusters (Fig. 5.4), as well as the inhibitory markers *Kcnip1* (Potassium (K) voltage-gated channel interacting protein 1) and *Gpc5* (Glypican 5) mRNA expression, co-expressed in the vGAT neurons the characterize the GABAergic neuronal clusters (Fig. 5.5).

Within the caudal POA glutamatergic population, I found both *Asic2* and *Ptprd* mRNA expression in ventromedial preoptic nucleus (VMPO), ventrolateral preoptic nucleus (VLPO), medial preoptic nucleus (MPA), medial preoptic area (MPO), lateral preoptic area (LPO) (Fig. 5.4). Comparing the co-expression levels of both *Asic2* and *Ptprd* between VMPO, VLPO, MPA, MPO and LPO revealed that vGLUT2 neurons in

MPA and VMPO expressed highest levels *Asic2* and *Ptprd* (Fig 5.4). Whereas, within the caudal POA GABAergic population, I found *Kcnip1* and *Gpc5* mRNA expression in VMPO, VLPO, MPA, MPO, LPO and AHA (Fig. 5.5). Comparing the co-expression levels of both *Kcnip1* and *Gpc5* between VMPO, VLPO, MPA, MPO, LPO and AHA revealed that vGAT neurons in MPO expressed highest levels *Kcnip1* and *Gpc5* (Fig 5.5).

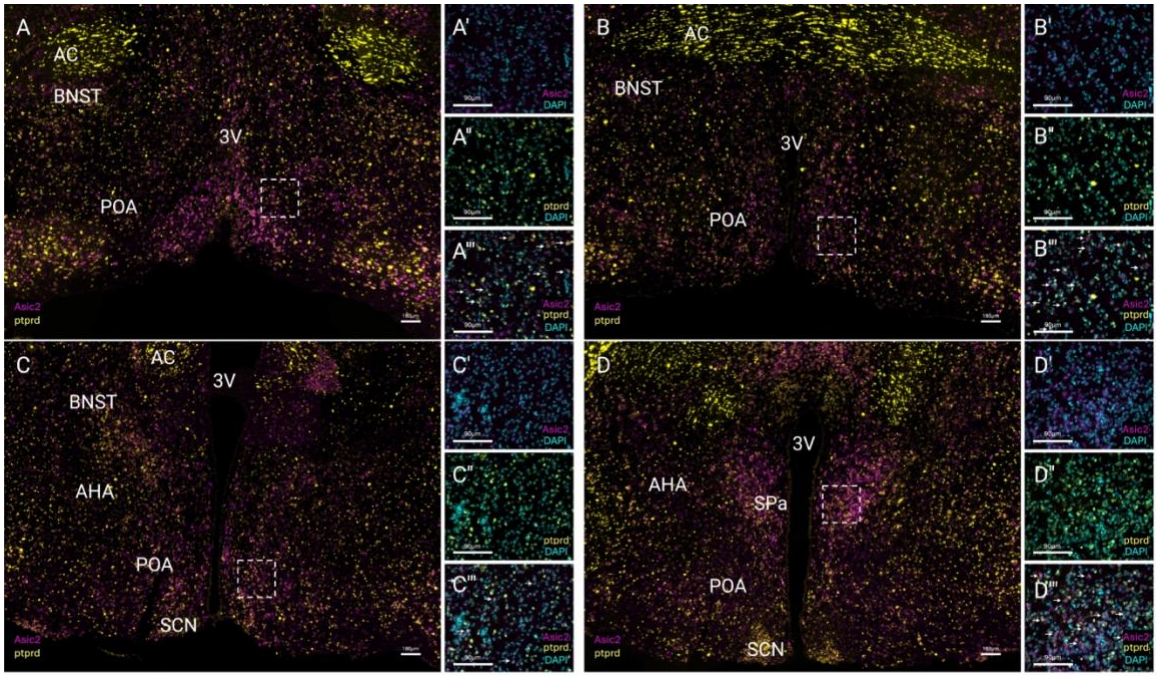

Figure 5.4: Asic2 and Ptprd mRNA expression in the caudal POA. RNAscope *in situ* hybridization representative images showing the regionally enriched distribution of Asic2 and Ptprd across the caudal POA (A-D). Magenta fluorescent dots represent Asic2 transcripts (one dot equals one transcript), yellow dots represent Ptprd transcripts and cyan dots represent DAPI in the nuclei. Four different bregma locations were chosen to represent the caudal POA: 0.26mm bregma (A), 0.02mm bregma (B),-0.34mm bregma (C) and -0.70mm bregma (D). Zoomed-in RNAscope images showing either Asic2 (A', B', C', D') or Ptprd (A'', B'', C'', D'') mRNA expression pattern overlaid with DAPI and a merge of all three (A''', B''', C''', D''') throughout the caudal POA. Asic2 = Acid-sensing ion channel 2. Ptprd = Protein tyrosine phosphatase receptor type D. DAPI = 4′,6-diamidino-2-phenylindol. AC = Anterior commissure. AHA = Anterior hypothalamic area. BNST = Bed nucleus of stria terminalis. 3V = 3rd ventricle. POA = Preoptic area. Spa = Subparaventricular hypothalamus. SCN = Suprachiasmatic nucleus. Scalebars = 180 µm (A, B, C, D) and 90 µm (A', A'', A''', B', B'', B''', C', C'', C''', D', D'', D'''). The schematics were created using The Mouse Brain in Stereotaxic Coordinates Fourth Edition (Paxinos and Franklin).

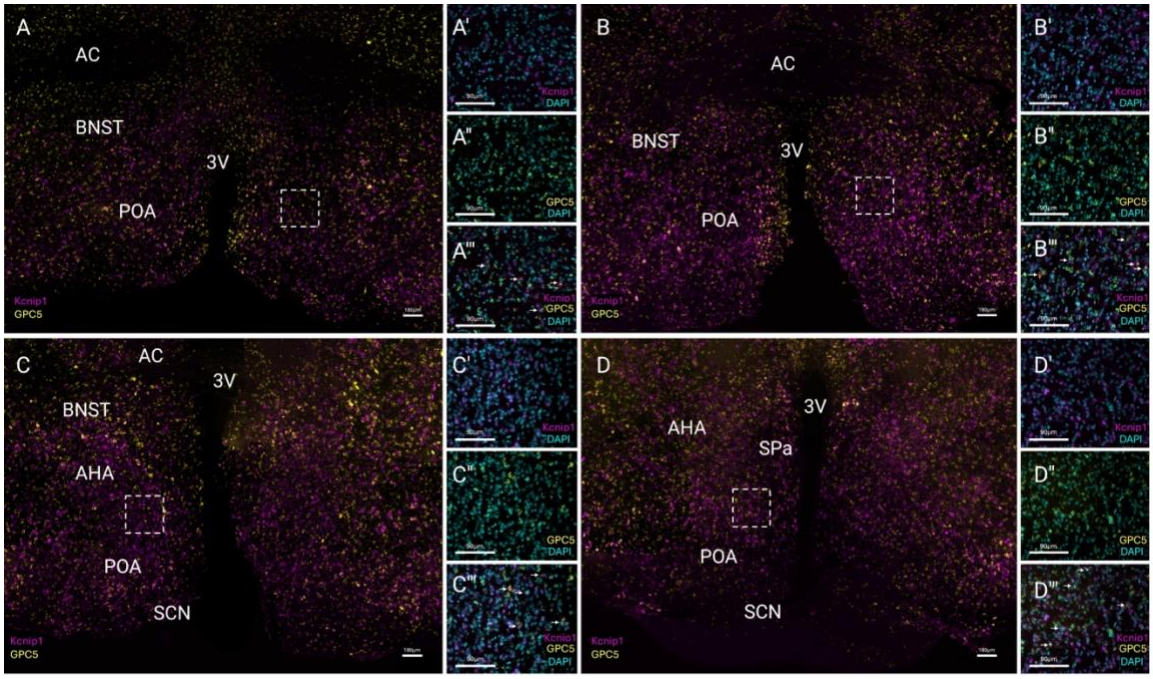

Figure 5.5: Kcnip1 and Gpc5 mRNA expression in the caudal POA. RNAscope *in situ* hybridization representative images showing the regionally enriched distribution of Kcnip1 and Gpc5 across the caudal POA (A-D). Magenta fluorescent dots represent Kcnip1 transcripts (one dot equals one transcript), yellow dots represent Gpc5 transcripts and cyan dots represent DAPI in the nuclei. Four different bregma locations were chosen to represent the caudal POA: 0.26mm bregma (A), 0.02mm bregma (B),-0.34mm bregma (C) and -0.70mm bregma (D). Zoomed-in RNAscope images showing either Kcnip1 (A', B', C', D') or Gpc5 (A'', B'', C'', D'') mRNA expression pattern overlaid with DAPI and a merge of all three (A''', B''', C''', D''') throughout the caudal POA. Kcnip1 = Potassium (K) voltage-gated channel interacting protein 1. Gpc5 = Glypican 5. DAPI = 4′,6-diamidino-2-phenylindol. AC = Anterior commissure. AHA = Anterior hypothalamic area. BNST = Bed nucleus of stria terminalis. 3V = 3rd ventricle. POA = Preoptic area. Spa = Subparaventricular hypothalamus. SCN = Suprachiasmatic nucleus. Scalebars = 180 µm (A, B, C, D) and 90 µm (A', A'', A''', B', B'', B''', C', C'', C''', D', D'', D'''). The schematics were created using The Mouse Brain in Stereotaxic Coordinates Fourth Edition (Paxinos and Franklin).

Discussion

Here, I combined the power of scRNA-seq and multiplex RNAscope *in situ* hybridization (RNAscope-ISH), to create a spatially resolved and functionally aware transcriptomic atlas of the POA of the mouse anterior hypothalamus in obese and glucose-intolerant mice. These methods identified major cell and neuronal subpopulations with correlated gene expression profiles, providing cross validations for both methods. Moreover, the two methods are complementary: scRNA-seq measured more genes than RNAscope-ISH and helped define marker genes for RNAscope-ISH; whereas the latter provided spatial context of specific cells at high resolution, as well as more accurate detection and quantification of weakly expressed genes, including functionally important genes such as neuropeptides and hormone receptors. As a result, the combined data provided a more complete picture of the transcriptional diversity and spatial organization of individual cells in the preoptic region. Transcriptional changes were compared between animals on HFD (the obese and diabetic mice group) and a control diet (the lean and glucose-tolerant mice group), where the obese and diabetic phenotype in the mice were confirmed by weekly body weight and body composition measurements and glucose tolerance tests. I observed a remarkable diversity of neurons in this region, comprising 26 different neuronal clusters within the POA and 34 different neuronal clusters within the BNST. Further molecular characterizations of the cell types revealed 7 excitatory neuronal clusters and 19 inhibitory neuronal clusters in POA and 11 excitatory neuronal clusters and 23 inhibitory neuronal clusters in the BNST.

Within the excitatory POA clusters I found *Asic2* and *Ptprd* genes to be over expressed in the obese and diabetic mice whereas within the inhibitory POA clusters I

found *Kcnip1* and *Gpc5* genes to be over expressed in the obese and diabetic mice. RNAscope-ISH revealed *Asic2* and *Ptprd* co-localized in the VMPO, VLPO, MPA, MPO and LPO with highest expression levels in the MPA and VMPO. Whereas, within the caudal POA GABAergic population, I found *Kcnip1* and *Gpc5* mRNA expression in VMPO, VLPO, MPA, MPO, LPO and AHA with highest expression levels in the in MPO.

ASIC2 is a member of the acid-sensing ion channels (ASICs) family that are proton-gated cation channels, crucial for detecting pH changes in the nervous system. These channels play a significant role in neuronal signaling, including the sensation of pain and mechano-transduction, which converts mechanical stimuli into electrical signals (Peng, Ahmad et al. 2004, Kweon, Cho et al. 2016). ASIC2 is expressed in both the central and peripheral nervous systems and contributes to various physiological processes, including taste and fear conditioning. There is no direct evidence linking ASIC2 to obesity or type 2 diabetes. However, ASICs' role in modulating autonomic nervous system activity may indirectly influence energy expenditure and appetite regulation, thereby affecting metabolic processes (Ohbuchi, Sato et al. 2010 117). ASIC2 has been implicated in neurological disorders involving chronic pain. It may contribute to conditions like migraines and certain neurodegenerative diseases due to its involvement in neuronal excitability (Kweon, Cho et al. 2016).

PTPRD is a receptor-type protein tyrosine phosphatase involved in cell signaling pathways that regulate cellular processes such as growth, differentiation, and synaptic development. PTPRD functions by removing phosphate groups from tyrosine residues on proteins, thereby modulating their activity and interactions. Recent research has identified

PTPRD as a receptor for asprosin, a fasting-induced adipokine produced by white adipose tissue. Asprosin plays a crucial role in energy homeostasis by crossing the blood-brain barrier and binding to PTPRD in the hypothalamus to stimulate appetite and increasing hepatic glucose production thereby increasing glucose release into the bloodstream. Asprosin binding to PTPRD triggers production of hunger-stimulating neuropeptides, such as AgRP, thereby increasing appetite and food intake (Feng, Liu et al. 2023 118). Elevated asprosin levels have been observed in individuals with obesity and insulin resistance, suggesting a role in the pathophysiology of metabolic disorders (Feng, Liu et al. 2023 119). The interaction between PTPRD and asprosin offers a promising target for obesity treatment. By inhibiting asprosin signaling through PTPRD, it may be possible to reduce appetite and food intake, leading to weight loss. Animal studies have shown that blocking asprosin can decrease appetite and body weight, suggesting that targeting this pathway could be an effective therapeutic strategy for managing obesity and its related complications (Zhang, Reis et al. 2020 120). Research is ongoing to develop small molecules or antibodies that can specifically inhibit the asprosin-PTPRD interaction. Such therapeutics could potentially normalize appetite regulation and improve metabolic health in individuals with obesity and type 2 diabetes. Additionally, understanding the broader signaling networks and physiological effects of PTPRD and asprosin can help identify other therapeutic targets and pathways involved in energy homeostasis (Zhang, Reis et al. 2020 120, Feng, Liu et al. 2023 118). Thus, PTPRD's interaction with asprosin plays a crucial role in regulating energy balance and appetite. Targeting this pathway offers a novel approach to developing anti-obesity

therapies, which could help address the growing prevalence of obesity and related metabolic disorders.

KCNIP1 belongs to the Kv channel-interacting proteins (KChIPs) that modulate voltage-gated potassium channels, crucial for controlling neuronal excitability and cardiac function by influencing potassium ion flow (Rhodes, Carroll et al. 2004 122). While the direct impact of KCNIP1 on obesity and type 2 diabetes is not well-documented, its regulation of neuronal activity might affect hypothalamic control of appetite and energy balance, potentially linking KCNIP1 to metabolic regulation (Xia, Xiong et al. 2010 121). KCNIP1 is implicated in neurological disorders due to its role in neuronal signaling and is also studied for its role in cardiovascular diseases, given its involvement in cardiac repolarization and arrhythmias (Xia, Xiong et al. 2010 123).

GPC5 is a glypican involved in modulating cell growth, differentiation, and morphogenesis by influencing signaling pathways such as Wnt and Hedgehog. Glypicans are heparan sulfate proteoglycans attached to the cell surface (Filmus and Capurro 2014). GPC5 is implicated in various cancers, including lung and prostate cancer, where it may influence tumor growth and progression. Its role in developmental processes also links it to congenital disorders affecting morphogenesis (Muller, Velazquez Camacho et al. 2023). Thus, these genes contribute to various physiological processes and can influence disease states, including metabolic disorders like obesity and type 2 diabetes, through different mechanisms and pathways. Understanding these genes' roles offers insights into potential therapeutic targets for metabolic and other diseases.

Additionally, this study also provides a molecular and cellular map of the neuronal and non-neuronal types within the BNST. Within the excitatory BNST clusters I

found *Foxp2* and *Col11a1* (Collagen Type XI Alpha 1 Chain) genes to be over expressed in the obese and diabetic mice whereas within the inhibitory POA clusters I found *Ryr3* (Ryanodine Receptor 3), *TrpC4* (Transient Receptor Potential Cation Channel Subfamily C Member 4) and *Dgkg* (Diacylglycerol Kinase Gamma) genes to be over expressed in the obese and diabetic mice. RNAscope-ISH of these over-expressed genes within the BNST will provide a detailed spatial map for targets within the BNST that are over expressed in the obese and diabetic mice.

FOXP2 is a transcription factor that plays a crucial role in the development of language and speech in humans. It is involved in the regulation of genes necessary for neural development, particularly in brain regions associated with speech and language processing (Vargha-Khadem, Gadian et al. 2005). Although primarily known for its role in speech and language, FOXP2 has been linked to metabolic processes. Some studies suggest that it might influence energy balance and feeding behavior through its expression in the brain, though direct associations with obesity or type 2 diabetes are not well-established. Mutations in FOXP2 can lead to developmental verbal dyspraxia, a disorder affecting the coordination of speech muscles, and may be associated with other neurodevelopmental disorders such as autism spectrum disorder (ASD) and schizophrenia (Lai, Fisher et al. 2001).

COL11A1 is a component of type XI collagen, which plays a role in the development and maintenance of cartilage, bone, and other connective tissues. It is essential for the proper formation of the extracellular matrix and skeletal development (Li, Ikeda et al. 2011). In type 2 diabetes, COL11A1 is downregulated along with other extracellular matrix and adhesion molecules (Li, Ikeda et al. 2011). Alterations in

collagen composition and structure can impact the mechanical properties of connective tissues, potentially influencing mobility and physical activity levels, which are indirectly related to obesity and metabolic health. Mutations in COL11A1 are associated with connective tissue disorders such as Stickler syndrome and Marshall syndrome, which can lead to skeletal abnormalities, hearing loss, and vision problems (Richards, McNinch et al. 2010).

RYR3 is a calcium release channel located in the sarcoplasmic reticulum of muscle cells and other tissues. It plays a key role in calcium signaling, which is crucial for muscle contraction, cellular metabolism, and various physiological processes (Zalk, Lehnart et al. 2007). RYR3 has been implicated in the regulation of glucose metabolism and insulin secretion. Abnormal calcium signaling through RYR3 may contribute to insulin resistance and beta-cell dysfunction, potentially impacting the development of type 2 diabetes. RYR3 is involved in various physiological processes, and its dysregulation may be linked to muscle-related disorders and certain cancers. However, its specific contributions to these conditions are not yet fully understood (Santulli, Lewis et al. 2018).

TRPC4 is a member of the TRP channel family, involved in calcium influx and cellular signaling. It plays a role in various physiological processes, including vascular function, neurotransmission, and sensory perception (Phelan, Mock et al. 2012). TRPC4 is implicated in the regulation of insulin secretion and glucose homeostasis. Its role in calcium signaling suggests that it may influence pancreatic beta-cell function and insulin sensitivity, which are critical factors in the pathogenesis of type 2 diabetes. Dysregulation of TRPC4 has been associated with cardiovascular diseases, kidney disorders, and

neurological conditions. Its involvement in calcium signaling pathways makes it a potential target for therapeutic interventions in these diseases (Dietrich, Kalwa et al. 2007, Camacho Londono, Tian et al. 2015).

DGKG is an enzyme involved in lipid signaling pathways, responsible for the conversion of diacylglycerol (DAG) to phosphatidic acid (PA). It plays a role in cell signaling, membrane trafficking, and lipid metabolism (Fukumoto, Tamada et al. 2018). DGKG may influence metabolic processes related to obesity and type 2 diabetes through its role in lipid signaling and metabolism. Alterations in DGKG expression or activity can affect lipid accumulation and insulin sensitivity, potentially contributing to metabolic disorders (Chibalin, Leng et al. 2022 134). DGKG has been linked to neurological disorders and certain cancers. Its role in lipid signaling pathways suggests that it may impact cell proliferation, survival, and differentiation, making it a potential target for cancer therapies (Topham and Prescott 1999).

This dataset, the largest of its kind till date, allowed me to map the spatial organization of neuronal and non-neuronal cell populations over expressed in POA and BNST of obese and diabetic mice. The identification of marker gene combinations and spatial locations defining the neuronal populations in the POA and BNST provides necessary tools for the precise targeting and perturbation of these populations, thus enabling future functional studies. Overall, my study provides the first transcriptomic map of the POA and BNST in obese and diabetic mice that can be leveraged to find the next generation of targets for obesity and diabetes therapeutics.

Conclusion

The integration of snRNA-seq and multiplex RNAscope in situ hybridization provided a comprehensive and spatially detailed transcriptomic atlas of the POA and BNST in obese and glucose-intolerant mice. This approach revealed the intricate cellular landscape and highlighted gene expression changes in response to a high-fat diet. The combined methods demonstrated complementary strengths: snRNA-seq facilitated the identification of diverse gene expressions, while RNAscope-ISH provided spatial resolution and precise quantification of gene expression, particularly for genes with low expression levels. The study uncovered specific neuronal clusters within the POA and BNST, indicating a complex network of excitatory and inhibitory neurons that may contribute to metabolic dysregulation in obesity and diabetes.

Overall, this research establishes a foundational understanding of the cellular and molecular mechanisms underpinning metabolic disorders, offering potential avenues for the development of targeted therapies to combat obesity and type 2 diabetes. The integration of transcriptomic profiling with spatial analysis in this study exemplifies a powerful approach to unraveling complex biological systems and identifying key genetic contributors to disease.

Acknowledgement

I thank Britany App, Connor A. Mahler, Sylvia Robertson, Soumya Yennapureddy and Dr. Travis Johnson for completing parts of the experiments in this chapter.

Chapter 6: Discussions

Summary and conclusions

My dissertation provides a comprehensive examination of the neural circuits and molecular mechanisms underlying energy homeostasis, with a particular focus on the caudal portion of the POA, which despite being is a major thermoregulatory centre, has not been studied for body weight and energy homeostasis. Utilizing cutting-edge techniques such as snRNASeq and multiplex RNAscope in situ hybridization, this research delineates the transcriptional landscape and spatial organization of neuronal populations in the hypothalamus of obese and glucose-intolerant mice. These methods facilitated the identification of major cell types and subpopulations, offering cross-validations and complementary insights into gene expression and spatial context. The findings of this dissertation have significant implications for the understanding of energy homeostasis and the development of obesity treatments. The identification of specific neuronal populations and pathways that regulate thermogenesis and energy balance opens new avenues for therapeutic intervention. By targeting these pathways, it may be possible to develop more effective treatments for obesity and related metabolic disorders, potentially improving health outcomes for millions of individuals worldwide. The integration snRNASeq and RNAscope-ISH provides a powerful toolkit for future research, enabling the exploration of complex biological systems with unprecedented detail.

First, I found the role of VMN neurons in regulating tissue thermogenesis and energy expenditure in the context of diet-induced obesity. The use of genetic mouse

models, such as *Sf1*^{Cre} and *Adcyap1*^{Cre}, allowed for the identification of specific VMN neuronal populations that express the neuropeptide PACAP. These neurons were shown to project to the caudal POA, playing a crucial role in the stimulation of thermogenesis in both iBAT and iWAT. The study found that activation of VMN^{PACAP} neurons significantly reduces adiposity and enhances energy expenditure, highlighting the potential of this neurocircuit for the treatment of obesity. The findings underscore the importance of VMN neurons in energy homeostasis and provide a basis for future studies exploring therapeutic interventions targeting these pathways.

Then I delved into the distinct neuronal populations within the caudal POA and their contributions to energy balance regulation. Utilizing *vGLUT2*^{Cre} and *vGAT*^{Cre} mouse models allowed for the dissection of the roles of glutamatergic and GABAergic neurons in the POA. The findings revealed that glutamatergic neurons primarily contribute to thermogenesis and food intake regulation, which is crucial for reducing body weight and improving metabolic profiles. In contrast, GABAergic neurons mainly influence adiposity without significantly affecting food intake, indicating a more nuanced role in energy regulation. This distinction underscores the complexity and specificity of the POA's role in ameliorating diet-induced obesity and provides a foundation for future research to develop targeted interventions that modulate these neuronal pathways.

Then I employed snRNASeq to explore the cellular diversity of the POA and the BNST in obesity and diabetes. This comprehensive approach identified various neuronal subtypes that are enriched in obese and glucose-intolerant mice. The transcriptomic analysis revealed specific gene expression profiles associated with metabolic dysregulation, providing insights into potential therapeutic targets for obesity and type 2

diabetes. The cellular map generated offers a novel perspective on the complex interactions within these brain regions and highlights key neuronal populations that could be targeted for therapeutic interventions.

Significance of findings

The findings of my dissertation significantly advance our understanding of the neural mechanisms involved in energy homeostasis, highlighting the complex interactions between specific neuronal populations and molecular pathways in the hypothalamus. The identification of key genes and circuits offers novel insights into the pathophysiology of obesity and related metabolic disorders, providing a foundation for developing targeted therapies. My study underscores the importance of considering both central and peripheral signals in maintaining energy balance, emphasizing the need for integrative approaches to address metabolic health challenges.

My dissertation also presents a comprehensive exploration of the neural circuits regulating energy expenditure, with a central focus on how the VMN, the less explored caudal POA and its downstream pathways influence thermogenesis and body weight regulation. My dissertation builds upon our current worldview of how different but interconnected neural circuits work in concert to achieve sustained body weight reduction and prevent rebound weight gain. One key player in this system is the VMN^{PACAP} neurons, which I have shown to project densely to the caudal POA. These projections play a crucial role in activating thermogenesis, especially in brown and beige adipose tissues, through glutamatergic signaling. The activation of VMN^{PACAP} neurons drives energy expenditure and thermogenic responses, which in turn lead to sustained body

weight reduction, even without altering food intake. This establishes the VMN → POA circuit as a critical axis for energy homeostasis.

What makes this system even more interesting and intricate is the involvement of distinct, parallel circuits within the different parts of the caudal POA region that are activated by VMN^{PACAP} efferents. My research reveals that both glutamatergic and GABAergic neurons in the caudal POA potentially gets activated by the VMN^{PACAP} efferents to ameliorate diet-induced obesity, but through a variety of yet to be fully characterized mechanisms. Glutamatergic neurons primarily reduce food intake that could be due to a distinct set of cells from those that can raise and lower temperature; while GABAergic neurons appear to contribute to weight regulation through alternative pathways that does not directly influence thermogenesis or food intake. Activation of the glutamatergic neurons in the anterior region of the caudal POA (mentioned as rostral POA throughout my dissertation) showed torpor like response, which may have contributed to the weight loss, and this neuronal population is distinct from the glutamatergic neurons in the posterior region of the caudal POA (mentioned as caudal POA throughout my dissertation). Inhibiting this torpor-like mechanism has been proposed for treating obesity. However, my work would suggest that this strategy would not be successful. That being said, avoiding the torpor response, as our data would suggest for VMN^{PACAP} neurons, would be preferable to target energy expenditure. This data is consistent with the view that the VMN, and presumably caudal POA efferents, are suppressed in negative energy balance because torpor is activated in energy deficit. Together, these findings highlight that thermogenesis, and activity may not be the biggest

influencer of body weight loss and there are other mechanisms that can be targeted to achieve weight loss.

Moreover, the fact that the GABAergic neurons within both the rostral and caudal POA can reduce both fat and body weight, with not only preserving but improving lean muscle mass is the third most interesting and important highlight of my dissertation. The GABAergic neuronal populations curb diet-induced obesity without inducing locomotor activity, thermogenesis or feeding circuits and this underscores the need to dissect this neuronal population. This population has the potential to reveal novel central and peripheral mechanisms that may be targetable in the future for specific loss of adipose mass, while preserving muscle mass. Indeed, POA cells receive inputs from a variety of locations in the brain, as well as peripheral signals that influence functioning. These signals could also impact the ability for VMN^{PACAP} neurons to induce the appropriate physiologic response or impact VMN-independent functions. But this needs to be tested in a future experiment to elucidate the exact inputs influencing the GABAergic caudal POA neurons. Additionally, it may also happen that there are separate mechanisms engaged by the VMN^{PACAP} neurons or some other VMN neuronal subtype that ultimately engages the different sub-populations of GABAergic caudal POA neurons which ultimately lead to this similar weight loss response at the periphery but via separate pathways. This notion requires further testing, since these mechanisms could be driven by a food intake-independent population of glutamatergic neurons. Whether or not these cells are a part of the VMN^{PACAP} circuitry, dissecting the caudal POA neuronal population has the potential to be the next therapeutic target for obesity treatment.

The glutamatergic and GABAergic neurons of the POA represent separate yet complementary pathways that converge on the same physiological outcomes—namely, body weight and adipose mass reduction — albeit through different mechanisms. This parallelism within the less explored caudal POA suggests that different subsets of neurons are responsible for fine-tuning the body's response to energy surpluses and deficits, allowing for a more nuanced control of body weight and energy expenditure. This also highlights the important role the caudal POA neurons may play in body weight regulation. Bringing all this together, my findings suggests that the VMN, through the VMN^{PACAP} neurons, orchestrates a network of parallel but distinct circuits in the caudal POA that work together and potentially mediate signaling via the glutamatergic caudal POA neurons to modulate adipose tissue thermogenesis and body weight loss.

The complexity of this circuit is further highlighted by the findings from single-nuclei RNA sequencing, where I identified six specialized subtypes of neurons in the POA and BNST that are dysregulated in obesity and type-2 diabetes. This provides a novel molecular basis for understanding how energy imbalance and metabolic dysfunction are encoded in the brain. The identification of these distinct yet cooperative circuits emphasize the potential for targeting specific neuronal populations within the POA to achieve sustained weight loss and prevent metabolic dysfunction. This work not only advances our understanding of the neural regulation of energy balance but also suggests exciting new directions for developing obesity and diabetes treatments based on the modulation of these parallel circuits. Also, the potential for targeting the asprosin-PTPRD pathway, in particular, holds another promise for innovative therapeutic strategies aimed at restoring energy balance in obese and diabetic patients.

Discussion and limitations

The dissertation presents a comprehensive exploration of the hypothalamic circuits involved in energy homeostasis, leveraging state-of-the-art techniques such as snRNASeq, multiplex RNAscope in situ hybridization, and advanced genetic mouse models. These approaches have provided novel insights into the neuronal populations and pathways that regulate energy balance and metabolic health. However, several limitations and areas for improvement warrant further discussion. To address the limitations of traditional techniques in resolving the diverse cellular subtypes and their specific contributions to physiological processes, I employed snRNASeq to provide a comprehensive analysis of the caudal POA's cellular landscape. I chose snRNASeq over other sequencing techniques due to its distinct advantages. Unlike single-cell RNA sequencing (scRNASeq), snRNASeq is particularly efficient for neurons and frozen brain tissue, as it can capture the transcriptional profiles from nuclei rather than whole cells, thus avoiding the biases introduced by cell dissociation procedures. This method is also cost-effective compared to scRNASeq, allowing for high-throughput analysis of large numbers of nuclei at a reduced cost. Additionally, snRNASeq is advantageous over bulk RNA sequencing (RNA-seq) as it provides single-cell resolution, enabling the identification of distinct cellular subtypes and their specific gene expression profiles, which are often masked in bulk RNA-seq data (Kim, Kang et al. 2023). While scRNA-seq offers high resolution at the single-cell level, it can be limited by its sensitivity, particularly for detecting low-abundance transcripts. The complexity of the hypothalamic tissue and the diversity of cell types may lead to underrepresentation of rare or transient

cell populations. Additionally, although RNAscope provides spatial context, it may not capture the full transcriptomic diversity due to limited probe availability and potential issues with probe specificity. Combining RNAscope with other spatial transcriptomics techniques, such as Slide-seq or MERFISH, could provide broader coverage and greater resolution, allowing for a more detailed understanding of the spatial organization and interactions of neuronal populations. Also, the reliance on mouse models may limit the translatability of findings to human physiology, as differences in neural circuitry and metabolic regulation exist between species. Incorporating humanized mouse models or ex vivo cultures of human hypothalamic tissue, in the future studies could bridge this gap and provide more directly applicable insights. Additionally, leveraging CRISPR-Cas9 gene editing to model human-specific genetic variations in mice could enhance the relevance of the findings. While my study focused on neuronal populations, non-neuronal cells such as astrocytes and microglia also play crucial roles in hypothalamic function and energy regulation. Expanding the research to include glial cell populations through techniques such as ATAC-seq or ChIP-seq could reveal insights into epigenetic regulation and cell-cell interactions that contribute to metabolic homeostasis. Moreover, incorporating multi-omics approaches, including proteomics and metabolomics, could provide a holistic view of how central nervous system changes translate into systemic physiological effects. Longitudinal studies that monitor metabolic changes over time in response to neuronal manipulation could further elucidate these connections.

To pinpoint specific POA subtypes that regulate energy balance without influencing body temperature, it is essential to systematically dissect the distinct neuronal populations within the POA. By utilizing selective genetic tools, such as Cre-lox systems

in combination with chemogenetics or optogenetics, researchers can activate or inhibit specific neuronal subtypes and observe their impact on both thermogenesis and body weight regulation. For instance, distinguishing between the glutamatergic and GABAergic populations in the rostral versus caudal POA has already revealed differences in their roles in regulating thermogenesis, body composition and body weight. Future studies should focus on identifying a POA subtype that, when manipulated, exclusively promotes body weight loss without altering thermogenic responses. This would involve targeted manipulation of neurons that project to non-thermogenic effector sites, such as those involved in regulating appetite or metabolic rate, rather than thermogenesis. Such discoveries would be invaluable for developing obesity treatments that modulate energy balance without undesired effects on body temperature. In terms of physiological function, these POA circuits may either represent distinct pathways that converge on a common outcome or multiple circuits that are co-recruited under different conditions to fine-tune physiological responses. For instance, certain circuits might be preferentially activated by specific metabolic signals, such as leptin or ghrelin, while others respond to environmental stimuli like temperature or stress; one specific circuit might be recruited in response to cold exposure to enhance thermogenesis, while another is activated during caloric excess to modulate energy storage without increasing body temperature. These circuits, although functionally overlapping, could exhibit subtle differences in their outputs, allowing the organism to maintain energy homeostasis under a variety of conditions. This suggests a flexible and robust system where multiple POA pathways can be engaged to achieve similar goals, such as energy balance or temperature regulation, depending on the demands placed on the organism. In the context of energy

balance, one circuit might primarily reduce food intake, while another simultaneously increases energy expenditure, both working in concert to achieve overall metabolic stability. Understanding the nuances of these circuits—whether they act independently or in a coordinated manner—will be crucial for designing interventions that target specific aspects of energy balance without triggering off-target effects, such as unwanted changes in body temperature or metabolic rate.

One of the translational challenges of this dissertation work lies in the inherent differences between rodent and human physiology, particularly in the hypothalamic markers and genomic regulation. While rodents serve as valuable models for studying energy homeostasis due to their well-characterized hypothalamic circuits and the ease of genetic manipulation, there are significant physiological and anatomical differences that can affect the direct application of findings to humans. For instance, the human hypothalamus is more complex, with additional nuclei and distinct patterns of gene expression that may not have direct equivalents in rodents. Moreover, differences in metabolic rates, feeding behavior, and environmental interactions between species add layers of complexity when extrapolating rodent data to human conditions. However, recent advances such as the HypoMap developed by Giles Yeo and colleagues (Steuernagel, Lam et al. 2022) have provided a comprehensive comparative map of hypothalamic cell types across species, revealing a high degree of conservation in the main markers of individual cell types between rodents and humans. This suggests that while there are translational challenges, particularly in the specificity and context of gene expression, there is also a strong foundational similarity that supports the relevance of

rodent studies for understanding human hypothalamic function and guiding the development of therapeutic strategies.

The findings of this dissertation have important implications for understanding the mechanisms underlying obesity and metabolic disorders. The identification of specific neuronal populations and circuits involved in energy regulation suggests that targeted therapies could modulate these pathways to restore metabolic balance. However, the complexity of the hypothalamic network indicates that multifaceted approaches may be necessary to achieve effective therapeutic outcomes. The interaction between central and peripheral signals is crucial for maintaining energy homeostasis. Understanding how these systems communicate and influence each other could provide insights into the pathogenesis of metabolic disorders and potential therapeutic targets. The heterogeneity of neuronal responses observed in the study suggests that individualized approaches may be necessary to effectively target specific neural circuits involved in metabolic regulation. Personalized medicine strategies could tailor interventions based on individual genetic and physiological profiles.

Future directions

Building on the findings and addressing the limitations identified, I propose the following future research directions:

Future research should aim to integrate snRNASeq with other high-throughput techniques such as proteomics, metabolomics, and epigenomics. This multi-modal approach could provide a more comprehensive understanding of how gene expression correlates with protein activity, metabolic changes, and epigenetic modifications in the

regulation of energy homeostasis. Moreover, investigating the transcriptomic profile of the POA and BNST after activating the VMN^{PACAP} neurons, in obese and diabetic mice, would pinpoint the cellular subtypes behind the thermogenic and hyperglycemic responses that I saw (as mentioned in chapter 3 results) after activating the VMN^{PACAP} axons in the POA and BNST respectively. Understanding these layers of regulation will be crucial for elucidating the full spectrum of mechanisms controlling energy balance.

Exploring the impact of environmental factors such as diet, exercise, and stress on the identified neural circuits and molecular pathways is an essential next step. This research could elucidate how external stimuli modulate the expression and activity of genes like Asic2, Ptprd, Kcnip1, and Gpc5, thereby influencing metabolic outcomes. Investigating gene-environment interactions could also uncover how lifestyle interventions might mitigate the effects of genetic predispositions to obesity and metabolic disorders.

While my dissertation focused primarily on neuronal populations within the hypothalamus, the roles of glial cells and other non-neuronal populations in energy homeostasis remain largely unexplored. Future studies should examine how these cells contribute to the regulation of metabolic processes and interact with neuronal circuits to maintain energy balance. Glial cells, in particular, may play critical roles in modulating inflammation and neurovascular coupling, which are relevant to obesity and metabolic health.

Conducting longitudinal studies in animal models and extending the research to human tissues will be essential for validating the findings and enhancing their translational potential. Cross-species comparisons could identify conserved pathways and

mechanisms that are critical for energy homeostasis across different organisms, providing insights into potential therapeutic targets that are relevant to humans. The identification of PTPRD, the receptor for asprosin, within my brain region of interest, presents a promising therapeutic target. Future research should focus on developing small molecules or biologics that can modulate this pathway, potentially leading to effective treatments for obesity. Investigating the safety, efficacy, and mechanisms of action of such therapeutics in preclinical and clinical settings will be a crucial step toward translating basic research findings into clinical applications.

While this dissertation provided a detailed map of neuronal populations, the complexity of neural circuits and their dynamic interactions remain incompletely understood. Future studies should employ techniques such as optogenetics and chemogenetics to manipulate specific neuronal populations and dissect the functional connectivity and causal relationships within these circuits. The specific roles and interactions of neuropeptides and hormone receptors in the POA and BNST require further exploration. Understanding how these molecules modulate neuronal activity and contribute to energy homeostasis could reveal new targets for therapeutic intervention. Chronic low-grade inflammation is a hallmark of obesity and metabolic disorders, yet its effects on the identified neural circuits have not been fully elucidated. Investigating how inflammation influences gene expression, neuronal activity, and circuit dynamics could provide insights into the pathophysiology of obesity and potential anti-inflammatory strategies. Understanding how the brain adapts energy expenditure in response to changes in energy intake and expenditure remains an open question. Future research should explore the molecular and neural mechanisms that enable this adaptability, particularly in

the context of dietary interventions and weight loss. The interaction between the hypothalamus and other brain regions involved in reward processing, stress response, and circadian rhythm regulation warrants further investigation. Understanding how these systems integrate with energy homeostasis circuits could provide a holistic view of the neural regulation of metabolism.

Overall, the dissertation advances my understanding of the neural mechanisms involved in energy homeostasis and highlights promising avenues for developing novel obesity and diabetes therapies. Continued research in this area is essential for translating these findings into effective clinical interventions, with the potential to significantly impact public health outcomes. By addressing these questions and exploring these mechanisms, future research can build on the findings of this dissertation, advancing my understanding of energy homeostasis and paving the way for novel therapeutic strategies to combat obesity and metabolic disorders.

Appendices

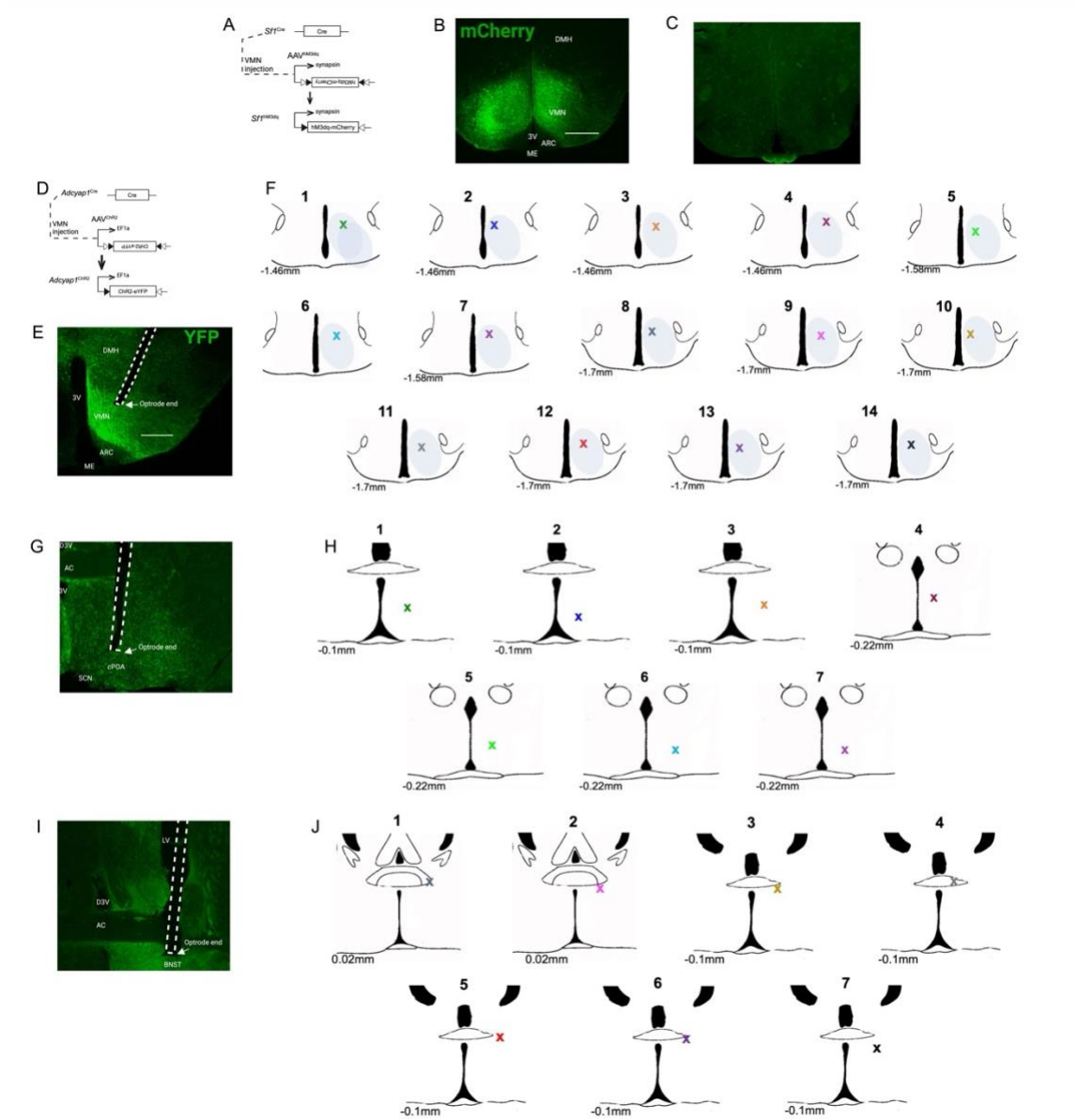

Supplementary figure S1: Schematic of *AAV*$^{DIO\text{-}hM3dq\text{-}mCherry}$ injection site in *Sf1*^{Cre} mice, *AAV*$^{DIO\text{-}ChR2\text{-}eYFP}$ injection site and optrode placements in *Adcyap1*^{Cre} mice. Design of the *AAV*$^{DIO\text{-}hM3dq\text{-}mCherry}$ virus that I injected into the VMN of either *Sf1*^{Cre} mice or their wild-type littermate controls (A). Brains from the mice in experiment 1 were collected and stained for mCherry. The presence of mCherry was used to determine the

spread of the virus, since the virus contained a mCherry tag. Representative image showing the location of *AAV*$^{DIO\text{-}hM3dq\text{-}mCherry}$ injections in *Sf1*^{Cre} mice (B) and their wild-type littermate controls (C) with the control having no Cre had no mCherry. Design of the *AAV*$^{DIO\text{-}ChR2\text{-}eYFP}$ virus that I injected into the VMN of *Adcyap1*^{Cre} mice to generate *Adcyap1*^{ChR2} mice for optogenetic experiments (D). Brains from the mice in experiment 1 were collected and stained for YFP. Representative images showing the location of *AAV*$^{DIO\text{-}ChR2\text{-}eYFP}$ virus injection at VMN (E) and location of the optrodes at either the VMN somas (E), the caudal POA efferents (G) or BNST efferents (I). Schematics representing AAV spread (shaded regions) at the VMN (C). Schematics representing AAV spread (blue shaded regions) at VMN (F) and optrode placement (denoted by "X") at either the VMN somas (F), the caudal POA efferents (H) or BNST efferents (J), for every animal included in the experiments in Figures 4 and 5. Each animal is numbered and represented by a different colored X. Scalebar = 460μm (B,E,G,I). 3V = 3rd ventricle. DMH = Dorsomedial hypothalamic nucleus. VMN = Ventromedial hypothalamic nucleus. ARC = Arcuate nucleus. ME = Median eminence. D3V = Dorsal 3rd ventricle. AC = Anterior commissure. cPOA = caudal preoptic area. SCN = Suprachiasmatic nucleus. LV = Lateral ventricle. BNST = Bed nucleus of stria terminalis. The schematics were created using The Mouse Brain in Stereotaxic Coordinates Fourth Edition (Paxinos and Franklin).

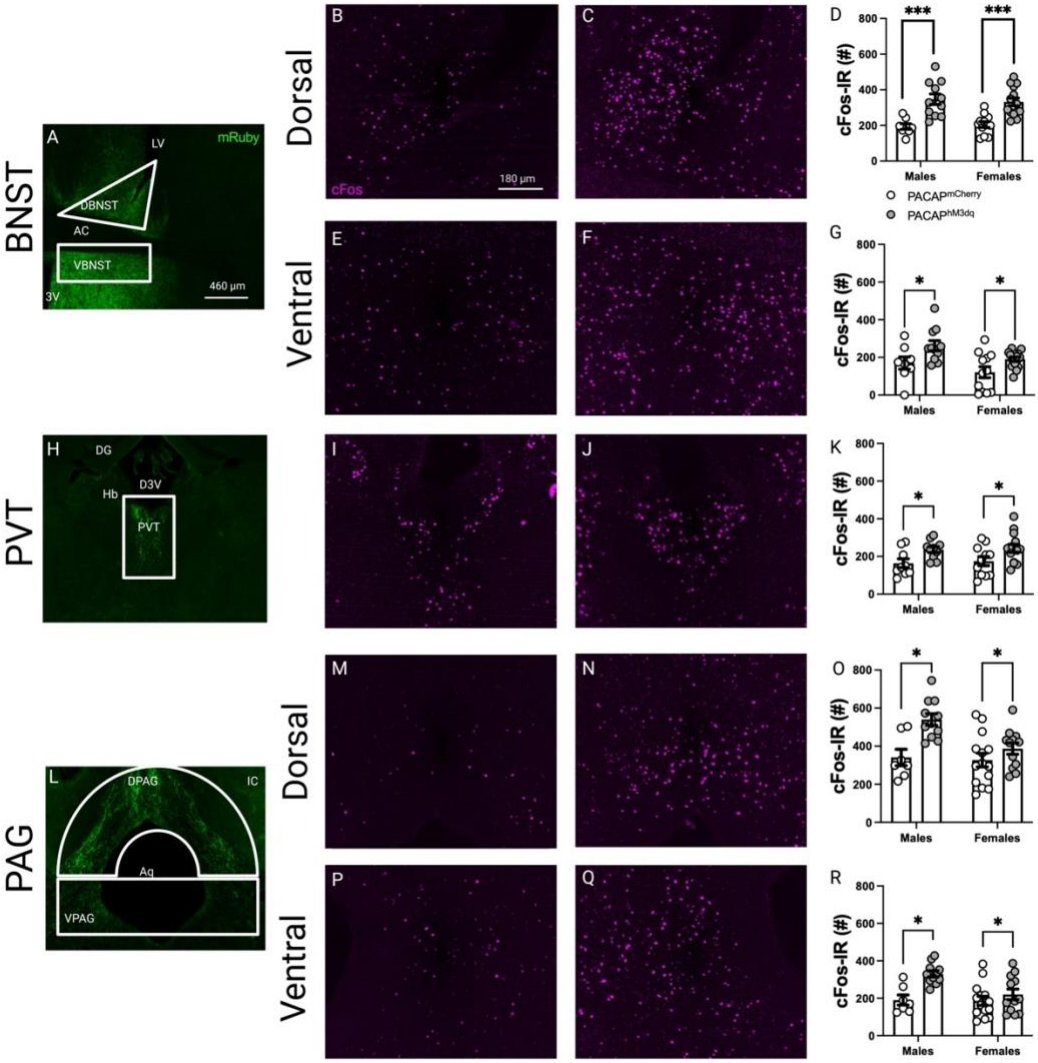

Supplementary figure S2: VMN^{PACAP} neurons project to sites outside of the POA and activate neurons in these sites in both sexes of mice. I looked at VMN^{PACAP} projections in the BNST (Fig. S2A-S2G), PVT (Fig. S2H-S2K) and PAG (Fig. S2L-S2R) by injecting *Adcyap1*^{Cre} mice with using *AAV*$^{DIO\text{-}syn\text{-}mRuby}$ via observing mRuby expression at the projection sites. I also used *AAV*$^{DIO\text{-}hSyn\text{-}hM3dq\text{-}mCherry}$ or *AAV*$^{DIO\text{-}hSyn\text{-}mCherry}$ to measure cFos induction at the projection sites. Brains from the tracing experiment were collected and stained for mRuby and also for cFos and mCherry. Representative traces showing cFos induction at all the projection sites after administering CNO to PACAP^{hM3dq} mice (Fig. S2C, S2F, S2J, S2N, S2Q) and PACAP^{mCherry} control mice (Fig. S2B, S2E, S2I, S2M, S2P). I also counted cFos at each of these projection sites (Fig. S2D, S2G, S2K,

S2O, S2R). N=6-10 mice. Scalebar = 460μm (A,H,L) and 180μm (B-C,E-F,I-J,M-N,P-Q). LV = Lateral ventricle. 3V = 3rd ventricle. AC = Anterior commissure. DBNST = Dorsal bed nucleus of stria terminalis. VBNST = Ventral bed nucleus of stria terminalis. DG = Dentate gyrus. D3V = Dorsal 3rd ventricle. Hb = Habenular commissure. PVT = Paraventricular thalamus. DPAG = Dorsal periaqueductal gray. VPAG = Ventral periaqueductal gray. IC = Inferior colliculus. Aq = Aqueduct. Data expressed as mean ± SEM and analyzed by student's t-test (H), *$p<0.05$, **$p<0.01$, ***$p<0.0001$

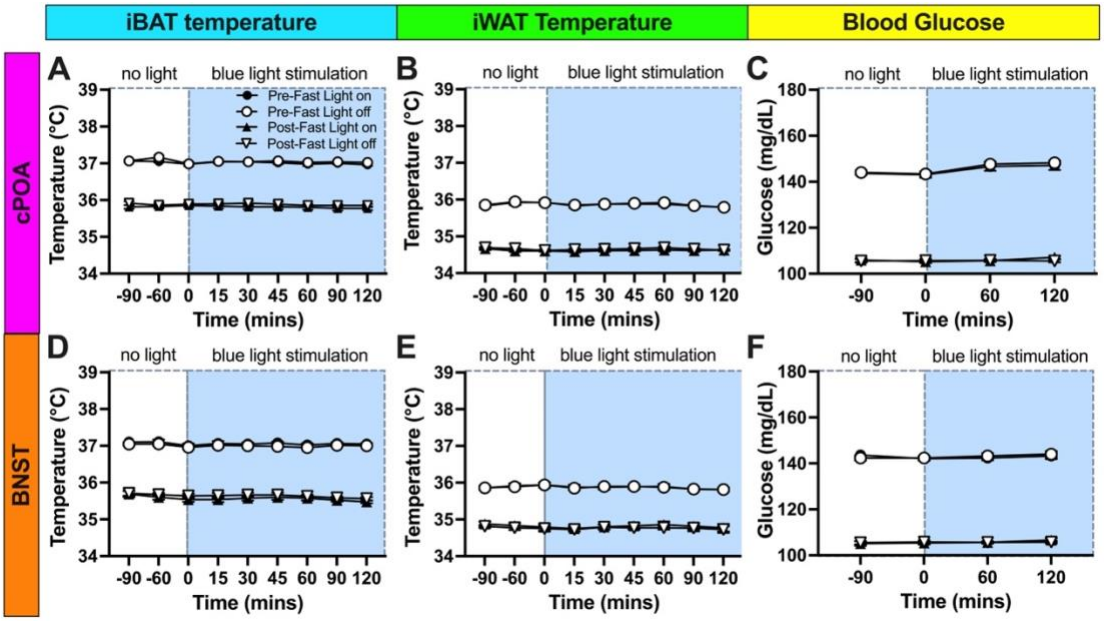

Supplementary figure S3: Stimulating VMN^{PACAP} à caudal POA neurons with blue light, in absence of ChR2, does not induce tissue thermogenesis in both sexes of mice. In *Adcyap1*^{Cre} mice, I introduced *AAV*$^{DIO\text{-}eYFP}$ into the VMN and implanted optical probes at either the caudal POA efferents (A-C), or BNST efferents (D-F) and then stimulated either of the optrodes with blue light for 2 hours and measured temperature above iBAT (A,D) and iWAT (B,E) and blood glucose (C,F). Data expressed as mean ±SEM and analyzed by two-way RM ANOVA, N=7-9, *p<0.05

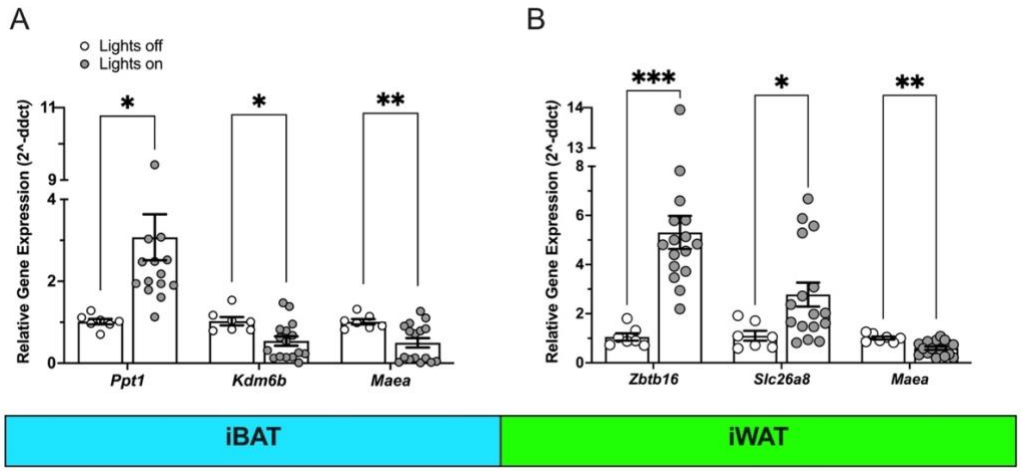

Supplementary figure S4: Validation of the top differentially expressed genes in iBAT and iWAT found in bulk RNA-sequencing. In *Adcyap1*^{Cre} mice, I introduced *AAV*$^{DIO\text{-}ChR2\text{-}eYFP}$ and implanted optrodes caudal POA efferents and temperature microchips at iBAT and iWAT. Then, I subjected the mice to blue light stimulation or without blue light stimulation for 2 hours and then the iBAT and iWAT were harvested from the mice after anesthesia, prior to transcardial perfusion. I then isolated total RNA from the iBAT and iWAT and performed qRT-PCR. Top 3 hits of differentially expressed genes from the RNA-sequencing results were validated using qRT-PCR. I calculated fold change (2^-ddct) of iBAT (A) or iWAT (B). All data expressed as mean ± SEM and analyzed by student's t-test. N=10-14 mixed male and female mice. *p<0.05, **p<0.01, ***p<0.0001

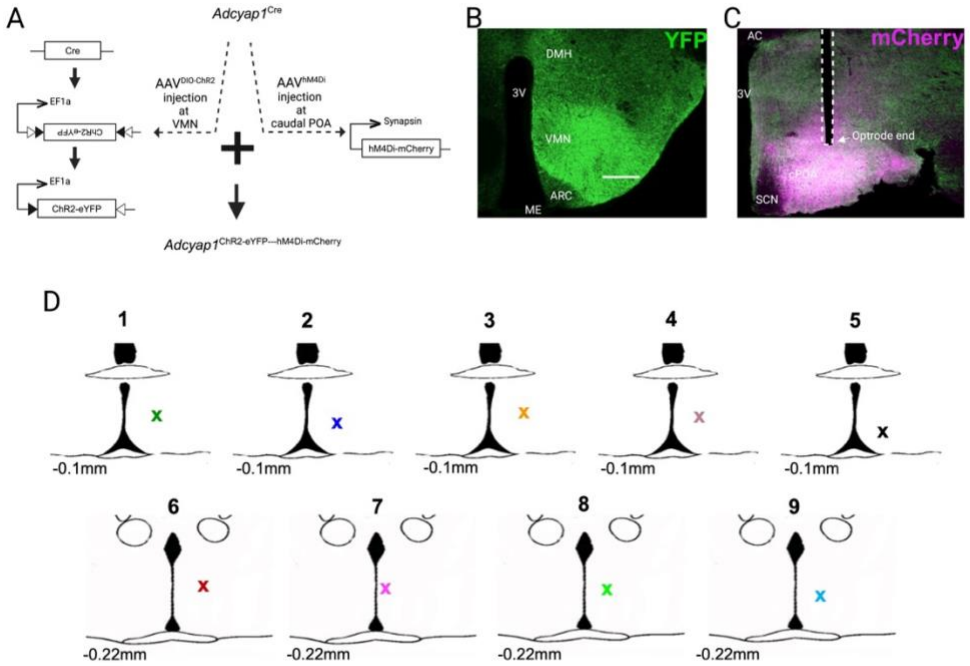

Supplementary figure S5: Schematic of *AAV$^{DIO\text{-}ChR2\text{-}eYFP}$* and *AAV$^{hM4Di\text{-}mCherry}$* injection site and optrode placements in *Adcyap1$^{ChR2\text{-}eYFP}$* mice. Design of the *AAV$^{DIO\text{-}ChR2\text{-}eYFP}$* and *AAV$^{hMDdi\text{-}mCherry}$* viruses that I injected into the VMN and caudal POA, respectively, of *Adcyap1^{Cre}* mice to generate *Adcyap1$^{ChR2\text{-}eYFP—hM4Di\text{-}mCherry}$* mice for optogenetic experiments (A). Brains from the mice in experiment 1 were collected and stained for YFP and mCherry. Representative images showing the location of *AAV$^{DIO\text{-}ChR2\text{-}eYFP}$* virus injection at VMN (B), location of the *AAV$^{hMDdi\text{-}mCherry}$* virus injection at caudal POA and location of the optrodes at the VMN efferents at the caudal POA (C). Schematics representing optrode placement (denoted by "X") VMN efferents at the caudal POA (D), for every animal included in the experiments in Figure 7. Each animal is numbered and represented by a different colored X. Scalebar = 460µm (B,C). 3V = 3rd ventricle. DMH = Dorsomedial hypothalamic nucleus. VMN = Ventromedial hypothalamic nucleus. ARC = Arcuate nucleus. ME = Median eminence. AC = Anterior commissure. cPOA = caudal preoptic area. SCN = Suprachiasmatic nucleus. The schematics were created using The Mouse Brain in Stereotaxic Coordinates Fourth Edition (Paxinos and Franklin).

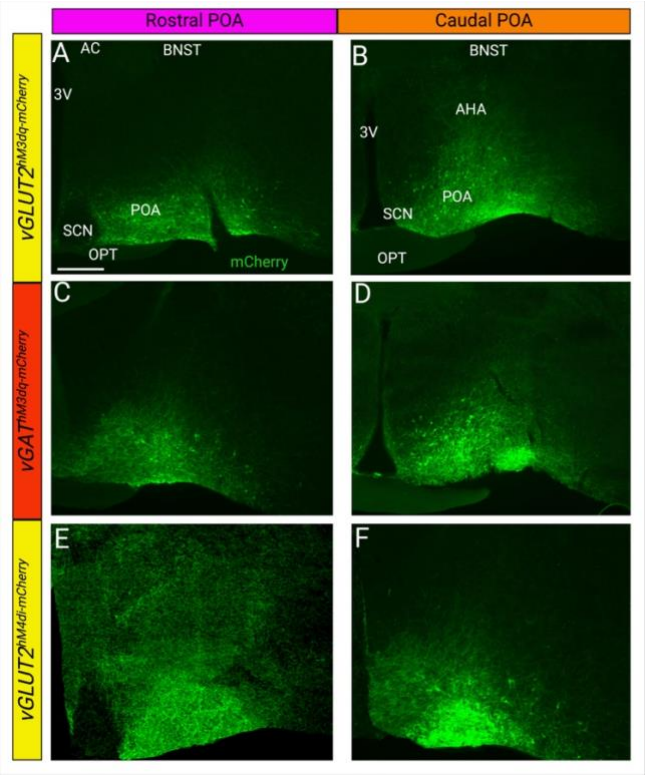

Supplementary figure S6: Schematic of *AAV*$^{DIO\text{-}hM3dq\text{-}mCherry}$ injection site in *vGLUT2*^{Cre} or *vGAT*^{Cre} mice, *AAV*$^{DIO\text{-}hM4di\text{-}mCherry}$ injection site in *vGLUT2*^{Cre} mice. I injected *AAV*$^{DIO\text{-}hM3dq\text{-}mCherry}$ virus into the rostral or caudal POA of either *vGLUT2*^{Cre} or *vGAT*^{Cre} mice and activated the *vGLUT2* $^{hM3dq\text{-}mCherry}$ or *vGAT* $^{hM3dq\text{-}mCherry}$ neurons by CNO IP injections. Brains from the mice were collected and stained for mCherry. The presence of mCherry was used to determine the spread of the virus, since the virus contained a mCherry tag. Representative image showing the location of *AAV*$^{DIO\text{-}hM3dq\text{-}mCherry}$ injections in *vGLUT2*^{Cre} (A-B) or *vGAT*^{Cre} (C-D) mice at either rostral (A, C) or caudal (B, D) POA. For a separate experiment, I injected *AAV*$^{DIO\text{-}h43iq\text{-}mCherry}$ virus into the rostral or caudal POA of *vGLUT2*^{Cre} mice and inhibited the *vGLUT2* $^{hM4di\text{-}mCherry}$ neurons by CNO IP injections. Brains from the mice were collected and stained for mCherry. The presence of mCherry was used to determine the spread of the virus. Representative image showing the location of *AAV*$^{DIO\text{-}hM4di\text{-}mCherry}$ injections in *vGLUT2*^{Cre} (E-F) either rostral (E) or caudal (F) POA. Scalebar = 460µm. 3V = 3rd ventricle. AC = Anterior commissure. POA = Preoptic area. SCN = Suprachiasmatic nucleus. OPT = Optic tract. BNST = Bed nucleus of stria terminalis. The schematics were created using The Mouse Brain in Stereotaxic Coordinates Fourth Edition (Paxinos and Franklin).

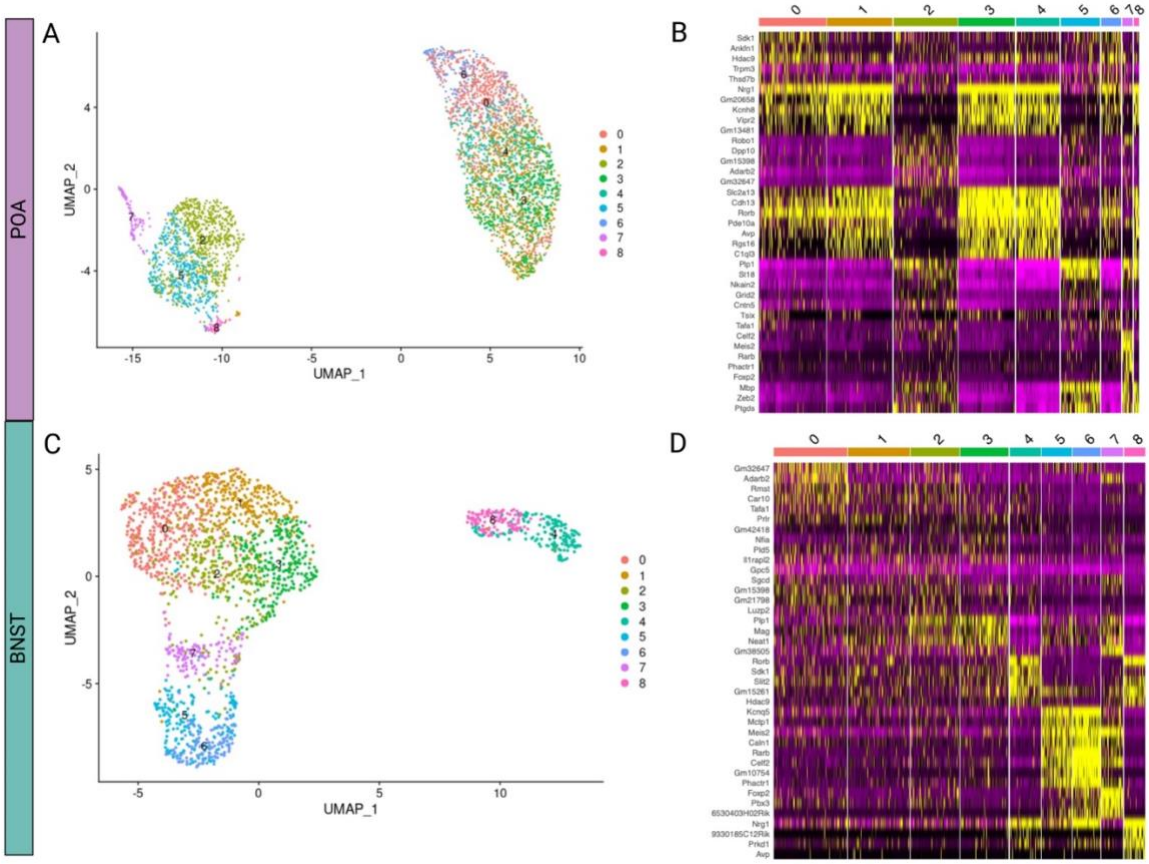

Supplementary figure S7: Single-nuclei RNA sequencing showing hybrid neuronal populations within POA and BNST. Over 200,000 single nuclei were analyzed from the POA and BNST of diet induced obese mice or control mice on chow diet, to identify the population of POA cells responsive to diabetes and obesity. Uniform Manifold Approximation and Projection (UMAP) for hybrid (expressing both excitatory and inhibitory markers) neuronal populations within POA (a) and BNST (C), with cells colored by cluster. Numbers on the UMAP indicate the cluster ID. Each color-coded cluster on the UMAP plot represents populations of cells that have the same gene expression profile. Total nuclei numbers for each UMAP plot are 200,000. Heatmap of differentially expressed genes per cluster within the hybrid neuron population in POA (B) or BNST (D). n = 10 females, 11 males (obese and glucose intolerant) and 9 females, 9 males (control).

References

Adjeitey, C. N., R. J. Mailloux, R. A. Dekemp and M. E. Harper (2013). "Mitochondrial uncoupling in skeletal muscle by UCP1 augments energy expenditure and glutathione content while mitigating ROS production." Am J Physiol Endocrinol Metab **305**(3): E405-415.

Andermann, M. L. and B. B. Lowell (2017). "Toward a Wiring Diagram Understanding of Appetite Control." Neuron **95**(4): 757-778.

Asadi, A., N. Shadab Mehr, M. H. Mohamadi, F. Shokri, M. Heidary, N. Sadeghifard and S. Khoshnood (2022). "Obesity and gut-microbiota-brain axis: A narrative review." J Clin Lab Anal **36**(5): e24420.

Bass, R., J. N. Brownell and V. A. Stallings (2021). "The Impact of Highly Effective CFTR Modulators on Growth and Nutrition Status." Nutrients **13**(9).

Basu, R., A. J. Elmendorf, B. Lorentz, C. A. Mahler, O. Lazzaro, B. App, S. Zhou, Y. Yamamoto, M. Suber, J. C. Wann, H. C. Roh, P. L. Sheets, T. S. Johnson and J. N. Flak (2024). "Ventromedial hypothalamic nucleus subset stimulates tissue thermogenesis via preoptic area outputs." Mol Metab **84**: 101951.

Basu, R. and N. J. Flak (2024). Hypothalamic neural circuits regulating energy expenditure, Academic Press.

Berg, T. and J. Jensen (2013). "Tyramine Reveals Failing alpha2-Adrenoceptor Control of Catecholamine Release and Total Peripheral Vascular Resistance in Hypertensive Rats." Front Neurol **4**: 19.

Betz, M. J. and S. Enerback (2018). "Targeting thermogenesis in brown fat and muscle to treat obesity and metabolic disease." Nat Rev Endocrinol **14**(2): 77-87.

Boelen, A., W. M. Wiersinga and E. Fliers (2008). "Fasting-induced changes in the hypothalamus-pituitary-thyroid axis." Thyroid **18**(2): 123-129.

Bozadjieva-Kramer, N., R. A. Ross, D. Q. Johnson, H. Fenselau, D. L. Haggerty, B. Atwood, B. Lowell and J. N. Flak (2021). "The Role of Mediobasal Hypothalamic PACAP in the Control of Body Weight and Metabolism." Endocrinology **162**(4).

Buhmann, H., C. W. le Roux and M. Bueter (2014). "The gut-brain axis in obesity." Best Pract Res Clin Gastroenterol **28**(4): 559-571.

Cai, D. and T. Liu (2011). "Hypothalamic inflammation: a double-edged sword to nutritional diseases." Ann N Y Acad Sci **1243**: E1-39.

Camacho Londono, J. E., Q. Tian, K. Hammer, L. Schroder, J. Camacho Londono, J. C. Reil, T. He, M. Oberhofer, S. Mannebach, I. Mathar, S. E. Philipp, W. Tabellion, F. Schweda, A. Dietrich, L. Kaestner, U. Laufs, L. Birnbaumer, V. Flockerzi, M. Freichel and P. Lipp (2015). "A background Ca2+ entry pathway mediated by TRPC1/TRPC4 is critical for development of pathological cardiac remodelling." Eur Heart J **36**(33): 2257-2266.

Cannon, B. and J. Nedergaard (2011). "Nonshivering thermogenesis and its adequate measurement in metabolic studies." J Exp Biol **214**(Pt 2): 242-253.

Caron, A. and D. Richard (2017). "Neuronal systems and circuits involved in the control of food intake and adaptive thermogenesis." Ann N Y Acad Sci **1391**(1): 35-53.

Cerri, M. (2017). "The Central Control of Energy Expenditure: Exploiting Torpor for Medical Applications." Annu Rev Physiol **79**: 167-186.

Chakhtoura, M., R. Haber, M. Ghezzawi, C. Rhayem, R. Tcheroyan and C. S. Mantzoros (2023). "Pharmacotherapy of obesity: an update on the available medications and drugs under investigation." EClinicalMedicine **58**: 101882.
Cheriyan, J., M. K. Kaushik, A. N. Ferreira and P. L. Sheets (2016). "Specific Targeting of the Basolateral Amygdala to Projectionally Defined Pyramidal Neurons in Prelimbic and Infralimbic Cortex." eNeuro **3**(2).
Cheriyan, J. and P. L. Sheets (2020). "Peripheral nerve injury reduces the excitation-inhibition balance of basolateral amygdala inputs to prelimbic pyramidal neurons projecting to the periaqueductal gray." Mol Brain **13**(1): 100.
Chibalin, A. V., Y. Leng, E. Vieira, A. Krook, M. Bjornholm, Y. C. Long, O. Kotova, Z. Zhong, F. Sakane, T. Steiler, C. Nylen, J. Wang, M. Laakso, M. K. Topham, M. Gilbert, H. Wallberg-Henriksson and J. R. Zierath (2022). "Downregulation of Diacylglycerol Kinase Delta Contributes to Hyperglycemia-Induced Insulin Resistance." Cell **185**(2): 397-398.
Clapham, J. C. (2012). "Central control of thermogenesis." Neuropharmacology **63**(1): 111-123.
Coll, A. P. and G. S. Yeo (2013). "The hypothalamus and metabolism: integrating signals to control energy and glucose homeostasis." Curr Opin Pharmacol **13**(6): 970-976.
Contreras, C., F. Gonzalez, J. Ferno, C. Dieguez, K. Rahmouni, R. Nogueiras and M. Lopez (2015). "The brain and brown fat." Ann Med **47**(2): 150-168.
Contreras, C., R. Nogueiras, C. Dieguez, G. Medina-Gomez and M. Lopez (2016). "Hypothalamus and thermogenesis: Heating the BAT, browning the WAT." Mol Cell Endocrinol **438**: 107-115.
Contreras, C., R. Nogueiras, C. Dieguez, K. Rahmouni and M. Lopez (2017). "Traveling from the hypothalamus to the adipose tissue: The thermogenic pathway." Redox Biol **12**: 854-863.
Cousin, B., S. Cinti, M. Morroni, S. Raimbault, D. Ricquier, L. Penicaud and L. Casteilla (1992). "Occurrence of brown adipocytes in rat white adipose tissue: molecular and morphological characterization." J Cell Sci **103 (Pt 4)**: 931-942.
Crestani, C. C., F. H. Alves, F. V. Gomes, L. B. Resstel, F. M. Correa and J. P. Herman (2013). "Mechanisms in the bed nucleus of the stria terminalis involved in control of autonomic and neuroendocrine functions: a review." Curr Neuropharmacol **11**(2): 141-159.
De Fano, M., D. Bartolini, C. Tortoioli, C. Vermigli, M. Malara, F. Galli and G. Murdolo (2022). "Adipose Tissue Plasticity in Response to Pathophysiological Cues: A Connecting Link between Obesity and Its Associated Comorbidities." Int J Mol Sci **23**(10).
De Souza, C. T., E. P. Araujo, S. Bordin, R. Ashimine, R. L. Zollner, A. C. Boschero, M. J. Saad and L. A. Velloso (2005). "Consumption of a fat-rich diet activates a proinflammatory response and induces insulin resistance in the hypothalamus." Endocrinology **146**(10): 4192-4199.
Dhillon, H., J. M. Zigman, C. Ye, C. E. Lee, R. A. McGovern, V. Tang, C. D. Kenny, L. M. Christiansen, R. D. White, E. A. Edelstein, R. Coppari, N. Balthasar, M. A. Cowley, S. Chua, Jr., J. K. Elmquist and B. B. Lowell (2006). "Leptin directly activates SF1 neurons in the VMH, and this action by leptin is required for normal body-weight homeostasis." Neuron **49**(2): 191-203.

Dietrich, A., H. Kalwa, B. Fuchs, F. Grimminger, N. Weissmann and T. Gudermann (2007). "In vivo TRPC functions in the cardiopulmonary vasculature." Cell Calcium **42**(2): 233-244.
Dinas, P. C., E. Nintou, M. Vliora, A. E. Pravednikova, P. Sakellariou, A. Witkowicz, Z. M. Kachaev, V. V. Kerchev, S. N. Larina, J. Cotton, A. Kowalska, P. Gkiata, A. Bargiota, Z. A. Khachatryan, A. A. Hovhannisyan, M. A. Antonosyan, S. Margaryan, A. Partyka, P. Bogdanski, M. Szulinska, M. Kregielska-Narozna, R. Czepczynski, M. Ruchala, A. Tomkiewicz, L. Yepiskoposyan, L. Karabon, Y. Shidlovskii, G. S. Metsios and A. D. Flouris (2022). "Prevalence of uncoupling protein one genetic polymorphisms and their relationship with cardiovascular and metabolic health." PLoS One **17**(4): e0266386.
Dodd, G. T., A. A. Worth, N. Nunn, A. K. Korpal, D. A. Bechtold, M. B. Allison, M. G. Myers, Jr., M. A. Statnick and S. M. Luckman (2014). "The thermogenic effect of leptin is dependent on a distinct population of prolactin-releasing peptide neurons in the dorsomedial hypothalamus." Cell Metab **20**(4): 639-649.
Eck, S. R., J. L. Palmer, C. C. Bavley, R. Karbalaei, E. Ordones Sanchez, J. Flowers, 2nd, A. Holley, M. E. Wimmer and D. A. Bangasser (2022). "Effects of early life adversity on male reproductive behavior and the medial preoptic area transcriptome." Neuropsychopharmacology **47**(6): 1231-1239.
Esterbauer, H., H. Oberkofler, Y. M. Liu, D. Breban, E. Hell, F. Krempler and W. Patsch (1998). "Uncoupling protein-1 mRNA expression in obese human subjects: the role of sequence variations at the uncoupling protein-1 gene locus." J Lipid Res **39**(4): 834-844.
Faber, C. L., M. E. Matsen, K. R. Velasco, V. Damian, B. A. Phan, D. Adam, A. Therattil, M. W. Schwartz and G. J. Morton (2018). "Distinct Neuronal Projections From the Hypothalamic Ventromedial Nucleus Mediate Glycemic and Behavioral Effects." Diabetes **67**(12): 2518-2529.
Federation, W. O. (2023). "Economic impact of overweight and obesity to surpass $4 trillion by 2035." from https://www.worldobesity.org/news/economic-impact-of-overweight-and-obesity-to-surpass-4-trillion-by-2035.
Feng, B., H. Liu, I. Mishra, C. Duerrschmid, P. Gao, P. Xu, C. Wang and Y. He (2023). "Asprosin promotes feeding through SK channel-dependent activation of AgRP neurons." Sci Adv **9**(8): eabq6718.
Filmus, J. and M. Capurro (2014). "The role of glypicans in Hedgehog signaling." Matrix Biol **35**: 248-252.
Finkelstein, E. A., J. G. Trogdon, J. W. Cohen and W. Dietz (2009). "Annual medical spending attributable to obesity: payer-and service-specific estimates." Health Aff (Millwood) **28**(5): w822-831.
Fischer, A. W., C. Schlein, B. Cannon, J. Heeren and J. Nedergaard (2019). "Intact innervation is essential for diet-induced recruitment of brown adipose tissue." Am J Physiol Endocrinol Metab **316**(3): E487-E503.
Fisher, F. M., S. Kleiner, N. Douris, E. C. Fox, R. J. Mepani, F. Verdeguer, J. Wu, A. Kharitonenkov, J. S. Flier, E. Maratos-Flier and B. M. Spiegelman (2012). "FGF21 regulates PGC-1alpha and browning of white adipose tissues in adaptive thermogenesis." Genes Dev **26**(3): 271-281.
Flak, J. N., D. Arble, W. Pan, C. Patterson, T. Lanigan, P. B. Goforth, J. Sacksner, M. Joosten, D. A. Morgan, M. B. Allison, J. Hayes, E. Feldman, R. J. Seeley, D. P. Olson, K.

Rahmouni and M. G. Myers, Jr. (2017). "A leptin-regulated circuit controls glucose mobilization during noxious stimuli." J Clin Invest **127**(8): 3103-3113.
Flak, J. N., P. B. Goforth, J. Dell'Orco, P. V. Sabatini, C. Li, N. Bozadjieva, M. Sorensen, A. Valenta, A. Rupp, A. H. Affinati, C. Cras-Meneur, A. Ansari, J. Sacksner, N. Kodur, D. A. Sandoval, R. T. Kennedy, D. P. Olson and M. G. Myers, Jr. (2020). "Ventromedial hypothalamic nucleus neuronal subset regulates blood glucose independently of insulin." J Clin Invest **130**(6): 2943-2952.
Flak, J. N. and M. G. Myers, Jr. (2016). "Minireview: CNS Mechanisms of Leptin Action." Mol Endocrinol **30**(1): 3-12.
Flak, J. N., C. M. Patterson, A. S. Garfield, G. D'Agostino, P. B. Goforth, A. K. Sutton, P. A. Malec, J. T. Wong, M. Germani, J. C. Jones, M. Rajala, L. Satin, C. J. Rhodes, D. P. Olson, R. T. Kennedy, L. K. Heisler and M. G. Myers, Jr. (2014). "Leptin-inhibited PBN neurons enhance responses to hypoglycemia in negative energy balance." Nat Neurosci **17**(12): 1744-1750.
Friedman, J. (2016). "The long road to leptin." J Clin Invest **126**(12): 4727-4734.
Fujikawa, T., C. M. Castorena, S. Lee and J. K. Elmquist (2017). "The hypothalamic regulation of metabolic adaptations to exercise." J Neuroendocrinol **29**(10).
Fujikawa, T., C. M. Castorena, M. Pearson, C. M. Kusminski, N. Ahmed, P. K. Battiprolu, K. W. Kim, S. Lee, J. A. Hill, P. E. Scherer, W. L. Holland and J. K. Elmquist (2016). "SF-1 expression in the hypothalamus is required for beneficial metabolic effects of exercise." Elife **5**.
Fukumoto, K., K. Tamada, T. Toya, T. Nishino, Y. Yanagawa and T. Takumi (2018). "Identification of genes regulating GABAergic interneuron maturation." Neurosci Res **134**: 18-29.
Gagnon, J., P. Mauriege, S. Roy, D. Sjostrom, Y. C. Chagnon, F. T. Dionne, J. M. Oppert, L. Perusse, L. Sjostrom and C. Bouchard (1996). "The Trp64Arg mutation of the beta3 adrenergic receptor gene has no effect on obesity phenotypes in the Quebec Family Study and Swedish Obese Subjects cohorts." J Clin Invest **98**(9): 2086-2093.
Gao, Q. and T. L. Horvath (2007). "Neurobiology of feeding and energy expenditure." Annu Rev Neurosci **30**: 367-398.
Gao, W., J. L. Liu, X. Lu and Q. Yang (2021). "Epigenetic regulation of energy metabolism in obesity." J Mol Cell Biol **13**(7): 480-499.
Guo, X., B. T. Keenan, B. C. Reiner, J. Lian and A. I. Pack (2024). "Single-nucleus RNA-seq identifies one galanin neuronal subtype in mouse preoptic hypothalamus activated during recovery from sleep deprivation." Cell Rep **43**(5): 114192.
Handschin, C. and B. M. Spiegelman (2006). "Peroxisome proliferator-activated receptor gamma coactivator 1 coactivators, energy homeostasis, and metabolism." Endocr Rev **27**(7): 728-735.
Hawke, Z., T. R. Ivanov, D. A. Bechtold, H. Dhillon, B. B. Lowell and S. M. Luckman (2009). "PACAP neurons in the hypothalamic ventromedial nucleus are targets of central leptin signaling." J Neurosci **29**(47): 14828-14835.
Hirschberg, P. R., P. Sarkar, S. B. Teegala and V. H. Routh (2020). "Ventromedial hypothalamus glucose-inhibited neurones: A role in glucose and energy homeostasis?" J Neuroendocrinol **32**(1): e12773.

Huo, L., K. Gamber, S. Greeley, J. Silva, N. Huntoon, X. H. Leng and C. Bjorbaek (2009). "Leptin-dependent control of glucose balance and locomotor activity by POMC neurons." Cell Metab **9**(6): 537-547.
Hyun, U. and J. W. Sohn (2022). "Autonomic control of energy balance and glucose homeostasis." Exp Mol Med **54**(4): 370-376.
Iglesias, P. and J. J. Diez (2007). "Influence of thyroid dysfunction on serum concentrations of adipocytokines." Cytokine **40**(2): 61-70.
Imai, J. and H. Katagiri (2022). "Regulation of systemic metabolism by the autonomic nervous system consisting of afferent and efferent innervation." Int Immunol **34**(2): 67-79.
Jenkins, J. S. (1972). "The hypothalamus." Br Med J **2**(5805): 99-102.
Kassir, R., T. Debs, P. Blanc, J. Gugenheim, I. Ben Amor, C. Boutet and O. Tiffet (2016). "Complications of bariatric surgery: Presentation and emergency management." Int J Surg **27**: 77-81.
Khodai, T. and S. M. Luckman (2021). "Ventromedial Nucleus of the Hypothalamus Neurons Under the Magnifying Glass." Endocrinology **162**(10).
Kim, N., H. Kang, A. Jo, S. A. Yoo and H. O. Lee (2023). "Perspectives on single-nucleus RNA sequencing in different cell types and tissues." J Pathol Transl Med **57**(1): 52-59.
King, B. M. (1991). "Ventromedial hypothalamic obesity: a reexamination of the irritative hypothesis." Neurosci Biobehav Rev **15**(3): 341-347.
Krude, H., H. Biebermann, W. Luck, R. Horn, G. Brabant and A. Gruters (1998). "Severe early-onset obesity, adrenal insufficiency and red hair pigmentation caused by POMC mutations in humans." Nat Genet **19**(2): 155-157.
Kweon, H. J., J. H. Cho, I. S. Jang and B. C. Suh (2016). "ASIC2a-dependent increase of ASIC3 surface expression enhances the sustained component of the currents." BMB Rep **49**(10): 542-547.
Labbe, S. M., A. Caron, D. Lanfray, B. Monge-Rofarello, T. J. Bartness and D. Richard (2015). "Hypothalamic control of brown adipose tissue thermogenesis." Front Syst Neurosci **9**: 150.
Lai, C. S., S. E. Fisher, J. A. Hurst, F. Vargha-Khadem and A. P. Monaco (2001). "A forkhead-domain gene is mutated in a severe speech and language disorder." Nature **413**(6855): 519-523.
Law, C. W., M. Alhamdoosh, S. Su, X. Dong, L. Tian, G. K. Smyth and M. E. Ritchie (2016). "RNA-seq analysis is easy as 1-2-3 with limma, Glimma and edgeR." F1000Res **5**.
Law, C. W., Y. Chen, W. Shi and G. K. Smyth (2014). "voom: Precision weights unlock linear model analysis tools for RNA-seq read counts." Genome Biol **15**(2): R29.
Leblanc, J., J. Dussault, D. Lupien and D. Richard (1982). "Effect of diet and exercise on norepinephrine-induced thermogenesis in male and female rats." J Appl Physiol Respir Environ Exerc Physiol **52**(3): 556-561.
Lee, M. S., H. J. Han, S. Y. Han, I. Y. Kim, S. Chae, C. S. Lee, S. E. Kim, S. G. Yoon, J. W. Park, J. H. Kim, S. Shin, M. Jeong, A. Ko, H. Y. Lee, K. J. Oh, Y. H. Lee, K. H. Bae, S. H. Koo, J. W. Kim, J. K. Seong, D. Hwang and J. Song (2018). "Loss of the E3 ubiquitin ligase MKRN1 represses diet-induced metabolic syndrome through AMPK activation." Nat Commun **9**(1): 3404.

Lee, Y. H., A. P. Petkova, A. A. Konkar and J. G. Granneman (2015). "Cellular origins of cold-induced brown adipocytes in adult mice." FASEB J **29**(1): 286-299.
Lenard, N. R. and H. R. Berthoud (2008). "Central and peripheral regulation of food intake and physical activity: pathways and genes." Obesity (Silver Spring) **16 Suppl 3**(Suppl 3): S11-22.
Li, J. N. and P. L. Sheets (2020). "Spared nerve injury differentially alters parabrachial monosynaptic excitatory inputs to molecularly specific neurons in distinct subregions of the central amygdala." Pain **161**(1): 166-176.
Li, T. S., S. Ikeda, M. Kubo, M. Ohshima, H. Kurazumi, Y. Takemoto, K. Ueda and K. Hamano (2011). "Diabetic impairment of C-kit bone marrow stem cells involves the disorders of inflammatory factors, cell adhesion and extracellular matrix molecules." PLoS One **6**(10): e25543.
Liao, C., M. P. de Molliens, S. T. Schneebeli, M. Brewer, G. Song, D. Chatenet, K. M. Braas, V. May and J. Li (2019). "Targeting the PAC1 Receptor for Neurological and Metabolic Disorders." Curr Top Med Chem **19**(16): 1399-1417.
Loncar, D. (1991). "Convertible adipose tissue in mice." Cell Tissue Res **266**(1): 149-161.
Lyly, A., S. K. Marjavaara, A. Kyttala, K. Uusi-Rauva, K. Luiro, O. Kopra, L. O. Martinez, K. Tanhuanpaa, N. Kalkkinen, A. Suomalainen, M. Jauhiainen and A. Jalanko (2008). "Deficiency of the INCL protein Ppt1 results in changes in ectopic F1-ATP synthase and altered cholesterol metabolism." Hum Mol Genet **17**(10): 1406-1417.
Lyons, C. E., M. Razzoli, E. Larson, D. Svedberg, A. Frontini, S. Cinti, L. Vulchanova, M. Sanders, M. Thomas and A. Bartolomucci (2020). "Optogenetic-induced sympathetic neuromodulation of brown adipose tissue thermogenesis." FASEB J **34**(2): 2765-2773.
Machado, N. L. S., S. S. Bandaru, S. B. G. Abbott and C. B. Saper (2020). "EP3R-Expressing Glutamatergic Preoptic Neurons Mediate Inflammatory Fever." J Neurosci **40**(12): 2573-2588.
Machado, N. L. S., F. Raffin, S. Kaur, A. S. Banks, N. Lynch, O. Fanari, O. R. Plascencia, S. Aten, J. D. Lima, S. S. Bandaru, R. D. Palmiter, E. Arrigoni and C. B. Saper (2023). "Prolonged activation of EP3 receptor-expressing preoptic neurons underlies torpor responses." Res Sq.
Maita, I., A. Bazer, J. U. Blackford and B. A. Samuels (2021). "Functional anatomy of the bed nucleus of the stria terminalis-hypothalamus neural circuitry: Implications for valence surveillance, addiction, feeding, and social behaviors." Handb Clin Neurol **179**: 403-418.
Meek, T. H., J. T. Nelson, M. E. Matsen, M. D. Dorfman, S. J. Guyenet, V. Damian, M. B. Allison, J. M. Scarlett, H. T. Nguyen, J. P. Thaler, D. P. Olson, M. G. Myers, Jr., M. W. Schwartz and G. J. Morton (2016). "Functional identification of a neurocircuit regulating blood glucose." Proc Natl Acad Sci U S A **113**(14): E2073-2082.
Moffitt, J. R., D. Bambah-Mukku, S. W. Eichhorn, E. Vaughn, K. Shekhar, J. D. Perez, N. D. Rubinstein, J. Hao, A. Regev, C. Dulac and X. Zhuang (2018). "Molecular, spatial, and functional single-cell profiling of the hypothalamic preoptic region." Science **362**(6416).
Morrison, S. F., C. J. Madden and D. Tupone (2014). "Central neural regulation of brown adipose tissue thermogenesis and energy expenditure." Cell Metab **19**(5): 741-756.

Muller, P., O. Velazquez Camacho, A. M. Yazbeck, C. Wolwer, W. Zhai, J. Schumacher, D. Heider, R. Buettner, A. Quaas and A. M. Hillmer (2023). "Why loss of Y? A pan-cancer genome analysis of tumors with loss of Y chromosome." Comput Struct Biotechnol J **21**: 1573-1583.
Munzberg, H., J. S. Flier and C. Bjorbaek (2004). "Region-specific leptin resistance within the hypothalamus of diet-induced obese mice." Endocrinology **145**(11): 4880-4889.
Munzberg, H., E. Qualls-Creekmore, H. R. Berthoud, C. D. Morrison and S. Yu (2016). "Neural Control of Energy Expenditure." Handb Exp Pharmacol **233**: 173-194.
Myers, M. G., Jr., R. L. Leibel, R. J. Seeley and M. W. Schwartz (2010). "Obesity and leptin resistance: distinguishing cause from effect." Trends Endocrinol Metab **21**(11): 643-651.
Nakamura, Y., T. Yahiro, A. Fukushima, N. Kataoka, H. Hioki and K. Nakamura (2022). "Prostaglandin EP3 receptor-expressing preoptic neurons bidirectionally control body temperature via tonic GABAergic signaling." Sci Adv **8**(51): eadd5463.
Neel, J. V. (1962). "Diabetes mellitus: a "thrifty" genotype rendered detrimental by "progress"?" Am J Hum Genet **14**(4): 353-362.
Nogueiras, R., P. Wiedmer, D. Perez-Tilve, C. Veyrat-Durebex, J. M. Keogh, G. M. Sutton, P. T. Pfluger, T. R. Castaneda, S. Neschen, S. M. Hofmann, P. N. Howles, D. A. Morgan, S. C. Benoit, I. Szanto, B. Schrott, A. Schurmann, H. G. Joost, C. Hammond, D. Y. Hui, S. C. Woods, K. Rahmouni, A. A. Butler, I. S. Farooqi, S. O'Rahilly, F. Rohner-Jeanrenaud and M. H. Tschop (2007). "The central melanocortin system directly controls peripheral lipid metabolism." J Clin Invest **117**(11): 3475-3488.
Novak, C. M. and J. A. Levine (2007). "Central neural and endocrine mechanisms of non-exercise activity thermogenesis and their potential impact on obesity." J Neuroendocrinol **19**(12): 923-940.
Ogden, C. L., S. Z. Yanovski, M. D. Carroll and K. M. Flegal (2007). "The epidemiology of obesity." Gastroenterology **132**(6): 2087-2102.
Ohbuchi, T., K. Sato, H. Suzuki, Y. Okada, G. Dayanithi, D. Murphy and Y. Ueta (2010). "Acid-sensing ion channels in rat hypothalamic vasopressin neurons of the supraoptic nucleus." J Physiol **588**(Pt 12): 2147-2162.
Organization, W. H. (2024). "Obesity and overweight."
Ottaway, N., P. Mahbod, B. Rivero, L. A. Norman, A. Gertler, D. A. D'Alessio and D. Perez-Tilve (2015). "Diet-induced obese mice retain endogenous leptin action." Cell Metab **21**(6): 877-882.
Pagès, H., M. Carlson, S. Falcon and N. Li (2021). AnnotationDbi: Manipulation of SQLite-based annotations in Bioconductor. R package version1. 54.1.
Pan, D., L. Huang, L. J. Zhu, T. Zou, J. Ou, W. Zhou and Y. X. Wang (2015). "Jmjd3-Mediated H3K27me3 Dynamics Orchestrate Brown Fat Development and Regulate White Fat Plasticity." Dev Cell **35**(5): 568-583.
Patel, M., J. Braun, G. Lambert, T. Kameneva, C. Keatch and E. Lambert (2023). "Central mechanisms in sympathetic nervous dysregulation in obesity." J Neurophysiol **130**(6): 1414-1424.
Peng, B. G., S. Ahmad, S. Chen, P. Chen, M. P. Price and X. Lin (2004). "Acid-sensing ion channel 2 contributes a major component to acid-evoked excitatory responses in

spiral ganglion neurons and plays a role in noise susceptibility of mice." J Neurosci **24**(45): 10167-10175.
Phelan, K. D., M. M. Mock, O. Kretz, U. T. Shwe, M. Kozhemyakin, L. J. Greenfield, A. Dietrich, L. Birnbaumer, M. Freichel, V. Flockerzi and F. Zheng (2012). "Heteromeric canonical transient receptor potential 1 and 4 channels play a critical role in epileptiform burst firing and seizure-induced neurodegeneration." Mol Pharmacol **81**(3): 384-392.
Pinol, R. A., A. S. Mogul, C. K. Hadley, A. Saha, C. Li, V. Skop, H. S. Province, C. Xiao, O. Gavrilova, M. J. Krashes and M. L. Reitman (2021). "Preoptic BRS3 neurons increase body temperature and heart rate via multiple pathways." Cell Metab **33**(7): 1389-1403 e1386.
Pinol, R. A. and M. L. Reitman (2022). "Preoptic bombesin-like receptor-3 neurons heat it up." Temperature (Austin) **9**(4): 306-309.
Plaisier, C. L., B. J. Bennett, A. He, B. Guan, A. J. Lusis, K. Reue and L. Vergnes (2012). "Zbtb16 has a role in brown adipocyte bioenergetics." Nutr Diabetes **2**(9): e46.
Polzin, B. J., C. Zhao, S. A. Stevenson, S. C. Gammie and L. V. Riters (2024). "RNA-sequencing reveals a shared neurotranscriptomic profile in the medial preoptic area of highly social songbirds and rats." Genes Brain Behav **23**(4): e12908.
Puigserver, P. and B. M. Spiegelman (2003). "Peroxisome proliferator-activated receptor-gamma coactivator 1 alpha (PGC-1 alpha): transcriptional coactivator and metabolic regulator." Endocr Rev **24**(1): 78-90.
Qi, Q. Y. D., A. Cox, S. McNeil and P. Sumithran (2024). "Obesity medications: A narrative review of current and emerging agents." Osteoarthr Cartil Open **6**(2): 100472.
Rashid, M., K. Kondoh, G. Palfalvi, K. I. Nakajima and Y. Minokoshi (2023). "Inhibition of high-fat diet-induced inflammatory responses in adipose tissue by SF1-expressing neurons of the ventromedial hypothalamus." Cell Rep **42**(6): 112627.
Rhodes, K. J., K. I. Carroll, M. A. Sung, L. C. Doliveira, M. M. Monaghan, S. L. Burke, B. W. Strassle, L. Buchwalder, M. Menegola, J. Cao, W. F. An and J. S. Trimmer (2004). "KChIPs and Kv4 alpha subunits as integral components of A-type potassium channels in mammalian brain." J Neurosci **24**(36): 7903-7915.
Richards, A. J., A. McNinch, H. Martin, K. Oakhill, H. Rai, S. Waller, B. Treacy, J. Whittaker, S. Meredith, A. Poulson and M. P. Snead (2010). "Stickler syndrome and the vitreous phenotype: mutations in COL2A1 and COL11A1." Hum Mutat **31**(6): E1461-1471.
Ritchie, M. E., B. Phipson, D. Wu, Y. Hu, C. W. Law, W. Shi and G. K. Smyth (2015). "limma powers differential expression analyses for RNA-sequencing and microarray studies." Nucleic Acids Res **43**(7): e47.
Roh, E., D. K. Song and M. S. Kim (2016). "Emerging role of the brain in the homeostatic regulation of energy and glucose metabolism." Exp Mol Med **48**(3): e216.
Rondini, E. A., L. Mladenovic-Lucas, W. R. Roush, G. T. Halvorsen, A. E. Green and J. G. Granneman (2017). "Novel Pharmacological Probes Reveal ABHD5 as a Locus of Lipolysis Control in White and Brown Adipocytes." J Pharmacol Exp Ther **363**(3): 367-376.
Sabatini, P. V., J. Wang, A. C. Rupp, A. H. Affinati, J. N. Flak, C. Li, D. P. Olson and M. G. Myers (2021). "tTARGIT AAVs mediate the sensitive and flexible manipulation of intersectional neuronal populations in mice." Elife **10**.

Santulli, G., D. Lewis, A. des Georges, A. R. Marks and J. Frank (2018). "Ryanodine Receptor Structure and Function in Health and Disease." Subcell Biochem **87**: 329-352.
Saper, C. B. and N. L. S. Machado (2022). "Identifying specific populations of preoptic thermoregulatory neurons: The way forward." Temperature (Austin) **9**(1): 12-13.
Satinoff, E. (1978). "Neural organization and evolution of thermal regulation in mammals." Science **201**(4350): 16-22.
Schneeberger, M., N. L. Brice, K. Pellegrino, L. Parolari, J. T. Shaked, K. J. Page, F. Marchildon, D. W. Barrows, T. S. Carroll, T. Topilko, V. M. Mulligan, R. Newman, K. Doyle, R. Burli, D. F. Barker, A. Glen, M. J. Ortuno, A. R. Nectow, N. Renier, P. Cohen, M. Carlton, N. Heintz and J. M. Friedman (2022). "Pharmacological targeting of glutamatergic neurons within the brainstem for weight reduction." Nat Metab **4**(11): 1495-1513.
Schneeberger, M., L. Parolari, T. Das Banerjee, V. Bhave, P. Wang, B. Patel, T. Topilko, Z. Wu, C. H. J. Choi, X. Yu, K. Pellegrino, E. A. Engel, P. Cohen, N. Renier, J. M. Friedman and A. R. Nectow (2019). "Regulation of Energy Expenditure by Brainstem GABA Neurons." Cell **178**(3): 672-685 e612.
Schwartz, M. W. and D. Porte, Jr. (2005). "Diabetes, obesity, and the brain." Science **307**(5708): 375-379.
Schwartz, M. W., S. C. Woods, D. Porte, Jr., R. J. Seeley and D. G. Baskin (2000). "Central nervous system control of food intake." Nature **404**(6778): 661-671.
Seale, P., B. Bjork, W. Yang, S. Kajimura, S. Chin, S. Kuang, A. Scime, S. Devarakonda, H. M. Conroe, H. Erdjument-Bromage, P. Tempst, M. A. Rudnicki, D. R. Beier and B. M. Spiegelman (2008). "PRDM16 controls a brown fat/skeletal muscle switch." Nature **454**(7207): 961-967.
Seoane-Collazo, P., J. Ferno, F. Gonzalez, C. Dieguez, R. Leis, R. Nogueiras and M. Lopez (2015). "Hypothalamic-autonomic control of energy homeostasis." Endocrine **50**(2): 276-291.
Settembre, C., A. Fraldi, D. L. Medina and A. Ballabio (2013). "Signals from the lysosome: a control centre for cellular clearance and energy metabolism." Nat Rev Mol Cell Biol **14**(5): 283-296.
Sidossis, L. and S. Kajimura (2015). "Brown and beige fat in humans: thermogenic adipocytes that control energy and glucose homeostasis." J Clin Invest **125**(2): 478-486.
Skolnikova, E., L. Sedova, B. Chylikova, A. Kabelova, F. Liska and O. Seda (2020). "Maternal High-Sucrose Diet Affects Phenotype Outcome in Adult Male Offspring: Role of Zbtb16." Front Genet **11**: 529421.
Smyth, G. K. (2005). Limma: linear models for microarray data. Bioinformatics and computational biology solutions using R and Bioconductor, Springer**:** 397-420.
Sternson, S. M. (2013). "Hypothalamic survival circuits: blueprints for purposive behaviors." Neuron **77**(5): 810-824.
Steuernagel, L., B. Y. H. Lam, P. Klemm, G. K. C. Dowsett, C. A. Bauder, J. A. Tadross, T. S. Hitschfeld, A. Del Rio Martin, W. Chen, A. J. de Solis, H. Fenselau, P. Davidsen, I. Cimino, S. N. Kohnke, D. Rimmington, A. P. Coll, A. Beyer, G. S. H. Yeo and J. C. Bruning (2022). "HypoMap-a unified single-cell gene expression atlas of the murine hypothalamus." Nat Metab **4**(10): 1402-1419.
Swanson, L. W. (2000). "Cerebral hemisphere regulation of motivated behavior." Brain Res **886**(1-2): 113-164.

Swanson, L. W. and H. G. Kuypers (1980). "A direct projection from the ventromedial nucleus and retrochiasmatic area of the hypothalamus to the medulla and spinal cord of the rat." Neurosci Lett **17**(3): 307-312.
Tan, C. L., E. K. Cooke, D. E. Leib, Y. C. Lin, G. E. Daly, C. A. Zimmerman and Z. A. Knight (2016). "Warm-Sensitive Neurons that Control Body Temperature." Cell **167**(1): 47-59 e15.
Tan, C. L. and Z. A. Knight (2018). "Regulation of Body Temperature by the Nervous System." Neuron **98**(1): 31-48.
Tanida, M., A. Hayata, N. Shintani, N. Yamamoto, Y. Kurata, T. Shibamoto, D. A. Morgan, K. Rahmouni and H. Hashimoto (2013). "Central PACAP mediates the sympathetic effects of leptin in a tissue-specific manner." Neuroscience **238**: 297-304.
Tanida, M., N. Shintani, Y. Morita, N. Tsukiyama, M. Hatanaka, H. Hashimoto, H. Sawai, A. Baba and K. Nagai (2010). "Regulation of autonomic nerve activities by central pituitary adenylate cyclase-activating polypeptide." Regul Pept **161**(1-3): 73-80.
Thaler, J. P., C. X. Yi, E. A. Schur, S. J. Guyenet, B. H. Hwang, M. O. Dietrich, X. Zhao, D. A. Sarruf, V. Izgur, K. R. Maravilla, H. T. Nguyen, J. D. Fischer, M. E. Matsen, B. E. Wisse, G. J. Morton, T. L. Horvath, D. G. Baskin, M. H. Tschop and M. W. Schwartz (2012). "Obesity is associated with hypothalamic injury in rodents and humans." J Clin Invest **122**(1): 153-162.
Timper, K. and J. C. Bruning (2017). "Hypothalamic circuits regulating appetite and energy homeostasis: pathways to obesity." Dis Model Mech **10**(6): 679-689.
Topham, M. K. and S. M. Prescott (1999). "Mammalian diacylglycerol kinases, a family of lipid kinases with signaling functions." J Biol Chem **274**(17): 11447-11450.
Torres Irizarry, V. C., Y. Jiang, Y. He and P. Xu (2022). "Hypothalamic Estrogen Signaling and Adipose Tissue Metabolism in Energy Homeostasis." Front Endocrinol (Lausanne) **13**: 898139.
Tran, L. T., S. Park, S. K. Kim, J. S. Lee, K. W. Kim and O. Kwon (2022). "Hypothalamic control of energy expenditure and thermogenesis." Exp Mol Med **54**(4): 358-369.
Tseng, Y. H., A. M. Cypess and C. R. Kahn (2010). "Cellular bioenergetics as a target for obesity therapy." Nat Rev Drug Discov **9**(6): 465-482.
van Veen, J. E., L. G. Kammel, P. C. Bunda, M. Shum, M. S. Reid, M. G. Massa, D. Arneson, J. W. Park, Z. Zhang, A. M. Joseph, H. Hrncir, M. Liesa, A. P. Arnold, X. Yang and S. M. Correa (2020). "Hypothalamic estrogen receptor alpha establishes a sexually dimorphic regulatory node of energy expenditure." Nat Metab **2**(4): 351-363.
Vargha-Khadem, F., D. G. Gadian, A. Copp and M. Mishkin (2005). "FOXP2 and the neuroanatomy of speech and language." Nat Rev Neurosci **6**(2): 131-138.
Vong, L., C. Ye, Z. Yang, B. Choi, S. Chua, Jr. and B. B. Lowell (2011). "Leptin action on GABAergic neurons prevents obesity and reduces inhibitory tone to POMC neurons." Neuron **71**(1): 142-154.
Wang, L., I. Z. Chen and D. Lin (2015). "Collateral pathways from the ventromedial hypothalamus mediate defensive behaviors." Neuron **85**(6): 1344-1358.
Wei, Q., S. Pinho, S. Dong, H. Pierce, H. Li, F. Nakahara, J. Xu, C. Xu, P. E. Boulais, D. Zhang, M. Maryanovich, A. M. Cuervo and P. S. Frenette (2021). "MAEA is an E3 ubiquitin ligase promoting autophagy and maintenance of haematopoietic stem cells." Nat Commun **12**(1): 2522.

Weir, J. B. (1949). "New methods for calculating metabolic rate with special reference to protein metabolism." J Physiol **109**(1-2): 1-9.
Wetmore, D. R., E. Joseloff, J. Pilewski, D. P. Lee, K. A. Lawton, M. W. Mitchell, M. V. Milburn, J. A. Ryals and L. Guo (2010). "Metabolomic profiling reveals biochemical pathways and biomarkers associated with pathogenesis in cystic fibrosis cells." J Biol Chem **285**(40): 30516-30522.
Wickham, H. (2016). "ggplot2: Elegant Graphics for Data Analysis." Springer-Verlag: New York.
Widen, E., M. Lehto, T. Kanninen, J. Walston, A. R. Shuldiner and L. C. Groop (1995). "Association of a polymorphism in the beta 3-adrenergic-receptor gene with features of the insulin resistance syndrome in Finns." N Engl J Med **333**(6): 348-351.
Wisse, B. E. and M. W. Schwartz (2009). "Does hypothalamic inflammation cause obesity?" Cell Metab **10**(4): 241-242.
Wu, J., P. Bostrom, L. M. Sparks, L. Ye, J. H. Choi, A. H. Giang, M. Khandekar, K. A. Virtanen, P. Nuutila, G. Schaart, K. Huang, H. Tu, W. D. van Marken Lichtenbelt, J. Hoeks, S. Enerback, P. Schrauwen and B. M. Spiegelman (2012). "Beige adipocytes are a distinct type of thermogenic fat cell in mouse and human." Cell **150**(2): 366-376.
Wu, J., H. Jun and J. R. McDermott (2015). "Formation and activation of thermogenic fat." Trends Genet **31**(5): 232-238.
Wu, L., L. Zhou, C. Chen, J. Gong, L. Xu, J. Ye, D. Li and P. Li (2014). "Cidea controls lipid droplet fusion and lipid storage in brown and white adipose tissue." Sci China Life Sci **57**(1): 107-116.
Xia, K., H. Xiong, Y. Shin, D. Wang, T. Deerinck, H. Takahashi, M. H. Ellisman, S. A. Lipton, G. Tong, G. Descalzi, D. Zhang, M. Zhuo and Z. Zhang (2010). "Roles of KChIP1 in the regulation of GABA-mediated transmission and behavioral anxiety." Mol Brain **3**: 23.
Yang, W. Z., H. Xie, X. Du, Q. Zhou, Y. Xiao, Z. Zhao, X. Jia, J. Xu, W. Zhang, S. Cai, Z. Li, X. Fu, R. Hua, J. Cai, S. Chang, J. Sun, H. Sun, Q. Xu, X. Ni, H. Tu, R. Zheng, X. Xu, H. Wang, Y. Fu, L. Wang, X. Li, H. Yang, Q. Yao, T. Yu, Q. Shen and W. L. Shen (2023). "A parabrachial-hypothalamic parallel circuit governs cold defense in mice." Nat Commun **14**(1): 4924.
Yang, X. and H. B. Ruan (2015). "Neuronal Control of Adaptive Thermogenesis." Front Endocrinol (Lausanne) **6**: 149.
Yang, Y. and Y. Xu (2020). "The central melanocortin system and human obesity." J Mol Cell Biol **12**(10): 785-797.
Yoo, E. S., J. Yu and J. W. Sohn (2021). "Neuroendocrine control of appetite and metabolism." Exp Mol Med **53**(4): 505-516.
Young, C. E. and Q. Tong (2021). "Corticotropin Releasing Hormone Signaling in the Bed Nuclei of the Stria Terminalis as a Link to Maladaptive Behaviors." Front Neurosci **15**: 642379.
Yu, G. (2022). "enrichplot: Visualization of Functional Enrichment Result."
Yu, S., M. Francois, C. Huesing and H. Munzberg (2018). "The Hypothalamic Preoptic Area and Body Weight Control." Neuroendocrinology **106**(2): 187-194.
Yu, S., E. Qualls-Creekmore, K. Rezai-Zadeh, Y. Jiang, H. R. Berthoud, C. D. Morrison, A. V. Derbenev, A. Zsombok and H. Munzberg (2016). "Glutamatergic Preoptic Area

Neurons That Express Leptin Receptors Drive Temperature-Dependent Body Weight Homeostasis." J Neurosci **36**(18): 5034-5046.
Zalk, R., S. E. Lehnart and A. R. Marks (2007). "Modulation of the ryanodine receptor and intracellular calcium." Annu Rev Biochem **76**: 367-385.
Zhang, J., D. Chen, P. Sweeney and Y. Yang (2020). "An excitatory ventromedial hypothalamus to paraventricular thalamus circuit that suppresses food intake." Nat Commun **11**(1): 6326.
Zhang, Y., I. A. Kerman, A. Laque, P. Nguyen, M. Faouzi, G. W. Louis, J. C. Jones, C. Rhodes and H. Munzberg (2011). "Leptin-receptor-expressing neurons in the dorsomedial hypothalamus and median preoptic area regulate sympathetic brown adipose tissue circuits." J Neurosci **31**(5): 1873-1884.
Zhang, Z., F. Reis, Y. He, J. W. Park, J. R. DiVittorio, N. Sivakumar, J. E. van Veen, S. Maesta-Pereira, M. Shum, I. Nichols, M. G. Massa, S. Anderson, K. Paul, M. Liesa, O. A. Ajijola, Y. Xu, A. Adhikari and S. M. Correa (2020). "Estrogen-sensitive medial preoptic area neurons coordinate torpor in mice." Nat Commun **11**(1): 6378.

Curriculum Vitae

Rashmita Basu

Education

PhD in **Pharmacology** **November 2024**
Indiana University

M.Sc. in **Biochemistry** **July 2015**
University of Calcutta, India

B.Sc. in **Microbiology** **July 2013**
University of Calcutta, India

Research Experience

PhD Graduate Research Assistant **August 2018 – October 2024**
Identification Of A Hypothalamic Neural System That Can Reduce Body Weight And Adipose Mass In Diet-Induced Obesity.
Department of Pharmacology & Toxicology, Indiana University School of Medicine, Indianapolis; Indiana Biosciences Research Institute, Indianapolis
Advisor: Dr. Jonathan Flak

- Spearheaded multiple research projects to characterize the therapeutic potential of specific neuronal populations, in the ventromedial hypothalamus (VMN) and preoptic area (POA) of the brain, to induce weight loss and energy expenditure in obese individuals using mice model.
- Identified PACAP (pituitary adenylate cyclase activating peptide) containing neurons in the VMN signal through caudal POA outputs to induce weight loss and promote energy expenditure using neural tracing, chemogenetics, optogenetics and transcriptomics.

Pitt-India-HTRTP Research Intern **July 2016 – October 2017**
Type-1 Interferon Signaling In Tuberculous Granulomas In Cynomolgus Macaques With SIV-TB Co-Injection.
University of Pittsburgh, Pennsylvania
Advisor: Dr. Joshua Mattila, Ph.D.

- Studied the immunotherapeutic role of type 1 interferons (IFN1) in enhancing macrophage immune functions in tuberculosis-SIV co-infection of non-human primate animal model using cynomolgus macaque monkeys.
- Elucidated IFN1 expression in macrophages and signaling, and how SIV infection modifies this at the level of the lung granulomas, using techniques including flow cytometry, ELISA, IHC, RT-qPCR, epifluorescence microscopy and different image analysis software including QuPath, ImageJ, CellProfiler, Nikon NIS elements.

Research Assistant **July 2015 – April 2016**
Role Of IL1β In Leishmaniasis.
Department of Biochemistry, University of Calcutta, Kolkata, India
Advisor: Dr. Anindita Ukil, Ph.D.

- Studied host-pathogen interaction in Leishmaniasis caused by *Leishmania donovani* infection with focus on the role of IL1β in disease pathophysiology.
- Elucidated the pro-inflammatory response exerted by IL-1β in response to the infection, activating macrophages and promoting a Th1 immune phenotype crucial for parasite clearance, using molecular and biochemistry techniques like qPCR, western blot, ELISA, fluorescence microscopy.

M.Sc Dissertation **November 2014 – May 2015**
Interaction Of Ellagic Acid With Human Serum Albumin: Pharmacological Analysis.
Department of Biochemistry, University of Calcutta, Kolkata, India
Advisor: Dr. Maitree Bhattacharyya, Ph.D.

- Studied the interaction between human serum albumin (HSA) and ellagic acid, a polyphenol compound found in fruits, as a potential small molecule pharmacotherapy candidate for human cancer treatment.
- HSA binds to and transports various endogenous and exogenous compounds across the bloodstream. We employed UV-Vis and Circular Dichroism spectroscopy, Isothermal Titration Calorimetry, fluorometric measures and cytotoxicity assays to study the interaction of ellagic acid with HSA in vitro, which provided us with important insights into the pharmacokinetics, bioavailability, cytotoxicity and thermodynamics of the HSA-ellagic acid complex.

M.Sc Summer Research Intern **June 2014 – August 2014**
Preparation And Characterization Of Sendai Virosomes And Study Of Its Interaction With Human Liver Cells.
Department of Biochemistry, University of Delhi, New Delhi, India
Advisor: Dr. Debi Prasad Sarkar, Ph.D.

- Isolated and purified Sendai virus particles, inactivating them, and reconstituting the viral envelope to prepare the functional virosomes.
- Characterized the virosomes by analyzing their morphology, size, protein composition, and functional capabilities using techniques like fluorometric assays, SDS-PAGE, and hemagglutination assays.
- Studied the interaction of the virosomes with human liver cells by examining cellular uptake, cytotoxicity, delivery efficiency, and changes in gene expression using fluorescence microscopy, flow cytometry, MTT assay, and RT-qPCR.

Awards

- IUI Graduate Student Travel Fellowship Award **2023**
- Paradise Travel Award, Department of Pharmacology, IUSOM **2022**

- GPSG Travel Award, IUI **2022**
- NIH Fogarty HIV-TB Research and Training Program Scholarship **2016**
- Indian Academy of Sciences Summer Research Scholarship **2014**
- Post-Graduate Indira Gandhi Scholarship for Single Girl Child **2013 - 2015**

Publications

- **Basu, R.** and Flak, J. N. (2024). Hypothalamic neural circuits regulating energy expenditure. *Vitamins and Hormones.* In press.
- **Basu, R.,** App, B., Mahler, C., et al. Inhibitory cells in the caudal preoptic area reduce adiposity and body weight in diet induced obesity. In preparation.
- **Basu, R.,** Elmendorf, A. J., Lorentz, B., et al. (2024). Ventromedial hypothalamic nucleus subset stimulates tissue thermogenesis via preoptic area outputs. *Molecular metabolism*, *84*, 101951.
- Lin, L., **Basu, R.**, Chatterjee, D., Templin, A. T., Flak, J. N., & Johnson, T. S. (2023). Disease-associated astrocytes and microglia markers are upregulated in mice fed high fat diet. *Scientific reports*, *13*(1), 12919.

Selected Presentations

- **Basu R**., Mahler C., Britany A., Robertson S., ……Flak J. "Identification Preoptic Area Cells Impacted By Obesity And Diabetes In Both Male And Female Mice". *Society for the Study of Ingestive Behavior***,** 2024.
- **Basu R**., Mahler C., Robertson S., …. Flak J. "Inhibitory Cells in The Caudal Preoptic Area Reduce Adiposity And Body Weight in Obese Mice". *The Obesity Society Annual Meeting***,** 2023.
- **Basu R**., Elmendorf A., Mahler C., Johnson D., Lorentz B., Roh H.C., Flak J. "Activating GABAergic Neurons in the Caudal Preoptic Area Promote Energy Expenditure in Diet-Induced Obesity". *American Diabetes Association Annual Meeting*, 2022.
- **Basu R**., Elmendorf A., Mahler C., Johnson D., Lorentz B., Roh H.C., Flak J. "Ventromedial Hypothalamic Nucleus → Caudal Preoptic Area Neural Circuit Reduces Adipose Mass in Diet-Induced Obesity". *Gordon Research Conference on Hypothalamus*, 2022.
- **Basu R**., Elmendorf A., Mahler C., Johnson D., Lorentz B., Roh H.C., Flak J. "Ventromedial Hypothalamic Nucleus → Caudal Preoptic Area Neural Circuit Reduces Body Weight And Adiposity in Diet-Induced Obesity". *Centre for Diabetes & Metabolic Diseases, Indiana University School of Medicine,* 2022

Volunteer Activities

- Organized departmental student events as member of the trainee events committee at the department of pharmacology, Indiana University School of Medicine.

- Volunteer at the science camps of Girls' STEM Institute at IUPUI, inspiring underrepresented girls in STEM education and at Longfellow Middle School's after-school STEM Club, to help inspire young minds and foster curiosity in STEM fields, which to me feels immensely fulfilling, aligning with my commitment to equitable education and empowerment beyond the scope of medicine.